

Copyright  
by  
Mary Minh Chau Nguyen  
2013

**The Dissertation Committee for Mary Minh Chau Nguyen Certifies that this is the approved version of the following dissertation:**

**The Development of Depsipeptides as Tissue Engineering Scaffolds:  
Synthesis, Characterization, and Self-Assembly into Hydrogels**

**Committee:**

---

Laura J. Suggs , Supervisor

---

Pengyu Ren

---

Joseph C. Salamone

---

Brent L. Iverson

---

Lauren J. Webb

---

Krishnendu Roy

**The Development of Depsipeptides as Tissue Engineering Scaffolds:  
Synthesis, Characterization, and Self-Assembly into Hydrogels**

**by**

**Mary Minh Chau Nguyen, B.Bio.Eng**

**Dissertation**

Presented to the Faculty of the Graduate School of

The University of Texas at Austin

in Partial Fulfillment

of the Requirements

for the Degree of

**Doctor of Philosophy**

**The University of Texas at Austin**

**May 2013**

## **Dedication**

To my parents.

## Acknowledgements

I would first like to thank my family for their endless support and encouragement. Thank you, Chris, for your patience, for dinners at Titayas, and helping me appreciate this great city of Austin.

Many thanks to the Chemistry folks for their invaluable conversations, column tutorials, access to the SDS, help with the IR, lending me glassware or chemicals or NMR tubes, and for keeping it real: Dr. Chelsea Martinez, Cameron Peebles, Marie, Dr. John Hardy, Annette Raigoza, Christina Ragain, Jason Duffer, and Will Bell. I am extremely grateful to the wonderful research staff at UT for sharing their knowledge and for always having time for my questions and requests, namely Dr. Shoulders, Steve Sorey, and Angela Spangenburg of the NMR facilities; Dr. Karin Keller of the MS Analysis facility; and Michelle Gadush and Marvin Mercado of the Peptide Synthesis Lab. I would also like to thank Rick Grey from the Johnston Lab for use of their osmometer, and Dr. Vince Lance and Steve Swinnea for their help collecting the WAXS data.

The first years of graduate school would not have been as enjoyable or memorable without my previous lab members and classmates: Dr. Charlie Drinnan, Mena Abdelmalek, Dr. Christie Zhang, and Dr. Hieu Nguyen. To Laura G, Laura R, Julie, Eunna, Kevin, and Ryan, thank you for the memories of high-caloric birthday celebrations, holiday parties with Eric, walks for frozen yogurt, my first UT football game, and for enjoying my cakes and cookies.

To Dr. Suggs, Dr. Ren, Dr. Iverson, Dr. Webb, Dr. Salamone, the Welch Foundation, and the National Institutes of Health for mentoring and funding my research efforts and professional development.

# **The Development of Depsipeptides as Tissue Engineering Scaffolds: Synthesis, Characterization, and Self-Assembly into Hydrogels**

Mary Minh Chau Nguyen, Ph.D

The University of Texas at Austin, 2013

Supervisor: Laura J. Suggs

The development of novel, peptide based structures for tissue engineering materials has been widely researched, and its popularity can be attributed to advancements in technological analysis methods. Using principles based on protein structure and organization, this work describes the novel self-assembly of depsipeptides, which incorporate alternating esters within a native peptide backbone.

Chapter 1 introduces and reviews peptide mimics for their utility for tissue engineering applications. Chapter 2 describes the methodology in synthesizing and characterization a depsipeptide library using both solution and solid phase methods. Chapter 3 discusses the effects of depsipeptide length, concentration, and sequence within a range of ionic concentrations and pH ranges on the self-assembly of depsipeptides into spherical nanostructures, fibers, or hydrogels. Chapter 4 describes proposed methods to increase the rate of gelation, followed by discussions of biocompatibility studies from other self-assembling peptide and modified-peptide systems *in vitro* and *in vivo*.

The work described in this dissertation demonstrates that the synthesis and self-assembly of a depsipeptide family which alternates esters into a native peptide backbone does not disrupt the formation of higher order structures. This study illustrates the

potential to synthesize a wide range of depsipeptides with variable side chains and hydrophobic character, as understanding these effects on self-assembly is imperative to the development of biomimetic materials for tissue engineering applications.

## Table of Contents

List of Tables .....	xi
List of Figures .....	xii
List of Schemes .....	xxiv
Chapter 1. Peptide Mimics as Biomaterials .....	1
1.1 Introduction .....	1
1.2 Naturally occurring peptide mimics .....	4
1.2.1 Elastin-like mimics .....	4
1.2.2 Silk-like mimics .....	6
1.3 Peptidomimetic families .....	7
1.3.1 Introduction .....	7
1.3.2 Peptoids .....	7
1.3.3 $\beta$ -peptides .....	10
1.4 Developing mimics with ester functionality .....	11
1.4.1 Depsipeptides for tissue engineering applications .....	11
1.4.2 Ease of synthesis .....	12
1.4.3 Controlled degradation of depsipeptides for future applications .....	12
Chapter 2. Synthesis of Alternating Depsipeptides: Incorporating Regular Esters into a Native Peptide Backbone through the Coupling of Depsi-dipeptide Building Blocks .....	19
2.1 Chapter Summary .....	19
2.1.1 Introduction .....	19
2.1.2 Goals .....	19
2.1.3 Approach .....	20
2.1.4 Results .....	20
2.2 Background .....	21
2.2.1 Polydepsipeptides: Challenges in Synthesis and Homopolymerizations .....	21



2.2.2	Solid Phase Peptide Synthesis .....	24
2.3	Results.....	25
2.3.1	Solution phase synthesis of Fmoc-depsidipeptides .....	25
2.3.2	Optimizing SPPS protocols for the Synthesis of Depsipeptides 30	
2.4	Conclusions.....	44
2.5	Experimental Methods.....	46
Chapter 3. Self-Assembly of Depsipeptides into Spherical Structures, Fibers, or Hydrogels.....		
3.1	Chapter Summary .....	94
3.1.1	Introduction.....	94
3.1.2	Goals .....	94
3.1.3	Approach.....	95
3.1.4	Results.....	95
3.2	Background.....	96
3.2.1	Depsipeptides as Self-Assembling Materials.....	96
3.2.2	Self-assembling peptides: Families and mechanisms.....	98
3.2.2.1	Amphiphilic peptides: balance of charge and hydrophobicity .....	98
3.2.2.2	Fmoc-peptides: role of aromatic interactions that drive self- assembly.....	104
3.3	Results.....	110
3.3.1	Depsipeptides (1) and (2): Effect of weak hydrophobic residues on charged residues.....	110
3.3.2	Depsipeptide (3): Formation of spherical nanostructures.....	113
3.3.3	Depsipeptide (4): Ordered morphology within ionic solutions	116
3.3.4	Depsipeptide (5): Self-assembly of a novel gel structure .....	120
3.3.4.1	Gelation in ionic concentrations from pH 6-9 .....	120
3.3.4.2	Effect of high ionic concentration on self-assembly.....	132
3.3.4.3	Self-assembly at low pH promote gelation at lower concentrations .....	132
3.3.4.4	Flexible fibers are observed at low pH in water .....	135

3.3.4.5 Self-assembly and gelation processes are slow in water	137
3.3.4.6 Proposed self-assembly models .....	139
3.3.5 Depsipeptide (6): Self-assembly is effected by depsipeptide length .....	142
3.4 Conclusions.....	146
3.5 Experimental methods .....	147
Chapter 4. Developing Depsipeptides as Novel Biomaterials with Predictable Self-Assembling Characteristics with Hydrophobicity, Secondary Prediction, and Biocompatibility.....	153
4.1 Chapter Summary .....	153
4.2 Experimental results.....	154
4.2.1 Increasing overall hydrophobicity .....	154
4.2.3 Secondary analysis and self-assembly of depsipeptides: Peptide control .....	155
4.2.3 Biocompatibility of self-assembling peptides and modified peptides	156
4.2.3.1 Fmoc-FF/RGD gels as 3D scaffolds.....	156
4.2.3.2 PuraMatrix™: Commercial synthetic peptide that exhibits self-assembling behavior .....	158
4.3 Conclusions.....	159
References.....	160
Bibliography .....	161
Vita	169

## List of Tables

Table 1.1. Abbreviations of the 20 common amino acids. ....	3
Table 2.1 Depsipeptide purification details. Lactic acid is represented by Lac, and the gradient refers to the percentage of solvent B at which the depsipeptide was collected during HPLC. The yield was calculated from the equivalence value of the Fmoc-Ala-Wang resin which varied by lot, unless otherwise noted*.....	45
Table 3.1 Summary of self-assembly tests on depsipeptide (1) and depsipeptide (2). No gelation was observed. As a reference, physiological osmolarity is around 280-310 mmol/kg.....	111
Table 3.2 Summary of self-assembly tests on depsipeptide (3). Spherical nanostructures were observed in solution F. As a reference, physiological osmolarity is around 280-310 mmol/kg.....	114
Table 3.3 Summary of self-assembly experiments on depsipeptide (4) at 10 mg/ml. As a reference, physiological osmolarity is around 280-310 mmol/kg.....	118
Table 3.4 Summary of self-assembly experiments for depsipeptide (5). As a reference, physiological osmolarity is around 280-310 mmol/kg. .	121
Table 3.5 Summary of the self-assembly experiments of depsipeptide (6). No gels were observed. As a reference, physiological osmolarity is around 280-310 mmol/kg.....	144

## List of Figures

- Figure 1.1 Unique features and potential applications of protein-based biomaterials. While the examples shown above are derived from recombinant DNA technology, the overall strategy of developing complex, functional, and biologically relevant materials can be applied to synthetically made peptide based systems. Used with permission. [3]. .....2
- Figure 1.2 Histological section of ELP-chondrocyte constructs. Sections stained for: (A) cell morphology with H&E, S-GAG using toluidine blue (B), and collagen and extracellular matrix using Masson's trichrome (C). The scale bar is 50  $\mu\text{m}$ . Used with permission. [12].....5
- Figure 1.3 Chemical structures of peptidomimetic families. The structure of a native peptide backbone is provided for comparison. ....8

Figure 1.4 Secondary structure and self-assembly of peptoid families. The chemical structures of the peptoid residues are illustrated (A). CD of the tested peptoids (B) show that secondary folding is maintained despite changes to the backbone. Peptoid 1 is [H-(NLys-Nspe-Nspe)<sub>4</sub>-NH<sub>2</sub>] and is modified by substituting Pro at the 6 position (1-Pro<sub>6</sub>), NHis at the 6 and 12 position (1-NHis<sub>6,12</sub>), or NGlu at the 4 and 10 position (1-NGlu<sub>4,10</sub>) [28]. A model of the proposed self-assembly process for the peptoid Nspe<sub>15</sub>-NGlu<sub>15</sub> [29] (C). The hydrophobic and hydrophilic regions are represented in green and red respectively. The aromatic regions align with a distance of 1.66 nm while the distance between each chain is 4.8 Å. As self-assembly continues, the chains arrange into 2-D sheets with a height of 7.8 nm and become layered to form superhelices. Dimensions were verified with AFM and X-ray scattering. Both images used with permission.....9

Figure 2.1 General chemical structure of a MD .....22

Figure 2.2 Synthesis of depsi-dipeptides using pentafluorophenol activated esters. LC/MS of the crude samples from depsipeptide coupling with Lac and Fmoc-Asp(OBzl)-OPfp under various conditions (A). Reacting with DIPEA overnight reduces the number of products with undesired lactic acid residues at the C-terminal. Purification of Fmoc-Lys(Z)-Lac-OH on a silica column shows that Fmoc-Lys(Z)-OH was not removed (B). Fmoc-Lys(Z)-Lac-Lac-OH was also present in this mixture, suggesting that the reaction time is sensitive to the formation of this undesired by-product. Chemical structures of the products in the mixture are provided (C). .....27

Figure 2.3	MS of Fmoc-Lys(Boc)-Bt. Bt refers to benzotriazole, M is the mass of interest, M – Boc is without the protecting group, and the mass addition of 23 is due to a sodium adduct. ....	29
Figure 2.4	<sup>1</sup> H-NMR of Lac-Bn. Shifts correspond with data reported in literature [23]: 7.40-7.26 (m, 5H, benzene ring protons), 5.21 (s, 2H, PhCH <sub>2</sub> ), 4.32 (q, 1H, COCH, <i>J</i> = 7.2 Hz), 1.43 (d, 3H, CH <sub>3</sub> , <i>J</i> = 7.2 Hz). ....	31
Figure 2.5	Depsipeptide library. These depsipeptides have been successfully purified with HPLC. The structures are named according to the presence of functional groups starting at the N-terminal. For example, depsipeptide 1 has alternating lysine (K) and Lac residues, with a total sequence of 8. Alanine (A) is terminal amino acid. Aspartic acid (D) is represented by its standard one letter code. ....	32
Figure 2.7	MS of crude Fmoc-(Asp(OBzl)-Lac) <sub>6</sub> . Arrows represent an increase of mass unit 72, which is equivalent to a Lac residue. ....	37
Figure 2.8	Fragmentation data of Fmoc-(Lys(Z)-Lac) <sub>6</sub> . Before fragmentation, the MS show masses associated with Fmoc-(Lys(Z)-Lac) <sub>6</sub> and Fmoc-(Lys(Z)-Lac) <sub>4</sub> -Lys (A). Masses are isolated and ionized to investigate the identity of fragmentation products (B). ....	38
Figure 2.9	Cleaving cocktail A. Solution A was composed of 95/5 TFA and TIPS. ....	40
Figure 2.10	Cleaving cocktail B. Solution B was composed of 95/2/3 TFA/Water/TIPS. ....	41
Figure 2.11	Cleaving cocktail C. Solution C was composed of 95/2/3 TFA/DCM/TIPS. ....	42

Figure 2.12	Cleaving cocktail D. Solution D was composed of 50/48/2 TFA/DCM/TIPS .....	43
Figure 2.13	<sup>1</sup> H-NMR of Fmoc-Asp(OtBu)-Lac-Bn. Full scale.....	49
Figure 2.14	<sup>1</sup> H-NMR of Fmoc-Asp(OtBu)-Lac-Bn . Magnified from 1.0-2.8 ppm, with integrations.....	50
Figure 2.15	<sup>1</sup> H-NMR of Fmoc-Asp(OtBu)-Lac-Bn. Magnified from 3.4-5.2 ppm, with integrations.....	51
Figure 2.16	<sup>1</sup> H-NMR of Fmoc-Asp(OtBu)-Lac-Bn. Magnified from 7.2-8.0 ppm with integrations.....	52
Figure 2.17	<sup>13</sup> C-NMR of Fmoc-Asp(OtBu)-Lac-Bn.....	53
Figure 2.18	LCMS of Fmoc-Asp(OtBu)-Lac-Bn.....	54
Figure 2.19	MS of Fmoc-Asp(OtBu)-Lac-Bn in negative mode. ....	55
Figure 2.20	MS of Fmoc-Asp(OtBu)-Lac-Bn in positive mode. ....	56
Figure 2.21	<sup>1</sup> H-NMR of Fmoc-Lys(Boc)-Lac-Bn. Full spectrum.....	58
Figure 2.22	<sup>1</sup> H-NMR of Fmoc-Lys(Boc)-Lac-Bn. Magnified from 1.0-3.4 ppm with integrations.....	59
Figure 2.23	<sup>1</sup> H-NMR of Fmoc-Lys(Boc)-Lac-Bn. Magnified from 3.8-5.2 ppm with integrations.....	60
Figure 2.24	<sup>1</sup> H-NMR of Fmoc-Lys(Boc)-Lac-Bn. Magnified from 6.7-8.0 ppm with integrations.....	61
Figure 2.25	<sup>1</sup> H-NMR of Fmoc-Lys(Boc)-Lac-Bn.....	62
Figure 2.26	LCMS of Fmoc-Lys(Boc)-Lac-Bn. ....	63
Figure 2.27	MS of Fmoc-Lys(Boc)-Lac-Bn negative mode. ....	64
Figure 2.28	MS of Fmoc-Lys(Boc)-Lac-Bn positive mode. ....	65
Figure 2.29	<sup>1</sup> H-NMR of Fmoc-Asp(OtBu)-Lac-OH. Full spectrum.....	67

Figure 2.30	<sup>1</sup> H-NMR of Fmoc-Asp(OtBu)-Lac-OH. Magnified from 1.1-1.7 ppm, with integrations.....	68
Figure 2.31	<sup>1</sup> H-NMR of Fmoc-Asp(OtBu)-Lac-OH. Magnified from 2.50-2.85 ppm, with integrations.....	69
Figure 2.32	<sup>1</sup> H-NMR of Fmoc-Asp(OtBu)-Lac-OH. Magnified from 4.3-4.9 ppm, with integrations.....	70
Figure 2.33	<sup>1</sup> H-NMR of Fmoc-Asp(OtBu)-Lac-OH. Magnified from 7.3-8.0 ppm, with integrations.....	71
Figure 2.34	<sup>13</sup> C-NMR of Fmoc-Asp(OtBu)-Lac-OH.....	72
Figure 2.35	LCMS of Fmoc-Asp(OtBu)-Lac-OH.....	73
Figure 2.36	MS of Fmoc-Asp(OtBu)-Lac-OH in negative mode. ....	74
Figure 2.37	MS of Fmoc-Asp(OtBu)-Lac-OH in positive mode. ....	75
Figure 2.38	<sup>1</sup> H-NMR of Fmoc-Lys(Boc)-Lac-OH. Full spectrum. ....	77
Figure 2.39	<sup>1</sup> H-NMR of Fmoc-Lys(Boc)-Lac-OH. Magnified from 1.0-3.4 ppm, with integrations.....	78
Figure 2.40	<sup>1</sup> H-NMR of Fmoc-Lys(Boc)-Lac-OH. Magnified from 3.8-5.8 ppm, with integrations.....	79
Figure 2.41	<sup>1</sup> H-NMR of Fmoc-Lys(Boc)-Lac-OH. Magnified at 6.7-8.1 ppm, with integrations.....	80
Figure 2.42	<sup>13</sup> C-NMR of Fmoc-Lys(Boc)-Lac-OH. ....	81
Figure 2.43	LCMS of Fmoc-Lys(Boc)-Lac-OH. ....	82
Figure 2.44	MS of Fmoc-Lys(Boc)-Lac-OH in negative mode.....	83
Figure 2.45	MS of Fmoc-Lys(Boc)-Lac-OH in positive mode.....	84
Figure 2.46	HPLC of depsipeptide (1). ....	86
Figure 2.47	HPLC of depsipeptide (2). ....	87



Figure 2.48	HPLC of depsipeptide (3).....	88
Figure 2.49	HPLC of depsipeptide (4).....	89
Figure 2.50	HPLC of depsipeptide (5).....	90
Figure 2.51	HPLC of depsipeptide (6).....	91
Figure 3.1	Molecular dynamics model of (Gly-Lac) <sub>6</sub> (A) and (Lys-Lac) <sub>6</sub> (B). (Gly-Lac) <sub>6</sub> (A) folds into a left- or right-handed helix and (Lys-Lac) <sub>6</sub> has a polyproline II-type structure. Used with permission. [6].....	97
Figure 3.2	Self-assembly of a depsipeptide-amylin derivative. The chemical structure of the derivative with ester substitutions at the 24, 26, and 28 position (A). TEM shows the formation of helical nanotubes formed by the amylin(20-29) derivative (B). Arrow a: single strand; arrow b: two strands starting to intertwine; arrow c: helical ribbon; arrow d: (closed) peptide tube; arrows e and f; two helical tapes with pitches of 500 and 330 nm, respectively. Samples were aged for 3 weeks. Scale bar: 1 μm. Used with permission. [2].....	99
Figure 3.3	Sequences of self-complementary peptides derived from EAK-peptides. The self-assembling process of peptide RAD16-I into a nanofiber scaffolding hydrogel is driven by the interactions of many individual peptides. Used with permission. [14, 15].....	101
Figure 3.4	CD and AFM of RAD16-I after sonication. CD shows β-sheet spectra for all conditions (A). AFM images of RAD16-I (B) were collected after sonication: 1 min (a), 2 min (b), 8 min (c), 16 min (d), 32 min (e), and 64 min (f). Used with permission. [16].....	103

Figure 3.5: Molecular (A) and self-assembled structure (B) of Fmoc-FF. Fmoc-F was used to observe signals in a non-gelling sample. CD spectra show a minimum at 218 nm for Fmoc-FF, which indicates beta-sheet structure (b). FTIR of Fmoc-FF show two distinct peaks at 1630 and 1685  $\text{cm}^{-1}$ , which is consistent with an anti-parallel  $\beta$  sheet (c). Fluorescence emission spectrum of Fmoc-FF shows a peak-shift from 320 to 330 nm to higher wavelength indicating excimer formation and a new broad peak at 460 nm indicating the formation of higher order aggregates (d). A model structure was created to illustrate the self-assembly of Fmoc-FF into nanofibers (B). Details are provided in the text. In (a), (b), and (d), fluorenyl groups are colored orange and the phenyl groups are colored purple to illustrate the paired pi-stacked nature of the fluorenyl groups. Used with permission. [21].....106

Figure 3.6 The self-assembled hydrogel of Fmoc-FF/RGD. The chemical structures of the hydrogel building blocks (A). Upon mixing, Fmoc-FF and Fmoc-RGD self-assemble into a translucent hydrogel at 37°C (B) AFM shows an overlapping mesh of nanofibers, with bundles and entanglements (C) while TEM shows that the nanofibers as ‘flat ribbons’ (D). The proposed supramolecular model demonstrates the formation of the 3 nm fibrils and their further lateral assembly into larger ribbons (E). RGD sequences are presented on the fiber surface in red and the FF peptides are illustrated in blue. Used with permission. [23].....107

Figure 3.7	Circular dichromism (CD) spectra of Fmoc-Phe and structures 1 and 7 at pH 7 (A). 1 is Fmoc-Gly-Gly and 7 is Fmoc-Phe-Phe. Gel 7 shows the presence of $\pi$ - $\pi$ interactions between fluorenyl groups. The y-axis represents molar ellipticity and is in units of mdeg. Two-photon fluorescence microscopy shows the presence of DAPI-stained cells within the hydrogel structure of Fmoc-Phe-Phe (B). Scale bar: 50 $\mu$ m. Used with permission. [25].....	109
Figure 3.8	Emission spectra of Fmoc-peptides and Fmoc-depsidipeptides (A) and Fmoc-K-Lac-8 (B). The chemical structures and short-hand labels for the Fmoc-peptides and Fmoc-depsidipeptide are provided (C).....	112
Figure 3.9	Self-assembly data of depsipeptide (3). Emission spectra (A), CD spectra of Fmoc-peptides and Fmoc-depsidipeptides (B), CD of depsidipeptide (3) (C) and TEM (E-G) of depsipeptide 3. The molar ellipticity of the CD data is in units of deg cm <sup>2</sup> /dmol. Parallel alignment of fluorenyl groups within Fmoc-dipeptide families have been reported to self-assemble to form the hydrophobic core of micelles [29] , as illustrated by the cartoon model (D).....	115
Figure 3.10	TEM images of depsipeptide (4). The sample in water (A), PBS (B), PBS and 10 mM NaCl (C-F). The formation of amyloid fibers may provide insight on the self-assembly processes of depsipeptide (4), as seen with the lateral growth of granular aggregates into amyloid fibers (G). Used with permission. [30] .....	119

- Figure 3.11 Self-assembling data for depsipeptide (5). The emission spectra (A) was collected 2 days after the sample was prepared. The peak at 330 nm is indicative of anti-parallel stacking of the Fmoc-groups. Helical packing of the fluorenyl groups is evident in the CD data collected on 5-20 mg/ml (B and C) and is consistent with data reported in other Fmoc-gelling families [31]. The sampled in its gelled form takes the shape of the vial (D). The molar ellipticity of the CD data in (B and C) is in units of deg cm<sup>2</sup>/dmol.....122
- Figure 3.12 <sup>1</sup>H-NMR of depsipeptide (5) in solution (A) and in gelled (B) states. (A) was prepared in D<sub>2</sub>O with PBS and NaCl salts and (B) was prepared in solution F with 5% D<sub>2</sub>O.....124
- Figure 3.13 MS of depsipeptide (5) in buffer F in ungelled (A) and gelled (B) form. The structure is stable for up to 4 days.....125
- Figure 3.14 IR data for depsipeptides (3) and (5). Fmoc-peptides and Fmoc-depsidipeptides were dissolved in methanol and dried on gold-coated silica (A). Depsipeptide (3) was collected on a GATR accessory on a geranium crystal and plotted against depsipeptide (5) for comparison (B). Depsipeptide (5) was collected using both methods and plotted against each other (C), suggesting that the gel in the dried or solution state have similar folding patterns. The IR shifts of depsipeptide (5) in (B) and (C) were normalized at 1545 cm<sup>-1</sup>. .....126

Figure 3.15 Fibril formation for depsipeptide (5). TEM images were collected at various times after sample preparation: 18 hours (A), 4 days (B and C), and 3 weeks (D) WAXS data (E) shows  $d$ -spacing of 4.3 Å and 3.26 Å, the latter of which is associated with the crystal structure of NaCl from the buffer. The former value has been reported to be the distance between  $\pi$ - $\pi$  bonds of the fluorenyl group or between  $\beta$ -sheet forming peptides. The insert was collected on the gel.....128

Figure 3.16 Titration curves for Depsipeptide (3) (A) and depsipeptide (5) (B). The red curve was prepared with 10 mM NaCl. ....130

Figure 3.17 Self-assembly data of depsipeptide (5) in solution M. Emission (A) and CD (B). TEM images of the 10 mg/ml sample (C) show the formation of fibers. The molar ellipticity of the CD data is in units of deg  $\text{cm}^2/\text{dmol}$ . ....133

Figure 3.18 Self-assembly of depsipeptide (5) in solution N. Emission spectra (A) and CD data (B). The molar ellipticity of the CD data is in units of deg  $\text{cm}^2/\text{dmol}$ . TEM images at 5 mg/ml (C and D), 10 mg/ml (E and F), and 20 mg/ml (G).....134

Figure 3.19 Self-assembly of depsipeptide (5) in solution O. Emission spectra (A) and CD data (B). The molar ellipticity of the CD data is in units of deg  $\text{cm}^2/\text{dmol}$ . TEM images were collected on 20 mg/ml samples (C and D). ....136

Figure 3.20 Self-assembly of depsipeptide (5) in solution W. TEM images were collected on 10 mg/ml samples 18 hours (C) and 4 days (D) after dissolving in water. Fibers were observed in 5 mg/ml (E) and 20 mg/ml (F) samples after 4 days. Gels were observed after 3 weeks. ....138

Figure 3.21 The self-assembly of depsipeptide (5) at pH 7 is modeled by principles reported in  $\beta$ -sheet like peptides. Self-organization is driven by an electrostatic attraction involving both positively and negatively charged peptide molecules in short Fmoc-peptide families [39] (A). For depsipeptide (5), electrostatic attractions, stacking of the fluorenyl groups, and hydrogen bonding may result in the formation of nanofibers with  $\beta$ -sheet like superstructure (B). The fluorenyl groups of depsipeptide (5) are highlighted in pink (C) and upon folding into a fiber, are aligned in a helical manner. The modeled images from Fmoc-dipeptide families show similar self-assembling trends [21]. Used with permission.....141

Figure 3.22 Suggested self-assembling model for fiber of depsipeptide (5) at pH 3. The fluorenyl groups are stacked in a parallel fashion. The side chains have no modes of interaction with each other, as expected since the Asp charges are not exposed. It is likely that the rest of the molecule is exposed to the solvent, as illustrated by the bottle-like brush structure for a surfactant model [40], where the cylindrical core is aligned as an  $\alpha$ -helix and the red structures represent interactions with the solvent. Used with permission.....143

Figure 3.23 Emission spectra for depsipeptide (6) under various ionic concentrations. The samples were observed at pH 9 (A), pH 7 (B), and pH 3 (C) at 18 hours and 5 days. ....145

Figure 4.1 The Fmoc-FF/RGD hydrogel promotes cell adhesion with subsequent cell spreading and proliferation. The chemical structures Fmoc-RGD and Fmoc-RGE are provided (A). Cell adhesion and morphology in the Fmoc-FF/RGD and Fmoc-FF/RGE hydrogels (B). HDFa are well-spread in the Fmoc-FF/RGD hydrogels, and form a 3D cell network (B1), compared to the round morphology observed in the Fmoc-FF/RGE hydrogels (B2). The Fmoc-RGD concentration also influenced cell spreading, as hydrogels with 30–50% Fmoc-RGD shows over 90% cell spreading (C). Integrin blocking experiments (D) show that cells with unblocked  $\alpha 5\beta 1$  integrins spread and attach to RGD (D1), while cells with blocked  $\alpha 5\beta 1$  maintain rounded morphology (D2). Used with permission [3] .....157

## List of Schemes

- Scheme 2.1 Fmoc-depsidipeptide synthesis, where by a) Fmoc-peptide in DCM, DIC/DMAP, 0°C for 1 hr, 16 hours at room temperature. The sample was purified on a silica column in hexanes and ethyl acetate (67-82%); b) Pd/C in H<sub>2</sub> at 5 or 15 psi for up to 16 hours in dry methanol, and purified on a silica column in DCM and methanol (33-67%); c) Couple with Lac in DCM with DIPEA 0°C for 1 hour, then 16 hours at room temperature. Purification was attempted on a silica column in hexanes and ethyl acetate in combination with recrystallization. The synthesis of structures 1 [23] and 3 [22] have been described elsewhere.....26
- Scheme 2.2 Synthesis of oligodepsipeptides via standard Fmoc-SPPS methods. Coupling was achieved on a trityl chloride resin, whereby a) DIPEA (1 equiv) for 1.5 hours with mixing, followed by DMF and DCM washes; b) 20% piperidine in DMF for 5 minutes (x 3) followed by DMF and DCM washes; c) DIC (4 equiv) and DMAP (0.01 equiv) for 2 hours with mixing, followed by DMF and DCM washes; d) DIC (4 equiv) and Oxyma Pure (0.1 equiv) for 2 hours with mixing followed by DCM washes; e) mixing with cleaving cocktail (A: TFA/TIPS – 95/5; B: TFA/Water/TIPS – 95/2/3; C: TFA/DCM/TIPS – 95/2/3; D: TFA/DCM/TIPS – 50/48/2) for 3 hours followed by precipitation in cold ether or extraction in chloroform.....35



## Chapter 1. Peptide Mimics as Biomaterials

### 1.1 INTRODUCTION

Peptide-based biopolymers are a relatively new class of biomaterials, partly driven by our increasingly sophisticated understanding of protein structure and function. [1-3]. These next generation biomaterials are developed for a variety of applications, including tissue regeneration and drug delivery (Figure 1.1). Research on peptide-based materials for tissue engineering applications is devoted to synthesizing new materials from both natural and synthetic sources. Peptide-based materials possess the unique property of self-assembly, whereby the self-organization into higher ordered structures is influenced by the length, sequence, and composition of the chemical backbone within specific environmental conditions. In addition, the self-assembly and directed-assembly of peptides has been reported to yield functional biomaterials, as seen with leucine zipper-based materials, peptide amphiphiles,  $\beta$ -sheet forming ionic oligopeptides, and  $\beta$ -hairpin peptides. More details on the self-assembly of various peptide families will be provided in Chapter 3.

Peptide-based materials offer many potential advantages over synthetic materials. Short peptide motifs such as RGD, KNEED, YIGSR are ubiquitous ligands for cell receptors and mediate cellular behaviors such as attachment and spreading [4-7]. A table describing the 20 amino acids with their respective one letter and three letter symbols is provided (Table 1.1). Many peptide-based biomaterials are easily degraded by the body, thus making them desirable as drug delivery vehicles and tissue engineering scaffolds.

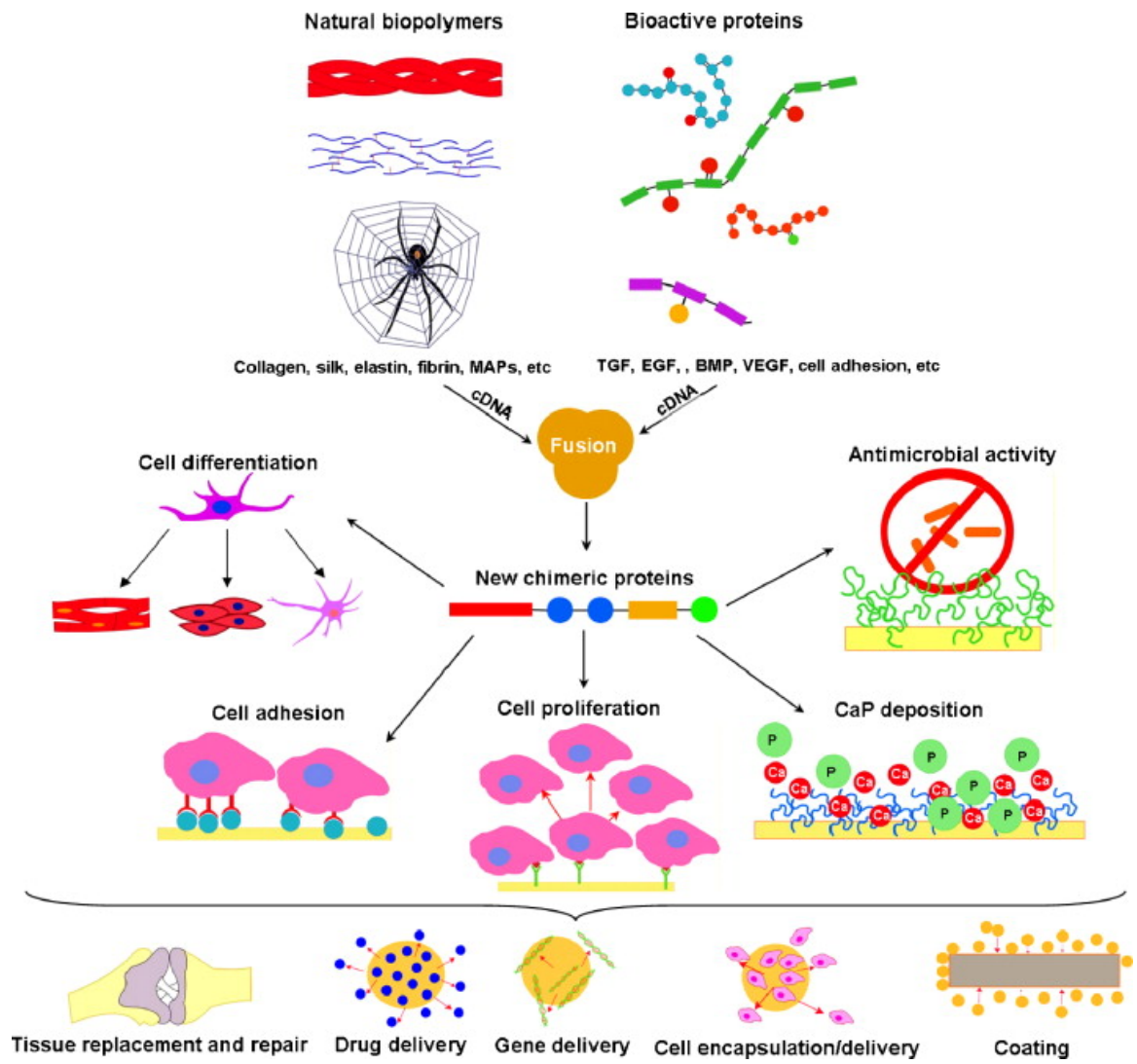


Figure 1.1 Unique features and potential applications of protein-based biomaterials. While the examples shown above are derived from recombinant DNA technology, the overall strategy of developing complex, functional, and biologically relevant materials can be applied to synthetically made peptide based systems. Used with permission. [3].

Amino acid	One letter symbol	Three letter symbol
Alanine	A	Ala
Arginine	R	Arg
Asparagine	N	Asn
Aspartic acid	D	Asp
Cysteine	C	Cys
Glutamic acid	E	Glu
Glutamine	Q	Gln
Glycine	G	Gly
Histidine	H	His
Isoleucine	I	Ile
Leucine	L	Leu
Lysine	K	Lys
Methionine	M	Met
Phenylalanine	F	Phe
Proline	P	Pro
Serine	S	Ser
Threonine	T	Thr
Tryptophan	W	Trp
Tyrosine	Y	Tyr
Valine	V	Val

Table 1.1. Abbreviations of the 20 common amino acids.

This chapter is intended to highlight the work of peptide mimics for their use in tissue engineering applications. Examples of naturally derived peptides based on elastin and silk will be discussed. Work on peptoids and  $\beta$ -peptides on tissue engineering applications will also be described in an effort to illustrate the self-assembling processes of peptide mimics with modified peptide backbones. The motivation to develop modified peptides with ester residues for the self-assembly of a hydrogel scaffold will also be described.

## **1.2 NATURALLY OCCURRING PEPTIDE MIMICS**

### **1.2.1 Elastin-like mimics**

Elastin-like polypeptide (ELP) based materials are an interesting family of peptides that have been investigated for self-assembly [1, 8]. Elastin is one of the most abundant extracellular matrix macromolecules, along with glycosaminoglycans (GAGs) and collagens, and it has the unique mechanical property of allowing repeated extension followed by elastic recoil. Elastin-like polypeptides are derived from the repeating motif, VPGXG, where X can be any amino acid other than proline [9]. Other derivatives of ELPs include KGGVG [10] and LGGVG [11] which both exhibit elastin-like properties despite substituting the first two residues of the peptide motif. The ability to synthesize an array of hydrogels with well-defined and varied properties allows these ELPs to be used in a wide range of applications. For example, ELPs have been shown to be ideal materials for cartilage scaffolds [12, 13]. Chondrocytes were encapsulated in ELP gel and maintained morphology and phenotype *in vitro* (Figure 1.2).

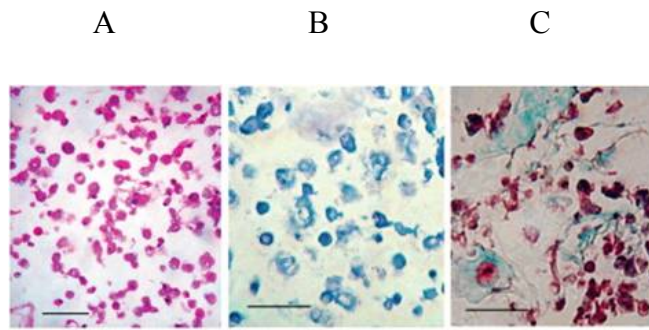


Figure 1.2 Histological section of ELP-chondrocyte constructs. Sections stained for: (A) cell morphology with H&E, S-GAG using toluidine blue (B), and collagen and extracellular matrix using Masson's trichrome (C). The scale bar is 50  $\mu\text{m}$ . Used with permission. [12]

After 15 days, the cells showed sulfated glycoaminoglycan (GAG) and collagen type II[12] production, and they also promoted the differentiation of human adipose-derived adult stem cells into chondrocytes [13]. Other applications of ELP hydrogels include small-diameter vascular grafts [14], urinary bladders [15], and stem cell sheets {Zhang, 2006 #818}.

### **1.2.2 Silk-like mimics**

Silk-like polymers (SLPs) aim to replicate the unique mechanical and physical properties of the natural protein. These features are in part due to its elastic properties exhibited by the presence of  $\alpha$ -helix and  $\beta$ -turns, as the strong intramolecular bonds within the folding regions are thought to be responsible for the stiffness of the fibers {Spohner, 2007 #822}.  $\beta$ -sheet peptide motifs have also been derived from silk ((GAGAGAS)<sub>m</sub>(GVGVP)<sub>n</sub>) [1, 16, 17], and modifications with peptide sequences or synthetic polymers do not alter functionality. For example, introducing polyethyleneglycol (PEG) [18] or polyethyleneoxide (PEO) and GAGA peptide sequences [19] within SLPs show that the native  $\beta$ -sheet structure was maintained. The relative ease of these modifications makes silk an ideal candidate for a range of tissue engineering applications, such as corneal regeneration [20], vascular grafts [21], bone regeneration [22], and drug delivery [23].

Peptide mimics based on naturally occurring proteins are synthesized through recombination techniques or with chemical methods. Recombinant DNA techniques have the advantages of high specificity in sequence, stereochemistry, and molecular weight [1], but are limited in how well the polypeptide of interest can be expressed. For

example, one of the main challenges in producing silk in large quantities is challenging due to the level of expression. The repeating gene sequence that codes for silk is not efficiently translated in *E. coli*, the most extensively used expression host.

### **1.3 PEPTIDOMIMETIC FAMILIES**

#### **1.3.1 Introduction**

The structure and function of peptide structures can be enhanced or mimics upon modification of the native peptide backbone [24]. Unlike the ELPs and SLPs discussed earlier, these classes of peptides are often extensions of the peptide structure or substitutions of the amide bond (Figure 1.3). Discussions of peptoids,  $\beta$ -peptides, and depsipeptides are presented with the motivation to use non-native polymer backbones in the development of self-assembling biomaterials.

#### **1.3.2 Peptoids**

Poly-N-substituted glycines, or peptoids, substitute functionality at the amide nitrogen. Peptoids have been reported for use as anti-cancer therapeutics [25] and lung surfactants [26]. An advantage of using peptoids, besides their resistance to proteomic enzymes [27], is that naturally occurring surfactants are expensive and vary batch to batch [26]. Peptoids have been reported to form helical secondary structures that are maintained among a family of structures [28]. Peptoid **1** [H-(NLys-Nspe-Nspe)<sub>4</sub>-NH<sub>2</sub>] is a 12-residue structure composed of Nspe and NLys, peptoid analogs of Phe and Lys respectively (Figure 1.4). When dissolved in 10 mM Tris buffer, the CD spectra reveals

$\alpha$ -helical structure, evident by the peak at 192 nm and 2 negative troughs at 206 and 220 nm.

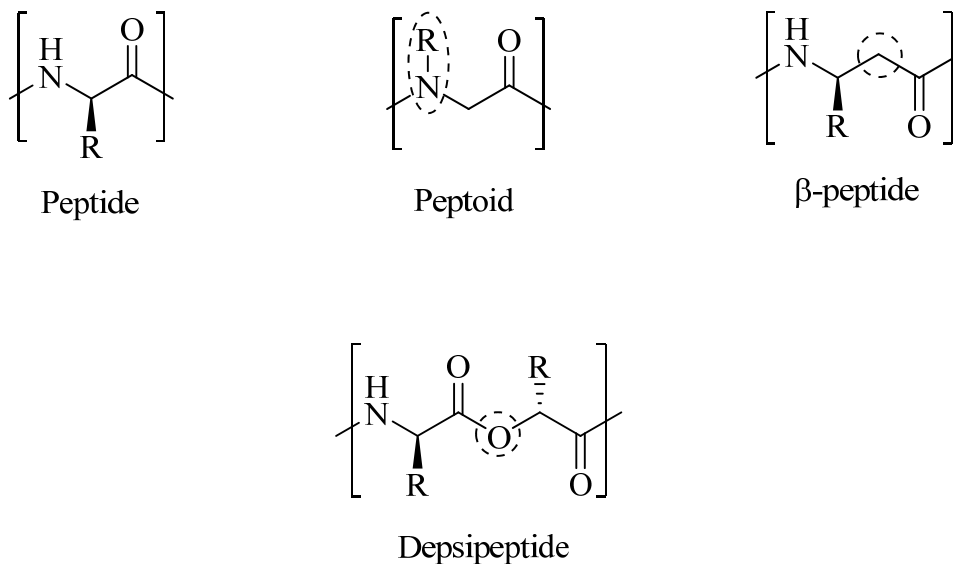


Figure 1.3 Chemical structures of peptidomimetic families. The structure of a native peptide backbone is provided for comparison.



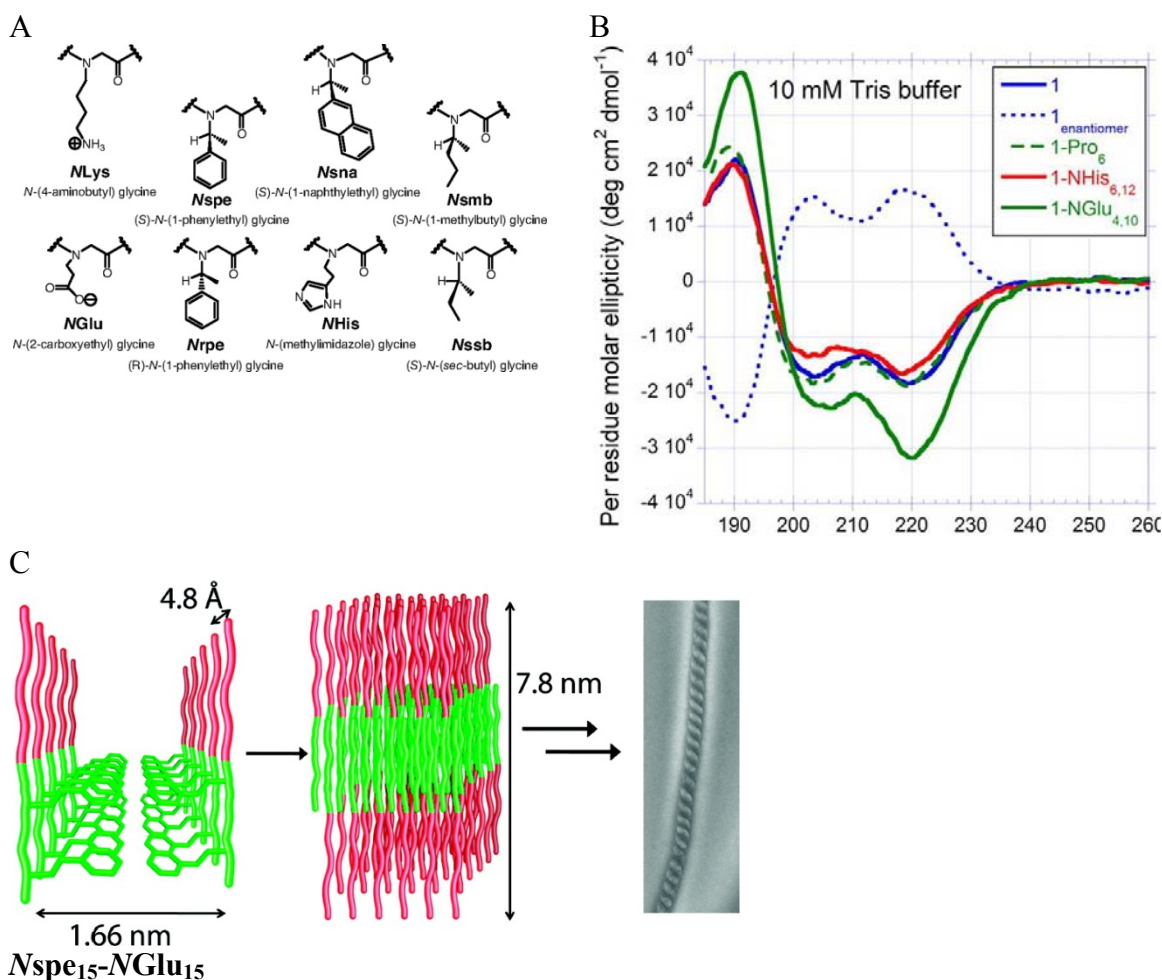


Figure 1.4 Secondary structure and self-assembly of peptoid families. The chemical structures of the peptoid residues are illustrated (A). CD of the tested peptoids (B) show that secondary folding is maintained despite changes to the backbone. Peptoid 1 is [H-(NLys-Nspe-Nspe)<sub>4</sub>-NH<sub>2</sub>] and is modified by substituting Pro at the 6 position (1-Pro<sub>6</sub>), NHis at the 6 and 12 position (1-NHis<sub>6,12</sub>), or NGlu at the 4 and 10 position (1-NGlu<sub>4,10</sub>) [28]. A model of the proposed self-assembly process for the peptoid Nspe<sub>15</sub>-NGlu<sub>15</sub> [29] (C). The hydrophobic and hydrophilic regions are represented in green and red respectively. The aromatic regions align with a distance of 1.66 nm while the distance between each chain is 4.8 Å. As self-assembly continues, the chains arrange into 2-D sheets with a height of 7.8 nm and become layered to form superhelices. Dimensions were verified with AFM and X-ray scattering. Both images used with permission.

Interestingly,  $\alpha$ -helical structure is maintained for all of the tested peptoids, including an enantiomeric analog. These results show that while peptoid backbones eliminate backbone chirality and hydrogen bonding, the formations of helical secondary structures through incorporations of bulky side chains are not hindered. [30, 31].

The supramolecular assembly of peptoids has also been reported [32-34]. The role of electrostatic and hydrogen bonding interactions in the hydrophilic block was found to be important in the self-assembly process of peptoid *Nspe<sub>15</sub>-NGlu<sub>15</sub>* (Figure 1.4A and C) [29]. Upon dissolution in water and analysis with scanning electron microscopy (SEM), atomic force microscopy (AFM), and X-ray scattering, sheet-like structures were observed within 24 hours and superhelical structures appeared after 4–7 days. A computational model suggests that during the self-assembling process, the sheets form a bilayer in which the hydrophobic groups are embedded in the interior of the sheet while the charged hydrophilic residues are exposed to the aqueous solution. These sheets are then layered within helices to form helical structures.

### 1.3.3 $\beta$ -peptides

$\beta$ -peptides are named such as the amino group is positioned at  $\beta$ -carbon.  $\beta$ -peptides have been reported to fold into a number of secondary formations [35-37] and display higher resistance to enzymatic degradation. For example, the  $\beta$ -peptide equivalent of Boc-(Val-Ala-Leu)<sub>2</sub>-OMe was characterized with CD, NMR, and X-ray crystallography to yield  $\beta$ -sheet-like or left-handed helices in solid or solution states respectively [38]. Interestingly, structural analysis of the native peptide shows the formation of random coils in solution. The  $\beta$ -peptide was stable to enzymatic

degradation at low pH for over 2 days, while the native peptide shows immediate cleaving.

## **1.4 DEVELOPING MIMICS WITH ESTER FUNCTIONALITY**

### **1.4.1 Depsipeptides for tissue engineering applications**

Depsipeptides are a class of peptides in which the chemical backbone is composed of ester and peptide bonds. Early work of synthetic depsipeptides have been reported in its polymer form as polydepsipeptides (PDPs) [39-54]. PDPs are unique, as they combine the synthetic characteristics of poly( $\alpha$ -hydroxy acids) and biological properties of polypeptides, such as tailored degradation rates[55] and protein structure[56] respectively. The chemical and biological properties of PDPs will be discussed in further detail in Chapters 2 and 3. Reports of detailed analysis of PDP secondary structure and subsequent self-assembly into higher order structures is scarce.

**The ability to control and maintain regular folding of a synthetic polymer is the first step towards engineering its biologic functionality, thus it is imperative to investigate to what extent the ester substitution affects the folding of depsipeptide structures.**

This project investigated short depsipeptides for their propensity to self-assemble into higher order structures. The desipeptide library was synthesized with solid phase methods with depsi-dipeptides as the coupling building block. Solid phase methods granted higher synthetic control of the total depsipeptide length and sequence, both of which would have been challenging with traditional polymerizations. The depsipeptides

were composed of hydrophilic and hydrophobic regions, motivated by the design of self-assembling peptides reported in the literature.

#### **1.4.2 Ease of synthesis**

The synthetic tools for peptide design have become widely available, allowing research groups to develop vast libraries of peptide structures. These developments are primarily due to the accessibility and optimization of solid phase peptide synthesis (SPPS). **Optimization of depsipeptide synthesis relied on the principles of SPPS, as each coupling step allows for complete control of the growing sequence.** The depsipeptides studied in this work were designed with alternating ester and peptide bonds, thus requiring the custom-development of depsi-dipeptides building blocks. The synthesis details are discussed in Chapter 2.

#### **1.4.3 Controlled degradation of depsipeptides for future applications**

Altering the peptide backbone with non-native substitutions can offer advantageous properties while preserving certain secondary folding characteristics. However, as seen with peptoids and  $\beta$ -peptides, these materials are often more resistant to degradation than their peptide counterparts. Depsipeptides have the ability to provide a more hydrolytically sensitive structure while maintaining secondary structure. The unique self-assembling processes of depsipeptides are discussed in Chapter 3.

Hydrolytic degradation of a mimetic biomaterial may have specific advantages for use in tissue engineering and specifically as an injectable, degradable hydrogel. Materials used for tissue engineering applications should be designed with rules that dictate their behavior under various conditions. In an effort to enhance the current library

of depsipeptides, synthetic methods to increase the overall hydrophobicity of the structure are provided in Chapter 4. *In vitro* and *in vivo* studies from other self-assembling peptide systems are also discussed to provide a template for future biocompatibility experiments and alternative applications.

## References

1. Chow, D., et al., *Peptide-based biopolymers in biomedicine and biotechnology*. Materials Science & Engineering R-Reports, 2008. **62**(4): p. 125-155.
2. Ratner, B.D. and S.J. Bryant, *Biomaterials: Where we have been and where we are going*. Annual Review of Biomedical Engineering, 2004. **6**: p. 41-75.
3. Gomes, S., et al., *Natural and genetically engineered proteins for tissue engineering*. Progress in Polymer Science, 2012. **37**(1): p. 1-17.
4. Deng, C., et al., *RGD peptide grafted biodegradable amphiphilic triblock copolymer poly(glutamic acid)-b-poly(L-lactide)-b-poly(glutamic acid): Synthesis and self-assembly*. Journal of Polymer Science Part a-Polymer Chemistry, 2007. **45**(15): p. 3218-3230.
5. Wong, J.Y., et al., *Identification and validation of a novel cell-recognition site (KNEED) on the 8th type III domain of fibronectin*. Biomaterials, 2002. **23**(18): p. 3865-3870.
6. Jun, H.-W. and J.L. West, *Modification of polyurethaneurea with PEG and YIGSR peptide to enhance endothelialization without platelet adhesion*. Journal of Biomedical Materials Research Part B: Applied Biomaterials, 2005. **72B**(1): p. 131-139.
7. Matsuda, A., et al., *Immobilization of laminin peptide in molecularly aligned chitosan by covalent bonding*. Biomaterials, 2005. **26**(15): p. 2273-2279.
8. Nettles, D.L., A. Chilkoti, and L.A. Setton, *Applications of elastin-like polypeptides in tissue engineering*. Advanced Drug Delivery Reviews, 2010. **62**(15): p. 1479-1485.
9. Urry, D.W., *Physical Chemistry of Biological Free Energy Transduction As Demonstrated by Elastic Protein-Based Polymers* The Journal of Physical Chemistry B, 1997. **101**(51): p. 11007-11028.
10. Martino, M. and A.M. Tamburro, *Chemical synthesis of cross-linked poly(KGGVG), an elastin-like biopolymer*. Biopolymers, 2001. **59**(1): p. 29-37.
11. Martino, M., A. Coviello, and A.M. Tamburro, *Synthesis and structural characterization of poly(LGGVG), an elastin-like polypeptide*. International Journal of Biological Macromolecules, 2000. **27**(1): p. 59-64.
12. Betre, H., et al., *Characterization of a Genetically Engineered Elastin-like Polypeptide for Cartilaginous Tissue Repair*. Biomacromolecules, 2002. **3**(5): p. 910-916.

13. Betre, H., et al., *Chondrocytic differentiation of human adipose-derived adult stem cells in elastin-like polypeptide*. *Biomaterials*, 2006. **27**(1): p. 91-99.
14. Heilshorn, S.C., J.C. Liu, and D.A. Tirrell, *Cell-binding domain context affects cell behavior on engineered proteins*. *Biomacromolecules*, 2005. **6**(1): p. 318-323.
15. Caves, J.M., et al., *Elastin-like protein matrix reinforced with collagen microfibers for soft tissue repair*. *Biomaterials*, 2011. **32**(23): p. 5371-5379.
16. Loo, Y., S.G. Zhang, and C.A.E. Hauser, *From short peptides to nanofibers to macromolecular assemblies in biomedicine*. *Biotechnology Advances*, 2012. **30**(3): p. 593-603.
17. Vandermeulen, G.W.M. and H.A. Klok, *Peptide/protein hybrid materials: Enhanced control of structure and improved performance through conjugation of biological and synthetic polymers*. *Macromolecular Bioscience*, 2004. **4**(4): p. 383-398.
18. Rathore, O. and D.Y. Sogah, *Self-Assembly of Beta-Sheets into Nanostructures by Poly(alanine) Segments Incorporated in Multiblock Copolymers Inspired by Spider Silk*. *Journal of the American Chemical Society*, 2001. **123**(22): p. 5231-5239.
19. Rathore, O. and D.Y. Sogah, *Nanostructure Formation through Beta-Sheet Self-Assembly in Silk-Based Materials*. *Macromolecules*, 2001. **34**(5): p. 1477-1486.
20. Lawrence, B.D., et al., *Silk film biomaterials for cornea tissue engineering*. *Biomaterials*, 2009. **30**(7): p. 1299-1308.
21. Soffer, L., et al., *Silk-based electrospun tubular scaffolds for tissue-engineered vascular grafts*. *Journal of Biomaterials Science, Polymer Edition*, 2008. **19**(5): p. 653-664.
22. Zhou, J., et al., *Electrospinning of silk fibroin and collagen for vascular tissue engineering*. *International Journal of Biological Macromolecules*, 2010. **47**(4): p. 514-519.
23. Lammel, A.S., et al., *Controlling silk fibroin particle features for drug delivery*. *Biomaterials*, 2010. **31**(16): p. 4583-4591.
24. Rotem, S. and A. Mor, *Antimicrobial peptide mimics for improved therapeutic properties*. *Biochimica Et Biophysica Acta-Biomembranes*, 2009. **1788**(8): p. 1582-1592.
25. Bouget, K., et al., *Hydrazino-aza and N-azapeptoids with therapeutic potential as anticancer agents*. *Bioorganic & Medicinal Chemistry*, 2003. **11**(23): p. 4881-4889.
26. Brown, N.J., J. Johansson, and A.E. Barron, *Biomimicry of Surfactant Protein C*. *Accounts of Chemical Research*, 2008. **41**(10): p. 1409-1417.

27. Miller, S.M., et al., *Proteolytic studies of homologous peptide and N-substituted glycine peptoid oligomers*. Bioorganic & Medicinal Chemistry Letters, 1994. **4**(22): p. 2657-2662.
28. Chongsiriwatana, N.P., et al., *Peptoids that mimic the structure, function, and mechanism of helical antimicrobial peptides*. Proceedings of the National Academy of Sciences, 2008. **105**(8): p. 2794-2799.
29. Murnen, H.K., et al., *Hierarchical Self-Assembly of a Biomimetic Diblock Copolypeptoid into Homochiral Superhelices*. Journal of the American Chemical Society, 2010. **132**(45): p. 16112-16119.
30. Wu, C.W., et al., *Peptoid Oligomers with  $\alpha$ -Chiral, Aromatic Side Chains: Sequence Requirements for the Formation of Stable Peptoid Helices*. Journal of the American Chemical Society, 2001. **123**(28): p. 6778-6784.
31. Wu, C.W., et al., *Structural and Spectroscopic Studies of Peptoid Oligomers with  $\hat{I}$ -Chiral Aliphatic Side Chains*. Journal of the American Chemical Society, 2003. **125**(44): p. 13525-13530.
32. Zhang, D.H., et al., *Polypeptoid Materials: Current Status and Future Perspectives*. Macromolecules, 2012. **45**(15): p. 5833-5841.
33. Sanii, B., et al., *Shaken, Not Stirred: Collapsing a Peptoid Monolayer To Produce Free-Floating, Stable Nanosheets*. Journal of the American Chemical Society, 2011. **133**(51): p. 20808-20815.
34. Kudirka, R., et al., *Folding of a single-chain, information-rich polypeptoid sequence into a highly ordered nanosheet*. Peptide Science, 2011. **96**(5): p. 586-595.
35. Hamuro, Y., J.P. Schneider, and W.F. DeGrado, *De Novo Design of Antibacterial  $\hat{I}$ -Peptides*. Journal of the American Chemical Society, 1999. **121**(51): p. 12200-12201.
36. Godballe, T., et al., *Antimicrobial  $\beta$ -Peptides and  $\alpha$ -Peptoids*. Chemical Biology & Drug Design, 2011. **77**(2): p. 107-116.
37. Deshmukh, R. and H.J. Purohit, *Peptide Scaffolds: Flexible Molecular Structures With Diverse Therapeutic Potentials*. International Journal of Peptide Research and Therapeutics, 2012. **18**(2): p. 125-143.
38. Seebach, D., et al.,  *$\beta$ -Peptides: Synthesis by Arndt-Eistert homologation with concomitant peptide coupling. Structure determination by NMR and CD spectroscopy and by X-ray crystallography. Helical secondary structure of a  $\beta$ -hexapeptide in solution and its stability towards pepsin*. Helvetica Chimica Acta, 1996. **79**(4): p. 913-941.



39. Bezemer, J.M., et al., *Amphiphilic poly(ether ester amide) multiblock copolymers as biodegradable matrices for the controlled release of proteins*. Journal of Biomedical Materials Research, 2000. **52**(1): p. 8-17.
40. Goodman, M. and K.C. Stueben, *Peptide Syntheses Via Amino Acid Active Esters*. J. Am. Chem. Soc., 1959. **81**(15): p. 3980-3983.
41. Mathias, L.J., et al., *Polydepsipeptides .6. Synthesis of Sequential Polymers Containing Varying Ratios of L-Alanine and L-Lactic Acid*. Macromolecules, 1978. **11**(3): p. 534-539.
42. Ouchi, T., A. Hamada, and Y. Ohya, *Biodegradable microspheres having reactive groups prepared from L-lactic acid-depsipeptide copolymers*. Macromolecular Chemistry and Physics, 1999. **200**(2): p. 436-441.
43. Ouchi, T., et al., *Synthesis of biodegradable amphiphilic AB-type diblock copolymers of lactide and depsipeptide with pendant reactive groups*. Journal of Polymer Science Part a-Polymer Chemistry, 2002. **40**(9): p. 1218-1225.
44. Ouchi, T., et al., *Synthesis and enzymatic hydrolysis of lactic acid depsipeptide copolymers with functionalized pendant groups*. Journal of Polymer Science Part a-Polymer Chemistry, 1997. **35**(2): p. 377-383.
45. Ouchi, T., et al., *Synthesis and enzymatic hydrolysis of polydepsipeptides with functionalized pendant groups*. Macromolecular Chemistry and Physics, 1996. **197**(6): p. 1823-1833.
46. Ouchi, T. and Y. Ohya, *Design of lactide copolymers as biomaterials*. Journal of Polymer Science Part a-Polymer Chemistry, 2004. **42**(3): p. 453-462.
47. Ouchi, T., et al., *Preparation of poly[DL-lactide-co-glycolide]-based microspheres containing protein by use of amphiphilic diblock copolymers of depsipeptide and lactide having ionic pendant groups as biodegradable surfactants by W/O/W emulsion method*. Polymer, 2004. **45**(5): p. 1583-1589.
48. Ouchi, T., et al., *Synthesis of Poly[(Glycolic Acid)-Alt-(L-Aspartic Acid)] and Its Biodegradation Behavior in-Vitro*. Makromolekulare Chemie-Rapid Communications, 1993. **14**(12): p. 825-831.
49. Shalaby, W. and D.F. Koelmel, *Copolymers of p-dioxanone and 2,5-morpholinediones and surgical devices form therefrom having accelerated absorption characteristics*. 1984, Ethicon, Inc.
50. Stewart, F.H.C., *The synthesis and polymerization of peptide p-nitrophenyl esters*. Australian Journal of Chemistry, 1965. **18**(6): p. 887-901.
51. Stewart, F.H.C., *The preparation of some sequential polypeptides by the p-Nitrophenyl ester method*. Australian Journal of Chemistry, 1966. **19**(8): p. 1503-1509.

52. Stewart, F.H.C., *Formation of depsipeptide ester bonds by accelerated active ester coupling*. Chemistry and Industry, 1967. **46**: p. 1960-1961.
53. Stewart, F.H.C., *Pentamethylbenzyl esters of  $\alpha$ -hydroxy acids and their use in depsipeptide synthesis*. Australian Journal of Chemistry, 1968. **21**(5): p. 1327-1335.
54. Stewart, F.H.C., *Synthesis of polydepsipeptides with regularly repeating unit sequences* Australian Journal of Chemistry, 1969. **22**(6): p. 1291-1298.
55. Schakenraad, J.M., et al., *Invivo and Invitro Degradation of Glycine Dl-Lactic Acid Copolymers*. Journal of Biomedical Materials Research, 1989. **23**(11): p. 1271-1288.
56. Ingwall, R.T., et al., *Polydepsipeptides. 7. Conformational Analysis of Poly(L-alanyl-L-alanyl-L-lactic acid)*. 1978. p. 540-545.

## **Chapter 2. Synthesis of Alternating Depsipeptides: Incorporating Regular Esters into a Native Peptide Backbone through the Coupling of Depsi-dipeptide Building Blocks**

### **2.1 CHAPTER SUMMARY**

#### **2.1.1 Introduction**

The depsipeptides designed for this project have alternating esters and peptides and are intended for use as hydrogel scaffolds. The synthesis of depsipeptides has been reported in the literature, but little work has been focused on relatively short depsipeptide sequences with regular repeats of esters. Optimizing a methodology such as this will not only control the synthesis, but also offer control over maintaining or modifying physical and biological properties associated with the ester bond.

The sequences of these structures are designed to alternate with hydrophobic and hydrophilic residues, namely lactic acid and either lysine or aspartic acid residues respectively. The following work describes the solution and solid phase peptide synthesis to produce the depsi-dipeptides building blocks and final structures respectively. This section will begin with a general discussion of solid phase peptide synthesis to briefly describe the aspects that apply to the depsipeptide system, namely the coupling methods, deprotection conditions, and resin characteristics.

#### **2.1.2 Goals**

The focus of this chapter is the synthesis of a family of depsipeptides in moderate yields using both solution and solid phase chemistry. Self-assembly of the purified products will be discussed in the next chapter.

### **2.1.3 Approach**

Design principles of dipeptides, didepsipeptides, and oligopeptides reported in the literature were used for our methodology. Coupling was achieved with either DCC or DIC, and the solid phase synthesis proceeded with general Fmoc-peptide strategies. The peptides of interest were charged in nature, thus careful selection of protecting groups were maintained throughout all synthesis processes. Efforts were taken to prevent hydrolysis of the ester bond, both in the solution and solid phase methods.

### **2.1.4 Results**

Several strategies for the synthesis of the depsipeptide building block were investigated. First, the ester of the Fmoc-peptide was activated with either pentafluorophenol or benzotriazole under various coupling conditions. While the final depsidipeptide was achieved with these strategies, purification was difficult. Lactic acid was protected with benzyl chloride, and upon coupling with the Fmoc-peptide, a protection version of the depsi-dipeptide was synthesized. Upon removing the benzyl group with hydrogenolysis, the depsipeptide building blocks were purified with a silica column and characterized with NMR and MS.

The synthesis of depsipeptides proceeded with general Fmoc-peptide methods. The coupling methods and selection of cleaving cocktails were optimized to reduce the effect of hydrolysis on the ester moiety. Depsipeptides were synthesized using standard Fmoc-peptide synthesis and were characterized and purified by HPLC and LCMS.

## **2.2 BACKGROUND**

### **2.2.1 Polydepsipeptides: Challenges in Synthesis and Homopolymerizations**

Polydepsipeptides (PDPs) are a unique set of resorbable polymers that have been developed for biomedical engineering applications. PDPs incorporate esters within a peptide backbone and can be synthesized through ring-opening polymerizations (ROPs) of morpholine-2,5-diones (MDs). MDs are 6-membered cyclic structures with an oxygen and amine at the 1- and 4-position and carbonyl groups at the 2- and 5-position (Figure 2.1). Functionality of the MD is designed within the 3- and 6-positions and successful synthesis of PDP homopolymers is dependent on the bulkiness of the side chains. For simplicity, PDPs will be described first by the ester side chain followed by the peptide moiety. Poly(glycolic acid-Asp(OBzl)) was synthesized with 78% conversion [1] while homopolymers of poly(lactic acid-Asp(OBzl)), poly(lactic acid-Lys(Z)), and poly(lactic acid-Cys(OBzl)) gave low monomer conversion rates (36-57%) [2]. Isolating the PDP was also difficult due to steric hindrance of the peptide side chains.

Repeatability of PDP synthesis among different research groups was challenging for the poly(glycolic acid-alt-Asp(OBzl)), as Ouchi et al. synthesized this PDP with a molecular weight range of 2200-3280 g/mol [1] while Wang et al. achieved higher molecular weights of 5800-13500 g/mol [3]. These differences may be attributed to hydrogen bonding of the MD, which was recrystallized in different solvents.

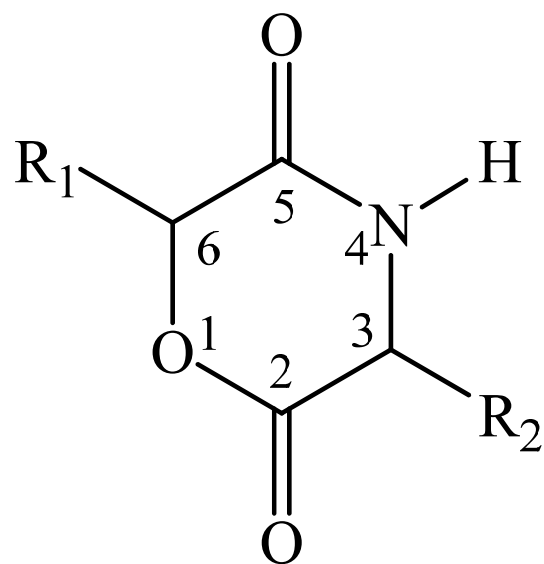


Figure 2.1 General chemical structure of a MD

Slight differences of the FTIR shift of the N-H region were observed, specifically 3196  $\text{cm}^{-1}$  for the higher molecular weight PDP and 3358  $\text{cm}^{-1}$  for the lower. The authors suggest that the monomer associated with the N-H stretch at the lower wavelength indicates a stronger hydrogen bond, which in turn affects the polymerization process to yield the PDP with higher molecular weights. Similarly, MDs of lactic acid and benzyl-protected aspartic acid recrystallized in ethyl acetate were successfully polymerized with a molecular weight range of 3200-4100 g/mol, while the same MD recrystallized in toluene did not polymerize [2, 4].

The yields of the MDs described above decrease with increasing functionality at the 3- and 6-positions (8-24.9%). Our group has successfully synthesized MDs with varying side chains using solid phase peptide synthesis [5]; however, forming the homopolymer of the PDP remains unsuccessful in terms of high yield and purification. The limitations of PDPs described above have been addressed with copolymerizations of polyesters and polypeptides [6-13]

In the case of developing a sequence of alternating esters and peptides of precise length and sequence, the synthesis of depsipeptides with less than 16 residues has been reported with general solid phase peptide chemistry methods. Kuilse et al. coupled  $\alpha$ -hydroxy acid protected lactic acid or mandelic acid to Boc-protected  $\alpha$ -amino acids on a Wang resin using diisocarbodiimide (DIC) and dimethylaminopyridine (DMAP) [14]. Spengler et al. devised a machine-assisted protocol for a family of depsipeptides based on a sequence of 26 residues with up to 6 ester substitutions [15]. The highest yields (30%) of the final product were seen with 1 or 2 ester substitutions, depending on the

depsipeptide sequence. Both bodies of work show that single and multiple esters are successfully incorporated into a peptide backbone without modification of traditional SPPS methods.

### **2.2.2 Solid Phase Peptide Synthesis**

Solid phase peptide synthesis (SPPS) has revolutionized peptide chemistry [16-18] partly due to the seminal work of Merrifield describing the assembly of peptides onto a solid phase in 1963 [19]. SPPS allows reactions to be carried out rapidly using an excess of the activated amino acid derivative, which is removed at the end of the reaction by simple washing operations. The synthesis steps can be performed in the same vessel without any transfer of materials, adding to the convenience of this method.

Commercially available resins are modified with appropriate handles, which enable anchoring of the protected C-terminal amino acid residue by the formation of ester or amide bonds. The first coupling step is one of the driving factors that influence the value of the final yield. To address this issue, pre-loaded, protected amino acids are available. Upon the first coupling to the resin, the chain grows from the C-terminus to the N-terminus as the protecting group is removed and coupled to another building block. This deprotection/coupling process is repeated until the desired sequence is obtained. In a final step, the peptide is released from the resin and, if applicable, the side chain protecting groups are removed simultaneously. Two main strategies are used for the temporary/permanent protecting groups: *N*-*tert*-butoxycarbonyl/benzyl (Boc/Bzl) or fluorenylmethyloxycarbonyl/*tert*-butyl ester (Fmoc/OtBu). For the Boc/Bzl strategy, both groups are acid labile with Boc removed by trifluoroacetic acid and Bzl removed by



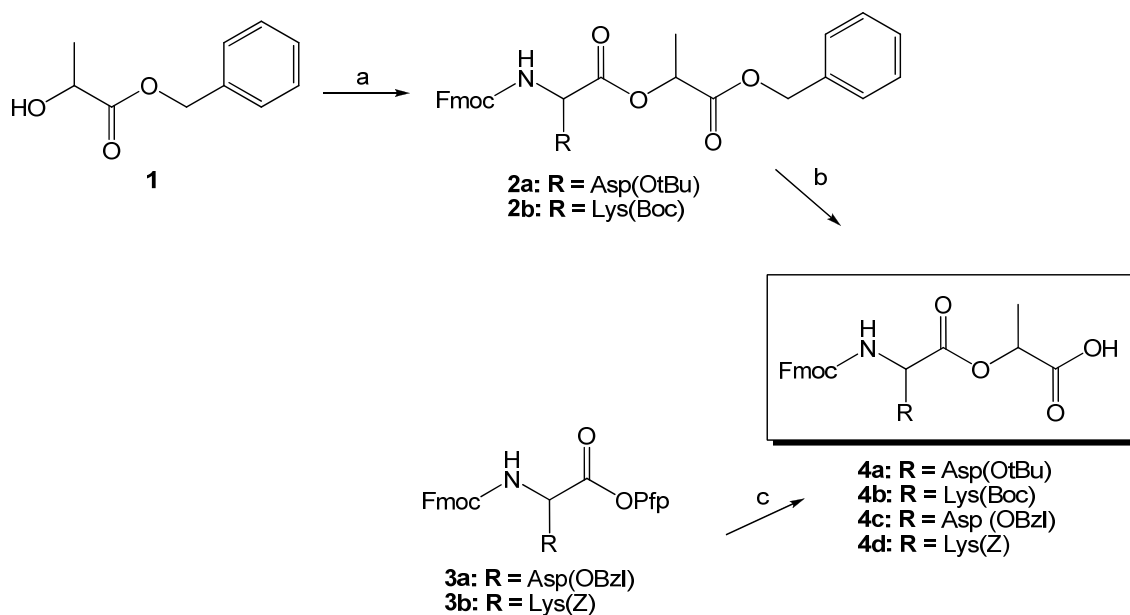
a stronger acid such as hydrofluoric acid. The Fmoc/OtBu method uses two different methods for removal, base or acid labile, respectively.

## **2.3 RESULTS**

### **2.3.1 Solution phase synthesis of Fmoc-depsidipeptides**

A general strategy towards the synthesis of depsipeptides includes the synthesis of unique building blocks and their incorporation into a peptide chain with common methods [20]. Design of the depsi-dipeptide building block must take into consideration the sensitivity of the ester bond and also the appropriate protecting strategies that will be used with SPPS as removal of base-labile groups has been shown to affect the stereochemistry of the ester bond [14, 21] while deprotection of acid-labile groups may hydrolyze the ester bond. Overall yield is also an important factor, as these materials would be used to couple using SPPS in a relatively high equivalence.

The initial synthesis of depsi-dipeptides was influenced by Fmoc-dipeptides with pentafluorophenol (Pfp)-activated esters [22] (Scheme 2.1). The synthesis and purification methods allowed for bulk synthesis in the absence of conditions that may affect the sensitivity of the ester bond. The esters of Fmoc-Lys(Z)-OH and Fmoc-Asp(OBzl)-OH were activated with Pfp and dicyclohexylcarbodiimide (DCC), recrystallized, and coupled to lactic acid (Lac) in dichloromethane (DCM). The coupling conditions were investigated with diisocarbodiimide (DIC) or diisopropylethylamine (DIPEA) in the presence or absence of the coupling agents dimethylaminopyridine (DMAP) or Oxyma Pure. The liquid chromatography and mass spectrometry (LC/MS) data show that the samples coupled with DIC were difficult to purify (Figure 2.2).



Scheme 2.1 Fmoc-depsidipeptide synthesis, where by a) Fmoc-peptide in DCM, DIC/DMAP, 0°C for 1 hr, 16 hours at room temperature. The sample was purified on a silica column in hexanes and ethyl acetate (67-82%); b) Pd/C in H<sub>2</sub> at 5 or 15 psi for up to 16 hours in dry methanol, and purified on a silica column in DCM and methanol (33-67%); c) Couple with Lac in DCM with DIPEA 0°C for 1 hour, then 16 hours at room temperature. Purification was attempted on a silica column in hexanes and ethyl acetate in combination with recrystallization. The synthesis of structures 1 [23] and 3 [22] have been described elsewhere.

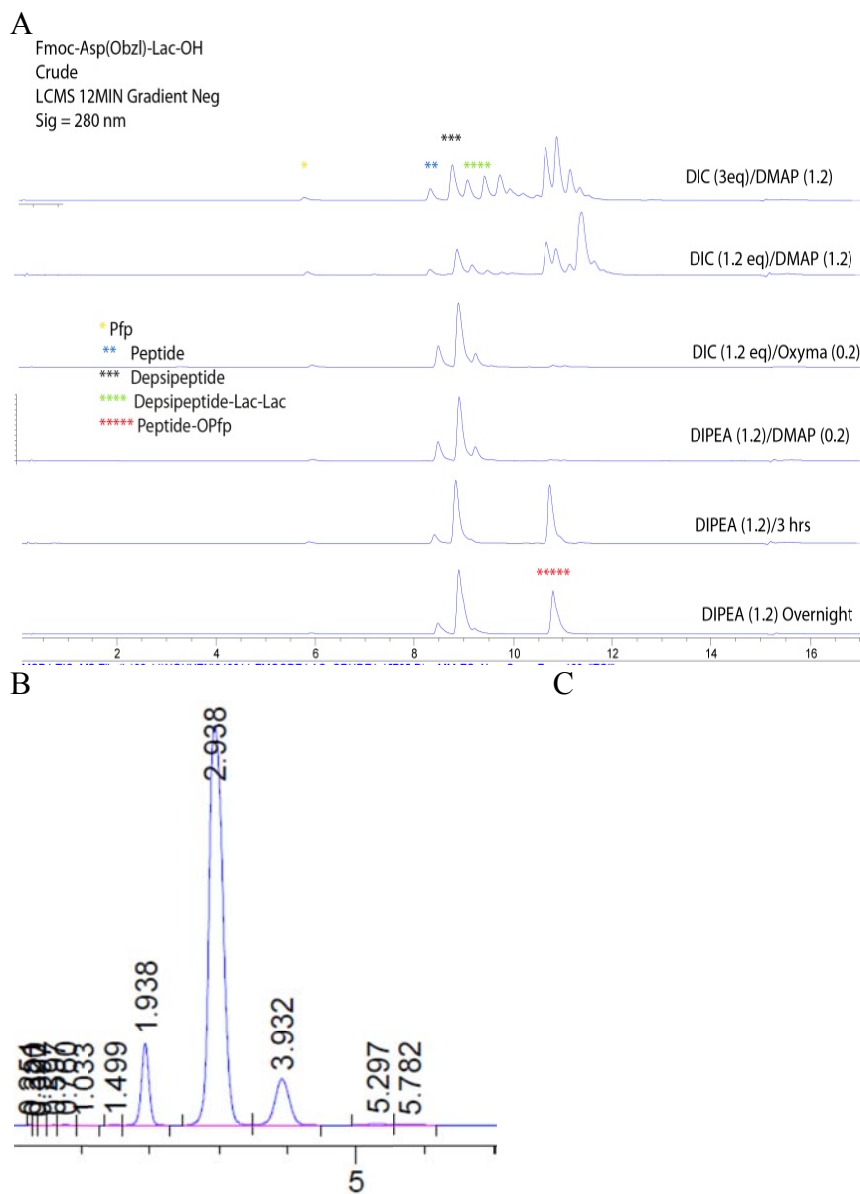


Figure 2.2 Synthesis of depsi-dipeptides using pentafluorophenol activated esters. LC/MS of the crude samples from depsipeptide coupling with Lac and Fmoc-Asp(OBzl)-OPfp under various conditions (A). Reacting with DIPEA overnight reduces the number of products with undesired lactic acid residues at the C-terminal. Purification of Fmoc-Lys(Z)-Lac-OH on a silica column shows that Fmoc-Lys(Z)-OH was not removed (B). Fmoc-Lys(Z)-Lac-Lac-OH was also present in this mixture, suggesting that the reaction time is sensitive to the formation of this undesired by-product. Chemical structures of the products in the mixture are provided (C).

Crude samples yielded structures with multiple lactic acid repeats at the C-terminal, i.e. Fmoc-Asp(OBzl)-Lac-Lac-OH and Fmoc-Asp(OBzl)-Lac-Lac-Lac-OH, and samples with DIC/DMAP and DIC/Oxyma Pure further increased the number of lactic acid repeats at the C-terminal. These by-products were not observed in DIPEA coupled samples, however the rate of conversion was relatively low.

The purification of Fmoc-Lys(Z)-OPfp was attempted on a silica column, however a significant amount of Fmoc-Lys(Z)-OH remained in all sample mixtures (Figure 2.2 B and C). Purification by recrystallization via vapor diffusion chamber in ethyl acetate or diethyl ether and hexanes was not successful. Alternative protection strategies to the Fmoc-peptides were examined. Benzotriazole (Bt) was coupled to the Fmoc-peptide with thionyl chloride in THF [24]. Upon multiple aqueous extractions and purification on a silica plug, Fmoc-Lys(Boc)-Bt was obtained with approximately 60% purity and 40% yield. Protecting with Bt has the advantage over the OPfp method in that excess peptide is not present. However, washing with aqueous HCl removes approximately 6% of the Boc protecting groups and excess Bt remains (Figure 2.3)

Protecting the ester moiety with a benzyl (Bn) group was another option in developing Fmoc-depsidipeptide building blocks. This method requires careful design of protection groups. N-terminal and side chain protecting groups must be unaffected upon final purification of the building block, as those ends will need to remain protected throughout SPPS. Thus, the cleaving method of the protecting group of the C-group of the depsidipeptide must neither affect the ester bond nor the other protecting groups.

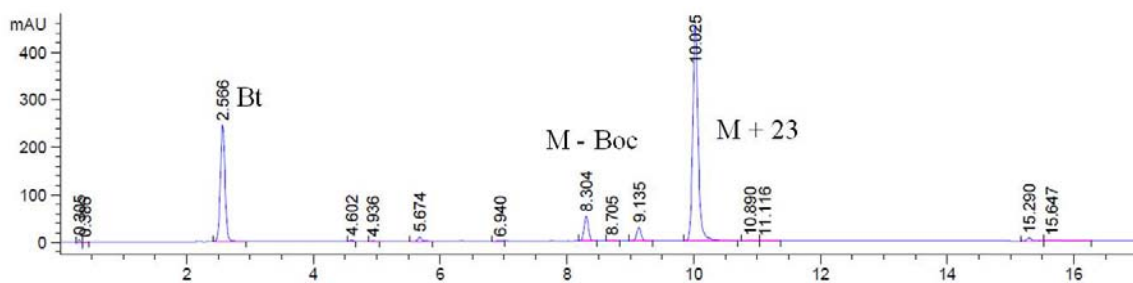


Figure 2.3 MS of Fmoc-Lys(Boc)-Bt. Bt refers to benzotriazole, M is the mass of interest, M – Boc is without the protecting group, and the mass addition of 23 is due to a sodium adduct.

The carbonyl group of Lac was initially investigated with benzyl chloroformate in pyridine [25]. Initial results show successful protection of Lac, however purification was difficult. The synthesis proceeded with benzyl chloride and lactic acid ethyl acetate with TEA [23]. The mixture was refluxed for 5 hours and purified via distillation. Pure Lac-Bn was synthesized and matched the proton nuclear magnetic resonance ( $^1\text{H-NMR}$ ) spectra as reported in the literature (Figure 2.4).

As stated earlier, coupling with Lac-Bn required a change to the original protection of the peptides used in the Pfp-activation methods. Excess Lac-Bn was coupled with Fmoc-Lys(Boc)-OH or Fmoc-Asp(OtBu)-OH in DCM with DIC and DMAP. The reactions were monitored by thin layer chromatography (TLC) and completed upon disappearance of the Fmoc-amino acid, as observed under UV. The samples were filtered to remove dicyclohexylurea, reduced under vacuum, and purified on silica in hexanes and ethyl acetate. The Bn group was removed in dry methanol with 10% palladium on activated carbon (Pd/C) under hydrogen gas ( $\text{H}_2$ ) and monitored with TLC. Hydrolysis products, specifically the Fmoc-amino acid, was evident in deprotections using commercial grade methanol, thus the absence of water is imperative for this step. The final depsi-dipeptide was purified on a silica column in DCM and methanol and was evaluated with  $^1\text{H-NMR}$  and LC/MS.

### **2.3.2 Optimizing SPPS protocols for the Synthesis of Depsipeptides**

A library of depsipeptides was synthesized from the depsi-dipeptide building blocks described in the previous section (Figure 2.5).

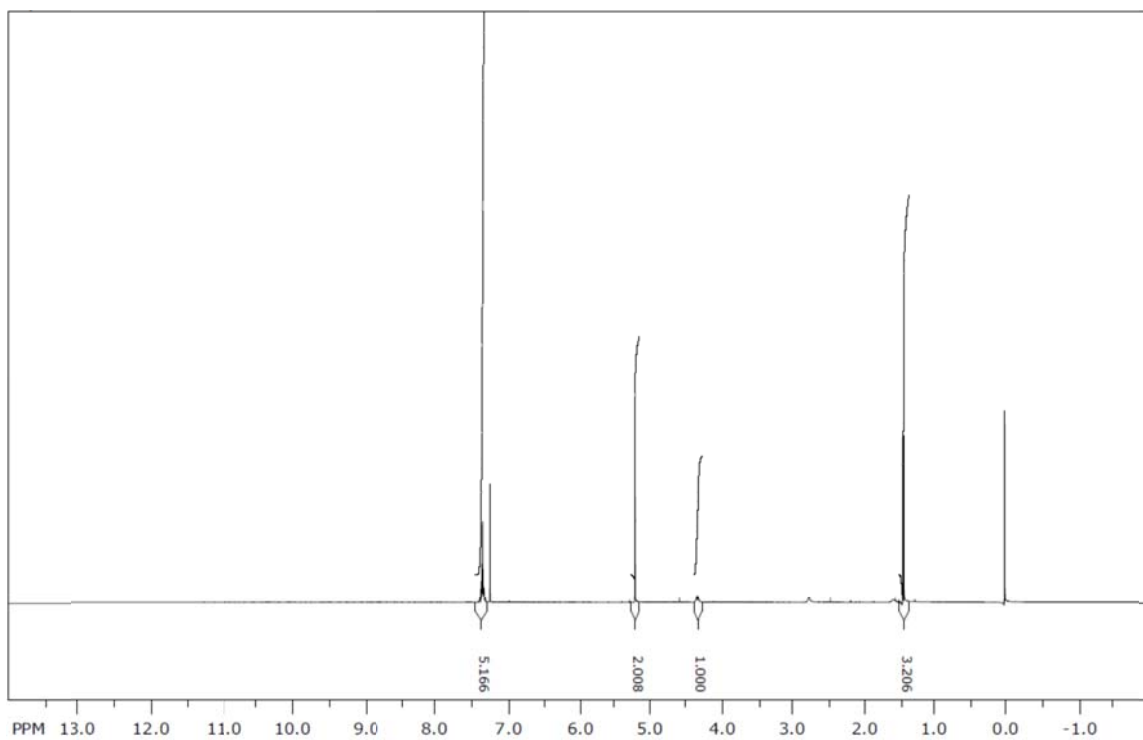


Figure 2.4 <sup>1</sup>H-NMR of Lac-Bn. Shifts correspond with data reported in literature [23]: 7.40-7.26 (m, 5H, benzene ring protons), 5.21 (s, 2H, PhCH<sub>2</sub>), 4.32 (q, 1H, COCH,  $J = 7.2$  Hz), 1.43 (d, 3H, CH<sub>3</sub>,  $J = 7.2$  Hz).

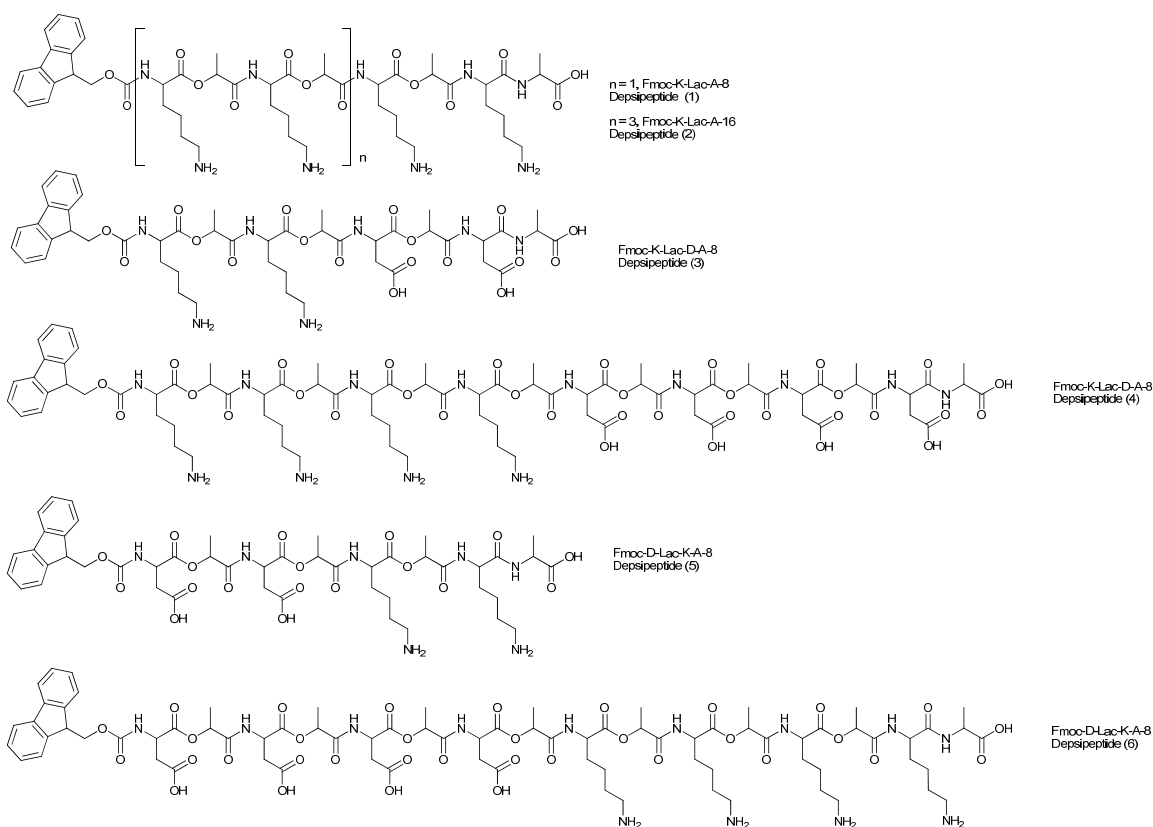


Figure 2.5 Depsipeptide library. These depsipeptides have been successfully purified with HPLC. The structures are named according to the presence of functional groups starting at the N-terminal. For example, depsipeptide 1 has alternating lysine (K) and Lac residues, with a total sequence of 8. Alanine (A) is terminal amino acid. Aspartic acid (D) is represented by its standard one letter code.



The depsipeptides investigated in this study incorporate alternating esters, thus a few conditions for SPPS must be determined. Optimization of these protocols proceeded with standard Fmoc strategies with ninhydrin monitoring. The target initial length of the depsipeptide was determined with segmented coupled SPPS (Figure 2.6A). It should be noted that the units used for coupling were not purified, which may affect the optimal length that could be achieved with this system.

The first steps of the synthesis were referenced from earlier work published on the synthesis of morpholine-diones [5]. Lac was coupled to a trityl-chloride resin with DIPEA, followed by coupling with Fmoc-amino acid and DIC/DMAP coupling and dried overnight. Three-fourths of the dried resin was transferred to a clean reaction vessel, cleaved off the resin, and used as the building block, S1. The remaining one-fourth of the depsipeptide was treated with 20% piperidine in DMF to remove the Fmoc group and coupled to S1 with DIC and Oxyma Pure. This process was repeated once, and MS of the crude samples revealed that the depsipeptide could be synthesized with 8 residues using this method. MS also shows a mass of 687, which may be excess S2 as fluorenyl groups are often cleaved due to the ionization process. The final yield of product with segmented coupling is very limiting, thus the synthesis of depsipeptides proceeded with linear growth (Scheme 2.2).

The ester group may be sensitive to the harsh solvents used with SPPS. Preliminary tests were conducted with crude samples of the depsi-dipeptide synthesized with Pfp-activated esters to ensure the Fmoc-depsipeptide was stable under general SPPS conditions.

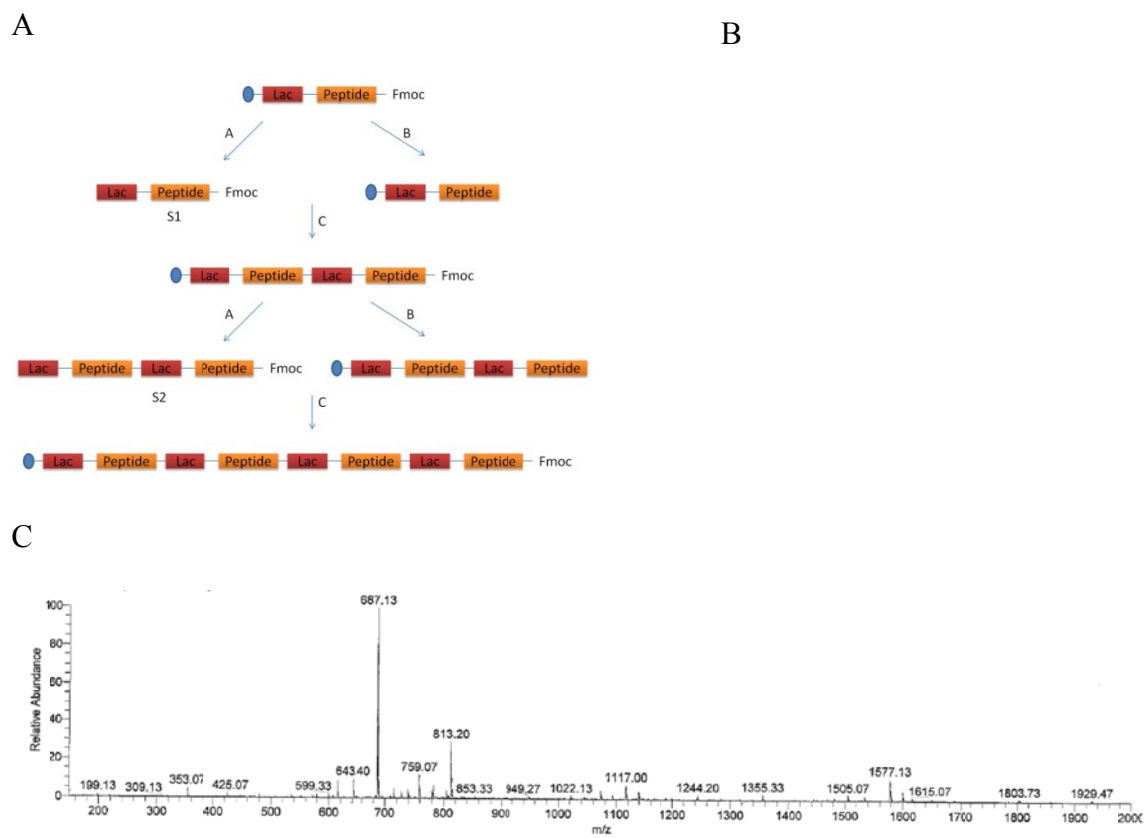
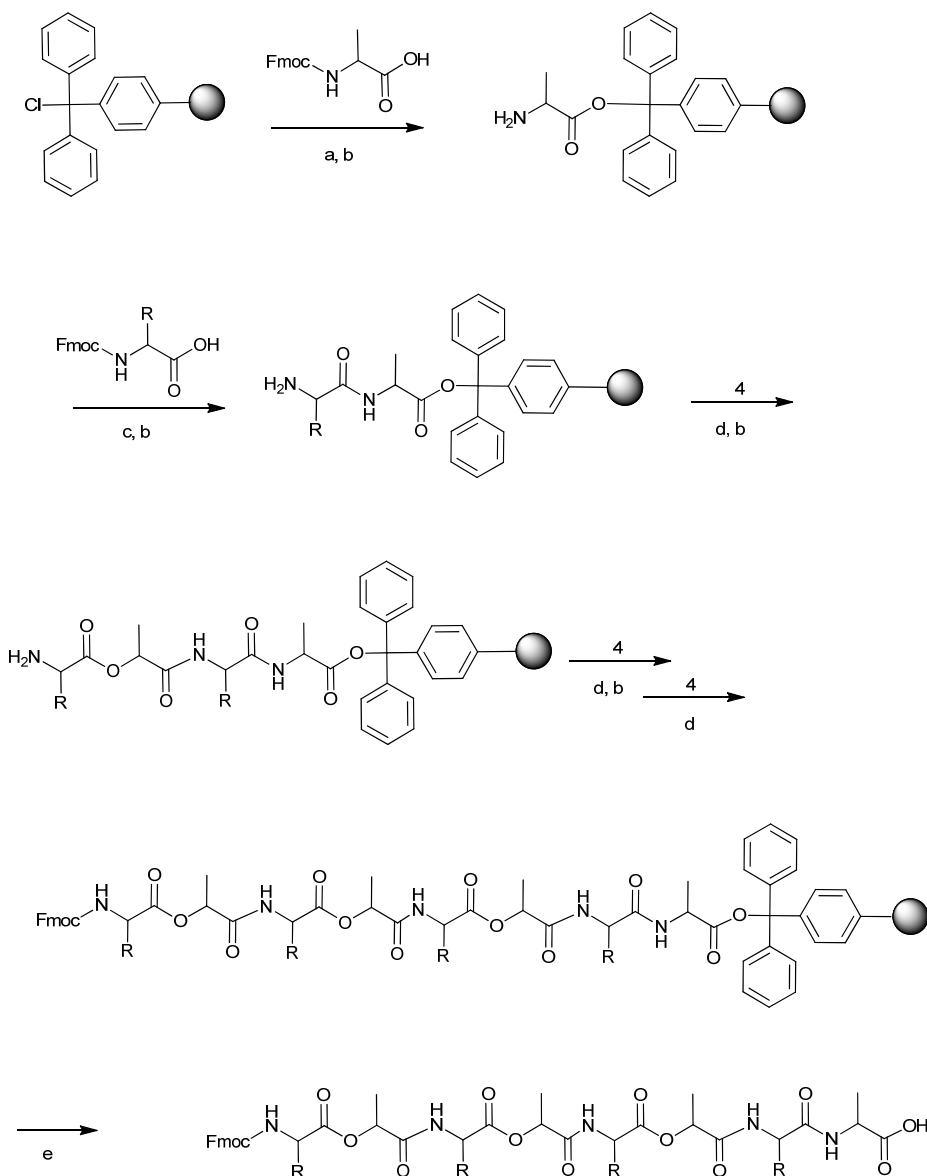


Figure 2.6 Schematic of segmented solid phase depsipeptide coupling (A) and MS of Fmoc-(Lys(Z)-Lac)<sub>4</sub> (C). Relevant chemical structures are provided (B).



**Scheme 2.2** Synthesis of oligodepsipeptides via standard Fmoc-SPPS methods. Coupling was achieved on a trityl chloride resin, whereby a) DIPEA (1 equiv) for 1.5 hours with mixing, followed by DMF and DCM washes; b) 20% piperidine in DMF for 5 minutes (x 3) followed by DMF and DCM washes; c) DIC (4 equiv) and DMAP (0.01 equiv) for 2 hours with mixing, followed by DMF and DCM washes; d) DIC (4 equiv) and Oxyma Pure (0.1 equiv) for 2 hours with mixing followed by DCM washes; e) mixing with cleaving cocktail (A: TFA/TIPS – 95/5; B: TFA/Water/TIPS – 95/2/3; C: TFA/DCM/TIPS – 95/2/3; D: TFA/DCM/TIPS – 50/48/2) for 3 hours followed by precipitation in cold ether or extraction in chloroform.

Tryl chloride resin was coupled with lactic acid with DIPEA, then subsequently coupled with Fmoc-Lys(Z)-OH or Fmoc-Asp(OBzl). After the washing and deprotection steps, the depsi-dipeptide was coupled/deprotected two additional times to obtain Fmoc-(Lys(Z)-Lac)<sub>6</sub> or Fmoc-(Asp(OBzl)-Lac)<sub>6</sub>.

The crude MS for Fmoc-(Asp(OBzl)-Lac)<sub>6</sub> shows a mass pertaining to the desired depsi-peptide as well as those with an additional mass unit of 72, which is indicative of additional Lac residues (Figure 2.7). Fragmented MS was used on Fmoc-(Lys(Z)-Lac)<sub>6</sub> to determine if the mass pattern was an aspect of fragmentation or if the ester bonds were hydrolyzed (Figure 2.8). This method is one way to monitor the ionization patterns that often occur with MS analysis. Before fragmentation, the dominating values from the crude sample are masses that pertain to Fmoc-(Lys(Z)-Lac)<sub>6</sub> and Fmoc-(Lys(Z)-Lac)<sub>4</sub>-Lys. The sample was isolated and ionized, resulting in ionization of the fluorenyl group to yield (Lys(Z)-Lac)<sub>6</sub>. The sample was again ionized to yield a mass of (Lys(Z)-Lac)<sub>4</sub>-Lys, which could pertain to ionization of the C-end ester or ionization of the fluorenyl group from Fmoc-(Lys(Z)-Lac)<sub>4</sub>-Lys. After the last ionization step, the dominating mass was of Fmoc-(Lys-Lac)<sub>6</sub>, resulting in ionization of the Z-group. These results suggest that the final sample consists of two different masses, Fmoc-(Lys(Z)-Lac)<sub>6</sub> and Fmoc-(Lys(Z)-Lac)<sub>4</sub>-Lys, with the latter being a deletion product as a result of the SPPS conditions. The fragmentation results also suggest that neither the end nor internal esters were ionized during the analysis. Replacing lactic acid with Fmoc-Ala-OH in the first coupling step facilitated the purification process, as fewer deletion products were detected in the crude MS samples (data not shown).

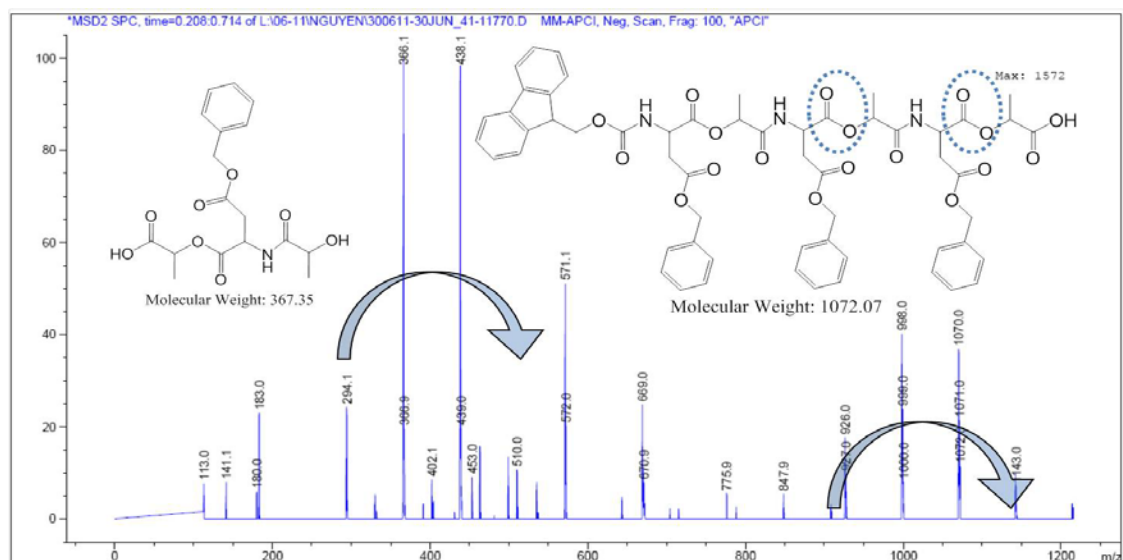
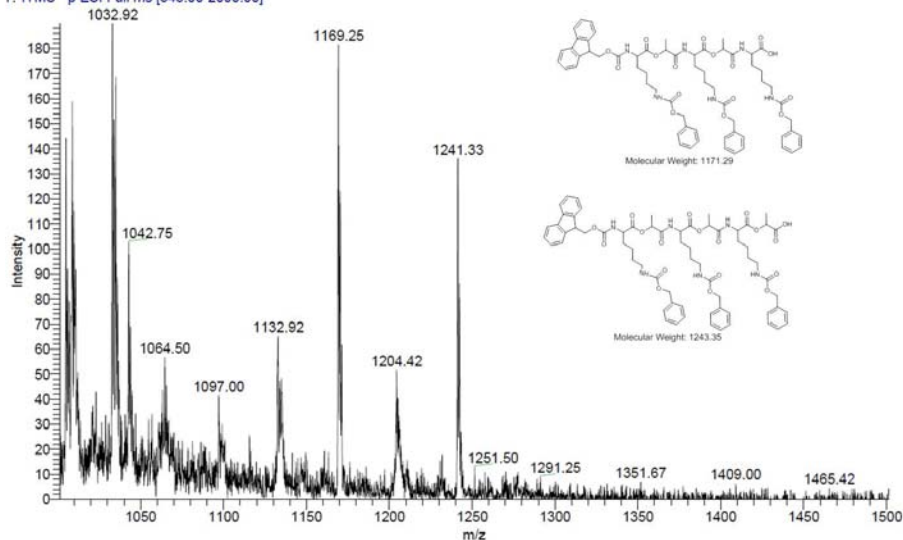


Figure 2.7 MS of crude Fmoc-(Asp(OBzl)-Lac)<sub>6</sub>. Arrows represent an increase of mass unit 72, which is equivalent to a Lac residue.

A

MSF1111-0114-iresneg1 #1-20 RT: 0.0001-0.0630 AV: 20 NL: 1.90E2  
 T: ITMS - p ESI Full ms [345.00-2000.00]



B

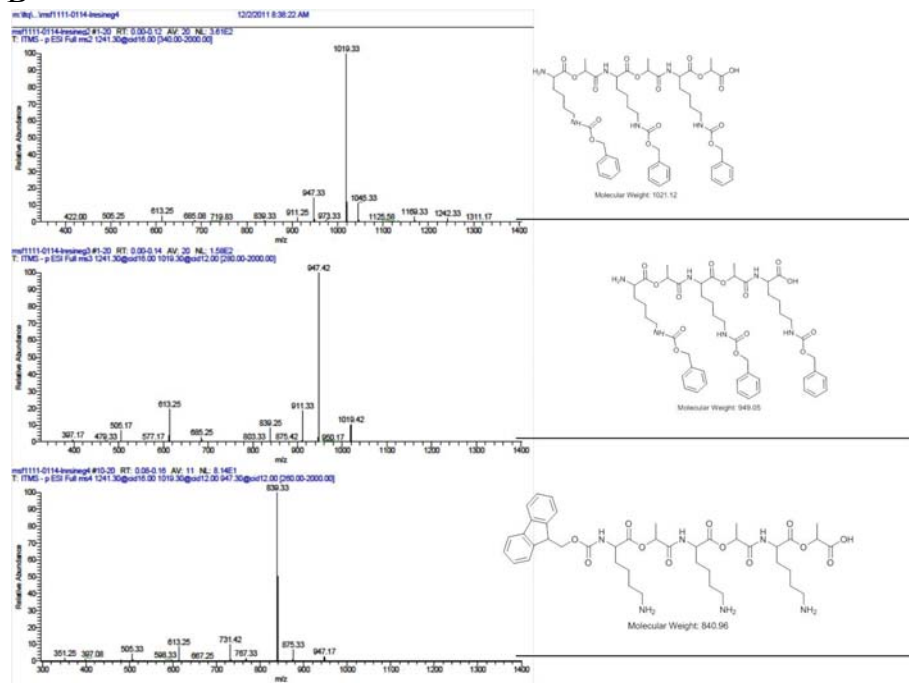


Figure 2.8 Fragmentation data of Fmoc-(Lys(Z)-Lac)<sub>6</sub>. Before fragmentation, the MS show masses associated with Fmoc-(Lys(Z)-Lac)<sub>6</sub> and Fmoc-(Lys(Z)-Lac)<sub>4</sub>-Lys (A). Masses are isolated and ionized to investigate the identity of fragmentation products (B)

SPPS of depsipeptides proceeded using Fmoc/OtBu strategies on a trityl-chloride resin. This new strategy required optimization of the cleaving cocktail, as higher acidic concentration is needed to simultaneously cleave the sequence off the resin and remove the Boc or OtBu protecting groups without hydrolyzing the ester bonds.

Four standard cleaving mixtures were tested on Fmoc-K-Lac-8 for 1 hour and show partial cleavage of the Boc-groups (Figures 2.9-2.12). The mixtures were composed of trifluoroacetic acid (TFA), dichloromethane (DCM), triisopropylsilane (TIPS), and/or water. Follow-up studies revealed that cocktails B and C completely removed the Boc groups after 2.5 hours (data not shown). Synthesis and cleavage of Fmoc-K-Lac-16 suggests that longer depsipeptide sequences are successfully synthesized with our method and the internal esters are not significantly affected by hydrolysis. Both Fmoc-D-Lac-8 and Fmoc-D-Lac-6 did not precipitate well in ether upon cleavage. The samples were extracted in chloroform prior purification attempts with HPLC. Purification was difficult and solubility characteristics varied batch to batch. Peptide sequences that contain the Asp residue commonly show the formation of lactam by-products, however attempts to identify this side reaction were not successful. Changes in a loss of oxygen, i.e. 16 mass units, would be expected for lactam formation, but this trend was not evident with MS. It is highly speculative that cyclization occurred, as both Asp-based depsipeptides were insoluble in water. It is interesting to note that despite the challenges of purifying Fmoc-D-Lac-8 or Fmoc-D-Lac-6, the addition of Lys to the sequences facilitates solubility, as seen with Fmoc-K-Lac-D-A-8 and Fmoc-K-Lac-D-A-16.

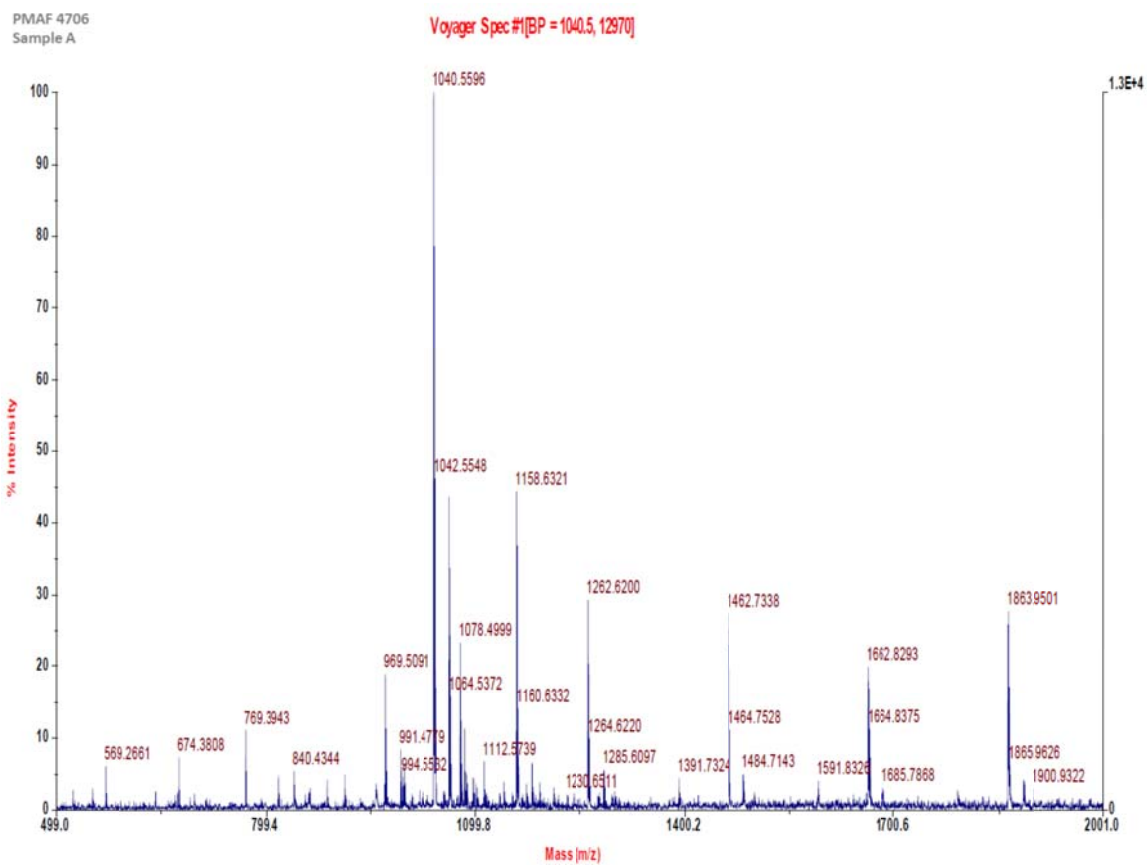


Figure 2.9 Cleaving cocktail A. Solution A was composed of 95/5 TFA and TIPS.



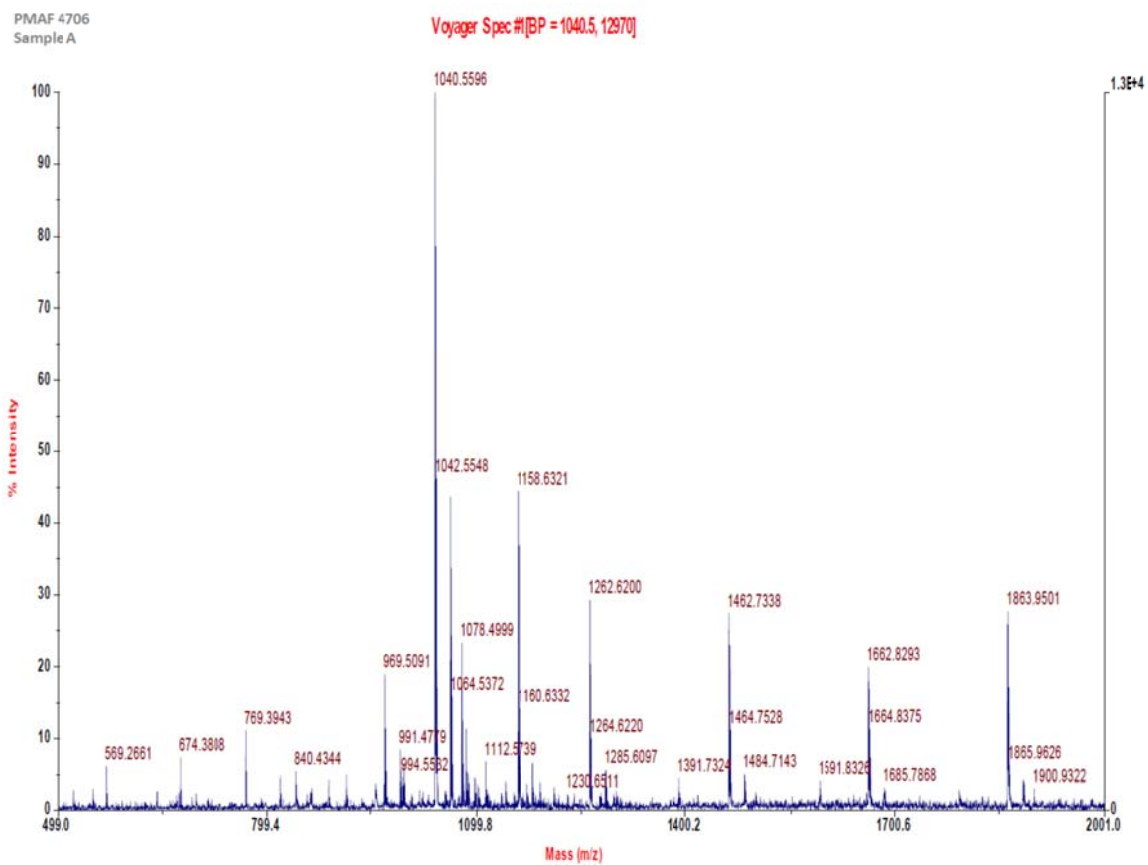


Figure 2.10 Cleaving cocktail B. Solution B was composed of 95/2/3 TFA/Water/TIPS

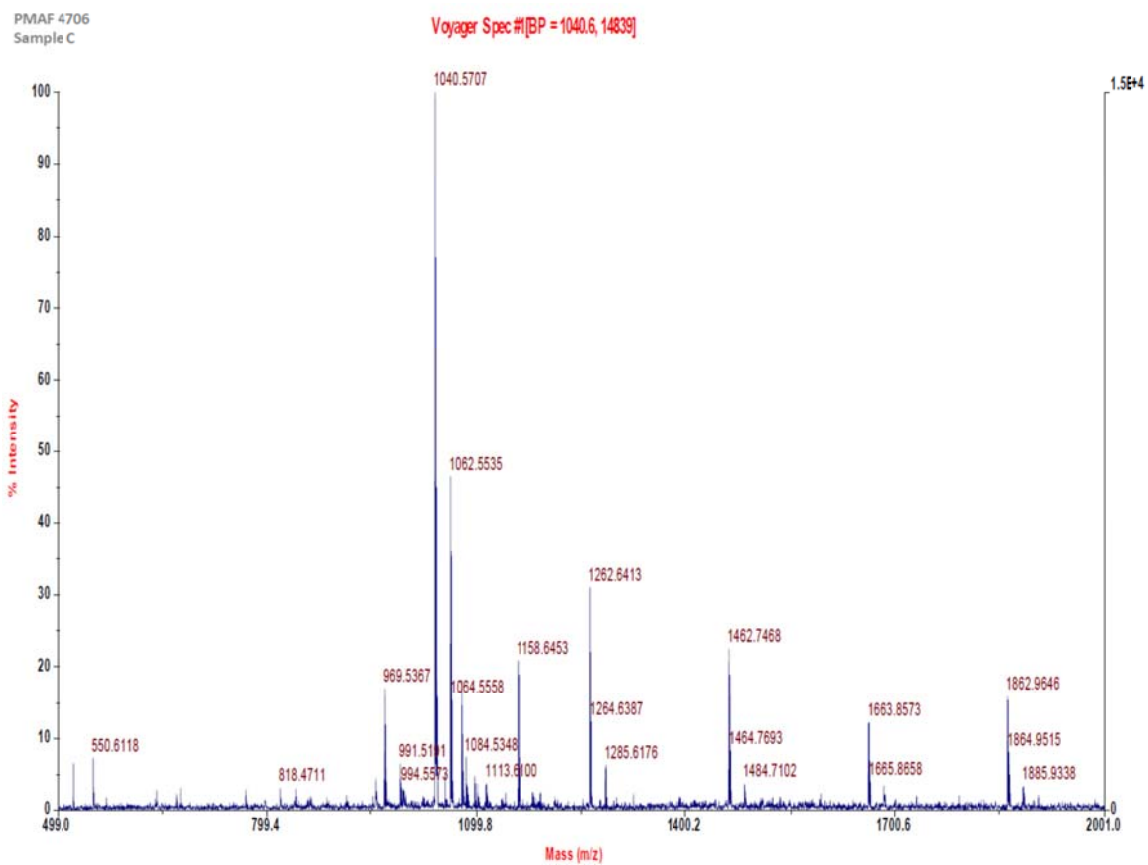


Figure 2.11 Cleaving cocktail C. Solution C was composed of 95/2/3 TFA/DCM/TIPS

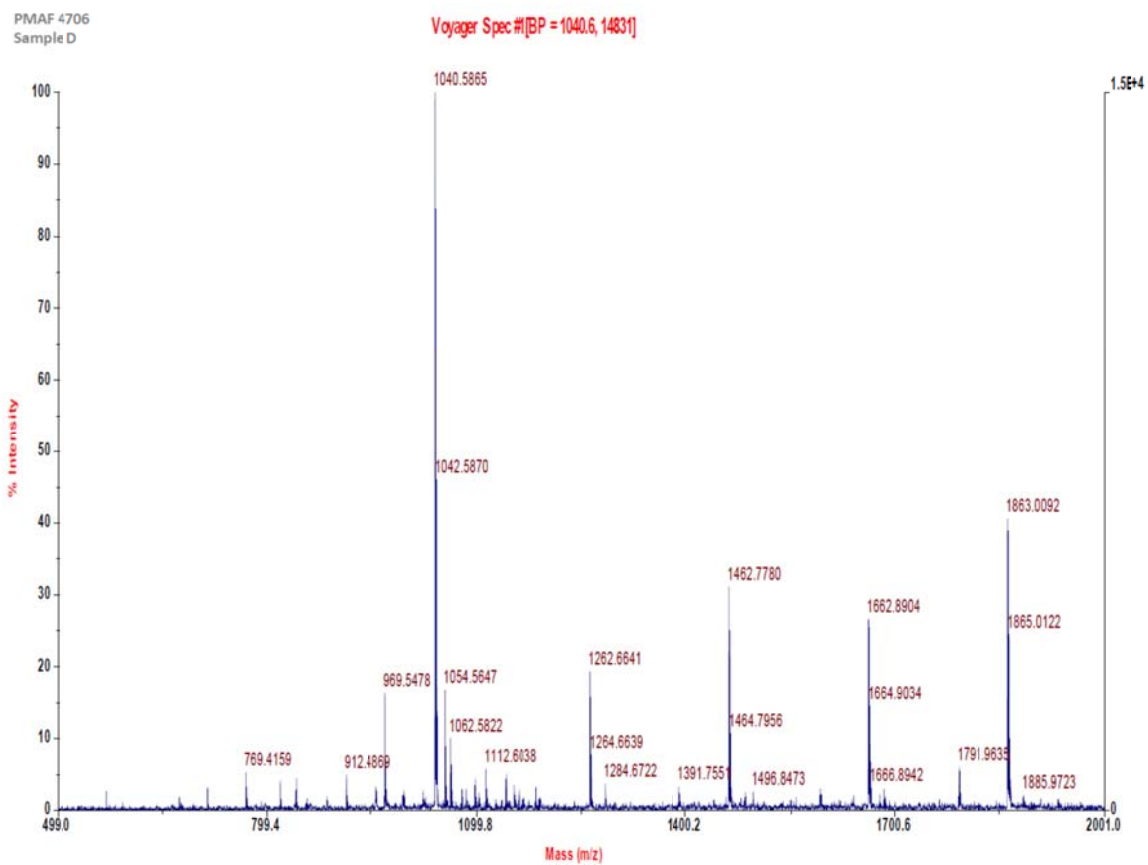


Figure 2.12 Cleaving cocktail D. Solution D was composed of 50/48/2 TFA/DCM/TIPS

The recovered yield of depsipeptides synthesized on the trityl chloride resin gave very low yields, thus a preloaded Fmoc-Ala-Wang resin was replaced by the trityl-chloride bead. The same strategies as stated above were utilized, with the exception of eliminating the first coupling step with Fmoc-Ala-OH. After purification with HPLC, the yield of Fmoc-K-Lac-8 increased from 4% to 36%. Fmoc-Ala-Wang resin was used for all other depsipeptides, showing additional evidence that our method can be used for a variety of depsipeptide sequences (Table 2.1) [26].

## 2.4 CONCLUSIONS

This chapter summarizes the design and synthesis of a family of depsipeptides to be further investigated for their ability to self-assemble into ordered hydrogels. The described methodology synthesized depsi-dipeptides in solution as building blocks for solid phase peptide synthesis. The solution methods gave relatively high yields, were repeatable, and did not disturb the stability of the ester bond. The building block was synthesized on the gram scale, which is ideal because of the relatively high coupling equivalences required for solid phase methods.

Solubility was affected by the sequences of the final depsipeptides. Depsipeptides designed with only Asp and Lac yield poor solubility and could not be purified, but both limitations were addressed upon the addition of adjacent Lys residues. The described work will be used in future studies to continue the development of novel depsipeptide structures.

Depsipeptide	Sequence	Gradient	Yield
Fmoc-K-Lac-8	Fmoc-Lys- <u>Lac</u> -Lys- <u>Lac</u> -Lys- <u>Lac</u> -Lys-Ala	28-30%	36%
Fmoc-K-Lac-16	Fmoc-Lys- <u>Lac</u> -Lys- <u>Lac</u> -Lys- <u>Lac</u> -Lys- <u>Lac</u> - Lys- <u>Lac</u> -Lys- <u>Lac</u> -Lys- <u>Lac</u> -Lys-Ala	25-26%	*2%
Fmoc-K-Lac-D-A-8	Fmoc-Lys- <u>Lac</u> -Lys- <u>Lac</u> -Asp- <u>Lac</u> -Asp-Ala	32-33%	*15%
Fmoc-K-Lac-D-A-16	Fmoc-Lys- <u>Lac</u> -Lys- <u>Lac</u> -Lys- <u>Lac</u> -Lys- <u>Lac</u> - Asp- <u>Lac</u> -Asp- <u>Lac</u> -Asp- <u>Lac</u> -Asp-Ala	35-37%	*3%
Fmoc-D-Lac-K-A-8	Fmoc-Asp- <u>Lac</u> -Asp- <u>Lac</u> -Lys- <u>Lac</u> -Lys-Ala	35-36.5%	52%
Fmoc-D-Lac-K-A-16	Fmoc-Asp- <u>Lac</u> -Asp- <u>Lac</u> -Asp- <u>Lac</u> -Asp- <u>Lac</u> -Lys- <u>Lac</u> -Lys- <u>Lac</u> -Lys- <u>Lac</u> -Lys-Ala	33-35%	*14%

Table 2.1 Depsipeptide purification details. Lactic acid is represented by Lac, and the gradient refers to the percentage of solvent B at which the depsipeptide was collected during HPLC. The yield was calculated from the equivalence value of the Fmoc-Ala-Wang resin which varied by lot, unless otherwise noted\*.

## 2.5 EXPERIMENTAL METHODS

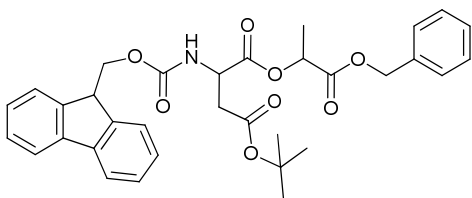
Abbreviations: Boc: tert-butyloxycarbonyl; OtBu: tert-butyl; Bn: benzyl; DCC, N,N'-Dicyclohexylcarbodiimide; DCM, dichloromethane; DMAP, 4-Dimethylaminopyridine; DMF, dimethylformamide; DIC, N,N'-Diisopropylcarbodiimide; DIPEA, N,N-diisopropylethylamine; Fmoc, 9-Fluorenylmethyloxycarbonyl; HPLC, high pressure liquid chromatography; Lac, lactic acid; Pd/C, palladium on carbon; Pfp, pentafluorophenol; TFA, trifluoroacetic acid; TIPS, triisopropylsilane. TFA, DCM, DMF, ethyl acetate, and diethyl ether were from Fisher Scientific. DIPEA, Pfp, and R-mandelic acid were from Acros Organics. Pd/C was purchased from Aldrich. Fmoc-amino acids, DMAP, and Oxyma Pure were purchased from EMD Biosciences. The side chain protecting groups were chosen as: Boc or Z for lysine and OtBu or OBzl for aspartic acid. Trityl chloride resin, Fmoc-Ala-Wang resin, and DIC were from Anaspec. Piperidine was from Alfa Aesar. L-lactic acid was from Biosynth.

Analytical thin layer chromatography (TLC) was performed on Whatman aluminum backed silica plates (UV<sub>254</sub>, 250 μm). Spots were visualized with UV light or a permanganate potassium stain. Column chromatography was performed manually on silica gel (230-400 mesh size, grade 60). <sup>1</sup>H-NMR, <sup>13</sup>C-NMR, and two dimensional spectra were obtained on a Varian 500 MHz and 500 MHz spectrometers. Chemical shifts are given in ppm with respect to internal standard TMS for <sup>1</sup>H-NMR and <sup>13</sup>C-NMR. Analytical HPLC was performed using an automatic HPLC system (Beckman System Gold) with an analytical reversed-phase column, an UV detector operating at 214 nm, at a

flow rate of 1 mL/min. A Vydac C18 column (300 Å, 5 µm, 3.1 x 150 mm) was used. Preparative HPLC was performed using a GE Biosciences AKTA 10 system on a Biorad HiPore RP C18 column (300 Å, 5 µm, 3.1 x 150 mm), and an UV detector operating at 214 nm or Biorad BioLogic DuoFlow on a Gemini C18 column (300 Å, 5 µm, 250 x 10mm) and a UV detector operating at 214 nm. The depsipeptides were characterized using liquid chromatography mass spectroscopy (LC-MS) and electrospray mass spectrometry (ESI-MS). They were performed on an Agilent 1200 series HPLC, an Agilent 6130 single quadrupole mass spectrometer or a Gemini column (C18, 55 µm, 2.1 x 50 mm), operating in a positive or negative ionization mode.

**General procedure for the removal of protecting groups for solid phase synthesis.** The Fmoc-protecting group was removed from the N-terminus with 20% piperidine in DMF. The solution was mixed for 5 minutes three times. The resin was washed with DMF. Cleavage of butyl-groups was investigated using the following cocktails: A: TFA/TIPS – 95/5; B: TFA/Water/TIPS – 95/2/3; C: TFA/DCM/TIPS – 95/2/3; D: TFA/DCM/TIPS – 50/48/2. The filtrate was precipitated into cold ether and purified with HPLC.

### Fmoc-Asp(OtBu)-Lac-Bn (3a)



Fmoc-Asp(OtBu)-OH (1.2 mmol) and Lac-Bn (1.0 mmol) was dissolved in DCM and placed on an ice bath. DIC (1.2 mmol) and DMAP (0.01 mmol) was added to the cold mixture and mixed for 1 hour. The reaction was stirred for 5 hours at room temperature and monitored by TLC. The solution was filtered and concentrated. The crude oil was purified on silica gel hexanes and ethyl acetate (67%).  $^1\text{H-NMR}$  (500 MHz,  $d_6$ -DMSO)  $\delta$  (ppm): 1.33-1.43 (m, 12H), 2.58 and 2.78 [dd,  $J = 4.76$ , 2H,  $\text{CH}_2\text{CH}_2\text{CO}$ ], 4.24 [t,  $J = 6.83$ , 1H,  $\text{CH}(\text{Fmoc})$ ], 4.34 [d,  $J = 6.66$ , 2H,  $\text{CH}_2(\text{Fmoc})$ ], 4.54 [m,  $J = 4.76$ , 1H,  $\text{NHCHCH}_2$ ], 7.32-7.44 (m, 9H), 7.70 [q,  $J = 7.07$ , 2H,  $\text{H}_{\text{Ar}}(\text{Fmoc})$ ], 7.89 [d,  $J = 7.51$ , 2H,  $\text{H}_{\text{Ar}}(\text{Fmoc})$ ], 7.96 [d,  $J = 8.24$ , 1H,  $\text{NH}$ ];  $^{13}\text{C-NMR}$  (125 MHz,  $d_6$ -DMSO)  $\delta$  (ppm): 170.77, 169.90, 168.75, 155.00, 143.74, 140.79, 135.50, 128.51, 128.26, 127.90, 127.87, 127.10, 125.18, 120.15, 80.63, 69.09, 66.44, 65.84, 50.43, 46.63, 36.81, 27.66, 16.59. MS (ESI+) calculated for  $\text{C}_{33}\text{H}_{35}\text{NO}_8$  [ $\text{M}^+ - \text{OtBu} - \text{H}$ ]: 517.53; found: 518.00



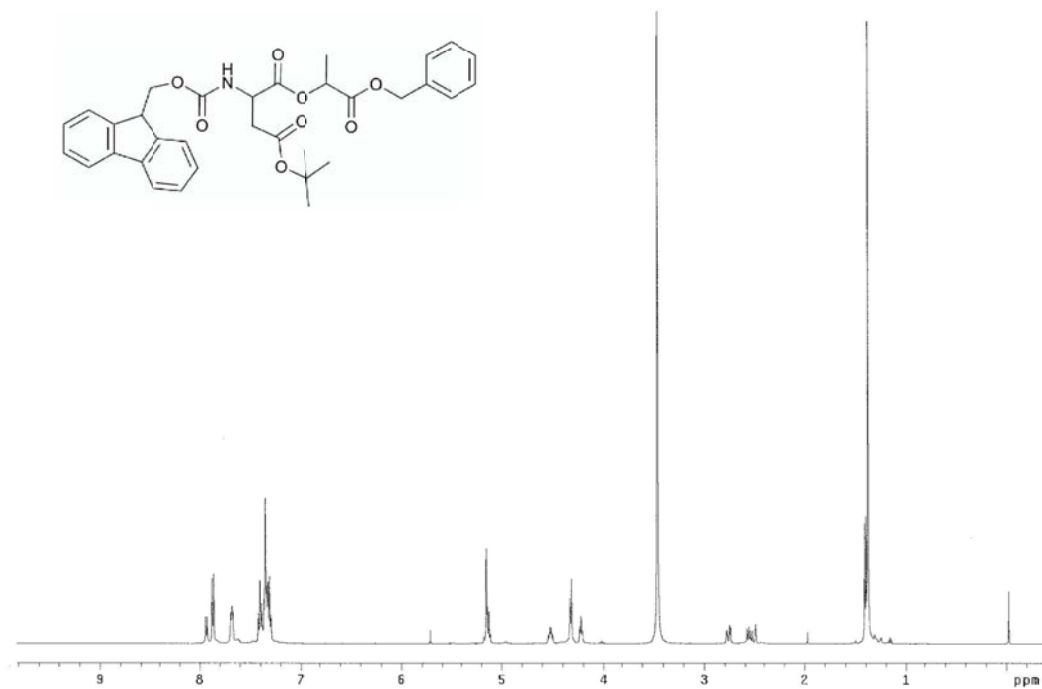


Figure 2.13  $^1\text{H-NMR}$  of Fmoc-Asp(OtBu)-Lac-Bn. Full scale.

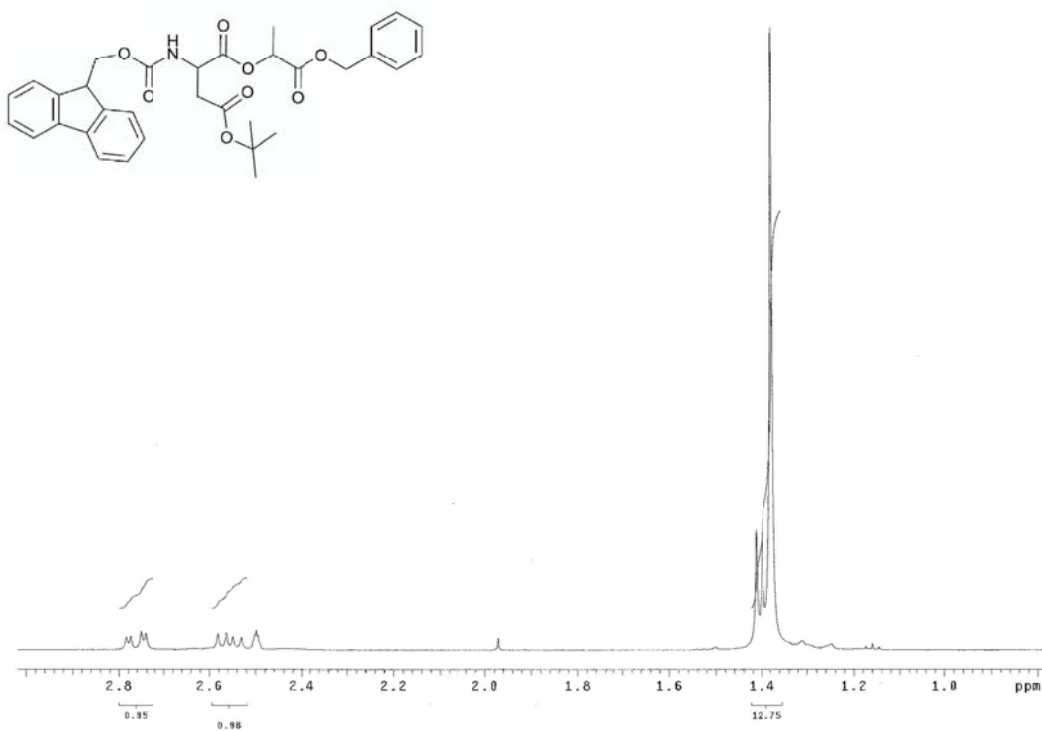


Figure 2.14 <sup>1</sup>H-NMR of Fmoc-Asp(OtBu)-Lac-Bn . Magnified from 1.0-2.8 ppm, with integrations.

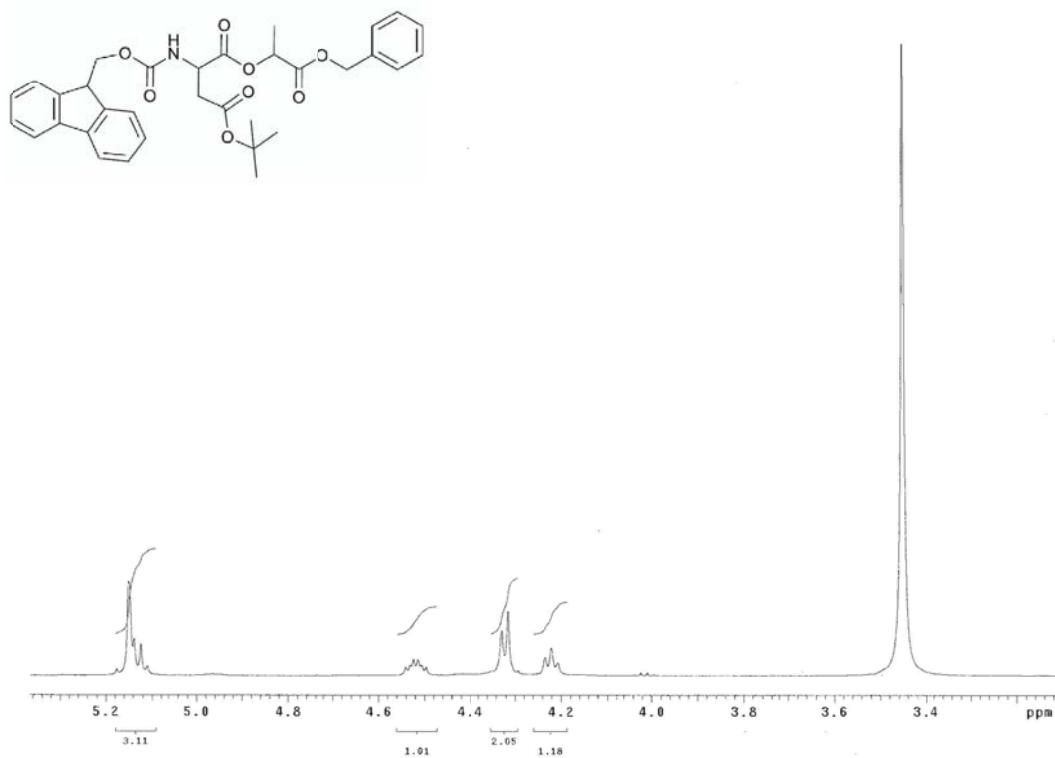


Figure 2.15 <sup>1</sup>H-NMR of Fmoc-Asp(OtBu)-Lac-Bn. Magnified from 3.4-5.2 ppm, with integrations.

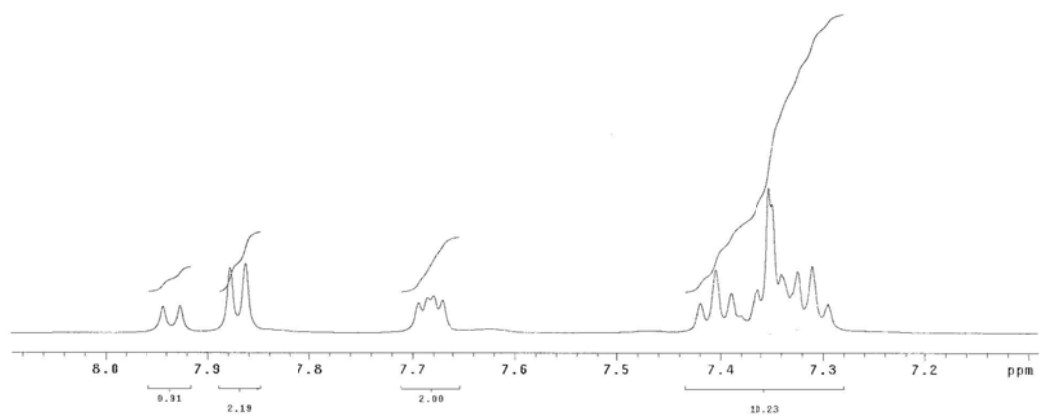
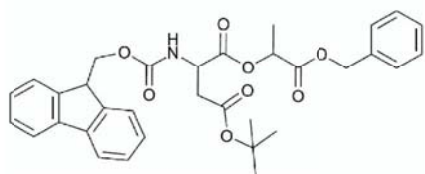


Figure 2.16  $^1\text{H-NMR}$  of Fmoc-Asp(OtBu)-Lac-Bn. Magnified from 7.2-8.0 ppm with integrations.

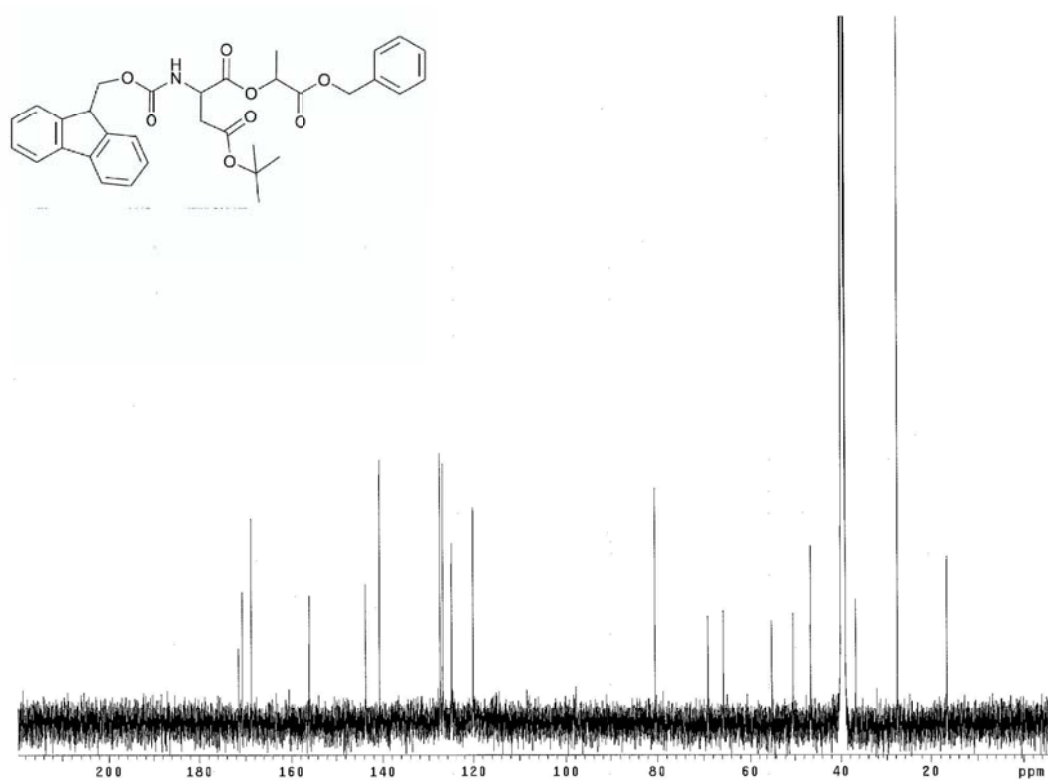


Figure 2.17  $^{13}\text{C}$ -NMR of Fmoc-Asp(OtBu)-Lac-Bn.

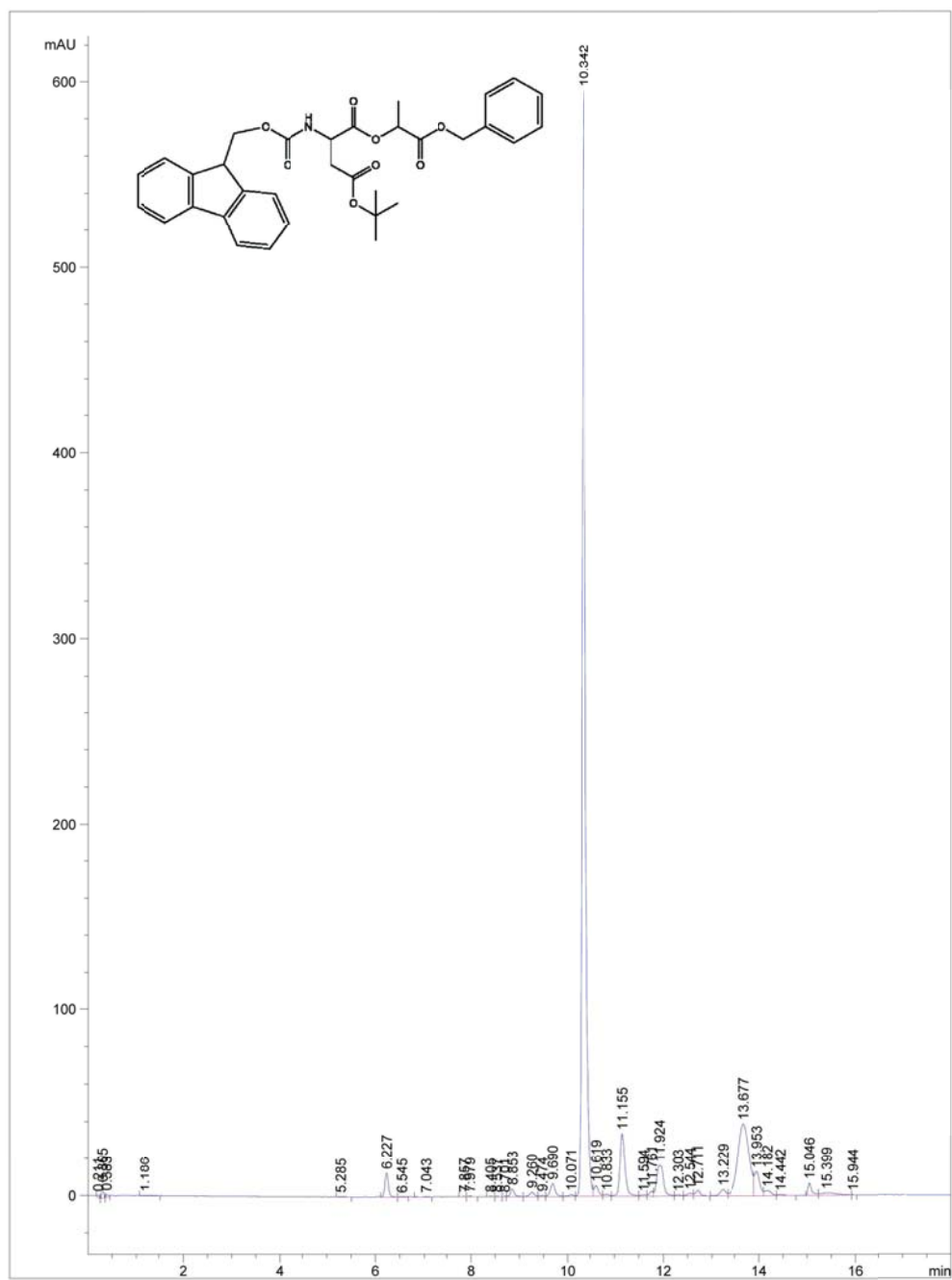


Figure 2.18 LCMS of Fmoc-Asp(OtBu)-Lac-Bn.

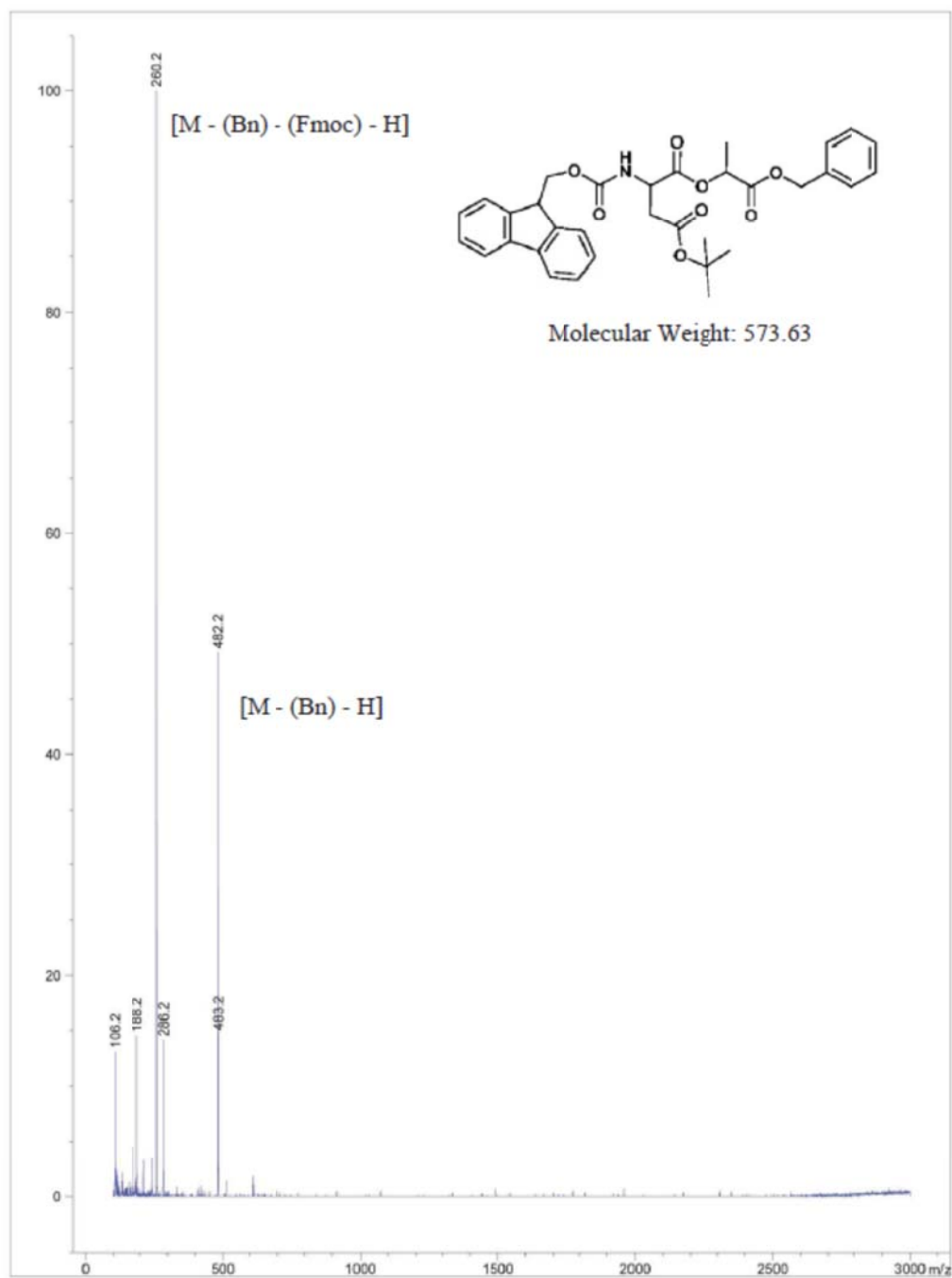


Figure 2.19 MS of Fmoc-Asp(OtBu)-Lac-Bn in negative mode.

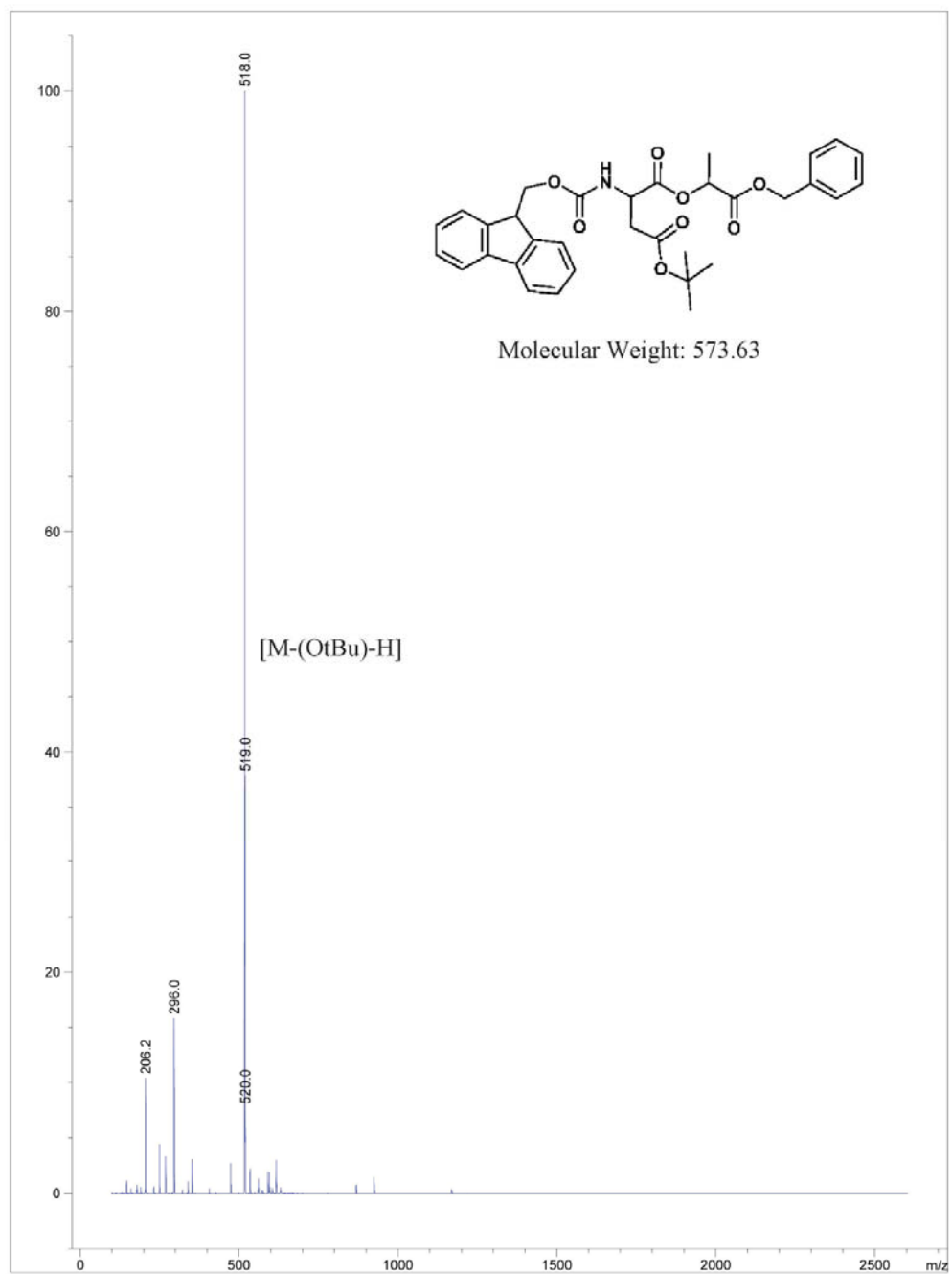
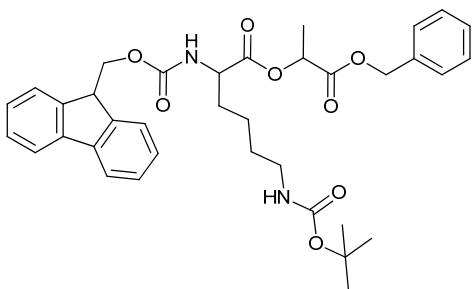


Figure 2.20 MS of Fmoc-Asp(OtBu)-Lac-Bn in positive mode.



### Fmoc-Lys(Boc)-Lac-Bn (3b)



Fmoc-Lys(Boc)-OH (1.2 mmol) and Lac-Bn (1.0 mmol) was dissolved in DCM and placed in an ice bath. DIC (1.2 mmol) and DMAP (0.01 mmol) was added to the cold mixture and mixed for 1 hour. The reaction was stirred for 5 hours at room temperature and monitored by TLC. Diisocarbonylurea was removed via filtration, and the mixture was concentrated. The crude oil was purified on silica gel with 37.5% EtOAc in hexanes (82%).  $^1\text{H-NMR}$  (500 MHz,  $d_6$ -DMSO)  $\delta$  (ppm): 1.24-1.45 (m, 16H), 1.56-1.73 (m, 2H), 2.88 [t,  $J = 5.13$ , 2H,  $\text{CH}_2\text{CH}_2\text{NH}$ ], 4.04 [m,  $J = 7.07$ , 1H,  $\text{NHCHCH}_2\text{CO}$ ], 4.21-4.32 (m, 3H), 5.10-5.15 (m, 3H), 6.75 [t,  $J = 5.61$ , 1H,  $\text{NH}$ ], 7.31-7.45 (m, 9H), 7.71 [d,  $J = 7.57$ , 2H,  $\text{H}_{\text{Ar}}(\text{Fmoc})$ ], 7.79 [d,  $J = 7.56$ , 1H,  $\text{NH}$ ], 7.89 [d,  $J = 7.56$ , 2H,  $\text{H}_{\text{Ar}}(\text{Fmoc})$ ];  $^{13}\text{C-NMR}$  (125 MHz,  $d_6$ -DMSO)  $\delta$  (ppm): 172.06, 169.96, 156.12, 155.54, 143.73, 140.68, 135.44, 128.43, 128.17, 127.90, 127.61, 127.02, 125.19, 120.08, 77.32, 68.66, 66.31, 65.67, 53.58, 46.58, 40.09, 30.15, 28.99, 28.23, 22.77, 16.63. MS (ESI-) calculated for  $\text{C}_{36}\text{H}_{42}\text{N}_2\text{O}_8$  [ $\text{M}^- - \text{H}$ ]: 630.73; found: 629.8

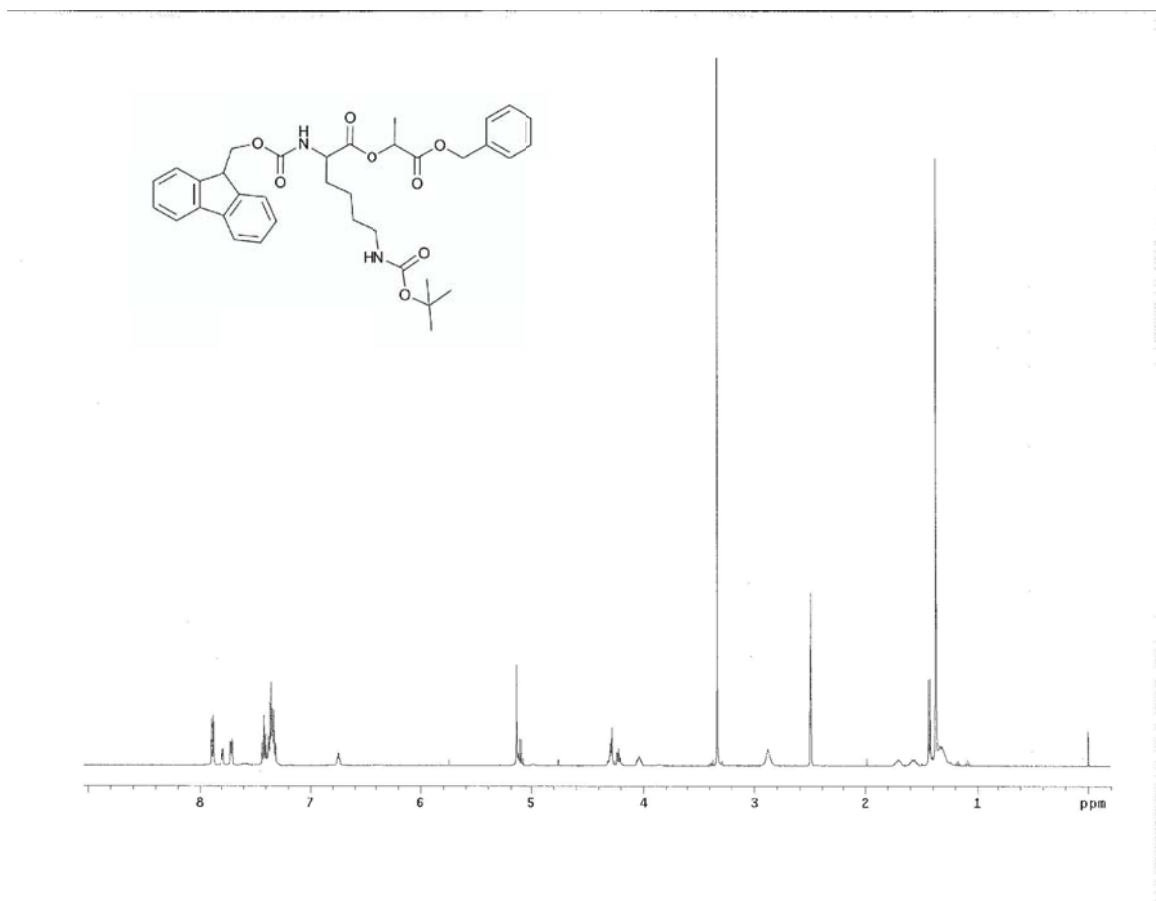


Figure 2.21 <sup>1</sup>H-NMR of Fmoc-Lys(Boc)-Lac-Bn. Full spectrum.

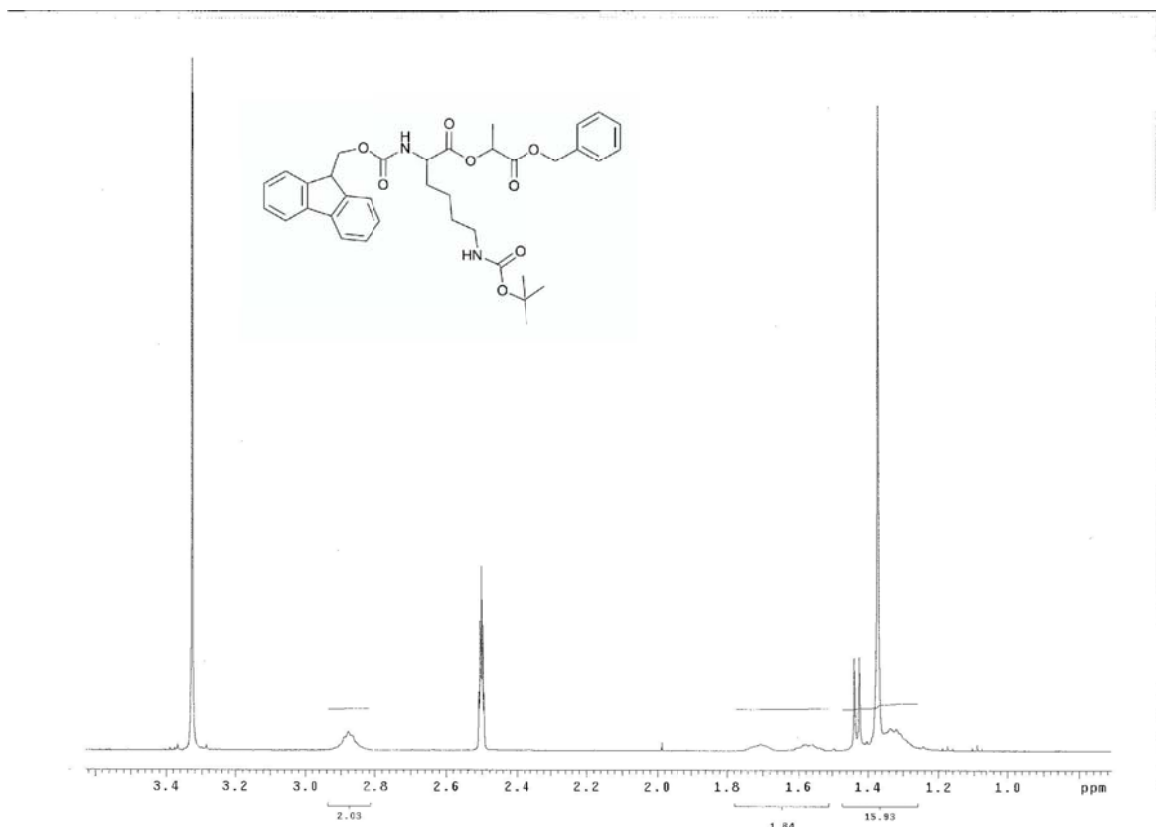


Figure 2.22  $^1\text{H-NMR}$  of Fmoc-Lys(Boc)-Lac-Bn. Magnified from 1.0-3.4 ppm with integrations.

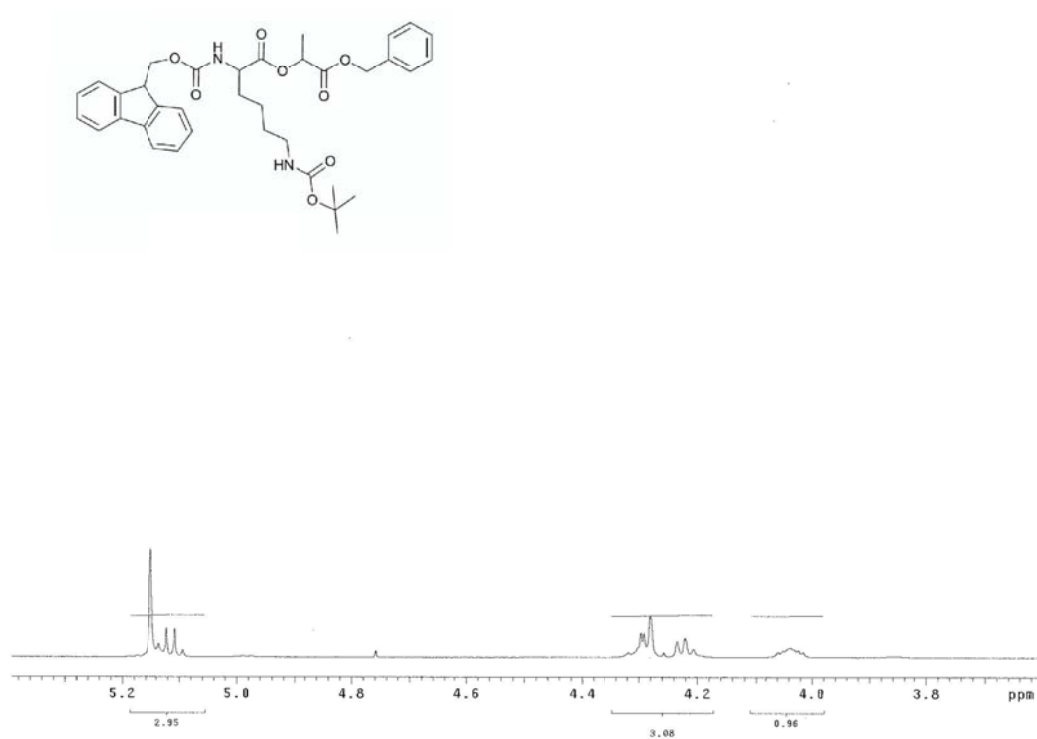


Figure 2.23 <sup>1</sup>H-NMR of Fmoc-Lys(Boc)-Lac-Bn. Magnified from 3.8-5.2 ppm with integrations.

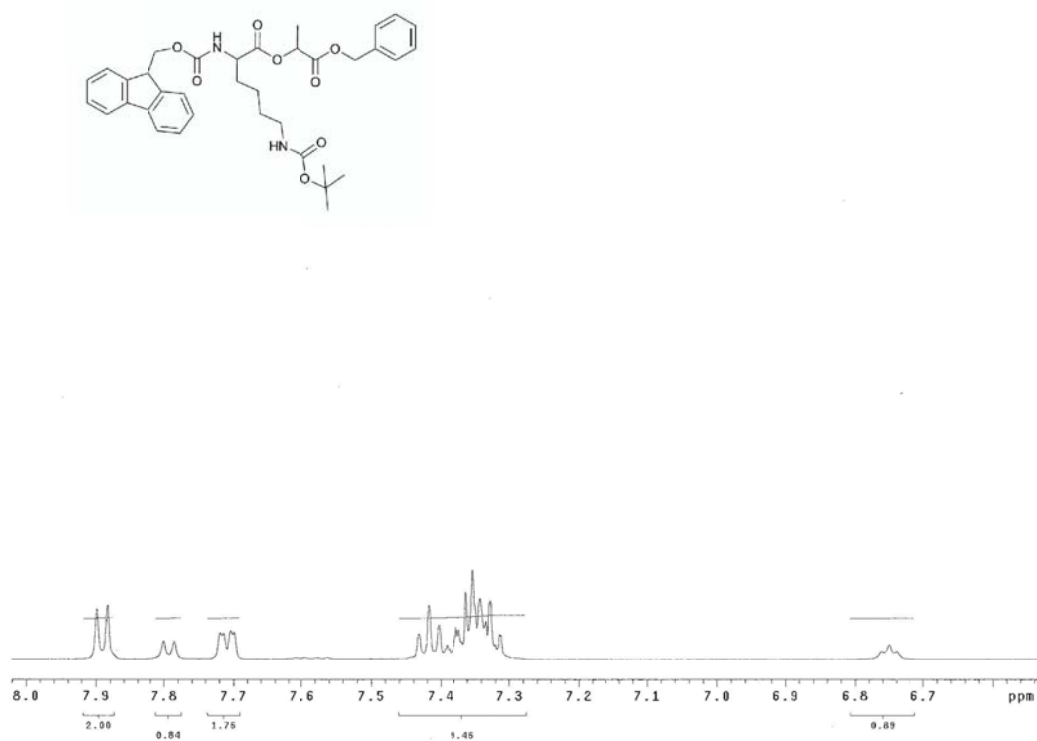


Figure 2.24 <sup>1</sup>H-NMR of Fmoc-Lys(Boc)-Lac-Bn. Magnified from 6.7-8.0 ppm with integrations.

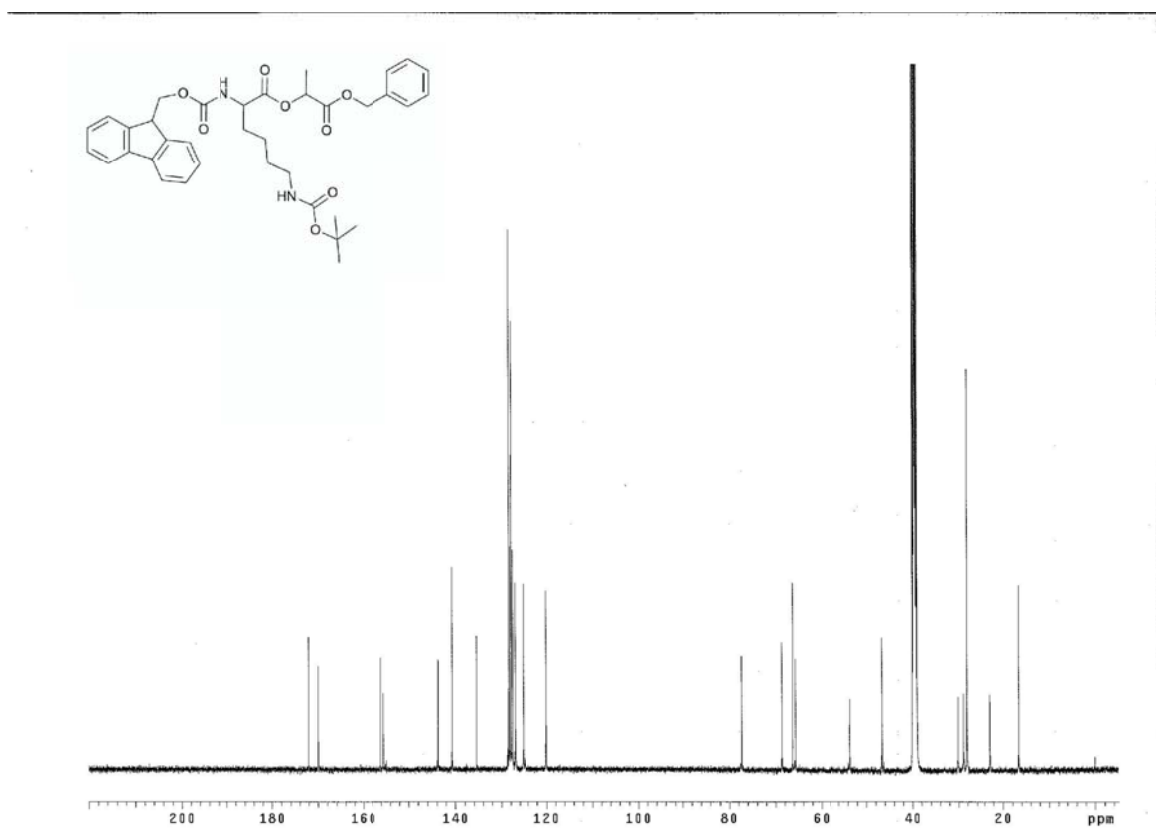


Figure 2.25 <sup>1</sup>H-NMR of Fmoc-Lys(Boc)-Lac-Bn.

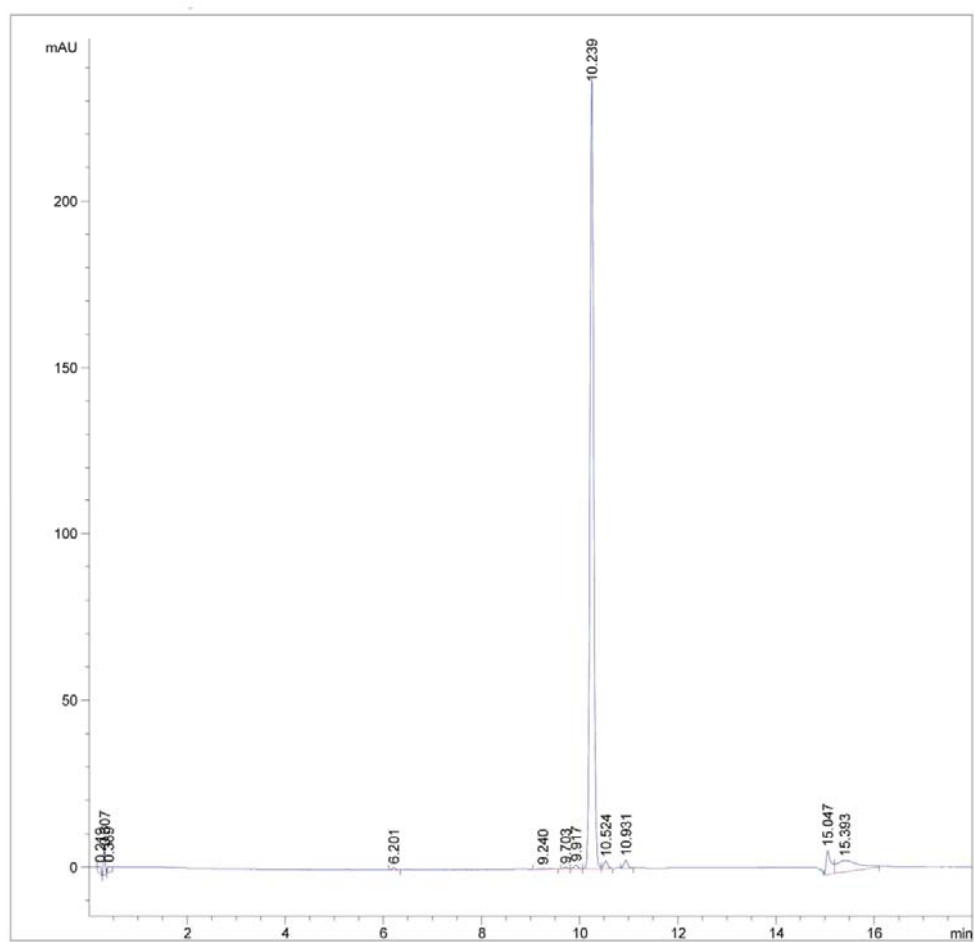
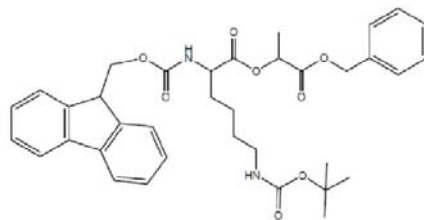
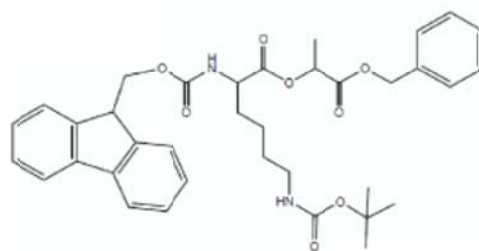


Figure 2.26 LCMS of Fmoc-Lys(Boc)-Lac-Bn.



Molecular Weight: 630.73

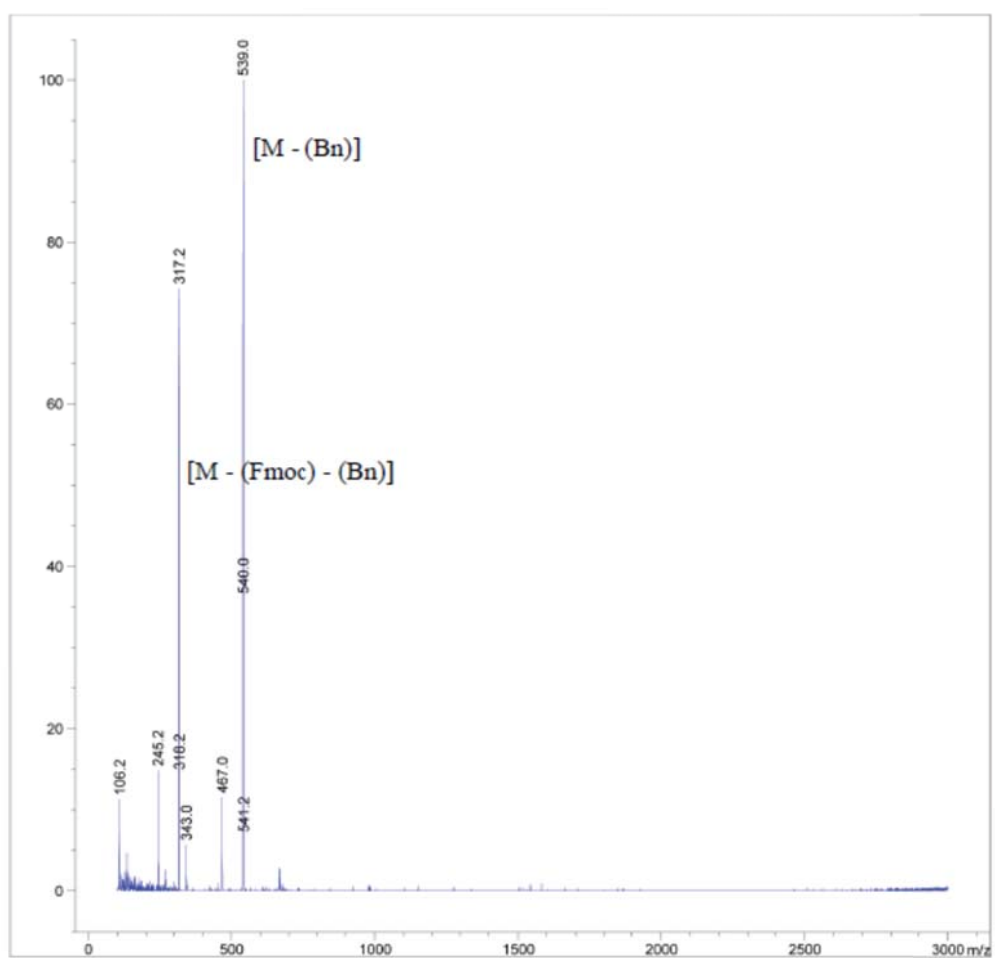
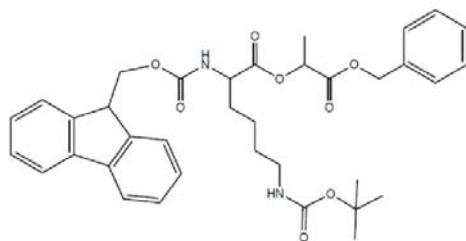


Figure 2.27 MS of Fmoc-Lys(Boc)-Lac-Bn negative mode.





Molecular Weight: 630.73

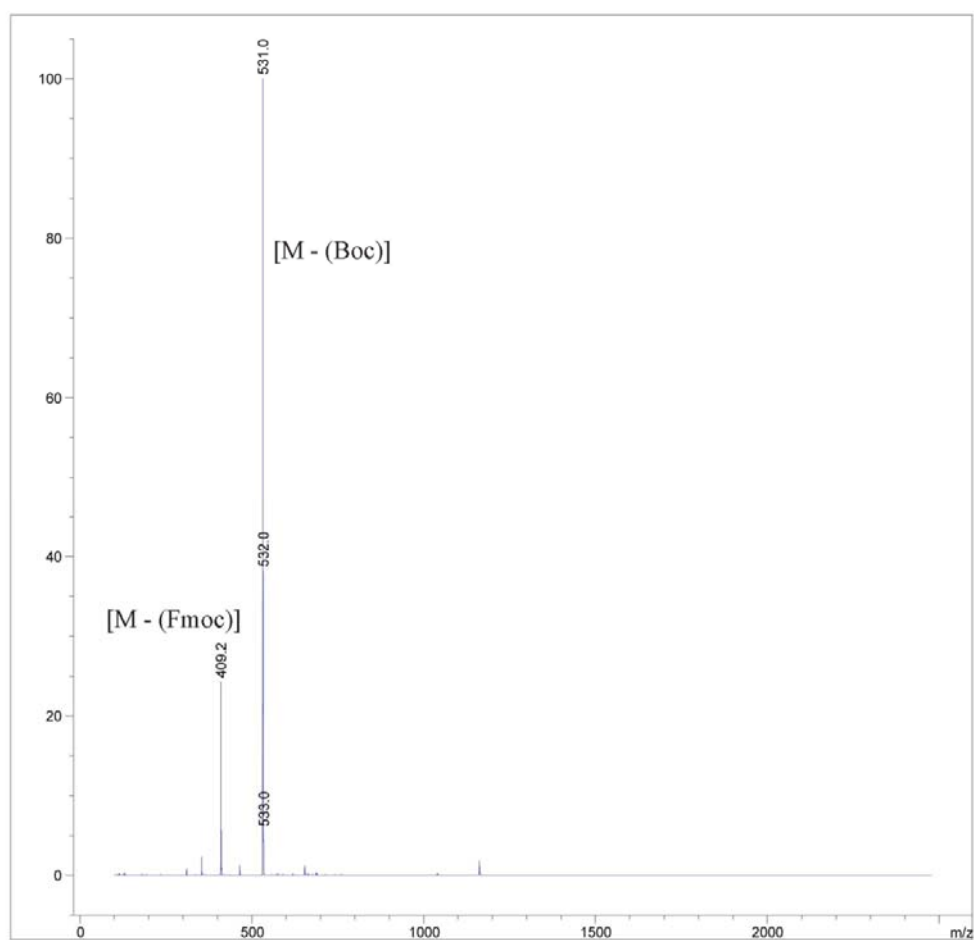
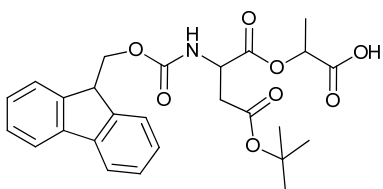


Figure 2.28 MS of Fmoc-Lys(Boc)-Lac-Bn positive mode.

### Fmoc-Asp(OtBu)-Lac-OH (4c)



(3a) was dissolved in dry methanol with 0.1 equiv Pd/C under H<sub>2</sub> at 5 psi for 8 hours or as monitored with TLC. The Pd/C was filtered through a pad of celite and concentrated in vacuo. The sample was purified on silica gel with 1% MeOH in DCM to yield 4c as white crystals (33%). <sup>1</sup>H-NMR (500 MHz, d<sub>6</sub>-DMSO) δ (ppm): 1.36-1.38 (m, 12H), 2.55 and 2.79 [dd, J = 4.64, 2H, CH<sub>2</sub>CH<sub>2</sub>CO], 4.22 [t, J = 7.08, 1H, CH(Fmoc)], 4.30 [d, J = 7.07, 2H, CH<sub>2</sub>(Fmoc)], 4.93 [q, J = 7.07, 1H, NHCHCH<sub>2</sub>], 7.31 [t, J = 7.32, 2H, H<sub>Ar</sub>(Fmoc)], 7.41 [t, J = 7.33, 2H, H<sub>Ar</sub>(Fmoc)], 7.68 [t, J = 7.08, 2H, H<sub>Ar</sub>(Fmoc)], 7.87-7.89 (d, 3H); <sup>13</sup>C-NMR (125 MHz, d<sub>6</sub>-DMSO) δ (ppm): 171.44, 170.64, 168.74, 155.79, 143.69, 140.68, 127.60, 127.01, 125.12, 120.09, 80.49, 69.05, 65.70, 50.33, 46.52, 36.74, 27.61, 16.62 (shift at 54.86 ppm is residual DCM). MS (ESI-) calculated for C<sub>26</sub>H<sub>29</sub>NO<sub>8</sub> [M<sup>-</sup> - H]: 483.51; found: 482.2

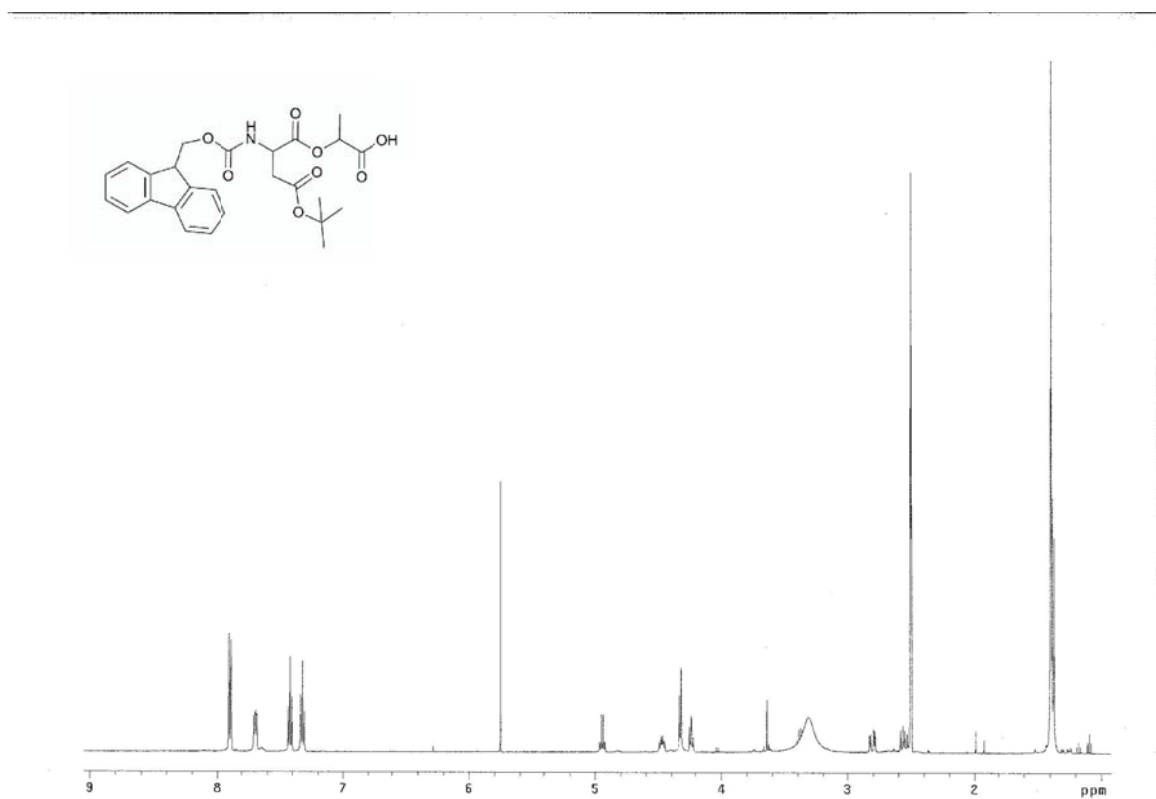


Figure 2.29 <sup>1</sup>H-NMR of Fmoc-Asp(OtBu)-Lac-OH. Full spectrum.

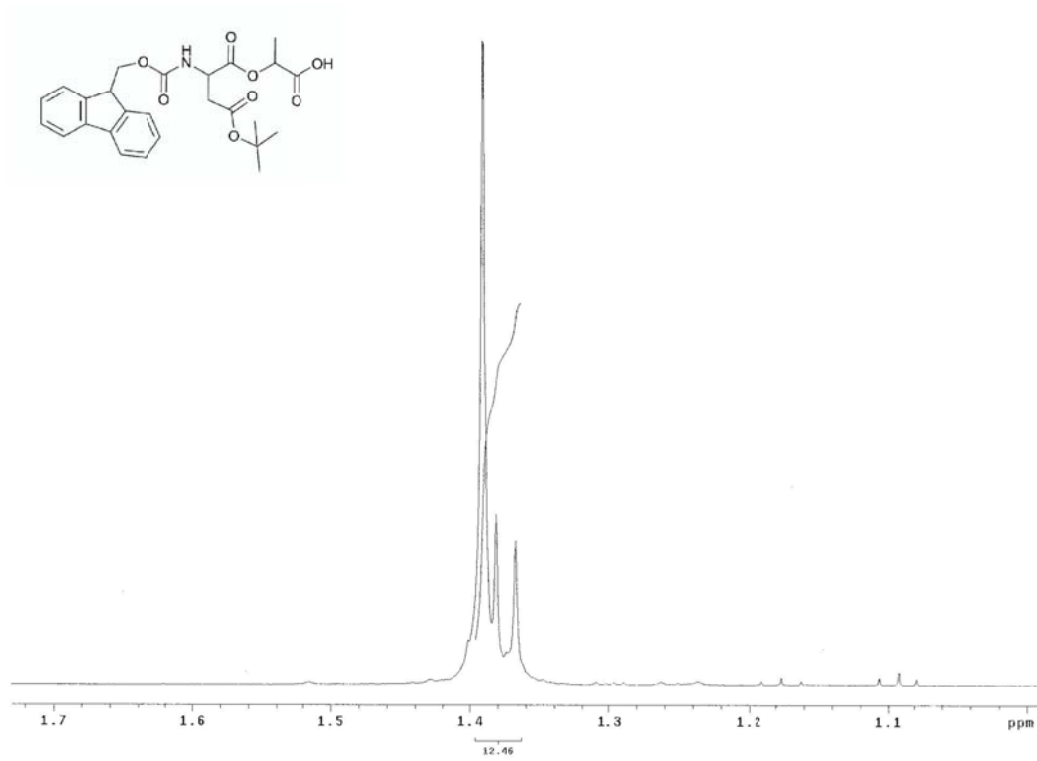


Figure 2.30 <sup>1</sup>H-NMR of Fmoc-Asp(OtBu)-Lac-OH. Magnified from 1.1-1.7 ppm, with integrations.

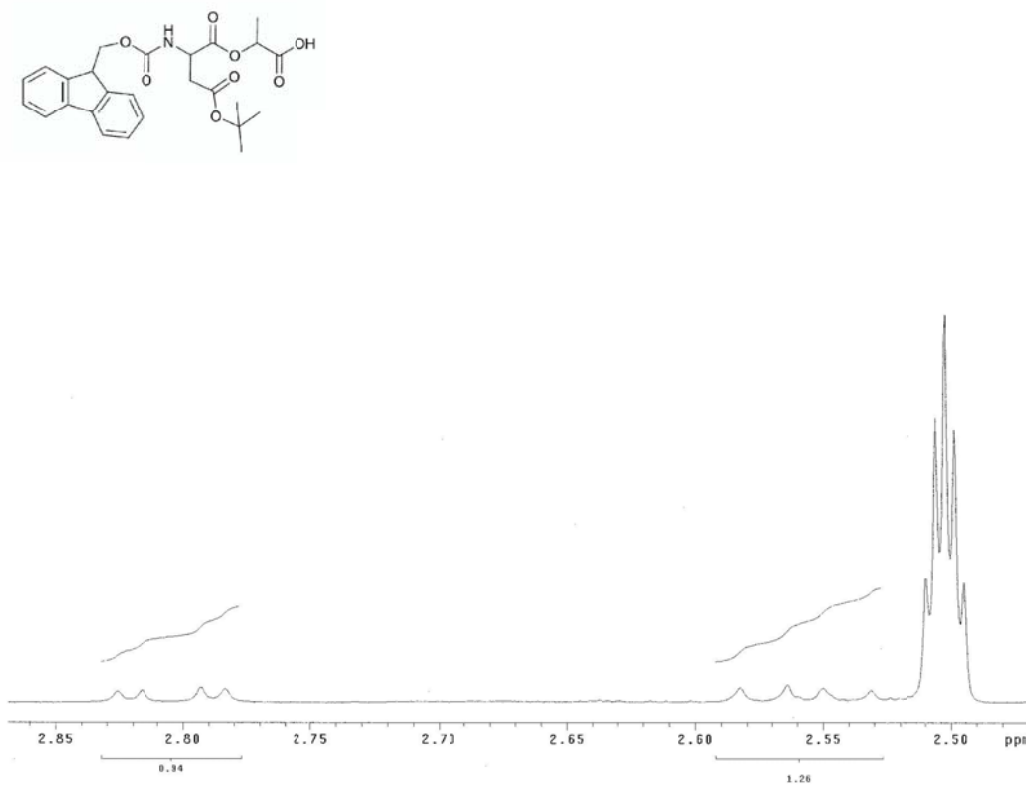


Figure 2.31 <sup>1</sup>H-NMR of Fmoc-Asp(OtBu)-Lac-OH. Magnified from 2.50-2.85 ppm, with integrations.

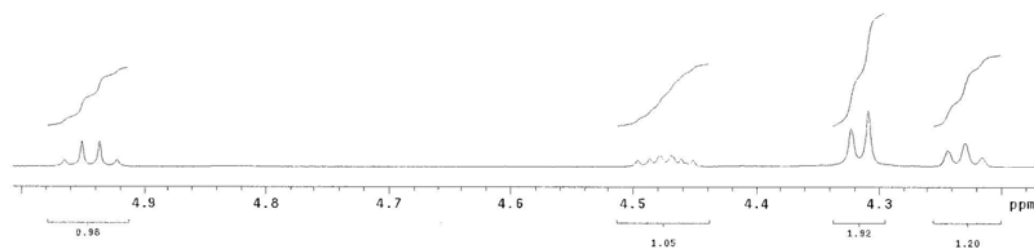
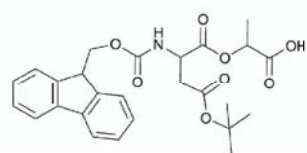


Figure 2.32 <sup>1</sup>H-NMR of Fmoc-Asp(OtBu)-Lac-OH. Magnified from 4.3-4.9 ppm, with integrations.

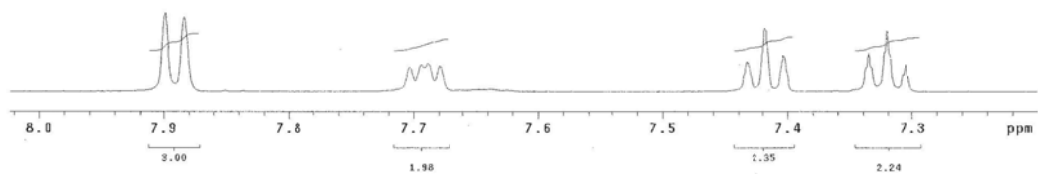
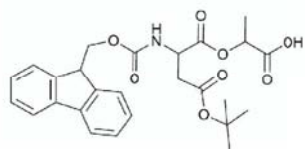


Figure 2.33 <sup>1</sup>H-NMR of Fmoc-Asp(OtBu)-Lac-OH. Magnified from 7.3-8.0 ppm, with integrations.

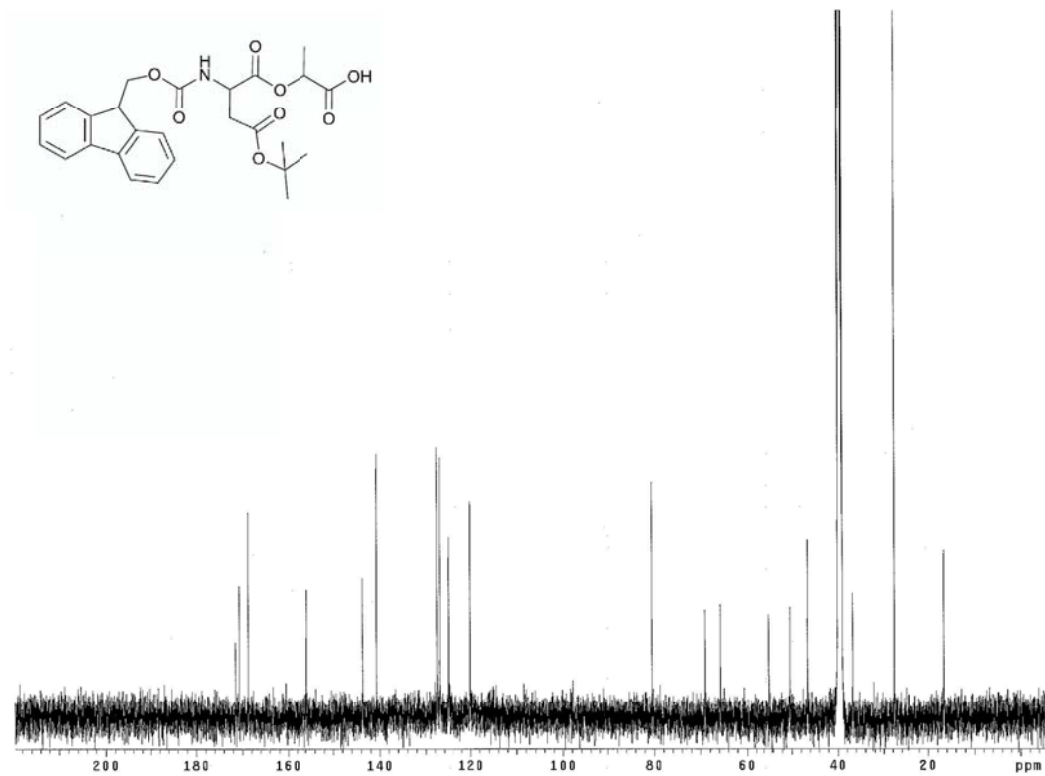


Figure 2.34  $^{13}\text{C}$ -NMR of Fmoc-Asp(OtBu)-Lac-OH.



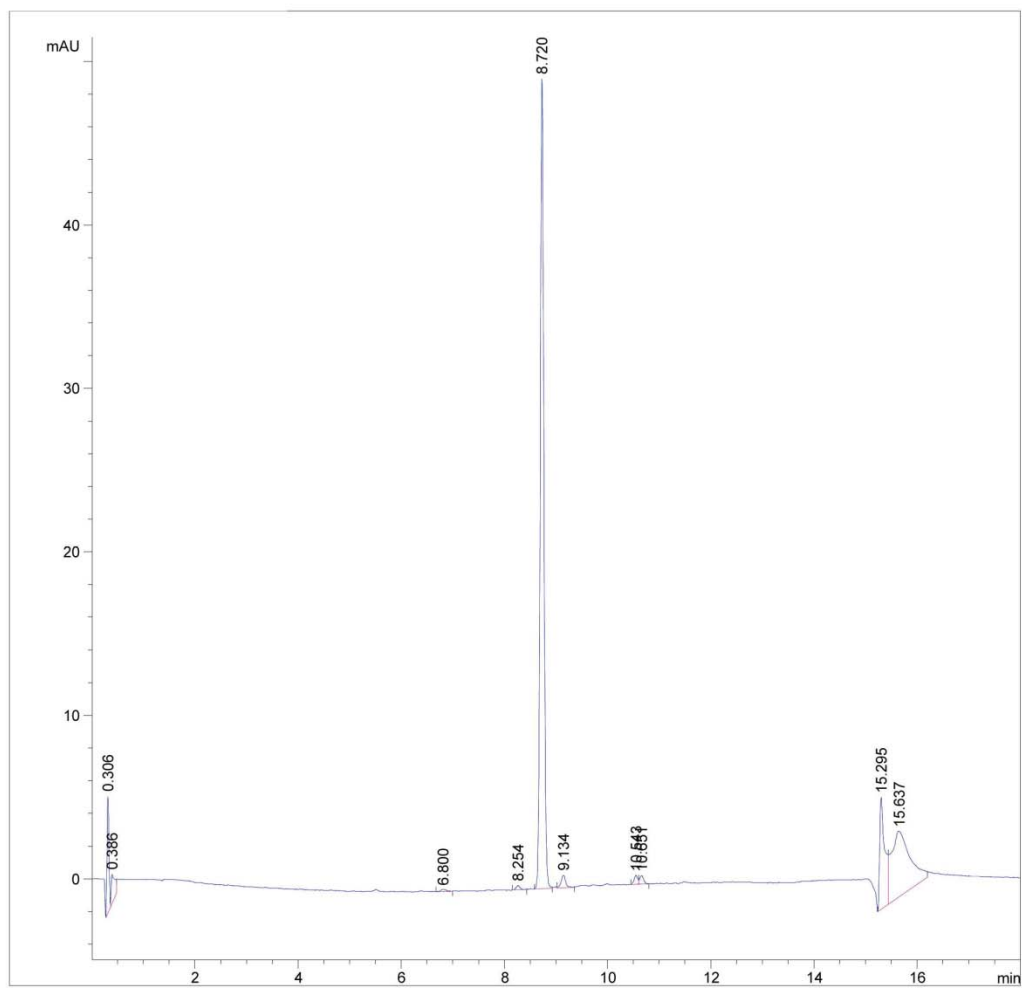
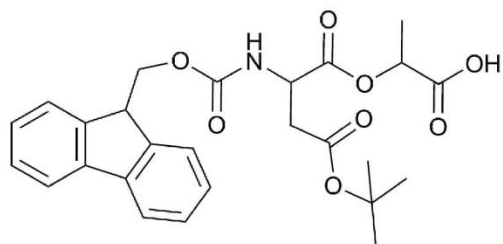
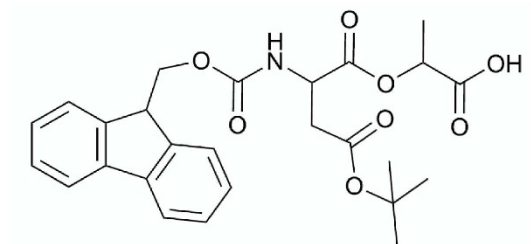


Figure 2.35 LCMS of Fmoc-Asp(OtBu)-Lac-OH.



Molecular Weight: 481.53

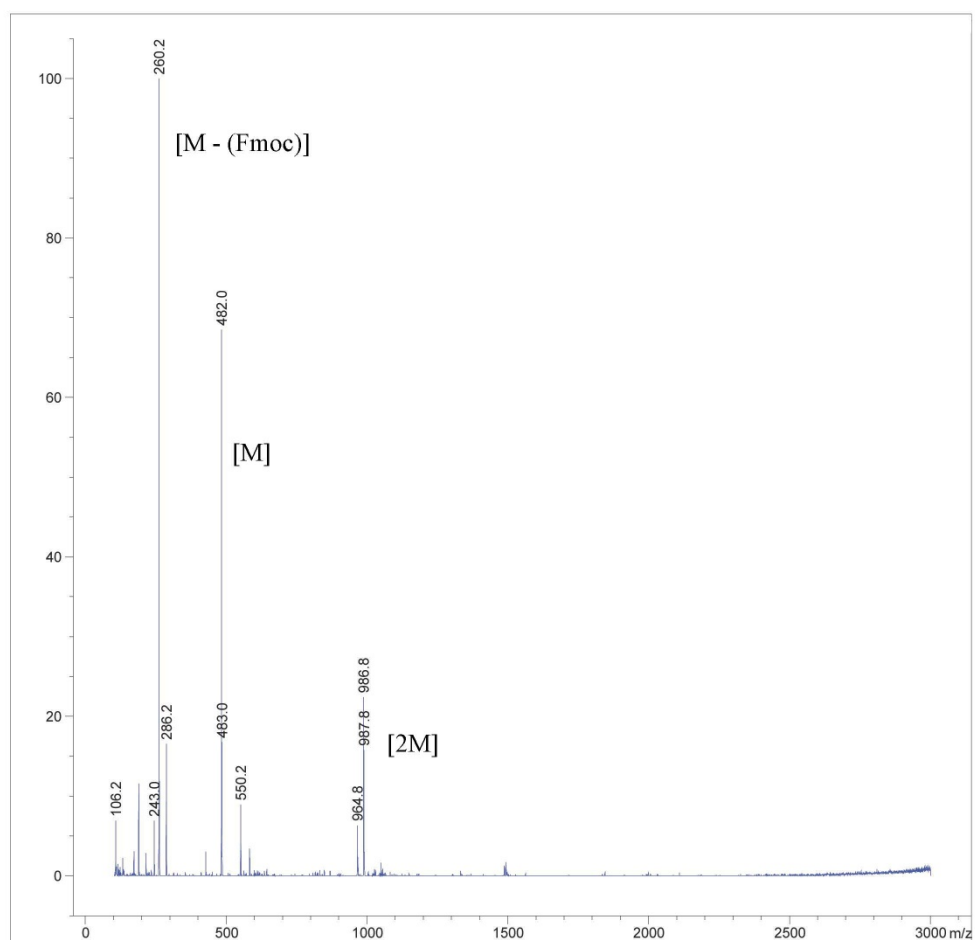
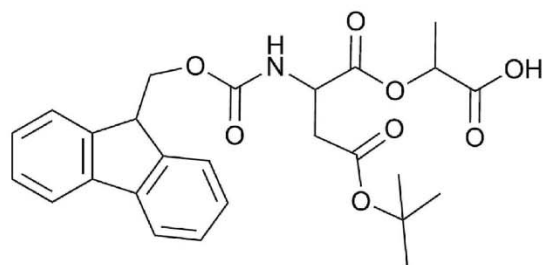


Figure 2.36 MS of Fmoc-Asp(OtBu)-Lac-OH in negative mode.



Molecular Weight: 481.51

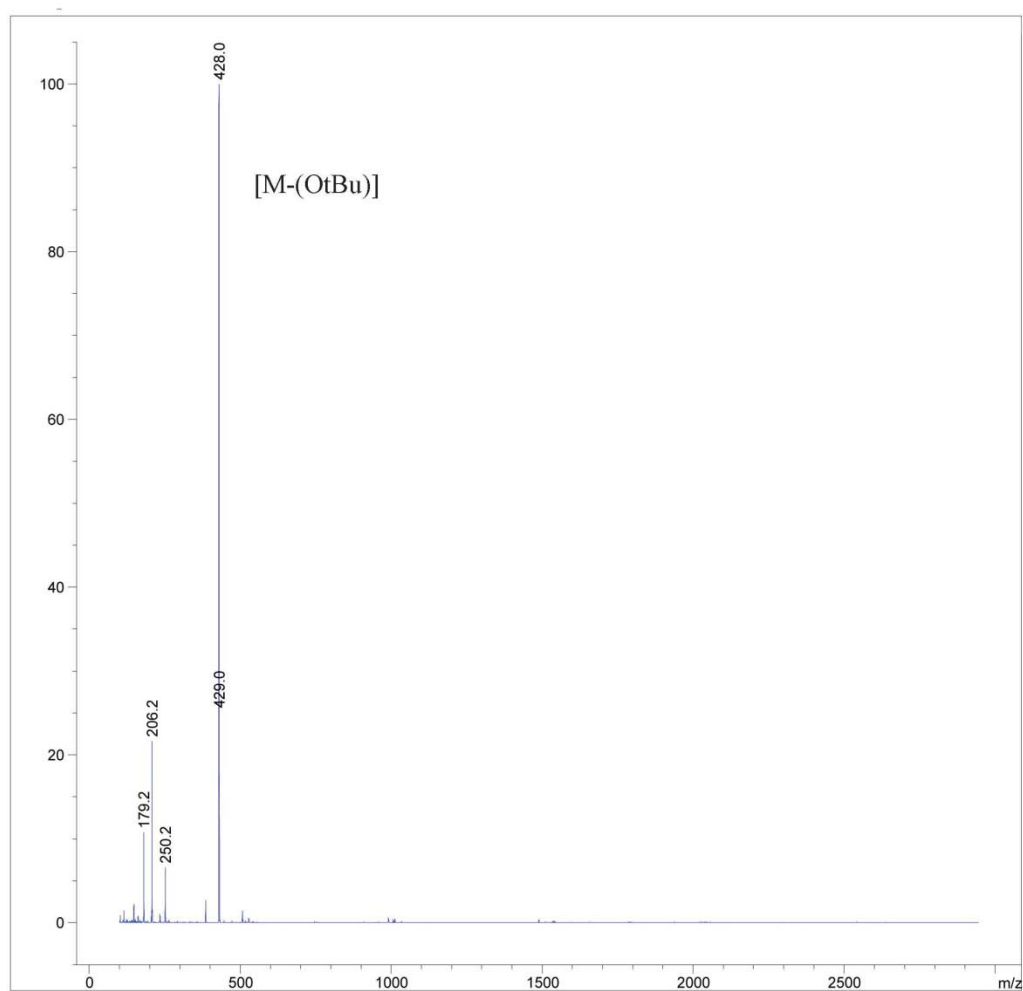
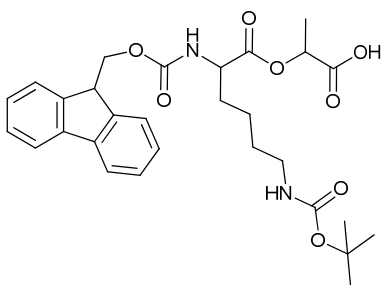


Figure 2.37 MS of Fmoc-Asp(OtBu)-Lac-OH in positive mode.

### Fmoc-Lys(Boc)-Lac-OH (4d)



(3b) was dissolved in dry methanol with 0.1 equiv Pd/C under H<sub>2</sub> at 12 psi for 9 hours or as monitored with TLC. The Pd/C was filtered through a pad of celite and concentrated in vacuo. The sample was eluted with 1-6% MeOH in DCM to yield 4d as white crystals in a yield of (67%). <sup>1</sup>H-NMR (500 MHz, d<sub>6</sub>-DMSO) δ (ppm): 1.34-1.47 (m, 16H), 1.60-1.79 (m, 2H), 2.90 [t, J = 5.96, 2H, CH<sub>2</sub>CH<sub>2</sub>NH], 4.04 [m, J = 5.03, 1H, NHCHCH<sub>2</sub>CO], 4.32-4.22 (m, 3H), 4.93 [q, J = 7.07, 1H, CH<sub>2</sub>CHCH<sub>3</sub>], 6.75 [t, J = 5.53, 1H, NH], 7.33 [t, J = 7.49, 2H, H<sub>Ar</sub>(Fmoc)]; 7.42 [t, J = 7.50, 2H, H<sub>Ar</sub>(Fmoc)], 7.72 [t, J = 6.90, 2H, H<sub>Ar</sub>(Fmoc)], 7.77 [d, J = 7.83, 1H, NH], 7.89 [d, J = 7.50, 2H, H<sub>Ar</sub>(Fmoc)]; <sup>13</sup>C-NMR (125 MHz, d<sub>6</sub>-DMSO) δ (ppm): 171.91, 171.84, 156.05, 155.47, 143.69, 140.62, 127.54, 126.96, 125.15, 120.01, 77.25, 68.59, 65.60, 53.52, 46.53, 30.12, 28.98, 28.18, 22.72, 16.63. MS (ESI-) calculated for C<sub>29</sub>H<sub>36</sub>N<sub>2</sub>O<sub>8</sub> [M<sup>-</sup> - H]: 540.60; found: 539.00.

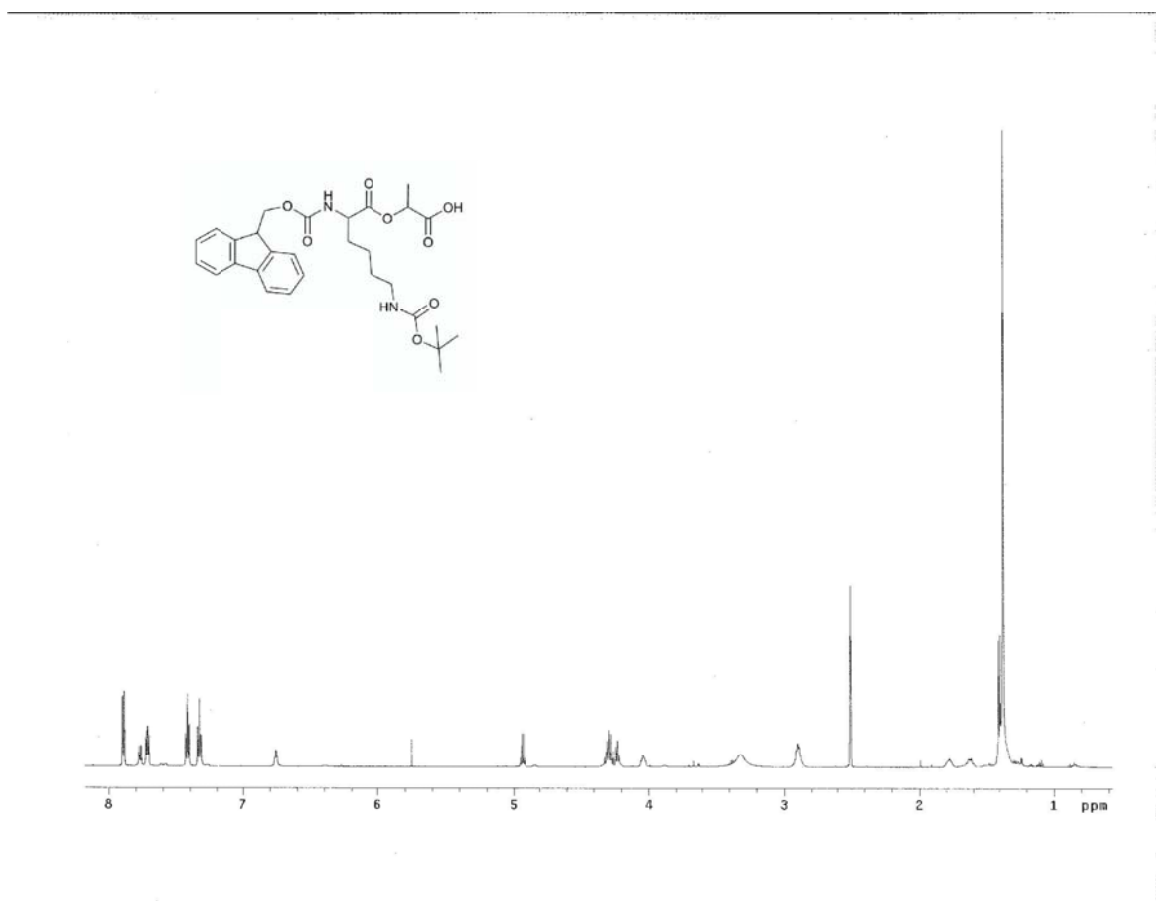


Figure 2.38 <sup>1</sup>H-NMR of Fmoc-Lys(Boc)-Lac-OH. Full spectrum.

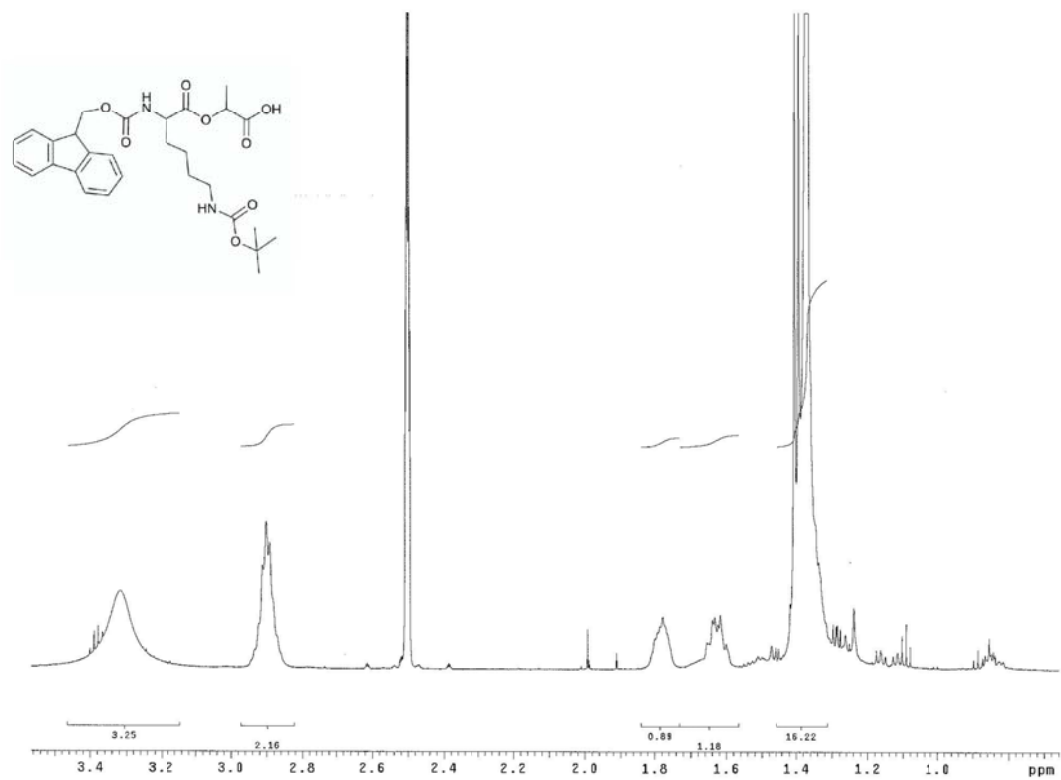


Figure 2.39 <sup>1</sup>H-NMR of Fmoc-Lys(Boc)-Lac-OH. Magnified from 1.0-3.4 ppm, with integrations.

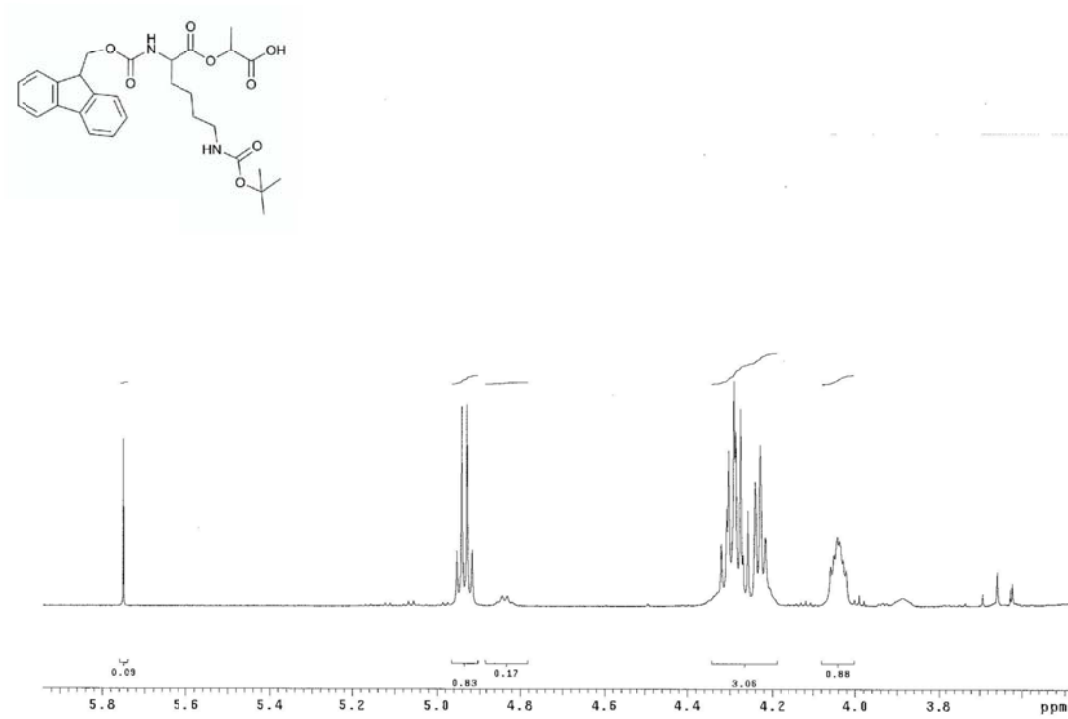


Figure 2.40 <sup>1</sup>H-NMR of Fmoc-Lys(Boc)-Lac-OH. Magnified from 3.8-5.8 ppm, with integrations.

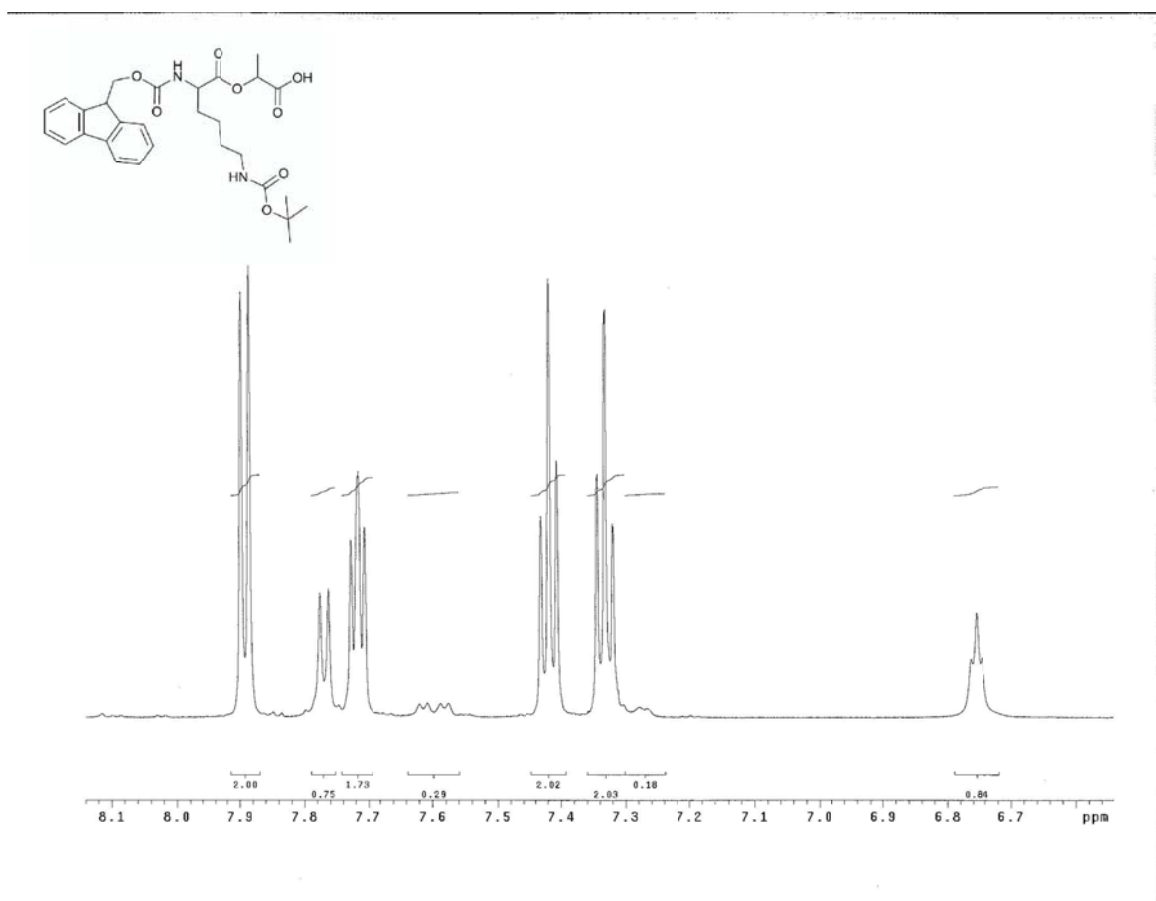


Figure 2.41 <sup>1</sup>H-NMR of Fmoc-Lys(Boc)-Lac-OH. Magnified at 6.7-8.1 ppm, with integrations.



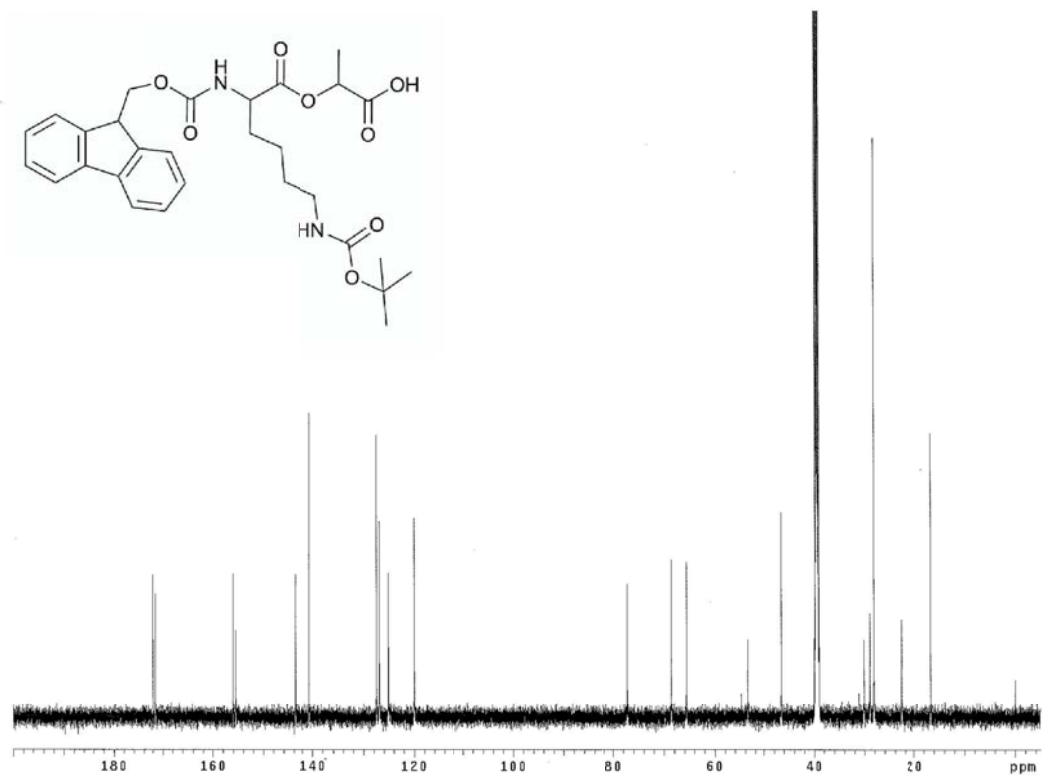


Figure 2.42 <sup>13</sup>C-NMR of Fmoc-Lys(Boc)-Lac-OH.

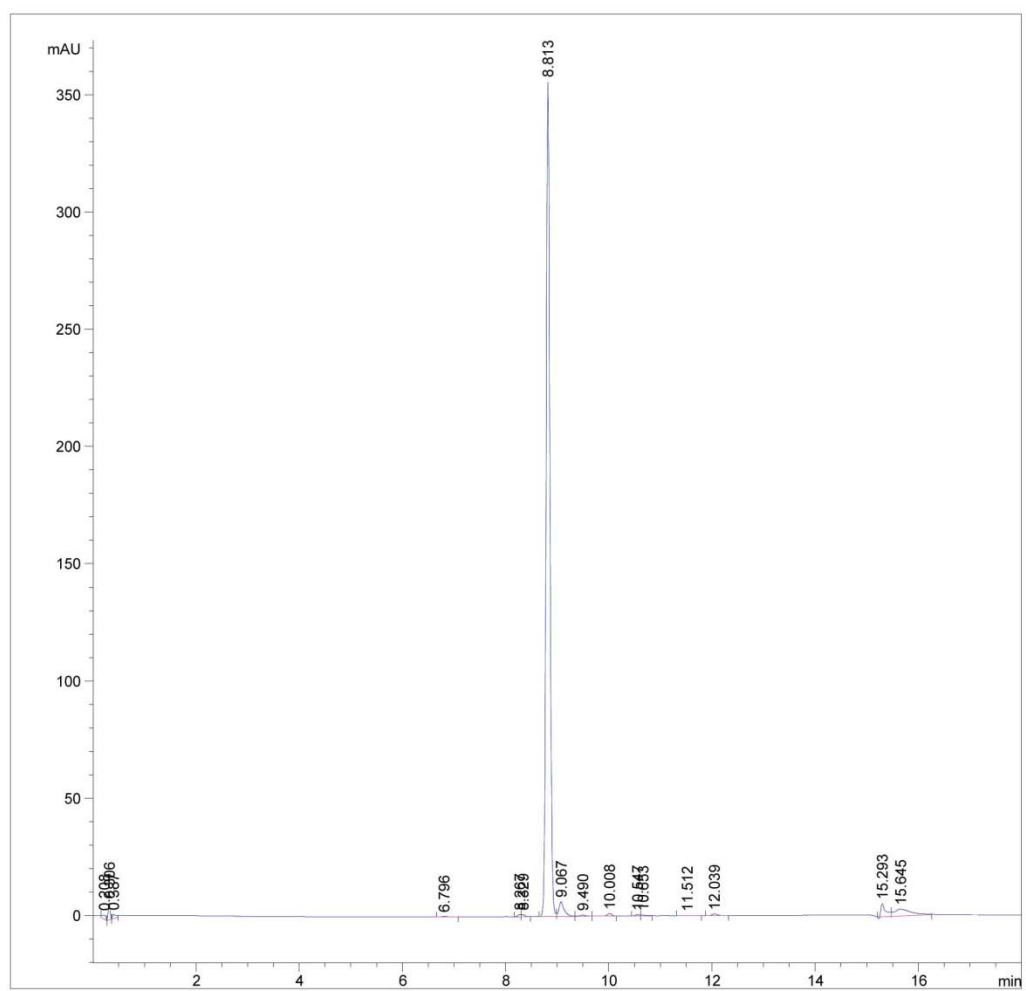
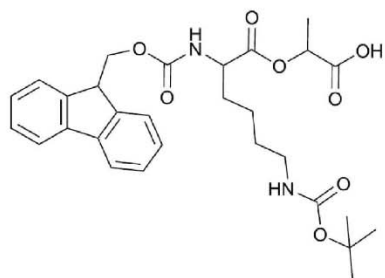
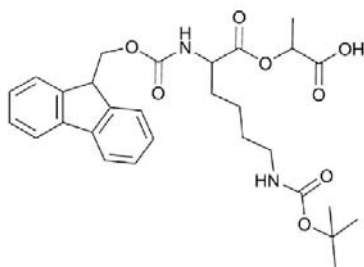


Figure 2.43 LCMS of Fmoc-Lys(Boc)-Lac-OH.



Molecular Weight: 540.60

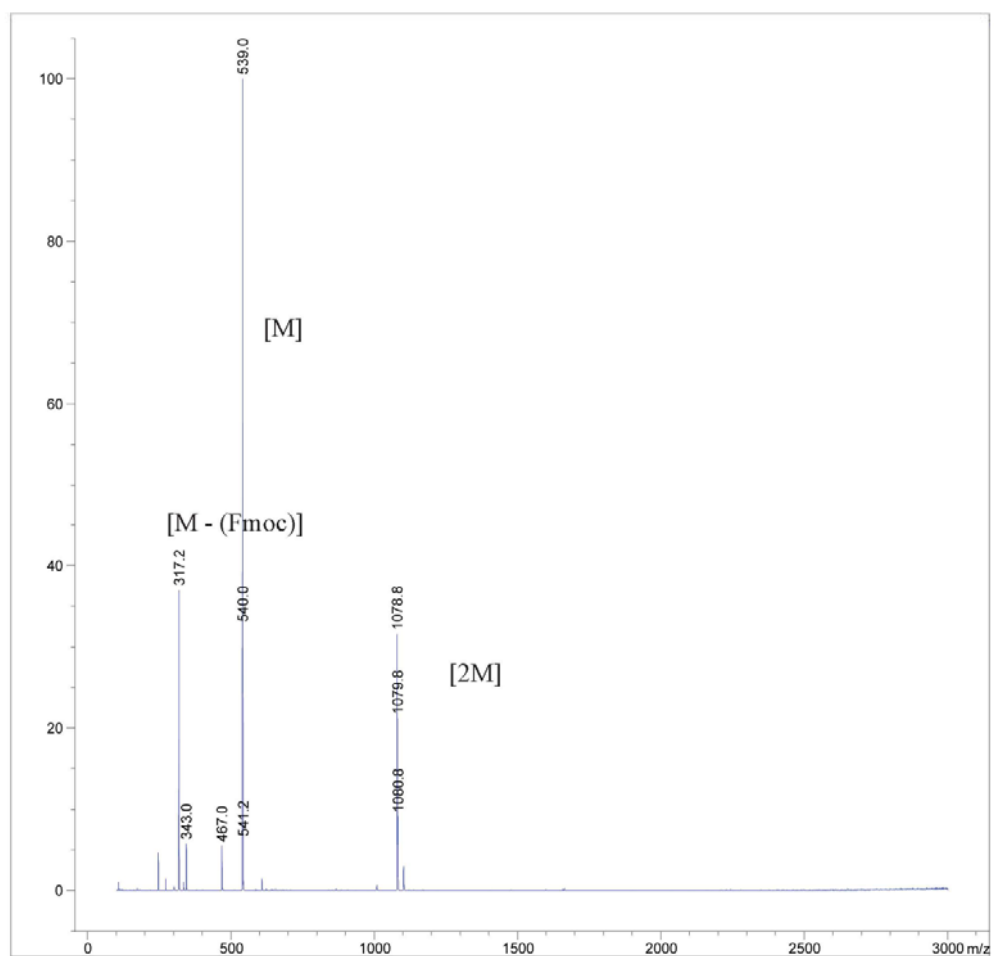
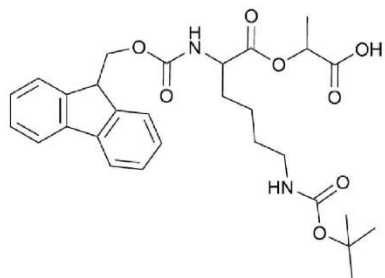


Figure 2.44 MS of Fmoc-Lys(Boc)-Lac-OH in negative mode



Molecular Weight: 540.60

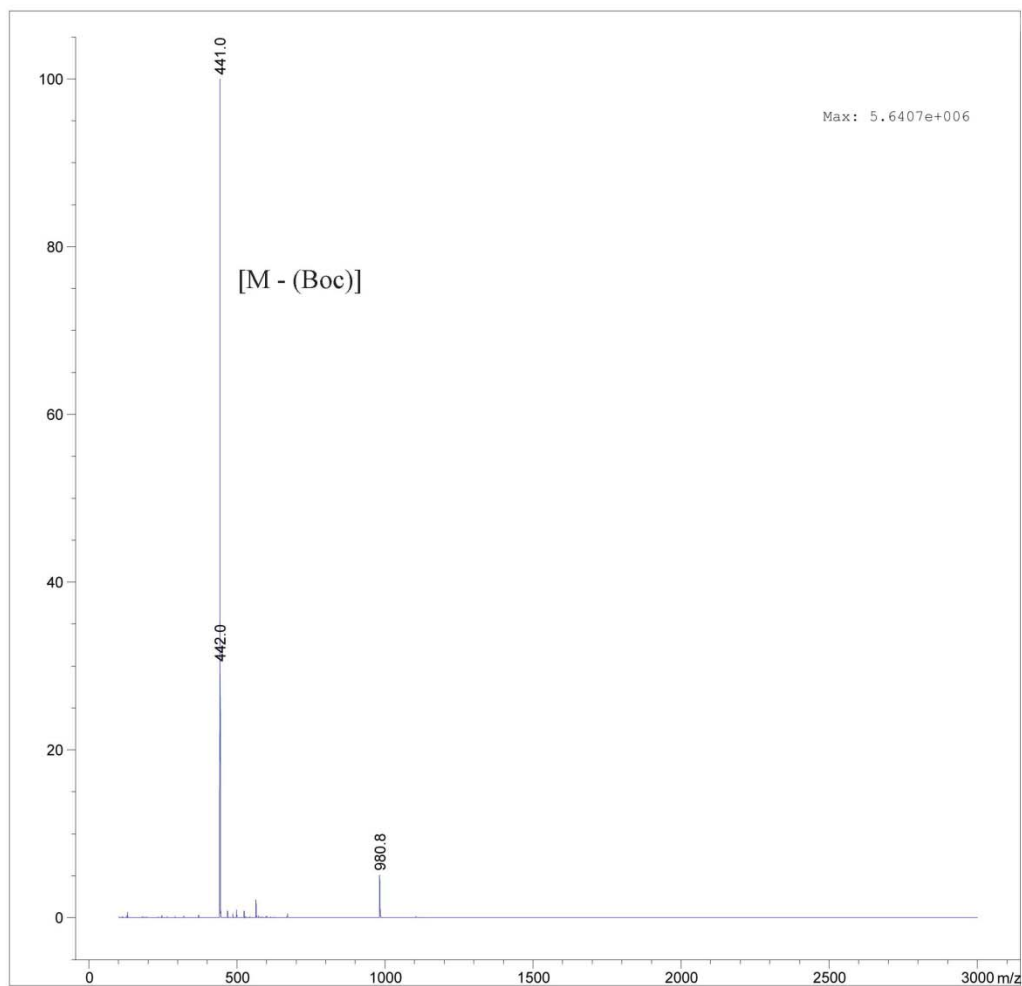


Figure 2.45 MS of Fmoc-Lys(Boc)-Lac-OH in positive mode

**Preparation of depsipeptides on solid phase synthesis.** The depsipeptides prepared with this method are shown in Figure . Functionalized peptides were added to the resin with DIC/DMAP as per standard Fmoc SPPS protocols. Fmoc-Ala-Wang resin (0.25 equiv) was swelled in DCM. The Fmoc group was removed with 20% pyridine in DMF and washed. Fmoc-peptide-OH (1 equiv) was dissolved in DCM and DMF and was added to the reaction vessel with DIC (0.75 equiv) and DMAP (0.05 equiv). After 2 hours the sample was washed with DCM and DMF. The Fmoc group was removed with pyridine in DMF and washed. Fmoc-depsidipeptide (1 equiv) was dissolved in DCM with Oxyma Pure (0.2 equiv) and was added to the reaction vessel upon a 2 minute preactivation time with DIC (0.75 equiv). After 2 hours the sample was washed with DCM and DMF. The Fmoc-removal, coupling, and washing steps were repeated with the Fmoc-depsidipeptide until the desired length was achieved. The oligodepsipeptide was removed from the resin accordingly and purified with HPLC.

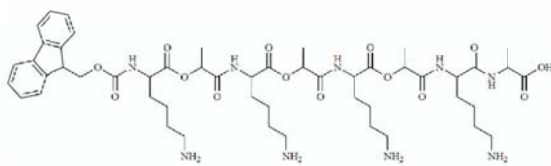
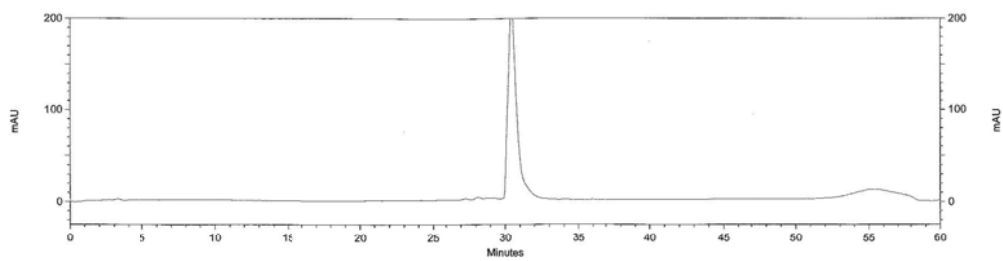


Figure 2.46 HPLC of depsipeptide (1).

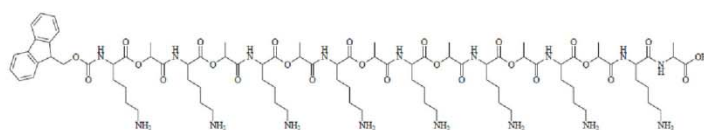
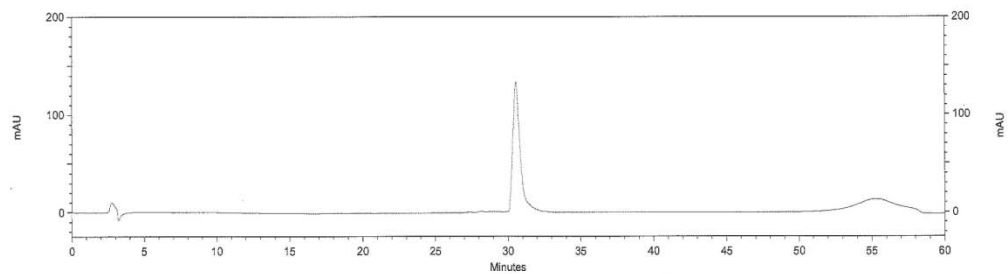


Figure 2.47 HPLC of desipeptide (2).

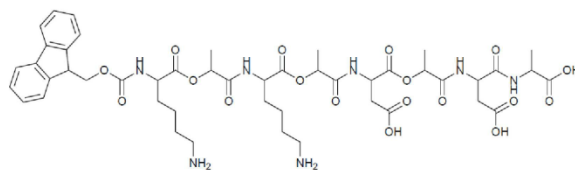
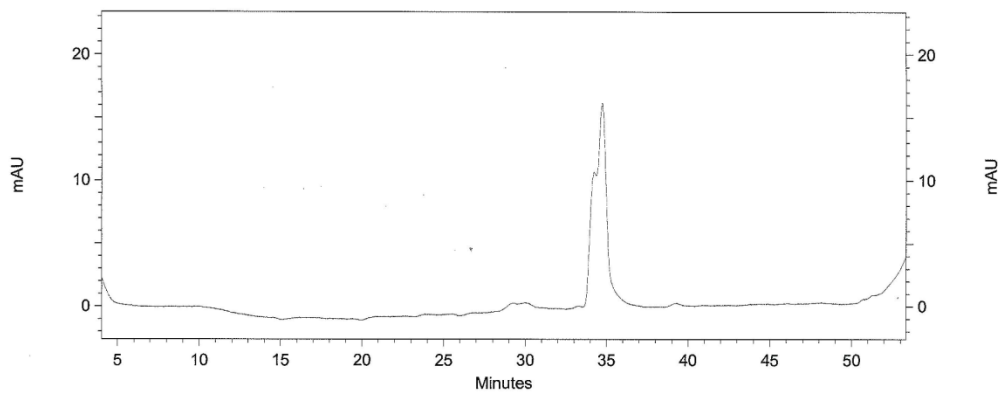


Figure 2.48 HPLC of depsipeptide (3).



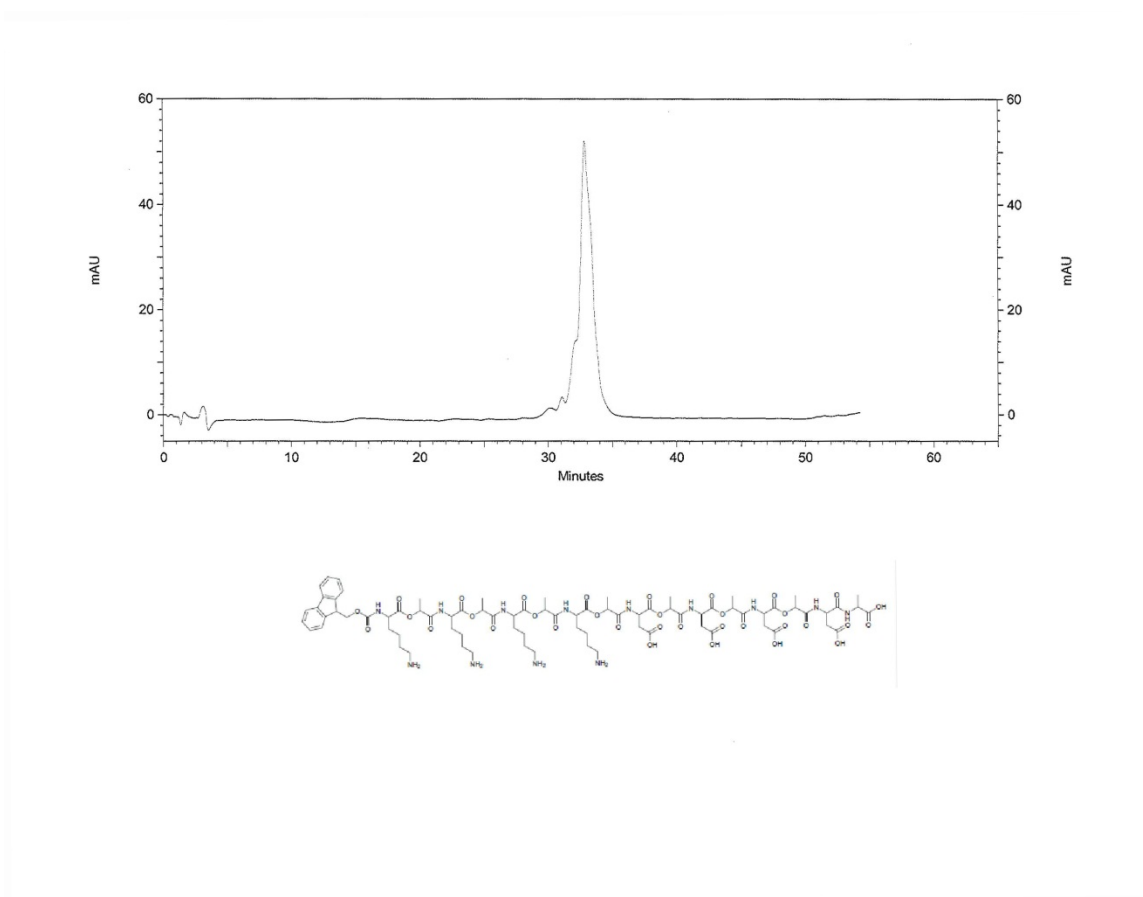


Figure 2.49 HPLC of depsipeptide (4).



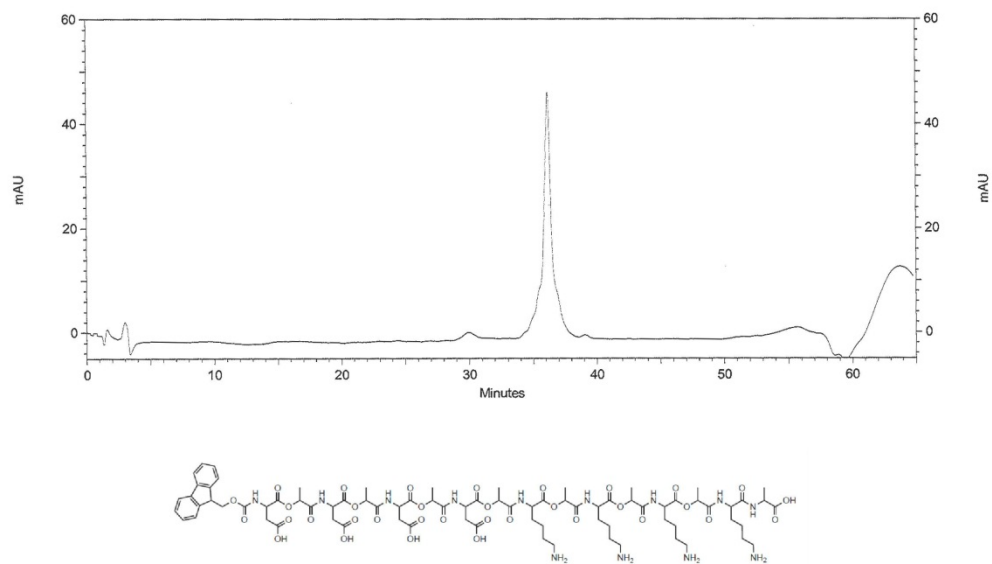


Figure 2.51 HPLC of depsipeptide (6).

## References

1. Ouchi, T., et al., *Synthesis of Poly[(Glycolic Acid)-Alt-(L-Aspartic Acid)] and Its Biodegradation Behavior in-Vitro*. Makromolekulare Chemie-Rapid Communications, 1993. **14**(12): p. 825-831.
2. Veld, P., P.J. Dijkstra, and J. Feijen, *Synthesis of Biodegradable Polyesteramides with Pendant Functional-Groups*. Makromolekulare Chemie-Macromolecular Chemistry and Physics, 1992. **193**(11): p. 2713-2730.
3. Wang, D. and X.D. Feng, *Synthesis of poly(glycolic acid-alt-L-aspartic acid) from a morpholine-2,5-dione derivative*. Macromolecules, 1997. **30**(19): p. 5688-5692.
4. Feng, Y., D. Klee, and H. Hocker, *Synthesis of poly[(lactic acid)-alt- or co-((S)-aspartic acid)] from (3S,6R,S)-3-[(benzyloxycarbonyl)methyl]6-methylmorpholine-2,5-dione*. Macromolecular Chemistry and Physics, 2002. **203**(5-6): p. 819-824.
5. Abdelmelek, M., et al., *Synthesis of Morpholine-2,5-dione Monomers for the Preparation of Polydepsipeptides*, in *Biomaterials*. 2010, American Chemical Society. p. 185-196.
6. Helder, J., et al., *Synthesis of Poly[Oxyethylidenecarbonylimino-(2-Oxoethylene)] [Poly(Glycine-D,L-Lactic Acid)] by Ring-Opening Polymerization*. Makromolekulare Chemie-Rapid Communications, 1985. **6**(1): p. 9-14.
7. Dijkstra PJ, F.J., *Synthetic Pathways to Polydepsipeptides*. Macromol Symp, 2000. **153**: p. 67-76.
8. Barrera, D.A., et al., *Copolymerization and Degradation of Poly(Lactic Acid Co-Lysine)*. Macromolecules, 1995. **28**(2): p. 425-432.
9. Ouchi, T., et al., *Synthesis and enzymatic hydrolysis of lactic acid depsipeptide copolymers with functionalized pendant groups*. Journal of Polymer Science Part a-Polymer Chemistry, 1997. **35**(2): p. 377-383.
10. Bezemer, J.M., et al., *Amphiphilic poly(ether ester amide) multiblock copolymers as biodegradable matrices for the controlled release of proteins*. Journal of Biomedical Materials Research, 2000. **52**(1): p. 8-17.
11. Ouchi, T., et al., *Synthesis of a block copolymer of L-lactide and depsipeptide with pendant thiol groups*. Designed Monomers and Polymers, 2000. **3**(3): p. 279-287.
12. Ouchi, T., et al., *Preparation of poly[DL-lactide-co-glycolide]-based microspheres containing protein by use of amphiphilic diblock copolymers of depsipeptide and lactide having ionic pendant groups as biodegradable surfactants by W/O/W emulsion method*. Polymer, 2004. **45**(5): p. 1583-1589.
13. Ouchi, T. and Y. Ohya, *Design of lactide copolymers as biomaterials*. Journal of Polymer Science Part a-Polymer Chemistry, 2004. **42**(3): p. 453-462.

14. Kuisle, O., E. Quinoa, and R. Riguera, *A general methodology for automated solid-phase synthesis of depsides and depsipeptides. Preparation of a valinomycin analogue*. Journal of Organic Chemistry, 1999. **64**(22): p. 8063-8075.
15. Spengler, J., B. Kokschi, and F. Albericio, *Simple machine-assisted protocol for solid-phase synthesis of depsipeptides*. Biopolymers, 2007. **88**(6): p. 823-828.
16. Coin, I., M. Beyermann, and M. Bienert, *Solid-phase peptide synthesis: from standard procedures to the synthesis of difficult sequences*. Nature Protocols, 2007. **2**(12): p. 3247-3256.
17. Brown, N.J., J. Johansson, and A.E. Barron, *Biomimicry of Surfactant Protein C*. Accounts of Chemical Research, 2008. **41**(10): p. 1409-1417.
18. Amblard, M., et al., *Methods and Protocols of modern solid phase peptide synthesis*. Molecular Biotechnology, 2006. **33**(3): p. 239-254.
19. Merrifield, R.B., *Solid Phase Peptide Synthesis .1. Synthesis Of A Tetrapeptide*. Journal of the American Chemical Society, 1963. **85**(14): p. 2149-&.
20. Cudic, P. and M. Stawikowski, *Pseudopeptide synthesis via Fmoc solid-phase synthetic methodology*. Mini-Reviews in Organic Chemistry, 2007. **4**(4): p. 268-280.
21. Kuisle, O., E. Quinoa, and R. Riguera, *Solid phase synthesis of depsides and depsipeptides*. Tetrahedron Letters, 1999. **40**(6): p. 1203-1206.
22. Kisfaludy, L. and I. Schon, *Preparation And Applications Of Pentafluorophenyl Esters Of 9-Fluorenylmethyloxycarbonyl Amino-Acids For Peptide-Synthesis*. Synthesis-Stuttgart, 1983(4): p. 325-327.
23. Fan, W., et al., *Enhanced Brain Targeting of Tegafur Using Novel Lactyl Cholesterol Liposome as a Carrier*. Letters in Drug Design & Discovery, 2009. **6**(7): p. 542-547.
24. Katritzky, A.R., et al., *N-Fmoc-protected(alpha-dipeptidoyl)benzotriazoles for efficient solid-phase peptide synthesis by segment condensation*. Chemical Biology & Drug Design, 2008. **72**(3): p. 182-188.
25. Avan, I., et al., *Benzotriazole-Mediated Syntheses of Depsipeptides and Oligoesters*. Journal of Organic Chemistry, 2011. **76**(12): p. 4884-4893.
26. Nguyen, M.M., N. Ong, and L. Suggs, *A general solid phase method for the synthesis of depsipeptides*. Organic & Biomolecular Chemistry, 2013. **11**(7): p. 1167-1170.

## **Chapter 3. Self-Assembly of Depsipeptides into Spherical Structures, Fibers, or Hydrogels**

### **3.1 CHAPTER SUMMARY**

#### **3.1.1 INTRODUCTION**

Depsipeptides are a unique class of materials that incorporate esters in the peptide backbone and have potential as self-assembling materials for tissue engineering scaffolds. Depsipeptides have been studied as polydepsipeptides for biomaterials or as models to investigate the folding and self-assembling studies of peptides with ester substitutions.

Self-assembling peptide systems can be categorized as natural or unnatural systems. Natural systems are based on structures of known natural existing proteins, such as  $\beta$ -sheets,  $\beta$ -turns,  $\alpha$ -helices, and coiled-coils. In general, self-assembly into a gel based on a number of factors including the ionic strength of the solution, peptide length, peptide sequence, temperature, and pH. Unnatural systems include peptide families that incorporate the covalent linking of other molecules, peptide amphiphiles, or  $\pi$ - $\pi$  interactions.

#### **3.1.2 Goals**

The goal of this work is to observe the self-assembly of depsipeptides into biologically relevant hydrogels. The depsipeptides under investigation are designed with hydrophilic and hydrophobic groups that have been shown to promote higher order structures with different families of peptides. Investigation of these structures will support the notion that self-assembling materials are not isolated to structures with native peptide backbones.

### **3.1.3 Approach**

Gelation was investigated for depsipeptides 1-6 under various ionic concentrations and pH values. The self-assembly process was analyzed with emission spectra, IR, CD, and TEM. Emission spectroscopy was used to observe the orientation of the fluorenyl group. IR and CD are commonly used methods to detect the secondary structure of proteins and peptides. These strategies are based on X-ray crystallography data from native peptide backbones, thus folding patterns such as those seen for  $\alpha$ -helices,  $\beta$ -sheets, and random coils may not be applicable to our system. Instead, these methods were used to detect the differences between two depsipeptides or changes in orientation due to environmental conditions. TEM was used to observe the morphology of the nanostructures under various pH, ionic concentrations, and depsipeptide concentrations over time.

### **3.1.4 Results**

The self-assembly of peptides into higher order structures, such as hydrogels, is a dynamic process. A common feature of self-assembling families is the order of the chemical groups, often identified by the secondary structure of the peptide under various environmental conditions. Results show that the order of depsipeptides influenced the formation of higher order structures into micelles, fibers, or hydrogels. Spherical nanostructures were observed in depsipeptide (3) when prepared in a high ionic solution at pH 7. The fluorenyl groups were oriented in a parallel manner, which has been reported to promote the formation of micelles in Fmoc-dipeptides. Depsipeptide (5) was the only structure within the reported synthetic library that formed a gel under certain

conditions. Gels were observed as soon as 18 hours or after 3 weeks. The formation of fibers were also detected in non-gelling samples of depsipeptide (5). The structures of the longest sequences within our library, depsipeptide (4) and (6), did not show signs of gelation.

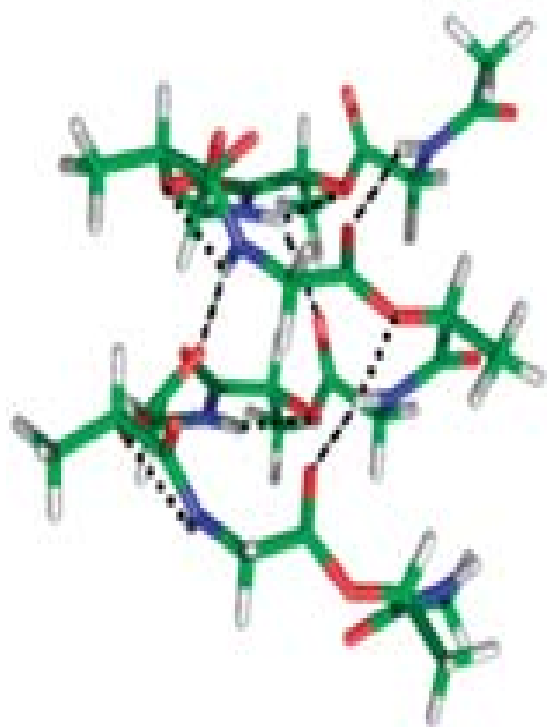
## **3.2 BACKGROUND**

### **3.2.1 Depsipeptides as Self-Assembling Materials**

Ester substitutions within peptides are a common strategy to analyze protein folding, function, and self-assembly [1, 2]. Peptide folding and self-assembly is driven by non-covalent interactions such as hydrogen-bonding,  $\pi$ - $\pi$ , electrostatic, or hydrophobic interactions between peptides, peptide side chains, and/or terminal protecting groups. The incorporation of esters into the peptide backbone reduces the potential for hydrogen bonding interactions, however depsipeptides have been shown to form a variety of ordered secondary structures. In the case of the family of (Leu-Leu-Lac)<sub>n</sub> residues, secondary structure is dependent on the length of the repeating unit [3-5]. Crystals of the depsipeptides were formed under various solvent conditions, and under x-ray crystallography, a transition from  $\beta$ -strands to  $\alpha$ -helices was observed when n=3. A computational study of a (Gly-Lac)<sub>6</sub> and (Lys-Lac)<sub>6</sub> show the potential for regular, helical folding patterns (Figure 3.1) using quantum mechanics calculations and molecular modeling [6]. Under simulated annealing, (Gly-Lac)<sub>6</sub> folded into well-defined, left-handed and right-handed helices, while (Lys-Lac)<sub>6</sub> formed a polyproline-II like helical structure.



A



B

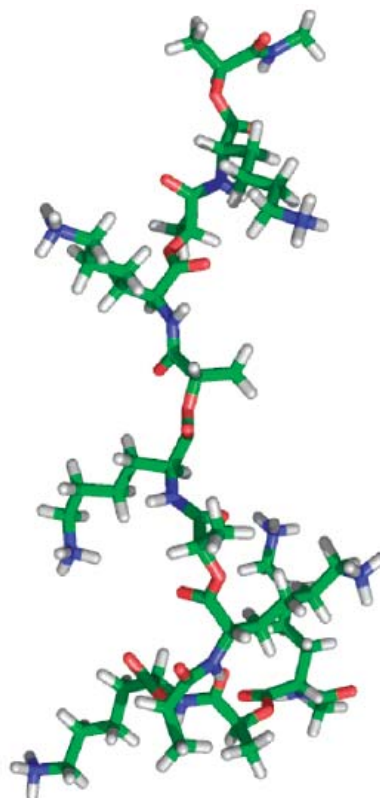


Figure 3.1 Molecular dynamics model of (Gly-Lac)<sub>6</sub> (A) and (Lys-Lac)<sub>6</sub> (B). (Gly-Lac)<sub>6</sub> (A) folds into a left- or right-handed helix and (Lys-Lac)<sub>6</sub> has a polyproline II-type structure. Used with permission. [6]

Hydrogel formation from depsipeptides of amyloid derivatives was dependent on the number and location of the ester substitutions within the 10 residue sequence [2]. Specifically, amylin(20-29) derivatives were modified at positions 24, 26, and 28 by incorporation of ester bond moieties (Figure 3.2). These newly designed amylin derivatives did not form traditional amyloid fibrils but gave rise to the formation of helical ribbons and peptide nanotubes, as observed by transmission electron microscopy (TEM). Amyloid fibril formation of the modified depsipeptides was unexpected, as a single amide bond replacement prevented gelation. Interestingly, the depsipeptide did not exhibit beta-sheet conformation, which is traditionally observed for amylin fibers. These results suggest that self-assembly is sensitive to the location of the ester substitution, and that folding other than  $\beta$ -sheet character is responsible for the self-assembly of the depsipeptide derivative .

### **3.2.2 Self-assembling peptides: Families and mechanisms**

#### ***3.2.2.1 Amphiphilic peptides: balance of charge and hydrophobicity***

A unique family of short self-assembling peptides with alternating hydrophobic and hydrophilic residues have been termed EAK, RAD, and KFE, based on the repeat of amino acids and are well cited in the literature [7] [8-10]. EAK16-II was first discovered while studying the left-handed Z-DNA binding protein zuotin [11].



CD studies of EAK16-II indicate strong  $\beta$ -sheet characteristics, suggesting the hydrophobic Ala side chains are on one side of the sheet and the charged Lys and Glu side chains are on the other. The  $\beta$ -sheet conformation further proposes that complementary patterns with pairs of positively and negatively charged ionic groups may be staggered, promoting specific interactions and packed fibril formations.

The self-assembly of EAK16-II motivated the design of other peptides within this family. For example, RAD-I replaces the positively charged Lys residue with Arg and the negatively charged Glu with Asp. RAD-1 has been shown to promote vascularization and the recruitment of endothelial cells in a rabbit heart model [12] and is now commercially available as PuraMatrix. RAD-I organizes into a hydrophobic and hydrophilic face, similar to the EAK16-II peptide. The structure adopts a  $\beta$ -sheet configuration through self-complementary ionic interactions, resulting in ordered nanostructures, which further assemble to form the nanofiber scaffold (Figure 3.3).

Predicting the self-assembly of a material is not straight forward, as illustrated by the folding studies of KFE [13]. Replacing Ala with Phe results in a more hydrophobic peptide, resulting in slightly different self-assembly trends. The driving forces for the self-assembly of KFE12 is driven by the hydrophobic nature of Phe groups and efficient masking of the charged side chains under various conditions. The critical coagulation concentration (CCC) was observed for KFE8, KFE12, and KFE16 (Figure 3.3). The KFE8 and KFE16 exhibit the same CCC, while KFE12 has a lower value from 0.1-1.0 mM NaCl.

Name	Sequence
EAK16-II	AEAEAKAKAEAEAKAK
RAD16-I	RADARADARADARADA
RAD16-II	RARADADARARADADA
KFE12	FKFEFKFEFKFE
KIE12	IKIEIKIEIKIE
KVE12	VKVEVKVEVKVE
KFE8	FKFEFKFE
KFE16	FKFEFKFEFKFEFKFE

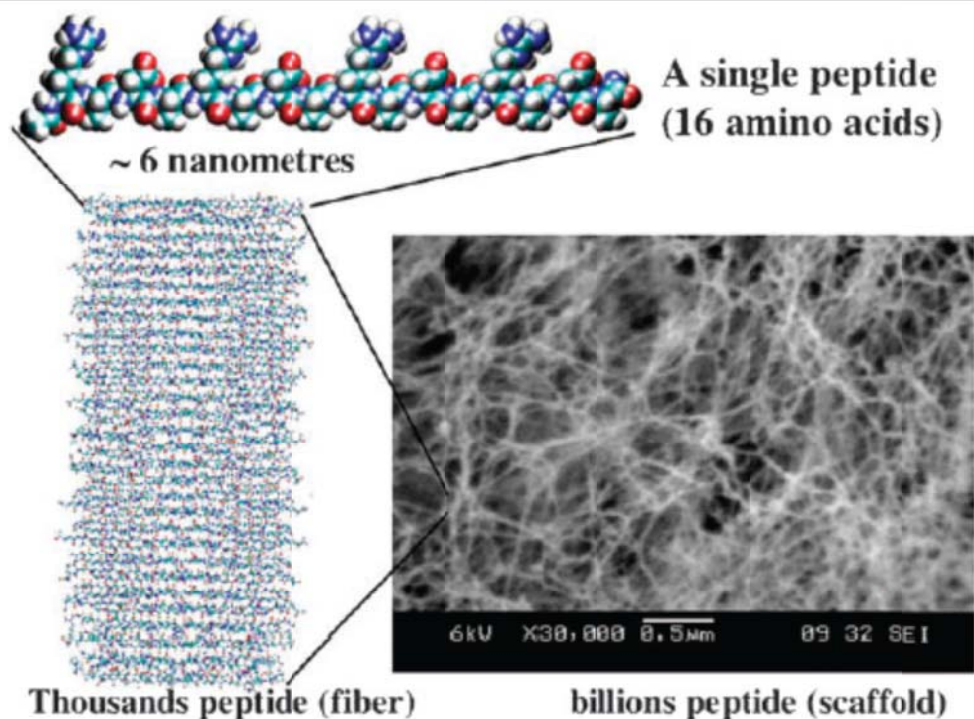


Figure 3.3 Sequences of self-complementary peptides derived from EAK-peptides. The self-assembling process of peptide RAD16-I into a nanofiber scaffolding hydrogel is driven by the interactions of many individual peptides. Used with permission. [14, 15].

Consistent with other peptide families in this system, each molecule must pack together as a  $\beta$ -strand with other oligopeptides to form a  $\beta$ -sheet, suggesting that KFE8 is not long enough to maintain this structure. On the other hand, KFE16 may cause the bond angles to become less flexible, preventing the stabilization of  $\beta$ -strand due to chain entanglements. These results suggest that an optimal length for peptide systems exist, and increasing the number of ionic interactions does not necessarily drive self-assembly.

Analysis of self-assembled structures often focuses on changes to physical properties or secondary structure. However, these factors may not have the same influences on morphology. RAD16-1 was found to assemble into a gel after dissolved in water and Tris-HCl buffer, as observed with circular dichroism (CD) and AFM [16]. The samples were exposed to 30 minutes of sonication, which can break hydrogen, ionic, and hydrophobic bonds. While analysis with CD shows that  $\beta$ -sheet characteristic was maintained under all tested conditions, the fiber length was significantly shortened from microns to the nanometer scale (Figure 3.4). The fibers reassembled to original dimensions after 2 hours. Similar trends were observed with the same peptide under pH changes [17]. CD results indicate that  $\beta$ -sheet structures were maintained within a broad range of pH values, with a slight increase in unordered folding from pH 4.5-9.5. Within this pH range, the presence of both short nanofibers and aggregates were observed. The distorted  $\beta$ -strand and unordered structures seen at higher pH may due to the formation of salt bridges. These results suggest that careful selection of analysis techniques must be considered to investigate self-assembling peptides, as secondary folding data may not accurately reflect the morphological changes of the fiber networks.

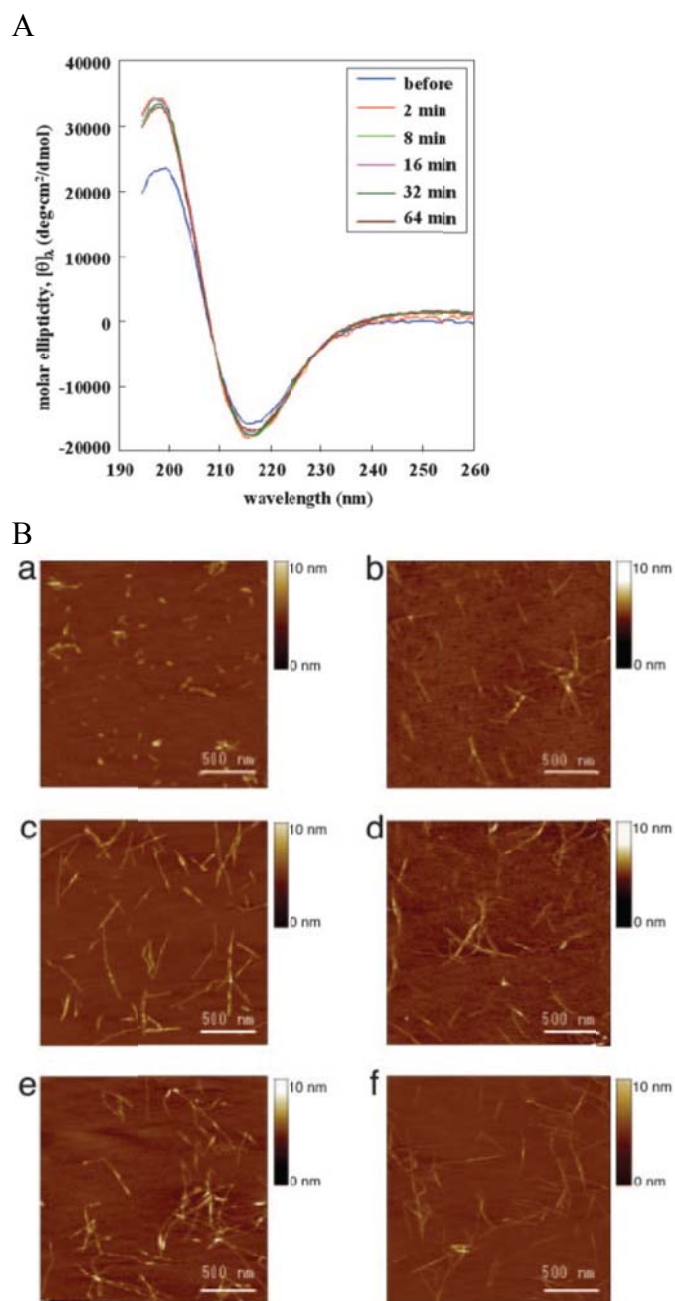


Figure 3.4 CD and AFM of RAD16-I after sonication. CD shows  $\beta$ -sheet spectra for all conditions (A). AFM images of RAD16-I (B) were collected after sonication: 1 min (a), 2 min (b), 8 min (c), 16 min (d), 32 min (e), and 64 min (f). Used with permission. [16]

### ***3.2.2.2 Fmoc-peptides: role of aromatic interactions that drive self-assembly***

Self-assembly has been studied on short peptide structures with conjugated aromatic groups at the N-terminal, such as with Fmoc or naphthalene. The next section will discuss the organizational properties associated with Fmoc-peptides families.

These small molecules should be easily removed through the renal system upon implantation as biomaterials, making them ideal for tissue engineering applications. Investigation of Fmoc-peptides as implantable materials was motivated from the study of 12 Fmoc-amino acids as anti-inflammatory agents [18]. Within a range of inflammation models in animals, the activities of the Fmoc-amino acids were shown to block recruitment of T-lymphocytes and neutrophils from inflammatory lesions and also inhibit enzymes in the synthetic pathway.

Fmoc-peptides are relatively small molecules, with a molecular weight of less than 1000 Da and usually self-assemble in water to form long, fibrous structures. In general, the ability to form a stable gel is determined by the overall hydrophobicity of the Fmoc-dipeptide [19]. Gelation was investigated in with Fmoc-dipeptides composed of Gly, Ala, Val, Leu, or Phe. Syneresis was observed in less hydrophobic Fmoc-dipeptides while self-supporting gels resulted within the intermediate hydrophobic structures and very hydrophobic structures. In addition, the dipeptides were found to assemble at different rates, possibly due to differences in  $pK_a$ .

The fluorenyl group plays an important role in self-assembly into hydrogels within these short peptide families. The mechanism of self-assembly leading to hydrogelation has been proposed on Fmoc-Phe-Phe [20-22] which has found to be



generally consistent for a range of gelled Fmoc-dipeptides. It is important to note that while the Fmoc-group helps in the ordering of the peptide backbone, the residues of the side chains can affect gelation and gelation strength. The Fmoc-Phe-Phe model proposes the peptide as a dimensional ribbon, formed by lateral association of nanotubes (Figure 3.5). This hierarchical assembly is based on the secondary structure data collected from IR, fluorescence, and CD [21]. IR data suggest that anti-parallel  $\beta$ -sheets are formed between dipeptides while emission spectra reveal that the Fmoc groups are stacked in an anti-parallel manner. CD analysis shows induced chirality of the Fmoc groups as well as a signal consistent with the formation of  $\beta$ -sheets. The model suggests that pairs of Fmoc-Phe-Phe structures are stacked in an anti-parallel sheet with another stack of Fmoc-Phe-Phe pairs positioned alongside the first sheet. The arrangement is staggered by one peptide, allowing the fluorenyl groups to interlock. The second sheet is rotated such that the fluorenyl groups interact along their full length and this twist, along with the incorporation of additional  $\beta$ -sheets, form a cylinder. This higher order structure has a width of approximately 30Å, 28 monomers per turn, and an inner diameter of 7Å diameter. The dimensions of the model were confirmed with TEM and WAXS.

Derivatives of Fmoc-Phe-Phe gels have been investigated by incorporating Fmoc-Arg-Gly-Asp within multicomponent systems [23]). Similar to the Fmoc-Phe-Phe model, the peptide sequences are self-assembled through inter-molecular hydrogen bonds forming anti-parallel  $\beta$ -sheet structures (Figure 3.6 ). The Fmoc-groups on both peptides interacted with one another and formed  $\pi$ - $\pi$  stacks to interlock the  $\beta$ -sheets.

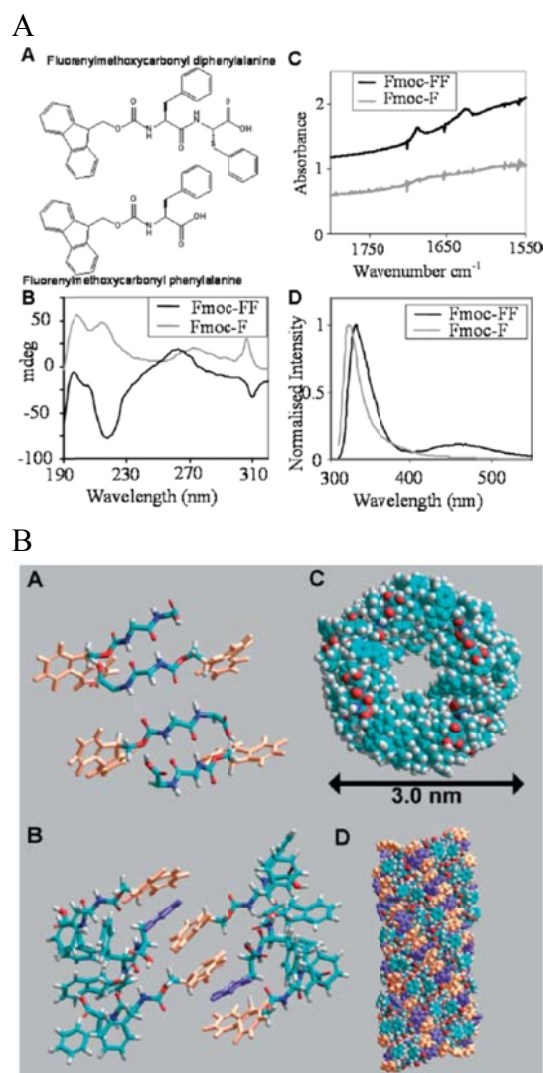


Figure 3.5: Molecular (A) and self-assembled structure (B) of Fmoc-FF. Fmoc-F was used to observe signals in a non-gelling sample. CD spectra show a minimum at 218 nm for Fmoc-FF, which indicates beta-sheet structure (b). FTIR of Fmoc-FF show two distinct peaks at 1630 and 1685  $\text{cm}^{-1}$ , which is consistent with an anti-parallel  $\beta$  sheet (c). Fluorescence emission spectrum of Fmoc-FF shows a peak-shift from 320 to 330 nm to higher wavelength indicating excimer formation and a new broad peak at 460 nm indicating the formation of higher order aggregates (d). A model structure was created to illustrate the self-assembly of Fmoc-FF into nanofibers (B). Details are provided in the text. In (a), (b), and (d), fluorenyl groups are colored orange and the phenyl groups are colored purple to illustrate the paired pi-stacked nature of the fluorenyl groups. Used with permission. [21]

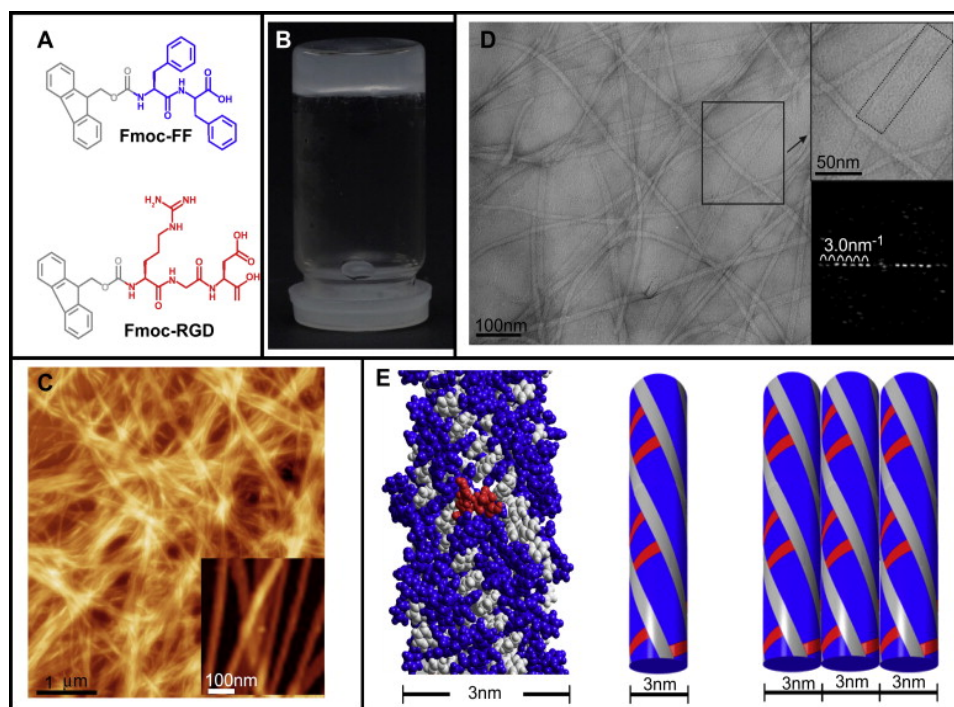


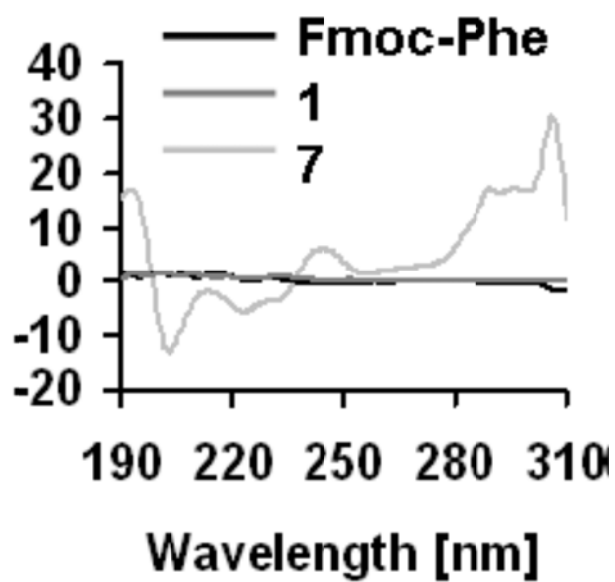
Figure 3.6 The self-assembled hydrogel of Fmoc-FF/RGD. The chemical structures of the hydrogel building blocks (A). Upon mixing, Fmoc-FF and Fmoc-RGD self-assemble into a translucent hydrogel at 37°C (B) AFM shows an overlapping mesh of nanofibers, with bundles and entanglements (C) while TEM shows that the nanofibers as ‘flat ribbons’ (D). The proposed supramolecular model demonstrates the formation of the 3 nm fibrils and their further lateral assembly into larger ribbons (E). RGD sequences are presented on the fiber surface in red and the FF peptides are illustrated in blue. Used with permission. [23]

As illustrated with the Fmoc-Phe-Phe model, the inherent twisted nature of  $\beta$ -sheets led to a cylindrical structure of 3 nm in diameter. These then further extended longitudinally into a supramolecular nano-fibrils with Arg-Gly-Asp sequences presented at the surface, aligning parallel to each other into larger flat ribbons. As suggested by the model, the exposure of the Arg-Gly-Asp sequences may present high accessibility to the cells.

The fluorenyl groups of Fmoc-dipeptides is a strong factor for self-assembly. A library of seven Fmoc-dipeptides was evaluated as gels for cell culture [20]. The samples were prepared by suspending Fmoc-dipeptides derived from with Gly, Ala, Leu, and Phe in purified water. Gelation was highly dependent on the interaction of the fluorenyl groups, as CD of all gels gave rise to peaks indicative of  $\pi$ - $\pi$  transitions in the Fmoc structure. In samples that did not form gels, no contribution from the aromatic region was observed with spectroscopic methods. Chondrocytes in either culture media alone or with Fmoc-dipeptides show cell proliferation for up to 7 days under both methods (Figure 3.7).

An important driving force in Fmoc-dipeptide self-assembly is the orientation of the fluorenyl group, but the design rules dictating assembly is not clear. For example, Fmoc-Phe-Gly forms a gel under 2 conditions while a simple change in the sequence to Fmoc-Gly-Phe does not [19]. In addition, a computational model of Fmoc-Ala-Ala suggests that self-assembled organizations converge into a condensed fibril structure mainly driven by stacking of Fmoc groups and hydrogen bonding between residues and with water rather than a hollow nanofiber [24].

A



B

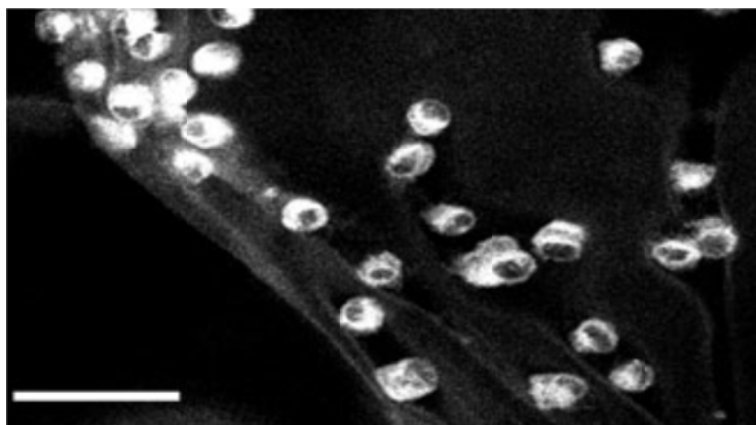
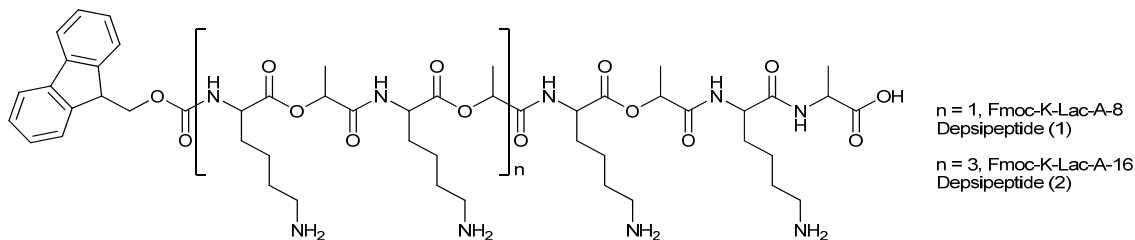


Figure 3.7 Circular dichroism (CD) spectra of Fmoc-Phe and structures 1 and 7 at pH 7 (A). 1 is Fmoc-Gly-Gly and 7 is Fmoc-Phe-Phe. Gel 7 shows the presence of  $\pi$ - $\pi$  interactions between fluorenyl groups. The y-axis represents molar ellipticity and is in units of mdeg. Two-photon fluorescence microscopy shows the presence of DAPI-stained cells within the hydrogel structure of Fmoc-Phe-Phe (B). Scale bar: 50  $\mu$ m. Used with permission. [25]

These results further illustrate the complexity of self-assembly and how changes in hydrophobicity and environmental conditions affect the kinetics of the organizational process.

### 3.3 RESULTS

#### 3.3.1 Depsipeptides (1) and (2): Effect of weak hydrophobic residues on charged residues



No gelation was found for depsipeptides (1) and (2) under conditions A – H (Table 3.1). The emission spectrum of depsipeptide (1) does not differ from the fluorescence data of the starting materials (Figure ). Gelation of short peptide families is often influenced by the degree of hydrophobicity of the side chains. For example, gelation with alternating Val, Leu, or Ala with Lys was investigated on various peptide lengths in water and saline concentrations [26]

Rigid gels were formed with peptides Leu-Lys-13, Val-Lys-9, Val-Lys-11, and Val-Lys-13 sequences. Ala-Lys-13 did not gel under the tested conditions, which further supports the influence of hydrophobicity on self-assembly. Interestingly, Val-Lys-10 and Val-Lys-12 also did not gel. The even numbered sequences have positive charges at both ends of the sequence, which may affect gelation in this system.

Solution	Conditions	Osmolarity (mmol/kg)
A	PBS, pH 6	295
B	PBS, pH 7	302
C	PBS, pH 8	303
D	PBS, pH 9	301
E	PBS + 10 mM NaCl, pH 6	510
F	PBS + 10 mM NaCl, pH 7	520
G	PBS + 10 mM NaCl, pH 8	520
H	PBS + 10 mM NaCl, pH 9	504

Table 3.1 Summary of self-assembly tests on depsipeptide (1) and depsipeptide (2). No gelation was observed. As a reference, physiological osmolarity is around 280-310 mmol/kg.

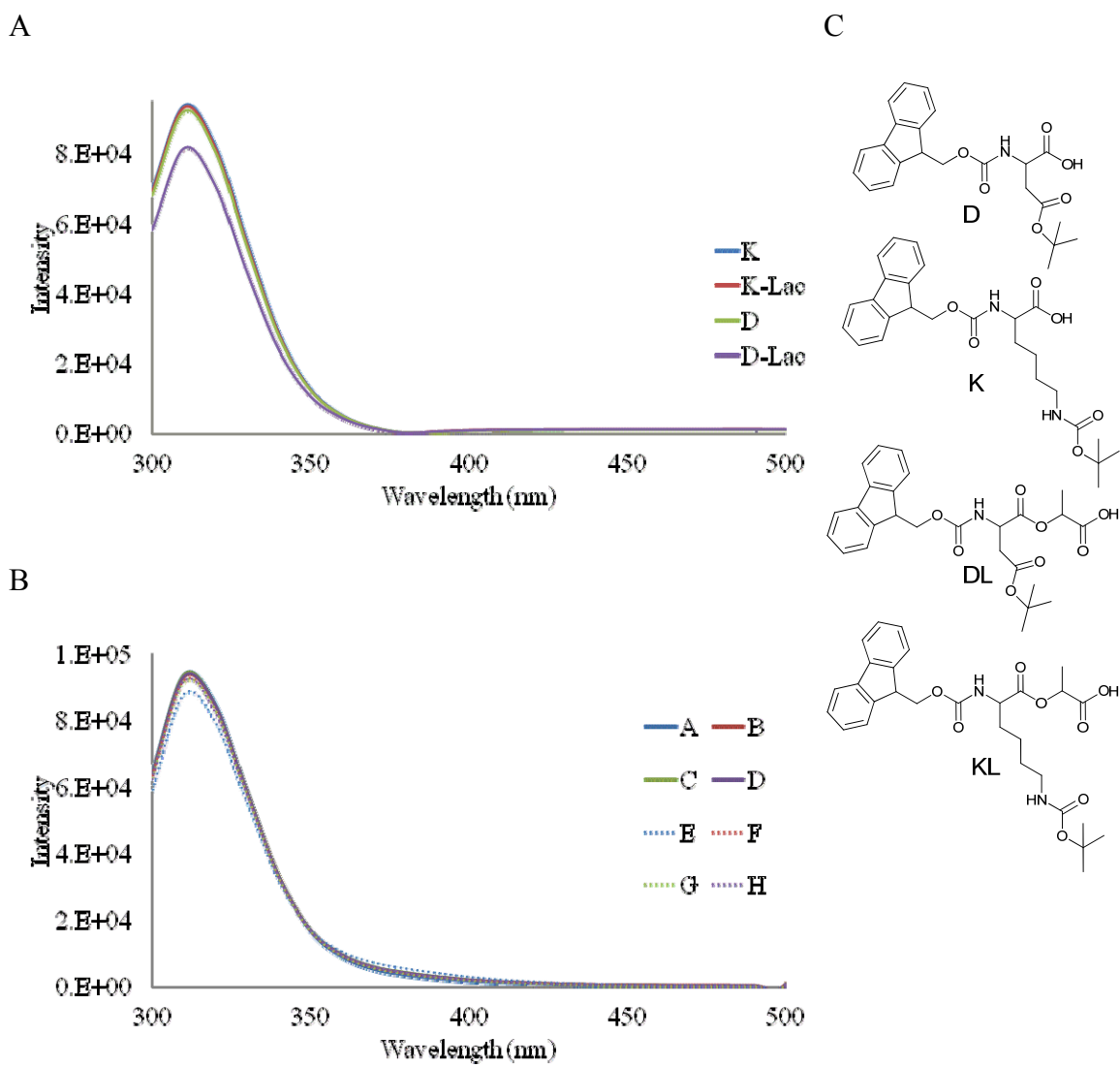
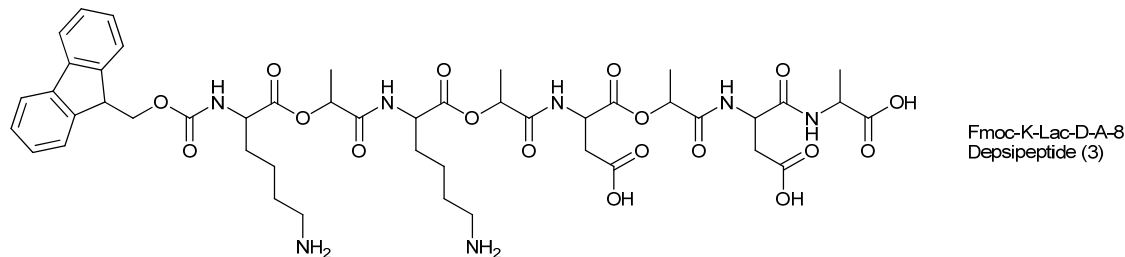


Figure 3.8 Emission spectra of Fmoc-peptides and Fmoc-depsidipeptides (A) and Fmoc-K-Lac-8 (B). The chemical structures and short-hand labels for the Fmoc-peptides and Fmoc-depsidipeptide are provided (C).



However, when N-terminal of Val-Lys-10 was capped with an acetyl group, the peptide sufficiently self-assembled to a gel [27].

### 3.3.2 Depsipeptide (3): Formation of spherical nanostructures



Depsipeptide (3) also did not form a gel under conditions A-L at 10 or 20 mg/ml (Table 3.2). The emission spectrum show no dependence on pH or salt concentration, however the 20 mg/ml samples yield a higher intensity at 370 nm (Figure A). Peaks within this region have been reported as parallel-alignment of the fluorenyl groups, which contribute to the self-assembly of select Fmoc-dipeptides into micelles [28, 29], with the Fmoc groups inside the core and the hydrophilic groups are in contact with the solvent (Figure 3.9 E). It is interesting to note that the broad shoulder at 370 nm observed in the emission spectra is absent in depsipeptide (1) (Figure 3.8), suggesting that the addition of Asp residues contributes to the parallel stacking of the fluorenyl groups.

The CD spectra of depsipeptide (3) shows increased chiral character in the concentrated depsipeptide samples (Figure 3.9 B). The negative peak at 234 nm does not correlate to commonly characterized secondary structures, although the peak patterns of the starting materials are quite similar. Charge repulsions or steric hindrance of the Lys side chains may prevent this structure to gel.

Solution	Conditions	Osmolarity (mmol/kg)
A	PBS, pH 6	295
B	PBS, pH 7	302
C	PBS, pH 8	303
D	PBS, pH 9	301
E	PBS + 10 mM NaCl, pH 6	510
F	PBS + 10 mM NaCl, pH 7	520
G	PBS + 10 mM NaCl, pH 8	520
H	PBS + 10 mM NaCl, pH 9	504
I	PBS + 2.5 mM NaCl, pH 6	337
J	PBS + 2.5 mM NaCl, pH 7	349
K	PBS + 2.5 mM NaCl, pH 8	346
L	PBS + 2.5 mM NaCl, pH 9	346

Table 3.2 Summary of self-assembly tests on depsipeptide (3). Spherical nanostructures were observed in solution F. As a reference, physiological osmolarity is around 280-310 mmol/kg.

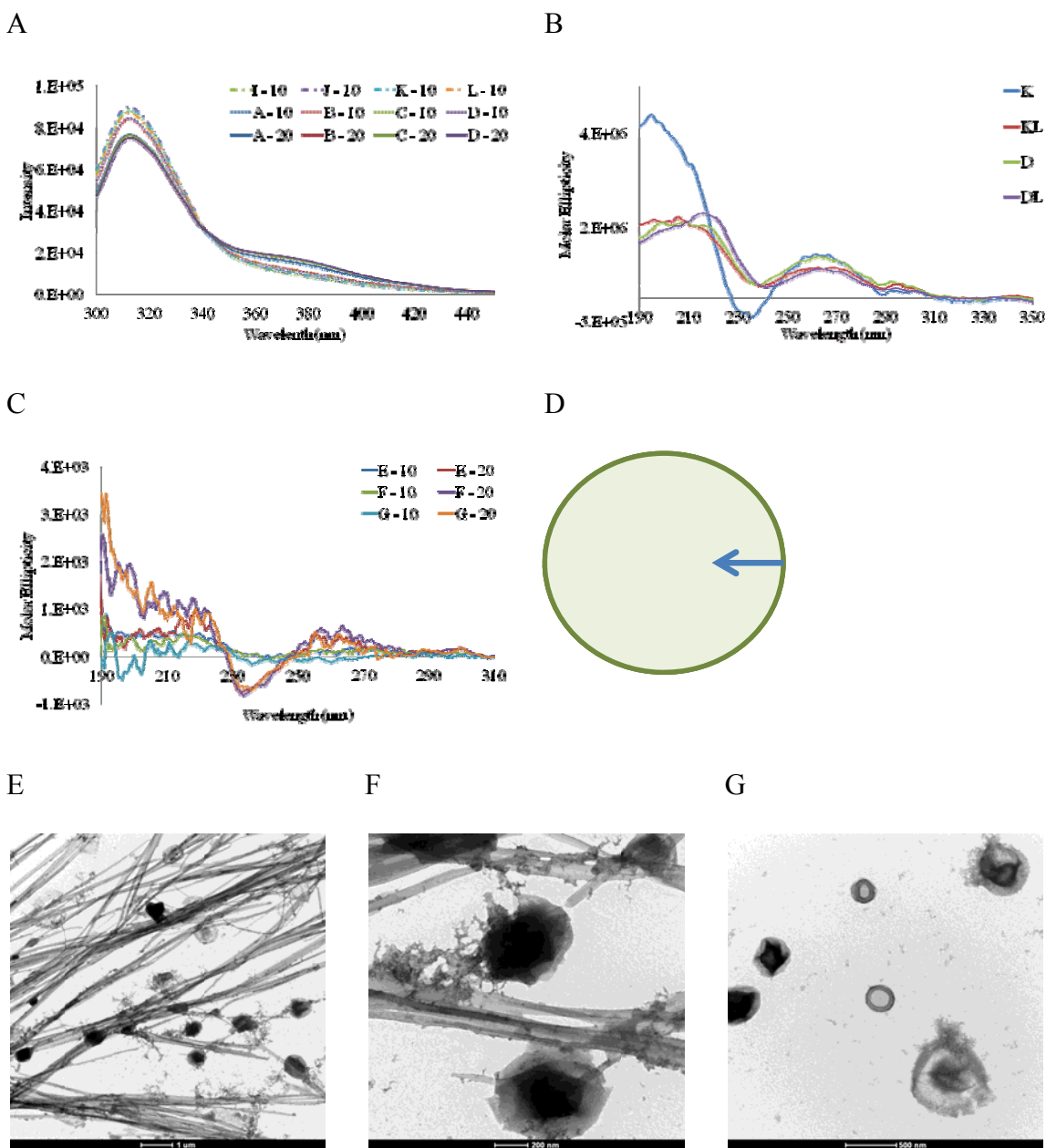
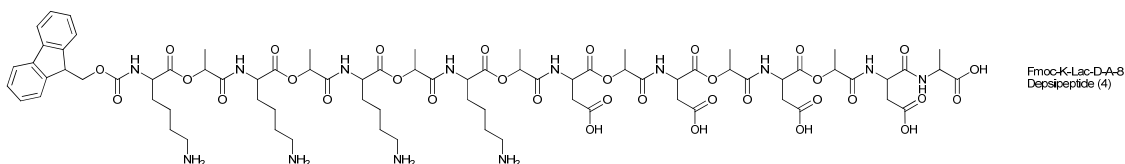


Figure 3.9 Self-assembly data of depsipeptide (3). Emission spectra (A), CD spectra of Fmoc-peptides and Fmoc-depsidipeptides (B), CD of depsidipeptide (3) (C) and TEM (E-G) of depsipeptide 3. The molar ellipticity of the CD data is in units of  $\text{deg cm}^2/\text{dmol}$ . Parallel alignment of fluorenyl groups within Fmoc-dipeptide families have been reported to self-assemble to form the hydrophobic core of micelles [29], as illustrated by the cartoon model (D).

For example, Fmoc-KKRGDK did not form a gel in ionic solutions within the pH range of 4-11, while Fmoc-GRDGG and Fmoc-VRDGV gelled at pH 3.4 (Xu, J Phys Chem, 2010). Authors suggest that the balance between hydrophobicity and hydrophilicity was extremely important for gelation, and that the polar characteristic of the Lys residue was not a driving force towards self-assembly.

The morphology of depsipeptide (3) was investigated with TEM with 20 mg/ml samples in sample F (Figure F-H). The sample was aged for over 4 weeks and show the presence of both straight fibers and spherical nanostructures with dimensions of about 50 and 250 – 500 nm in diameter, respectively. The self-assembly of the spherical nanostructures is supported by earlier reports of micelle formation for Fmoc-families [29], although the formation of the fibers is not easily explained. It is possible that depsipeptide (3) forms fibers within weeks of sample preparation, but additional experiments are needed to understand the self-assembly process. Future observations of these formations will be evaluated at earlier time points to investigate the effect of morphology on depsipeptide concentration. Dynamic light scattering tests will also be used to monitor the possible transition of spherical particles into fibers.

### 3.3.3 Depsipeptide (4): Ordered morphology within ionic solutions



Preliminary data on depsipeptide (4) was investigated with TEM after 18 hours at pH 7 under various ionic concentrations (Table 3.3). Gelation was not evident after 18 hours when prepared in solutions B, F, and W. TEM images show unordered aggregates in solution W (Figure 3.10). Upon the addition of salt, samples in solution B show globular-like aggregates with diameters of about 25 nm while higher order aggregates are observed upon the addition of 10 mM NaCl in solution F. Possible formation of these aggregates was captured in the F solution. Short fiber-like structures, 200-500 nm in length are found within the unordered aggregates and begin to form an interlaced-like network. These fibers are relatively flexible with lengths in the microns.

The formation of fibrils from spherical structures has been reported with amyloid peptides [30] and could offer insight on the self-assembly of depsipeptide (4). The purified protein contained oligomers as granular particles in 20-25  $\mu\text{m}$  in diameter, and grew to 35-40 nm just before fusion. Immediately after fusion, the diameter of the resulting particle was reduced to 20-25 nm while the length increased to 110 nm. Changes to the morphology dimensions indicate structural reorganization, which most likely involves changes in hydrogen-bonding. Elongation continued to give fibers up to 1  $\mu\text{m}$  in length with a further reduction in diameter to 17-20 nm. On day 9, the fiber grew to more than 4  $\mu\text{m}$ , but the diameter remained constant. While the TEM images collected on depsipeptide (4) do not show evidence of lateral fusion between particles, it is clear that well-defined fibers are sprouting from the unordered aggregates.

Solution	Conditions	Osmolarity (mmol/kg)	Observations
B	PBS, pH 7	302	Globular aggregates
F	PBS + 10 mM NaCl, pH 7	520	Short fibers
W	Water	30	Unordered aggregates

Table 3.3 Summary of self-assembly experiments on depsipeptide (4) at 10 mg/ml. As a reference, physiological osmolarity is around 280-310 mmol/kg

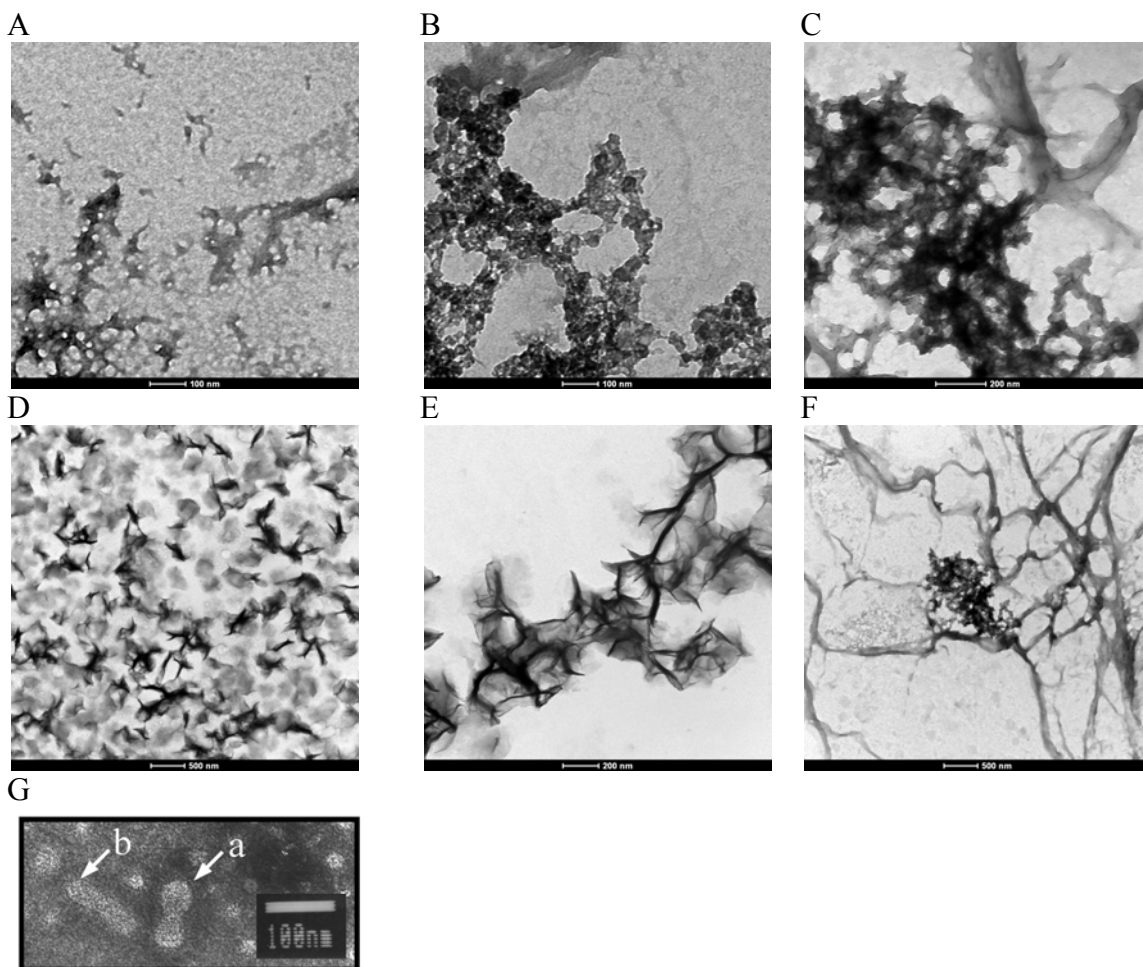
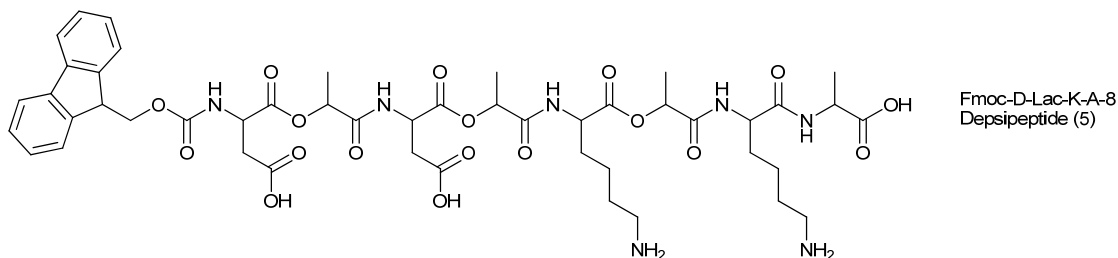


Figure 3.10 TEM images of depsipeptide (4). The sample in water (A), PBS (B), PBS and 10 mM NaCl (C-F). The formation of amyloid fibers may provide insight on the self-assembly processes of depsipeptide (4), as seen with the lateral growth of granular aggregates into amyloid fibers (G). Used with permission. [30]

Further examination on the self-assembly of depsipeptide (4) would include time-dependent analysis with emission, IR, and CD to observe changes in hydrogen-bonding patterns. DLS studies would also be used to monitor fiber formation.

### 3.3.4 Depsipeptide (5): Self-assembly of a novel gel structure

#### 3.3.4.1 Gelation in ionic concentrations from pH 6-9



Gelation was observed in depsipeptide (5) after 2 days in solutions F-H and after 6 days in solutions A-D (Table 3.4). After 2 days, the samples were observed under fluorescence. The gelled samples show a slight red shift from 310 nm to 330 nm as well as a decrease in intensity (Figure 3.11). The appearance of the shift at 330 nm is representative of anti-parallel alignment of the fluorenyl groups, which is further supported by the loss of intensity of the broad shoulder at 370 nm. Similar emission trends have been reported in Fmoc-families upon gelation [29]. Fmoc-Phe-Tyr was phosphorylated, contributing to its solubility in water. Gelation was observed upon dephosphorylation, and this transition was observed with fluorescence. Specifically, there was a loss of intensity at both 320 nm 370 nm, further supporting the observed gel formation. CD spectra of the gelled samples were collected after 2 weeks and show a unique pattern from 302 nm-250 nm.



Solution	Conditions	Osmolarity (mmol/kg)	Observations in 10 mg/ml unless noted
A	PBS, pH 6	295	Gel after 6 days
B	PBS, pH 7	302	Gel after 6 days
C	PBS, pH 8	303	Gel after 6 days
D	PBS, pH 9	301	Gel after 6 days
E	PBS + 10 mM NaCl, pH 6	510	Gel after 2 days
F	PBS + 10 mM NaCl, pH 7	520	Gel after 2 days
G	PBS + 10 mM NaCl, pH 8	520	Gel after 2 days
H	PBS + 10 mM NaCl, pH 9	504	Gel after 2 days
M	PBS + 100 mM NaCl, pH 7	447	Gel after 1 day at 5 and 20 mg/ml
N	PBS + 10 mM NaCl, pH 3	484	Flexible fibers at 20 mg/ml
O	Water, buffered to pH 3	30	No gel, flexible fibers
W	Water	30	Gel after 3 weeks

Table 3.4 Summary of self-assembly experiments for depsipeptide (5). As a reference, physiological osmolarity is around 280-310 mmol/kg.

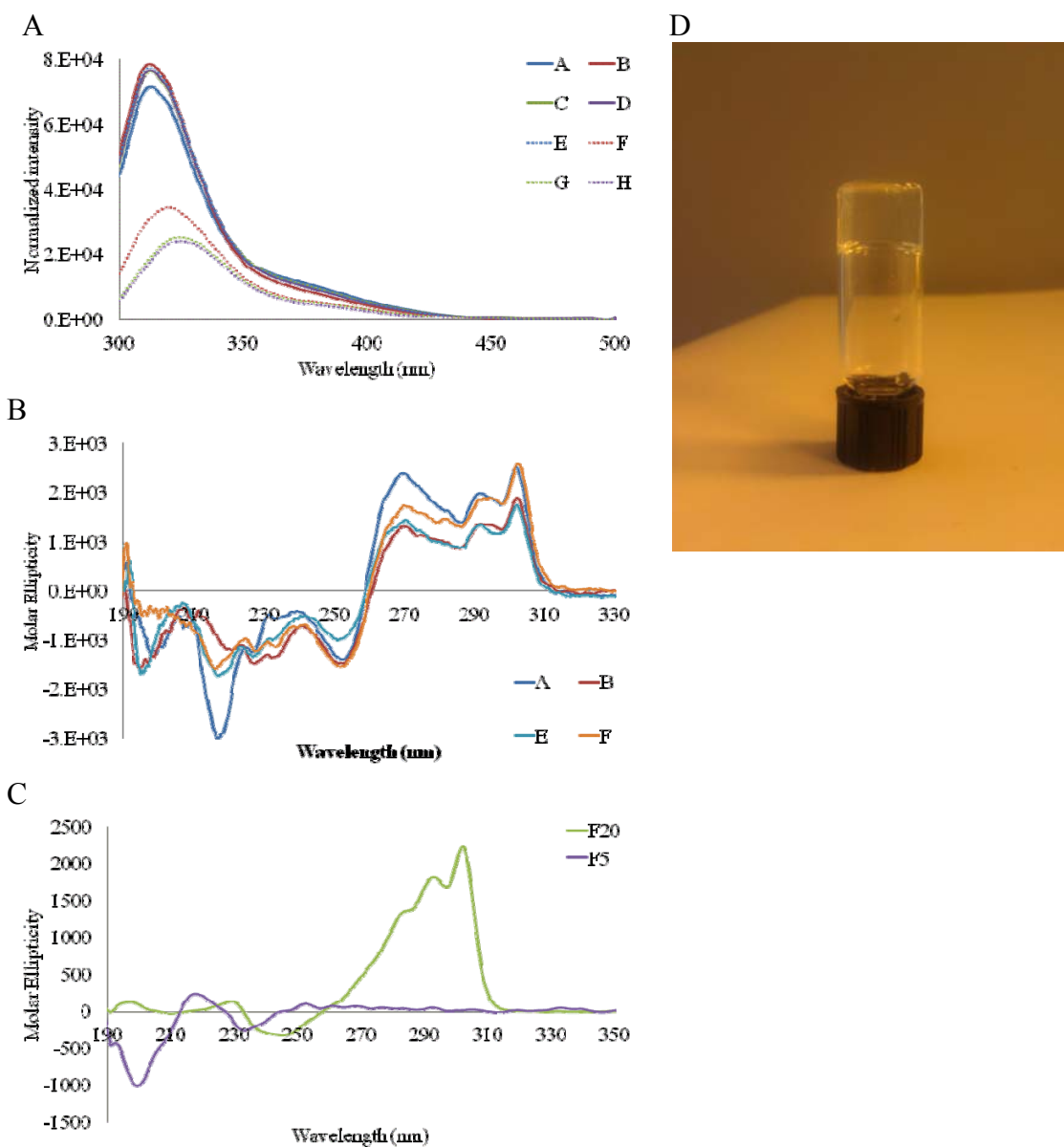


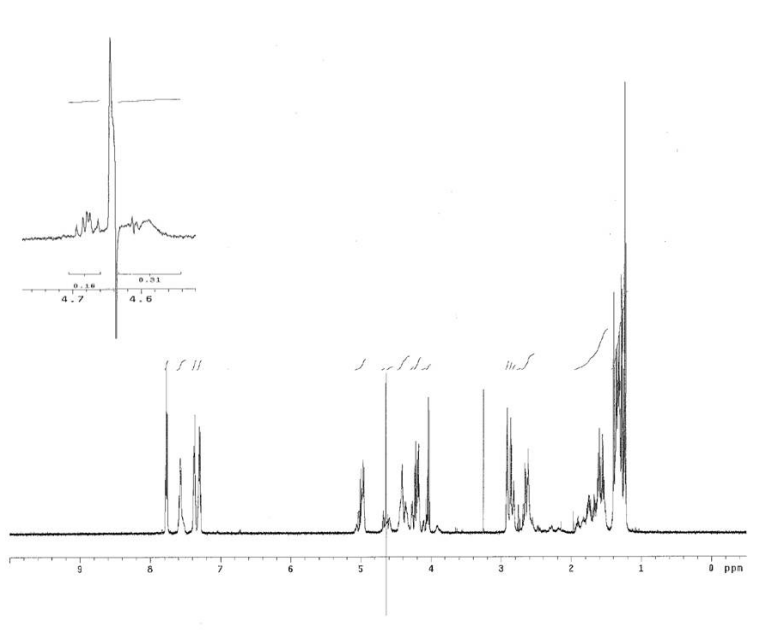
Figure 3.11 Self-assembling data for depsipeptide (5). The emission spectra (A) was collected 2 days after the sample was prepared. The peak at 330 nm is indicative of anti-parallel stacking of the Fmoc-groups. Helical packing of the fluorenyl groups is evident in the CD data collected on 5-20 mg/ml (B and C) and is consistent with data reported in other Fmoc-gelling families [31]. The sampled in its gelled form takes the shape of the vial (D). The molar ellipticity of the CD data in (B and C) is in units of  $\text{deg cm}^2/\text{dmol}$ .

CD spectra of other Fmoc-peptide families also have this unique pattern at higher wavelengths, which has been reported as helical stacking of the fluorenyl groups[31].

Depsipeptide (5) was also prepared at 5 mg/ml and 20 mg/ml in solution F, with the latter forming a gel overnight. Upon collecting the CD spectra, the gelled sample shows similar patterns at higher wavelengths while the 5 mg/ml sample has a negative peak at 200 nm, suggesting that fluorenyl packing is concentration dependent. The gelled sample was analyzed with  $^1\text{H-NMR}$  (Figure 3.12). A 10 mg/ml sample was prepared in a  $\text{D}_2\text{O}$  with PBS salts and NaCl to replicate solution F, but gelation was not observed even after 2 weeks.  $^1\text{H-NMR}$  was also collected in a 5%  $\text{D}_2\text{O}$  sample in solution F, which gelled after 4 days. Results show broadening of the chemical shifts, further supporting gel formation [32]. This is an important feature, as preparation of the samples was not successful for rheological analysis. The stability of gelled product was analyzed in buffer F with MS, and results show no significant changes after 4 days (Figure 3.13). Additional studies investigating both the enzymatic and ester hydrolysis of buffer F may be investigated in the future.

Molecular interactions of depsipeptide (3) and a gelled sample of depsipeptide (5) was investigated with IR (Figure 3.14). Interestingly, the shifts are quite different considering both structures possess the same functional groups. IR of Fmoc-peptides and Fmoc-depsidipeptides were prepared in methanol and compared against the self-assembled samples.

A



B

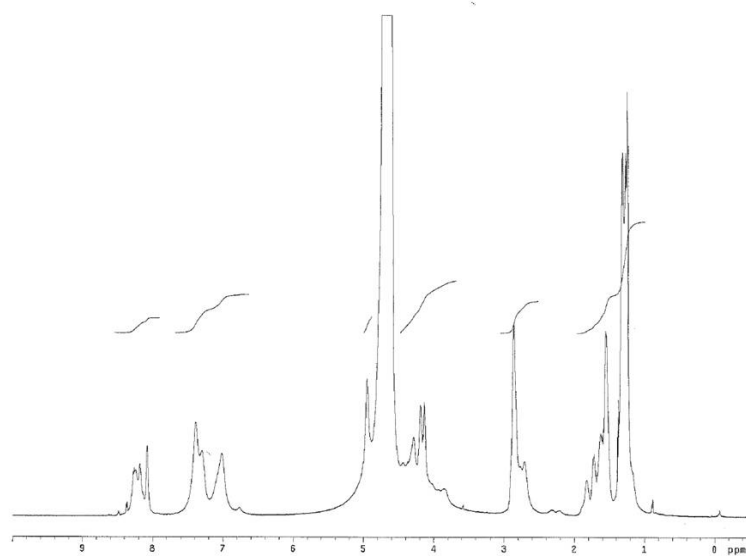


Figure 3.12  $^1\text{H}$ -NMR of depsipeptide (5) in solution (A) and in gelled (B) states. (A) was prepared in  $\text{D}_2\text{O}$  with PBS and NaCl salts and (B) was prepared in solution F with 5%  $\text{D}_2\text{O}$ .

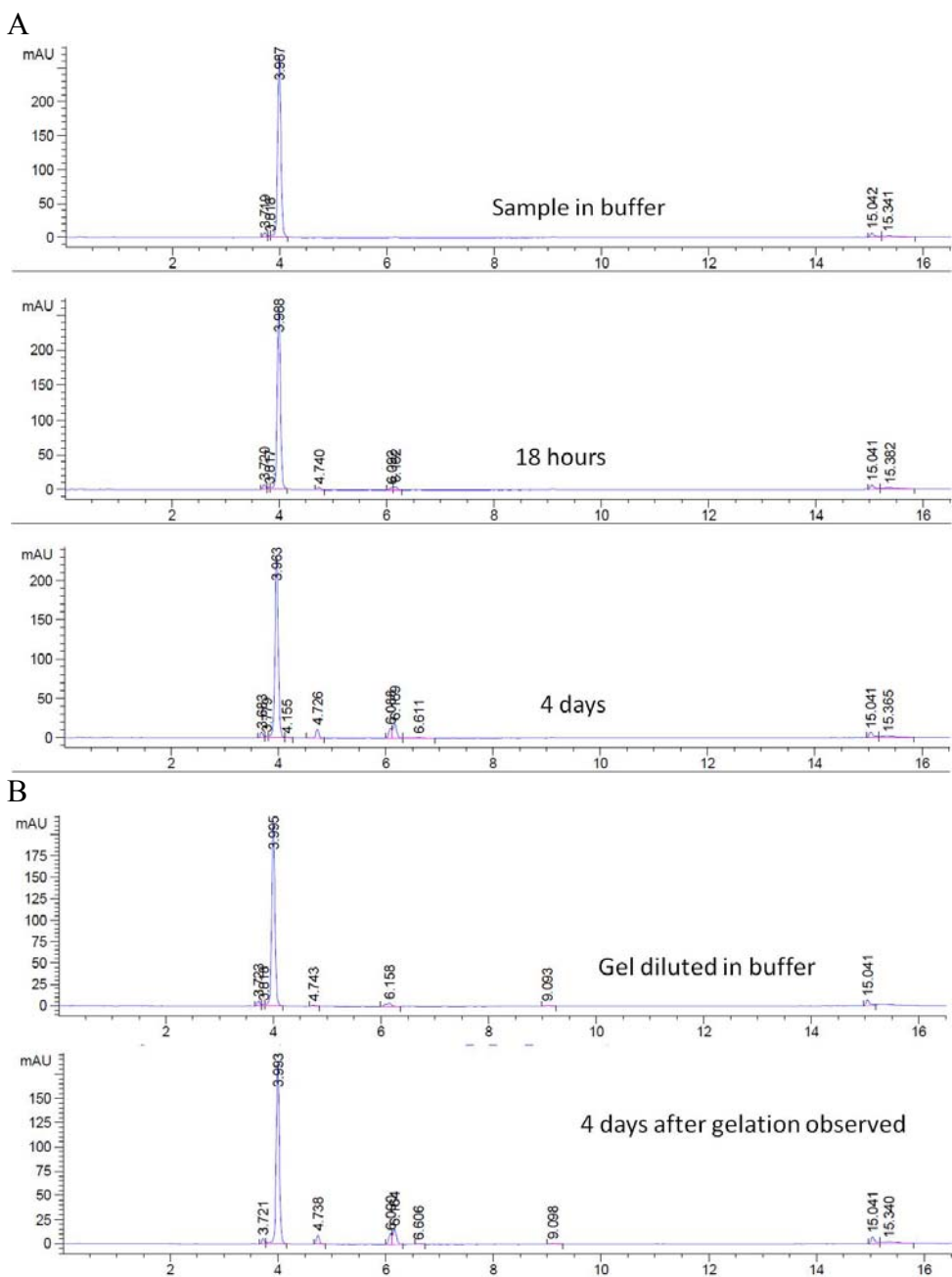


Figure 3.13 MS of depsipeptide (5) in buffer F in ungelled (A) and gelled (B) form. The structure is stable for up to 4 days.

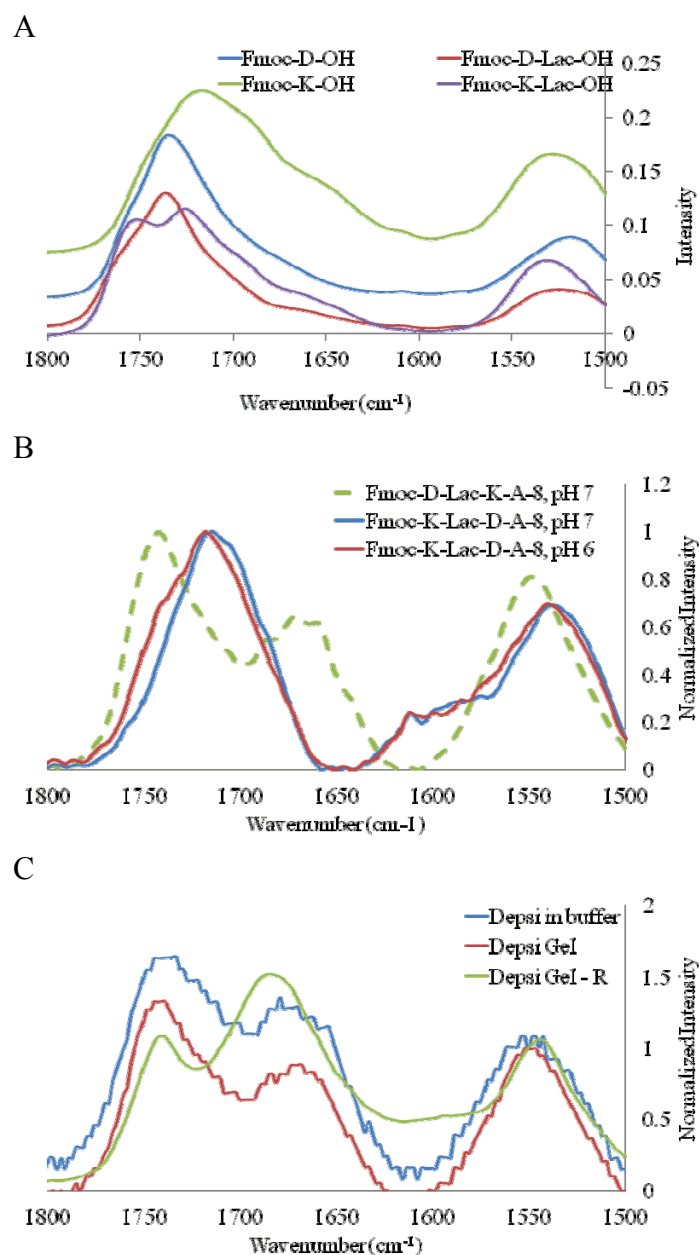


Figure 3.14 IR data for depsipeptides (3) and (5). Fmoc-peptides and Fmoc-depsidipeptides were dissolved in methanol and dried on gold-coated silica (A). Depsipeptide (3) was collected on a GATR accessory on a germanium crystal and plotted against depsipeptide (5) for comparison (B). Depsipeptide (5) was collected using both methods and plotted against each other (C), suggesting that the gel in the dried or solution state have similar folding patterns. The IR shifts of depsipeptide (5) in (B) and (C) were normalized at 1545 cm<sup>-1</sup>.

Depsipeptide (5) was investigated in both solution and dried states. The peaks were subtracted from buffer F and bare gold respectively and normalized at  $1545\text{ cm}^{-1}$ . Results show very little difference between the solution and dried samples, suggesting that the backbone configuration is not affected by the drying process. The depsipeptide was also prepared in buffer F at a relatively low concentration immediately before collecting on the IR, and the sample showed very little difference in the peaks in the Amide I and Amide II region. This may suggest that the self-assembly process begins immediately with specific backbone preferences.

The depsipeptides under investigation contain multiple ester substitutions, which reduce the number of hydrogen bonding sites. Considering that depsipeptide (3) and (5) share the same functional groups, the sequence of the depsipeptides not only affects the potential for gelation, but also the folding characteristics of the backbone. Future work to investigate these effects could be investigated on the peptide equivalent to determine how secondary structure changes with the presence of the ester bond. For example, the position and number of ester substitutions has been shown to affect the self-assembly of amylin(20-29) derivatives [2]. Despite lacking the traditional  $\beta$ -sheet structure of amyloid fibers, the authors suggest the structure may have formed anti-parallel  $\beta$ -sheet-like tapes, which in turn self-assembled into helical ribbons due to the intrinsic chirality of the depsipeptide.

TEM images of depsipeptide (5) were collected in sample F at various time points to observe the morphology of fibers throughout the gelation process (Figure 3.15).

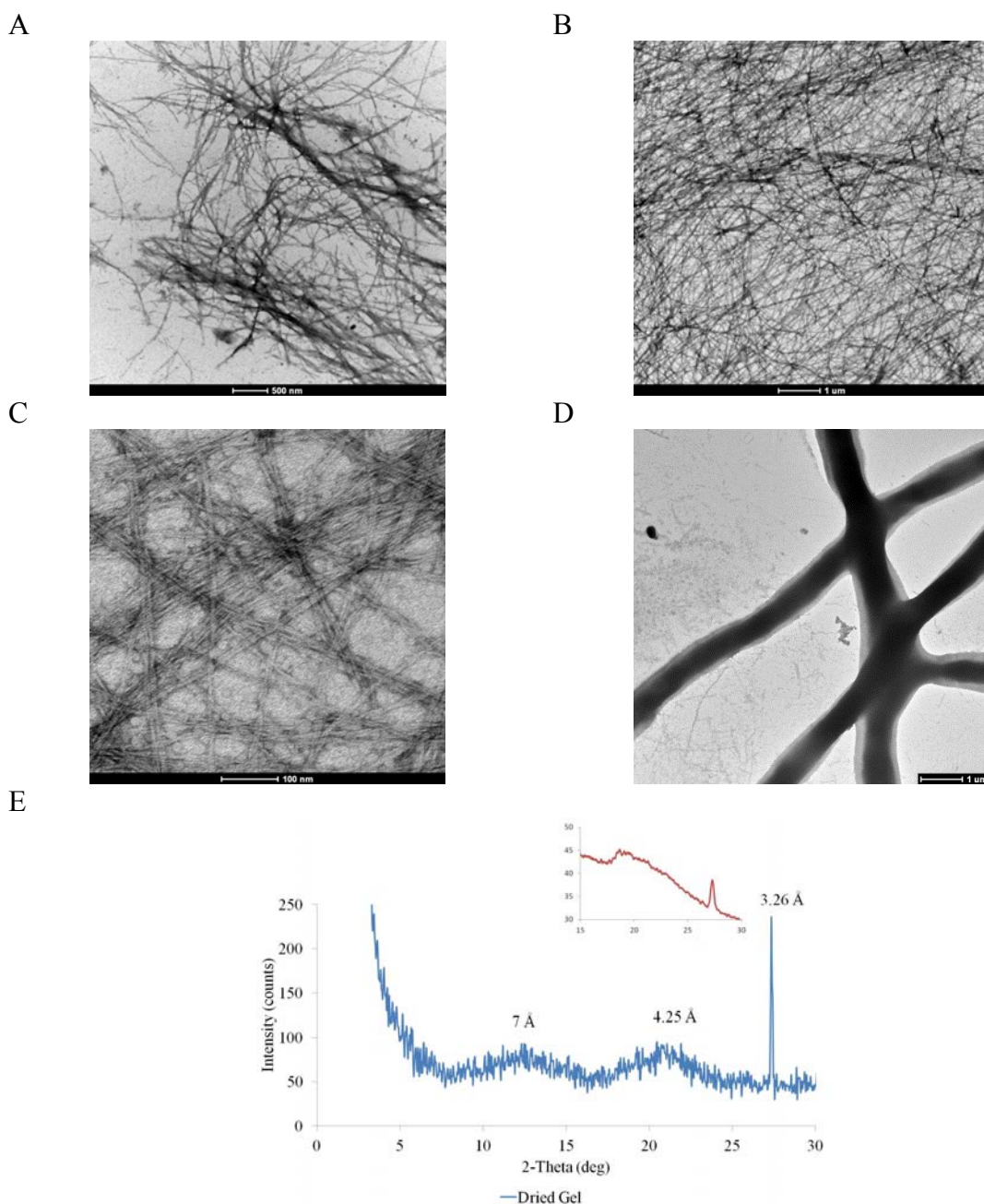


Figure 3.15 Fibril formation for depsiptide (5). TEM images were collected at various times after sample preparation: 18 hours (A), 4 days (B and C), and 3 weeks (D) WAXS data (E) shows  $d$ -spacing of 4.3 Å and 3.26 Å, the latter of which is associated with the crystal structure of NaCl from the buffer. The former value has been reported to be the distance between  $\pi$ - $\pi$  bonds of the fluorenyl group or between  $\beta$ -sheet forming peptides. The insert was collected on the gel.



Short fiber networks, with approximately 25 nm diameters, were evident 18 hours after the depsipeptide was prepared. A dense network formed after 4 days, and large fibers on the order of microns in diameter were observed after more than 3 weeks.

The gel was also analyzed with wide angle x-ray scattering to gain additional information on the fiber network. Upon analysis, the sample was left to dry at ambient temperature for over 48 hours. Results show a *d*-spacing value of 4.3 Å, which has been described as the distance between peptides within beta-sheets for a variety of Fmoc-dipeptide families [21, 33]. Fmoc-SF-OMe, Fmoc-SL-OMe, Fmoc-TF-OMe, and Fmoc-TL-OMe have reported the planar  $\pi$ -stacking of the Fmoc group to be correlated with a *d*-spacing of 7.6 Å and 3.8 Å (Hughes), which could be correlated to the *d*-spacing of 7 Å for depsipeptide (5). Further interpretation of this data is difficult due to the broadness of the peaks, thus additional experiments are needed. The distance of the  $\pi$ - $\pi$  stacking between the Fmoc groups has also been reported with a *d*-spacing of 4.3 Å [24, 34]. This observation may be more accurate for the depsipeptide structure, as typical  $\beta$ -sheet structure was not observed in CD or IR data. While it is clear that depsipeptide (5) self-assembles into an ordered structure upon fiber formation and gelation, no techniques currently exist to investigate the secondary folding of a depsipeptide backbone.

Titration tests were conducted on depsipeptide (3) and (5) in water, PBS, and PBS + 10 mM NaCl to investigate changes in pH under ionic environments (Figure 3.16). The titration curves of depsipeptide (3) have 2 isoelectric points, 8.33-8.10 and 4.96-4.65, among the 3 solutions tested.

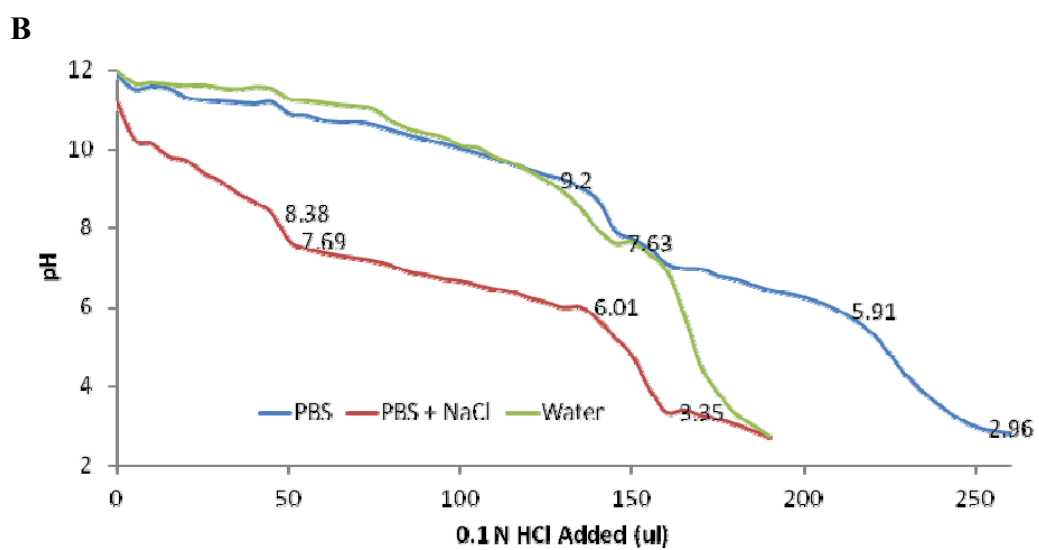
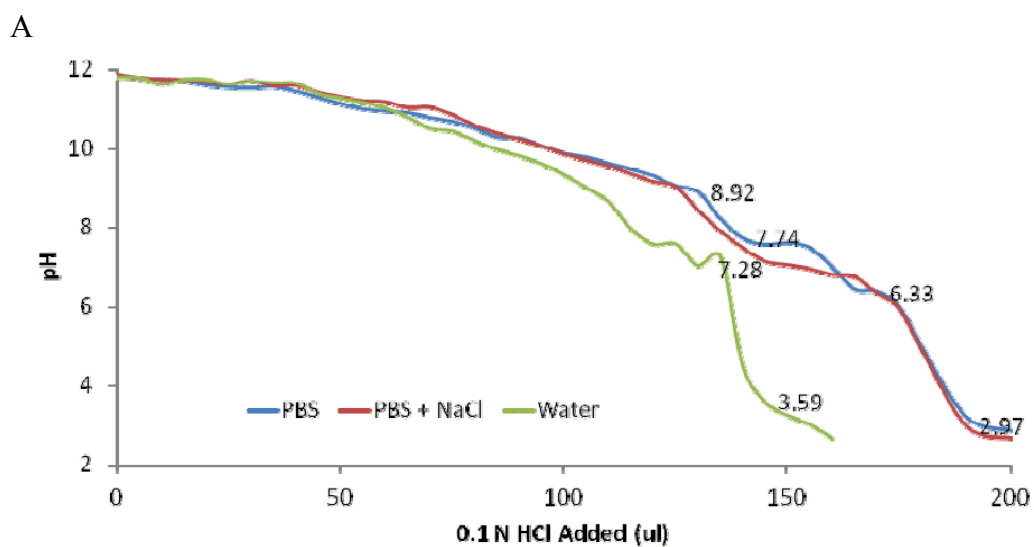


Figure 3.16 Titration curves for Depsipeptide (3) (A) and depsipeptide (5) (B). The red curve was prepared with 10 mM NaCl.

The decrease in pH becomes greater at pH less than 7.28 and 6.3 in the water and the ionic samples, respectively. The charged residues of depsipeptide (3) are screened by the ionic environments of both PBS and PBS with NaCl, illustrated by the shifts of both ionic curves when the pH is less than 10.52 [35, 36]. The titration curves of depsipeptide (5) also have 2 isoelectric points, 8.41-8.04 and 4.68-4.44. The rapid decrease in pH varies for all three solutions. The PBS solution screens the charges of the Lys and Asp residues in depsipeptide (5) at  $\text{pH} < 6.93$ , whereas the PBS+NaCl solution shows a much rapid change at all pH values tested.

The presence of salt can effect self-assembly by screening the charges of the Lys and Asp residues. It is possible that depsipeptide (5) may be more sensitive to the presence of salt. The depsipeptide is much more influenced by changes in pH in solutions with higher salt concentrations, where significant changes were only evident in depsipeptide (3) at pH values less than 7. Hofmeister effects can also contribute at high ionic strengths, due to the effects of ions on the properties of water. Clearly the solution with PBS and NaCl influences the properties of depsipeptide (4), suggesting that Hofmeister effects dominate in solutions with added NaCl.

The next set of studies investigates the role of salt and pH on fiber morphology and gelation of depsipeptide (5). The effect of various salts was reported to influence the fiber formation of islet amyloid polypeptide at pH 5.5 and pH 8.0 [37]. Because the polypeptide contains positively charged residues, screening effects are likely to stabilize amyloids. Results show that increasing the ionic strength of a Tris-HCl buffer increases the rate at which fibrils form. For example, upon adding 20 mM NaCl to the buffer,

amyloid formation was observed around 22 hours. The rate decreased to just over 2 hours upon adding 600 mM NaCl. The rate of fibril formation decreases with increasing ionic strength at pH 5.5, but variations were observed between different anions at constant ionic strength. This result suggests that the effects of salt on amyloid formation are complex and may be due to a combination of Hofmeister and screening effects.

#### ***3.3.4.2 Effect of high ionic concentration on self-assembly***

Solution M was prepared in PBS and 100 mM NaCl. Solution M has the highest ionic concentration of all the tested conditions, although the osmolarity value is comparable to those with an additional 10 mM NaCl added. Gels were formed in solution M after 20 hours in the 5 mg/ml and 20 mg/ml samples. The emission spectra are relatively similar in shape, with the 20 mg/ml sample having a higher intensity at 320 nm and 360 nm than the other concentrations (Figure 3.17A). CD analysis shows the presence of Fmoc-stacking due to the positive peaks at 300-250 nm for the gelled samples (Figure 3.17B), suggesting that the fluorenyl groups participate in the formation of gelation. TEM images of the 10 mg/ml sample show the presence of fibers (3.17C), despite not forming a gel.

#### ***3.3.4.3 Self-assembly at low pH promote gelation at lower concentrations***

Solution N was prepared in PBS with 10 mM NaCl and buffered to pH 3. In solution N, the samples at 5 mg/ml and 10 mg/ml gelled after 4 days. Emission curves are similar for gelled samples, while a loss of intensity and appearance of a broad shoulder at 370 nm is observed for the sample at 20 mg/ml (Figure 3.18A).

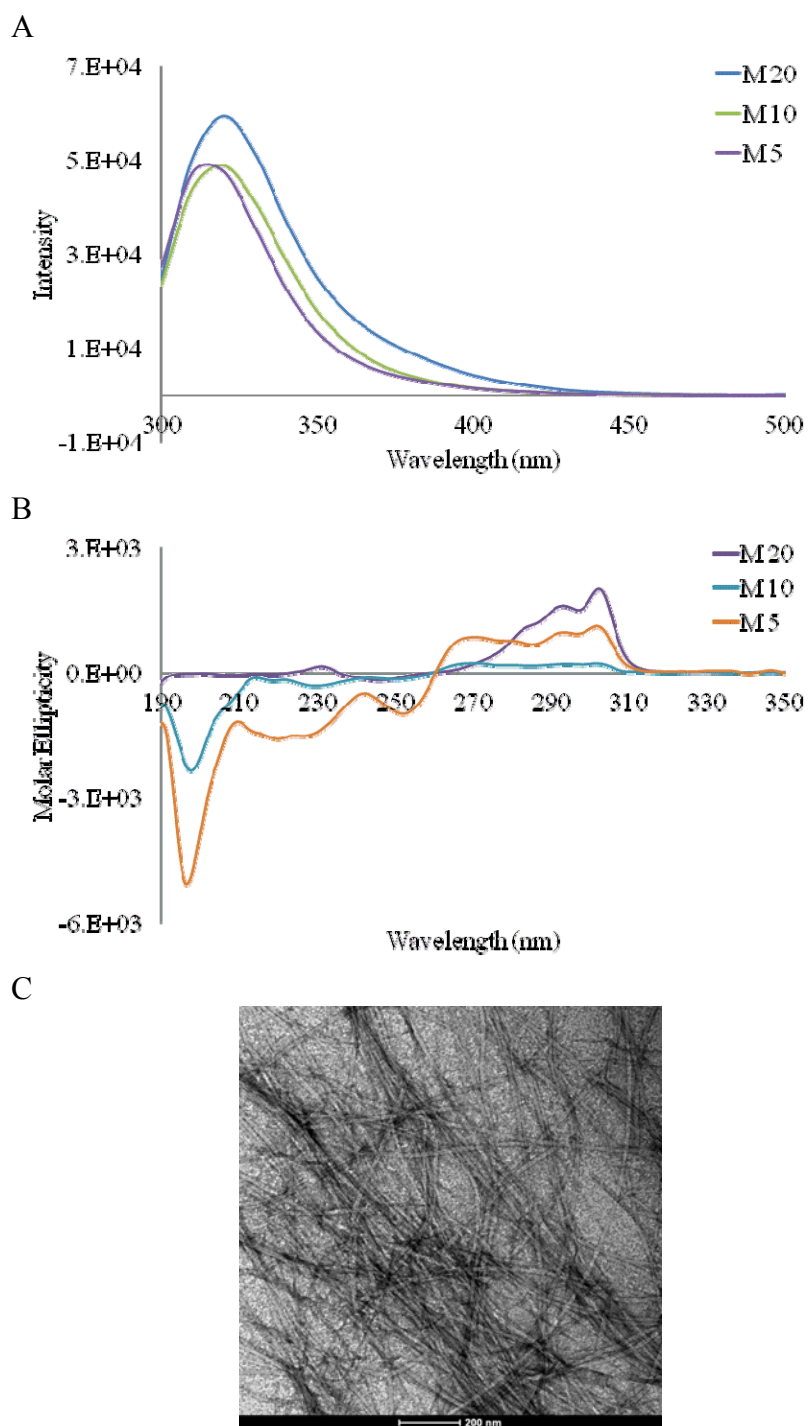


Figure 3.17 Self-assembly data of depsiptide (5) in solution M. Emission (A) and CD (B). TEM images of the 10 mg/ml sample (C) show the formation of fibers. The molar ellipticity of the CD data is in units of  $\text{deg cm}^2/\text{dmol}$ .

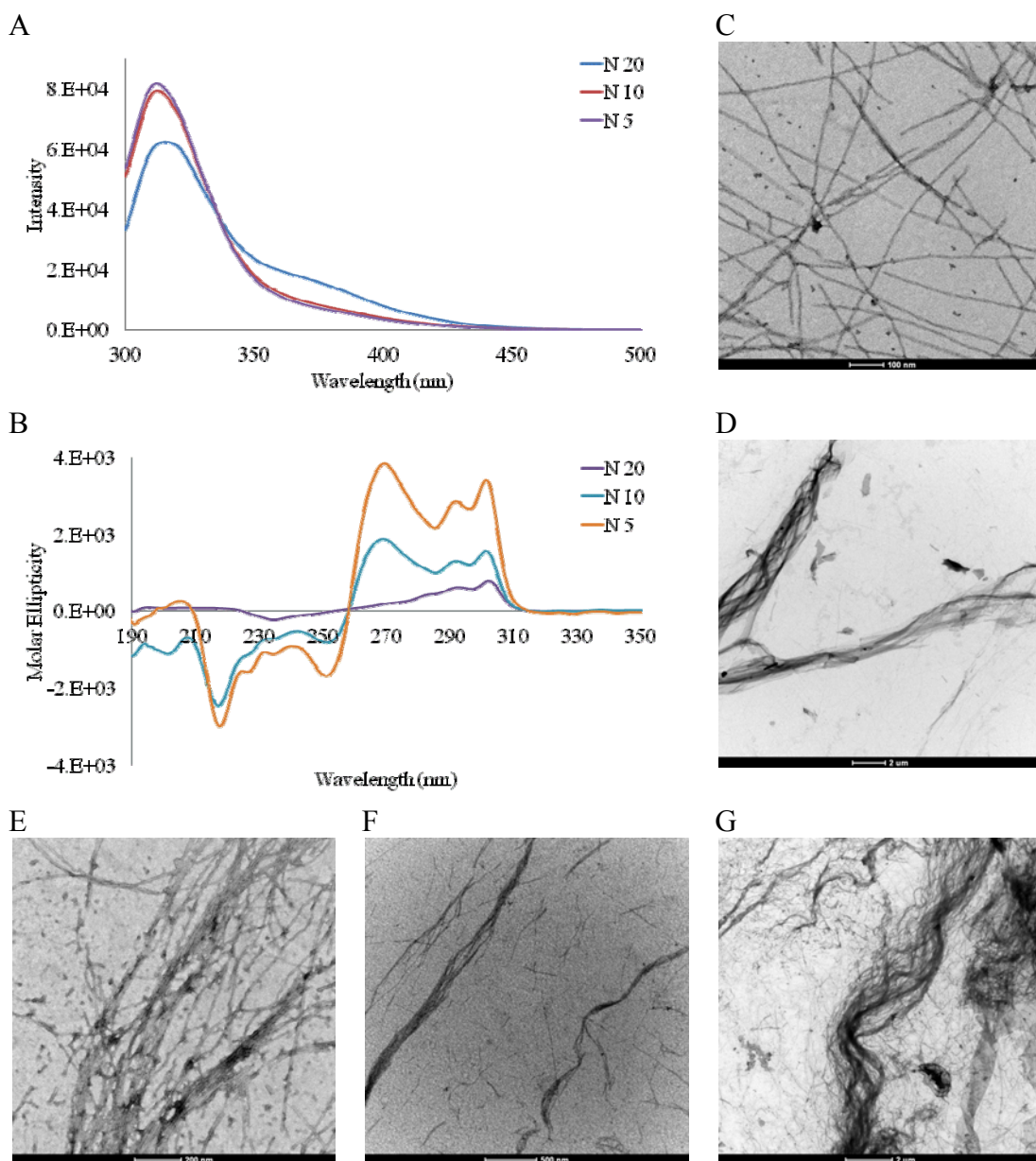


Figure 3.18 Self-assembly of depsipeptide (5) in solution N. Emission spectra (A) and CD data (B). The molar ellipticity of the CD data is in units of  $\text{deg cm}^2/\text{dmol}$ . TEM images at 5 mg/ml (C and D), 10 mg/ml (E and F), and 20 mg/ml (G).

The magnitude of the peaks collected from the CD spectra suggest higher fluorenyl packing for the 5 mg/ml sample (Figure 3.18B). The self-assembling trends of depsipeptide (5) behave differently at various pH. The formation of helical-like tubes are observed in both 5 mg/ml and 10 mg/ml samples, while the fibers in the 20 mg/ml sample are less stiff. Gels were formed in 10 mg/ml and 20 mg/ml at pH 7, while gels formed in 5 mg/ml and 10 mg/ml at pH 3. The emission spectra of ungelled samples prepared in PBS and 10 mM NaCl at both pH 7 and pH 3 show a broad shoulder at 370 nm, suggestions that for depsipeptide (5), this observation is an indicator that gelation does not occur. In addition, pH may affect the morphology of the fibers at higher concentrations. At lower pH, the carboxylic acid of the C-terminal and the Asp residues are more likely to be protonated, suggesting that repulsion of these groups may affect the supramolecular assembly into ordered gels.

#### ***3.3.4.4 Flexible fibers are observed at low pH in water***

Solution O was prepared with deionized water and buffered to pH 3 with 0.1 HCl. No gels were formed in solution O. The emission spectra is similar for samples at 5 mg/ml and 10 mg/ml, while a broad shoulder at 370 nm is observed for the 20 mg/ml sample (Figure 3.19 A). The CD data suggests the presence of Fmoc-stacking for all of the tested samples, although the negative troughs at 250 nm and 215-218 nm are absent in the 20 mg/ml samples. TEM images of the sample at 20 mg/ml show unordered fibers and are less dense than the flexible fibers observed in solution N (Figure 3.18), suggesting that the presence of salt may affect the packing of fiber formations.

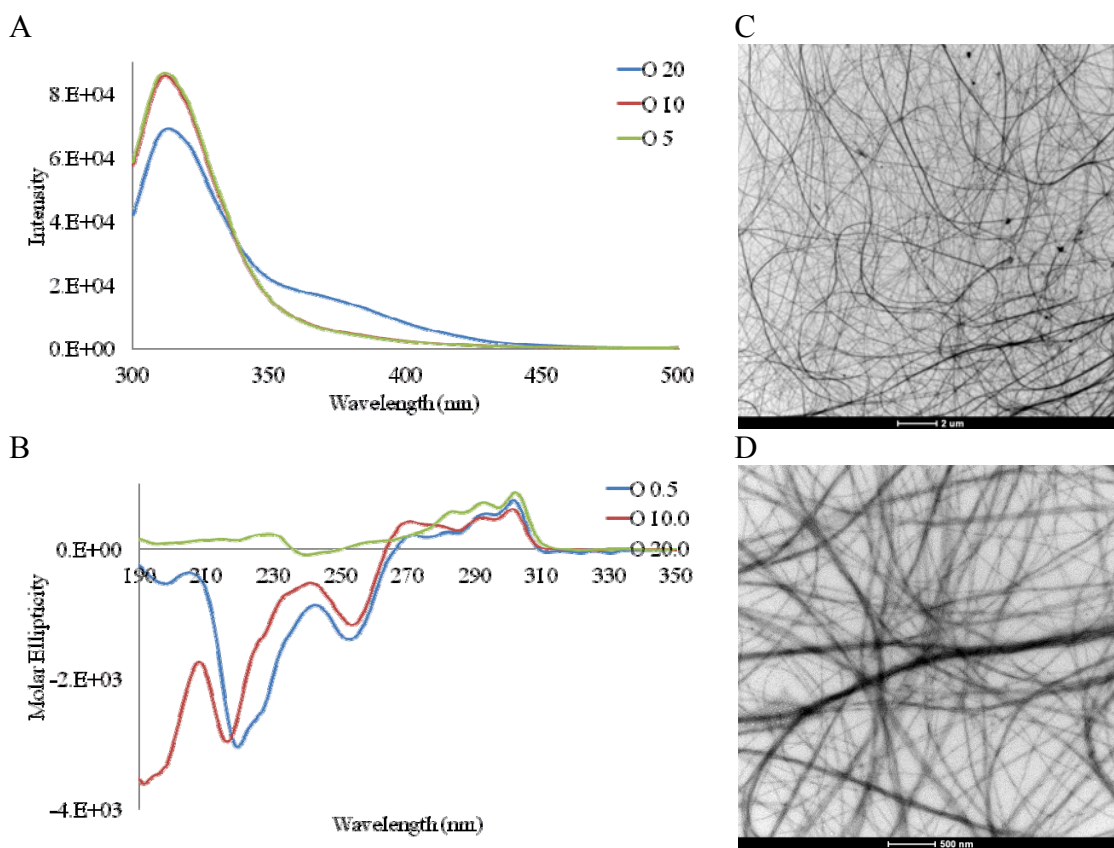


Figure 3.19 Self-assembly of depsipeptide (5) in solution O. Emission spectra (A) and CD data (B). The molar ellipticity of the CD data is in units of  $\text{deg cm}^2/\text{dmol}$ . TEM images were collected on 20 mg/ml samples (C and D).



This trend has been reported on the self-assembly of EAK peptides [38]. Globular aggregates and short fibrils were observed in the absence of NaCl, while fibers formed in the presence of salt. This observation was evident in only one of the evaluated concentrations, thus the effects of salt may also be concentration dependent.

#### ***3.3.4.5 Self-assembly and gelation processes are slow in water***

Depsipeptide (5) was investigated in solution W at 5, 10, and 20 mg/ml. The samples were dissolved in water and examined with emission spectra and TEM at 18 hours and 4 days. Gelation was observed after 3 weeks, suggesting that salt increases the rate of gelation. The emission spectrum shows a linear concentration dependence, illustrated by the peak magnitude at 370 nm for the 20 mg/ml sample (Figure 3.20A). After 4 days, the peak intensity at 320 nm decreases, although no other changes in the spectrum are present. The CD spectrum shows a positive peak from 270-310 nm (Figure 3.20B). TEM images of the sample at 10 mg/ml show the presence of spherical nanostructures after 18 hours (Figure 3.20C). Fibers were observed in all tested concentrations after 4 days (Figure 3.20D-F). The fibers have a relatively straight morphology, unlike the hair-like fibers observed in solution N (Figure 3.20G and H) and O (Figure 3.20C and D).

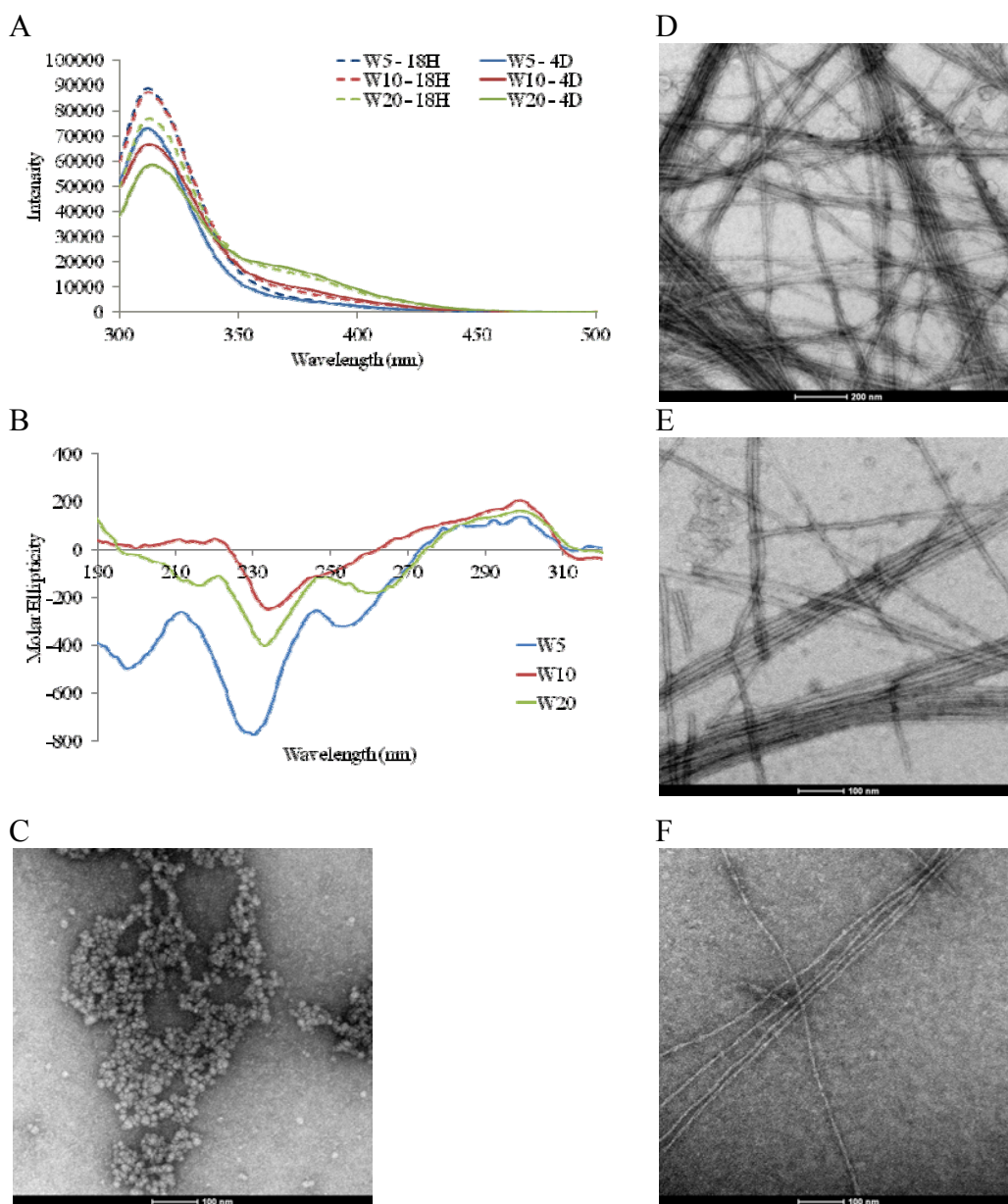


Figure 3.20 Self-assembly of depsipeptide (5) in solution W. TEM images were collected on 10 mg/ml samples 18 hours (C) and 4 days (D) after dissolving in water. Fibers were observed in 5 mg/ml (E) and 20 mg/ml (F) samples after 4 days. Gels were observed after 3 weeks.

The transition from the nanospheres to fibers is not evident, considering no intermediate products were observed from 18 hours to 4 days. However, it is likely that the Fmoc-group form a hydrophobic core when first exposed to water. Overtime, the electrostatic interactions from the charged Lys and Asp side chains are such that the formation of fibers is favorable.

#### ***3.3.4.6 Proposed self-assembly models***

Depsipeptide (5) self-assembles into fibers and hydrogels under various ionic concentrations and a wide range of pH values. These ordered structures are observed in water, PBS, and PBS with 10 mM NaCl. The morphology of fibers are less stiff at lower pH. The structural data reveals that the fluorenyl groups are aligned in an anti-parallel manner in gelled samples, while parallel stacking of the Fmoc group is observed in samples that do not aggregate. Data from the gelled samples is consistent with Fmoc-peptides that show helical stacking of the fluorenyl groups.

The self-assembling models of well-studied peptide families have been reported in the literature and heavily rely on secondary folding characteristics. Observations of secondary structures were absent in depsipeptide (5), however this may have been due to the chosen analysis methods. Interpreting secondary structure with CD and IR are based on principles of a native peptide backbone. The ester moiety of depsipeptides disrupts both flexibility and hydrogen bonding, thus one may argue that the backbone is too different to be used with these techniques. However, the possibility of the depsipeptide folding into an ordered structure has not been ruled out. Two models that are consistent

with the self-assembling data of depsipeptide (5) include  $\beta$ -sheet forming fibers and bottle-like brushes.

#### *3.3.4.6.1 $\beta$ -sheet forming fibers*

The self-assembly of  $\beta$ -sheet forming fibers has been reported on a number of Fmoc-peptide families. The model based on the coassembly of Fmoc-VRGDV and Fmoc-KKRGDK [39] suggests that self-assembly was driven by the electrostatic attraction between the Lys and Asp residues (Figure 3.21). The intramolecular bonding is highest when all of charged groups of depsipeptide (5) are exposed. Under this state, self-assembly is driven by the hydrophobic interactions between the anti-parallel stacked fluorenyl groups and the methyl groups of Lac, the electrostatic interactions between Lys and Asp, electrostatic bridge interactions between residues of the same charge and salt [39], and hydrogen bonding from the peptide residues. It should be noted here that fluorenyl groups are likely interacting with the structure on the adjacent side, as shown with the  $\beta$ -sheet model of Fmoc-dipeptides (Figure 3.5). The fluorenyl groups interact along their full length and are aligned anti-parallel from another structure. Additional  $\beta$ -sheet structures are incorporated until a cylinder is formed, such that the orientation of the fluorenyl groups drives their helical orientation around the organized structure.

#### *3.3.4.6.2 Bottle-brush like chains*

At low pH, the Asp residues are protonated and the electrostatic interactions with Lys are eliminated. The charge repulsion from the Lys groups may cause the fluorenyl groups to align in a parallel fashion, however helical stacking of the Fmoc groups are observed with CD (Figure 3.19 and 3.20).

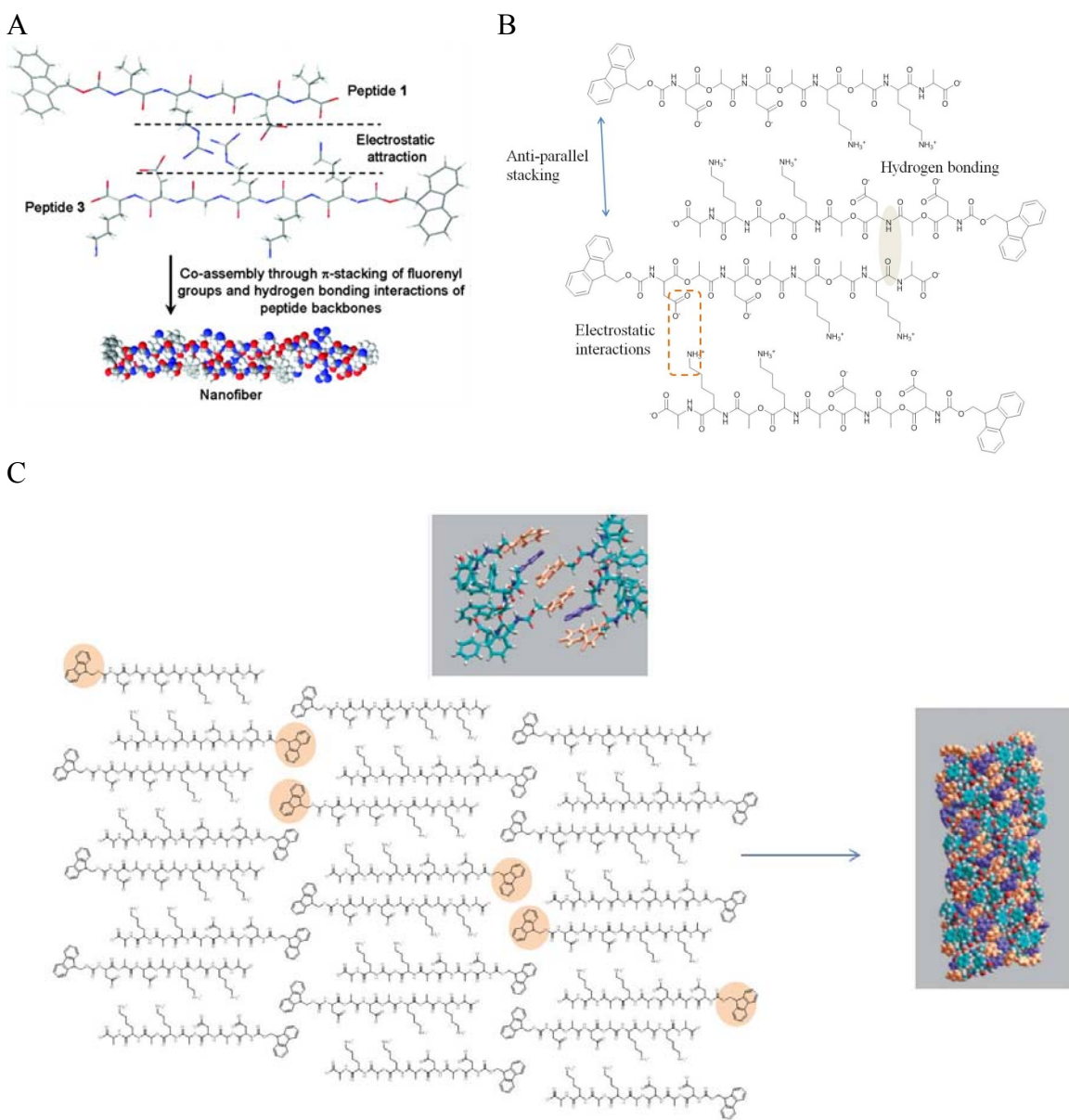
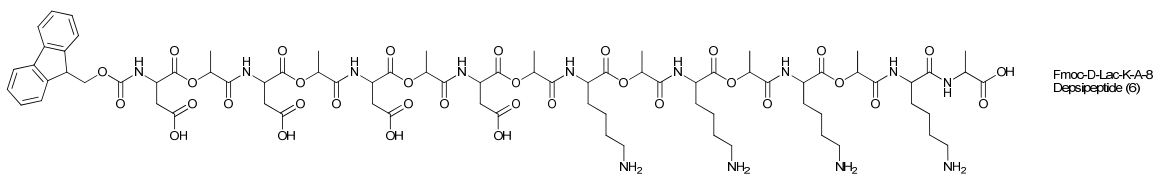


Figure 3.21 The self-assembly of depsipeptide (5) at pH 7 is modeled by principles reported in  $\beta$ -sheet like peptides. Self-organization is driven by an electrostatic attraction involving both positively and negatively charged peptide molecules in short Fmoc-peptide families [39] (A). For depsipeptide (5), electrostatic attractions, stacking of the fluorenyl groups, and hydrogen bonding may result in the formation of nanofibers with  $\beta$ -sheet like superstructure (B). The fluorenyl groups of depsipeptide (5) are highlighted in pink (C) and upon folding into a fiber, are aligned in a helical manner. The modeled images from Fmoc-dipeptide families show similar self-assembling trends [21]. Used with permission.

The fluorenyl groups could potentially form a hydrophobic core, with rest of the structure exposed radially from the center (Figure 3.22) and could possible form a bottle-like brush structure model [40]. Loss of the ionic interactions between Lys and Asp may result in weaker intramolecular bonding that could potentially explain the flexible morphologies of the fibers as observed in pH 3.

### 3.3.5 Depsipeptide (6): Self-assembly is effected by depsipeptide length



Depsipeptide (6) did not show gel formation in solutions B, D, F, H, N, O, P, Q, or W (Table 3.5). The emission spectra shows little change after 5 days (Figure 3.23). Additional work needs to be done to determine how important peptide length is for this depsipeptide, as sequence may be a driving factor for self-assembly. For example, changes in the position of charged residues affect fiber morphology, as seen with the helical peptides AEAEAKAK and AEAKAEAK [41]. Long rigid fibers with an average width of 7-9 nm were observed for AEAEAKAK. When the charges are alternated between the Ala residue as seen with the AEAKAEAK peptide, very few fibers are observed.

The charged residues of AEAEAKAK are present on each side of the helix. The opposing charges of Lys and Glu stabilize the  $\alpha$ -helical structure, facilitating the  $\alpha$ -helices to aggregate and form supramolecular fibers through hydrophobic interactions.

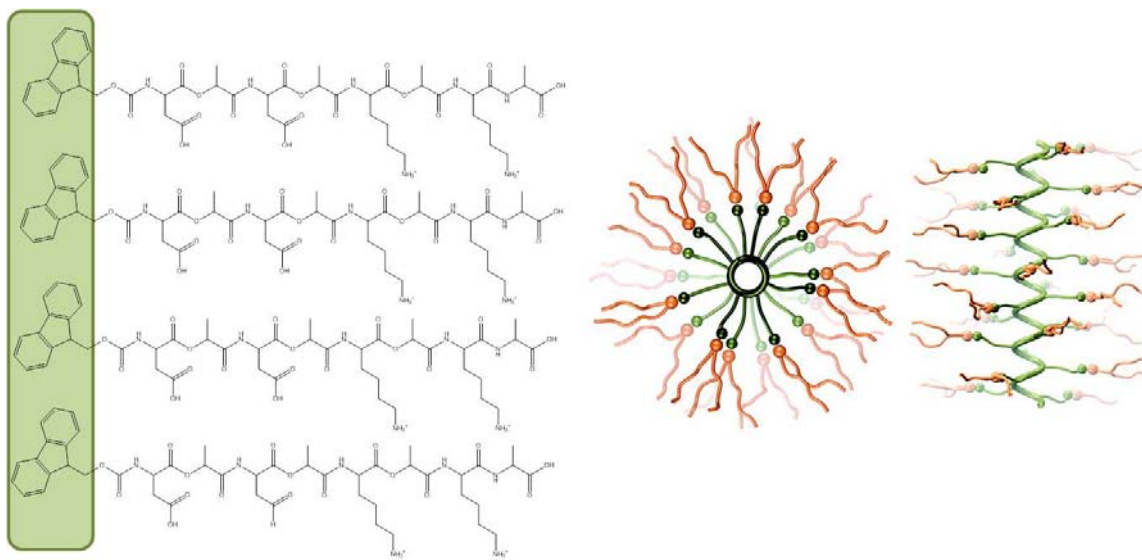


Figure 3.22 Suggested self-assembling model for fiber of depsipeptide (5) at pH 3. The fluorenyl groups are stacked in a parallel fashion. The side chains have no modes of interaction with each other, as expected since the Asp charges are not exposed. It is likely that the rest of the molecule is exposed to the solvent, as illustrated by the bottle-like brush structure for a surfactant model [40], where the cylindrical core is aligned as an  $\alpha$ -helix and the red structures represent interactions with the solvent. Used with permission

Solution	Conditions	Osmolarity (mmol/kg)
P	PBS, pH 3	298
B	PBS, pH 7	302
D	PBS, pH 9	301
N	PBS + 10 mM NaCl, pH 3	484
F	PBS + 10 mM NaCl, pH 7	520
H	PBS + 10 mM NaCl, pH 9	504
O	Water, buffered to pH 3	30
W	Water	30
Q	Water, buffered to pH 9	55

Table 3.5 Summary of the self-assembly experiments of depsipeptide (6). No gels were observed. As a reference, physiological osmolarity is around 280-310 mmol/kg.



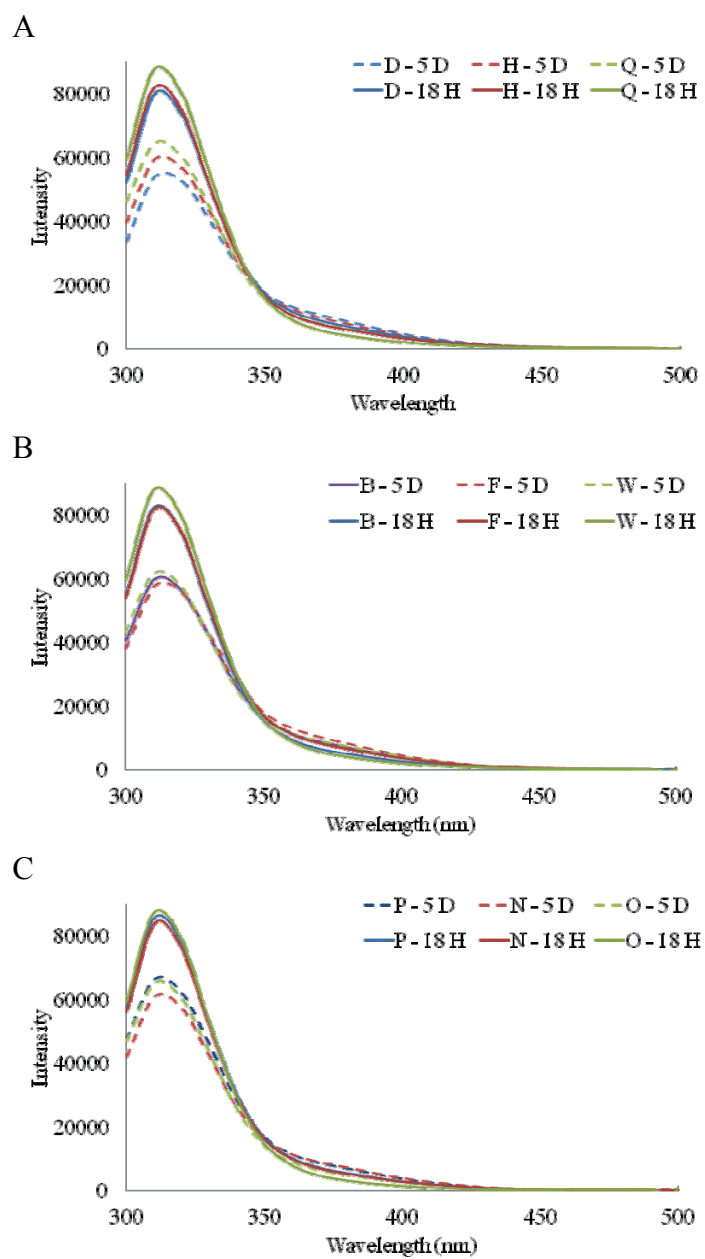


Figure 3.23 Emission spectra for depsiptide (6) under various ionic concentrations. The samples were observed at pH 9 (A), pH 7 (B), and pH 3 (C) at 18 hours and 5 days.

On the other hand, the orientation of the charged residues of AEAKAEAK are located the same sides of the helix. The charge repulsion disrupts the order of the  $\alpha$ -helix and further interferes with the self-assembly of this peptide in solution.

The process of self-assembly may also be longer due to the increased length of the peptide. For example, the gelation of X-VRGDV-OH was affected by length of the X moiety, which varied in alkyl chain length and named according to the number of carbons on the chain: C9, C11, C13, and C15 [42]. The  $pK_a$  values of C9 and C11 were easier to identify than for C13 and C15, suggesting that protonation and deprotonation processes occur slowly for structures with higher hydrophobic regions. At pH 7, all of the structures formed nanofibers. The formation of micelles was observed upon increasing to pH 11 for C9 and C11. No obvious morphology changes were observed for C13 and C15, suggesting that the nanofibers are tightly packed due to the strengthened hydrophobic interaction. CD and IR studies indicate that all structures maintain  $\beta$ -sheet conformation at pH 7 and pH 11, despite the differences in morphology.

### **3.4 CONCLUSIONS**

Short depsipeptide structures have been shown to self-assemble into ordered structures based on sequence, concentration, and pH. The organization of depsipeptide (3) into spherical nanostructures is driven by the parallel alignment of the fluorenyl groups. Similar to assemblies reported in Fmoc-dipeptide micelles, the fluorenyl structures form a hydrophobic core, with the hydrophilic regions exposed to the aqueous solution. Depsipeptide (5) forms into hydrogels within 18 hours-3 weeks of preparation, and the rate of gelation is dependent on compositions of the solution. Flexible fibers

were observed at lower pH, which most likely organize into bottle-brush like structures. The formation of dense fiber networks was observed at pH 7. The self-assembly process of these structures is driven by hydrogen bonding, electrostatic interactions, and fluorenyl stacking and most likely forms via  $\beta$ -sheet like organizations.

### 3.5 EXPERIMENTAL METHODS

**Depsipeptide preparation:** Samples were prepared to 5, 10, or 20 mg/ml in 200  $\mu$ l of the selected solution. The samples were allowed to sit at room temperature until gelation was observed via the inverted vial method.

**Fluorescence experiments:** Emission spectra were collected on a Molecular Dynamics plate reader provided by the DNA Sequencing Facility at the Institute of Cellular and Molecular Biology. Samples were read in 96-well black plates with an excitation of 265 nm from 300-500 nm and subtracted from the respective solution prior to data analysis.

**Circular dichroism (CD):** CD was collected on a Jasco J-815 CD Spectrometer. CD spectra were measured at 10.0 nm intervals over the range 180–350 nm in a 0.1 mm cylindrical cuvette. The optical chamber was continually flushed with N<sub>2</sub> gas. The samples were averaged over 3 runs and subtracted from the respective solution.

**Infrared Spectroscopy (IR):** IR experiments were performed in both the dry and solution state on a Bruker Vertex 70 Fourier transform infrared (FTIR) spectrometer provided by the Webb group in the Department of Chemistry. Samples were dried on silicon wafers coated with chromium and gold. The wafers were generously provided by the Webb group. The surfaces were cleaned with either hydrogen flame annealing or

with a piranha wash. The later method was followed by rinses in concentrated hydrogen chloride, high purity water, ethanol, and dried with N<sub>2</sub>. The spectrometer was equipped with a A518/Q horizontal reflection (Bruker) for illuminating the sample at a grazing angle of 80° with respect to the surface normal. The sample chamber was purged with N<sub>2</sub> for 1 hour prior starting experiments and handled by methods reported in the literature [43, 44]. Samples were collected on using a mercury cadmium telluride (MCT) detector, with 100 scans between 400 and 4000 cm<sup>-1</sup> at a resolution of 4 cm<sup>-1</sup>. A gelled sample of depsipeptide (5) in solution F was analyzed on a GATR reflector cell equipped with a germanium crystal. The sample (20 μl) was dropped on the surface and sandwiched with a wafer. The sample was referenced to buffer F on gold. Fmoc-Asp(OtBu)-OH, Fmoc-Lys(Boc)-OH, Fmoc-Asp(OtBu)-Lac-OH, and Fmoc-Lys(Boc)-OH were dissolved in methanol to a final concentration of 0.008-0.01 mM and collected at ambient temperature.

**<sup>1</sup>H-NMR:** Experiments were conducted on a Varian 500 MHz spectrometer. Chemical shifts are given in ppm. A bulk solution of D<sub>2</sub>O (1 mL) with phosphate buffer solution (PBS) salt and NaCl or solution F with 5% D<sub>2</sub>O was added to depsipeptide (5) to a final concentration of 10 mg/ml. Gelation under the second condition occurred the NMR-tube.

**Titration tests:** Dilute samples of depsipeptide (3) and depsipeptide (5) were brought to pH below 12 to avoid the removal of the Fmoc group. 0.1 N HCl (5 μl) was added to the solution and mixed for 1-2 minutes before recording the pH.

**TEM:** Samples were collected on a FEI Tecnai Transmission Electron Microscope. Samples (5  $\mu$ l) were dropped onto glow-discharged or untreated carbon coated copper grids for 10 seconds, removing the excess with filter paper. Water (5  $\mu$ l) was dropped on the grid in solutions that contained salts. This process was repeated twice, and then negatively stained with urenyl acetate (5  $\mu$ l).

**X-ray scattering:** Experiments on the dried gel was collected on a Scintag X1  $\theta$ - $\theta$  powder diffractometer with a copper X-ray source fitted with a solid-state detector and was generously provided by Dr. Steve Swinnea from the Department of Chemical Engineering. A gelled sample of depsipeptide (5) in solution F was dried for over 48 hours at room temperature. Peak analysis was performed using Jade v9.1.1 (Materials Data Inc.) software, and *d*-spacings were calculated assuming an X-ray wavelength of 1.54059 Å (Cu K- $\alpha$ 1). Experiments on the gel in solution state were collected on a Rigaku R-Axis Spider diffractometer and were generously provided by Dr. Vincent Lynch from the X-ray Diffraction Lab. The instrument was equipped with an image plate detector using a graphite monochromator and CuK $\alpha$  radiation ( $\lambda = 1.5418\text{\AA}$ ) and controlled using Rapid/XRD diffractometer control software. The integration of the two dimensional data into a one dimensional pattern was accomplished using 2DP software.

## References

1. Yang, X.Y., M. Wang, and M.C. Fitzgerald, *Analysis of protein folding and function using backbone modified proteins*. Bioorganic Chemistry, 2004. **32**(5): p. 438-449.
2. Elgersma, R.C., et al., *Self-assembly of amylin(20-29) amide-bond derivatives into helical ribbons and peptide nanotubes rather than fibrils*. Chemistry-a European Journal, 2006. **12**(14): p. 3714-3725.
3. Oku, H., et al., *Addition of a peptide fragment on an  $\alpha$ -helical depsipeptide induces  $\alpha/3(10)$ -conjugated helix: Synthesis, crystal structure, and CD spectra of Boc-Leu-Leu-Ala-(Leu-Leu-LaC)(3)-Leu-Leu-OEt*. Biopolymers, 2004. **75**(3): p. 242-254.
4. Oku, H., K. Yamada, and R. Katakai, *Conformational change from antiparallel beta-sheet to alpha-helix in a series of depsipeptide, -(Leu-Leu-Lac)(n)-: Syntheses, spectroscopic studies, and crystal structures of Boc-Leu-Lac-OEt and Boc-(Leu-Leu-Lac)(n)-OEt (n=1, 2)*. Biopolymers, 2008. **89**(4): p. 270-283.
5. Ohyama, T., et al., *Crystal structure of a depsipeptide, Boc-(Leu-Leu-Lac)(3)-Leu-Leu-OEt*. Biopolymers, 2001. **58**(7): p. 636-642.
6. Zhang, J.J., et al., *Molecular modeling of conformational properties of oligodepsipeptides*. Biomacromolecules, 2007. **8**(10): p. 3015-3024.
7. Loo, Y., S.G. Zhang, and C.A.E. Hauser, *From short peptides to nanofibers to macromolecular assemblies in biomedicine*. Biotechnology Advances, 2012. **30**(3): p. 593-603.
8. Gelain, F., A. Horii, and S.G. Zhang, *Designer self-assembling peptide scaffolds for 3-D tissue cell cultures and regenerative medicine*. Macromolecular Bioscience, 2007. **7**(5): p. 544-551.
9. Horii, A., et al., *Biological Designer Self-Assembling Peptide Nanofiber Scaffolds Significantly Enhance Osteoblast Proliferation, Differentiation and 3-D Migration*. PLoS ONE, 2007. **2**(2): p. e190.
10. Yang, Y., et al., *Designer self-assembling peptide nanomaterials*. Nano Today, 2009. **4**(2): p. 193-210.
11. Zhang, S.G., et al., *Spontaneous Assembly of a Self-Complementary Oligopeptide to Form a Stable Macroscopic Membrane*. Proceedings of the National Academy of Sciences of the United States of America, 1993. **90**(8): p. 3334-3338.
12. Davis, M.E., et al., *Injectable self-assembling peptide nanofibers create intramyocardial microenvironments for endothelial cells*. Circulation, 2005. **111**(4): p. 442-450.
13. Caplan, M.R., et al., *Control of self-assembling oligopeptide matrix formation through systematic variation of amino acid sequence*. Biomaterials, 2002. **23**(1): p. 219-227.
14. Hauser, C.A.E., et al., *Natural tri- to hexapeptides self-assemble in water to amyloid beta-type fiber aggregates by unexpected alpha-helical intermediate*

- structures*. Proceedings of the National Academy of Sciences of the United States of America, 2011. **108**(4): p. 1361-1366.
15. Mishra, A., et al., *Ultrasmall natural peptides self-assemble to strong temperature-resistant helical fibers in scaffolds suitable for tissue engineering*. Nano Today, 2011. **6**(3): p. 232-239.
  16. Yokoi, H., T. Kinoshita, and S. Zhang, *Dynamic reassembly of peptide RADA16 nanofiber scaffold*. Proceedings of the National Academy of Sciences of the United States of America, 2005. **102**(24): p. 8414-8419.
  17. Ye, Z.Y., et al., *Temperature and pH effects on biophysical and morphological properties of self-assembling peptide RADA16-1*. Journal of Peptide Science, 2008. **14**(2): p. 152-162.
  18. Burch, R.M., et al., *N-(Fluorenyl-9-Methoxycarbonyl) Amino-Acids, A Class Of Antiinflammatory Agents With A Different Mechanism Of Action*. Proceedings of the National Academy of Sciences of the United States of America, 1991. **88**(2): p. 355-359.
  19. Adams, D.J., et al., *Relationship between molecular structure, gelation behaviour and gel properties of Fmoc-dipeptides*. Soft Matter, 2010. **6**(9): p. 1971-1980.
  20. Jayawarna, V., et al., *Nanostructured hydrogels for three-dimensional cell culture through self-assembly of fluorenylmethoxycarbonyl-dipeptides*. Advanced Materials, 2006. **18**(5): p. 611-+.
  21. Smith, A.M., et al., *Fmoc-Diphenylalanine self assembles to a hydrogel via a novel architecture based on pi-pi interlocked beta-sheets*. Advanced Materials, 2008. **20**(1): p. 37-+.
  22. Ryan, D.M., T.M. Doran, and B.L. Nilsson, *Complementary pi-pi Interactions Induce Multicomponent Coassembly into Functional Fibrils*. Langmuir, 2011. **27**(17): p. 11145-11156.
  23. Zhou, M., et al., *Self-assembled peptide-based hydrogels as scaffolds for anchorage-dependent cells*. Biomaterials, 2009. **30**(13): p. 2523-2530.
  24. Mu, X., et al., *Experimental and Computational Studies Reveal an Alternative Supramolecular Structure for Fmoc-Dipeptide Self-Assembly*. Biomacromolecules, 2012. **13**(11): p. 3562-3571.
  25. Jayawarna, V., et al., *Introducing chemical functionality in Fmoc-peptide gels for cell culture*. Acta Biomaterialia, 2009. **5**(3): p. 934-943.
  26. Geisler, I.M. and J.P. Schneider, *Evolution-Based Design of an Injectable Hydrogel*. Advanced Functional Materials, 2012. **22**(3): p. 529-537.
  27. Bowerman, C.J., et al., *Tuning beta-Sheet Peptide Self-Assembly and Hydrogelation Behavior by Modification of Sequence Hydrophobicity and Aromaticity*. Biomacromolecules, 2011. **12**(7): p. 2735-2745.
  28. Tang, C., R.V. Ulijn, and A. Saiani, *Effect of Glycine Substitution on Fmoc-Diphenylalanine Self-Assembly and Gelation Properties*. Langmuir, 2011. **27**(23): p. 14438-14449.

29. Sadownik, J.W., J. Leckie, and R.V. Ulijn, *Micelle to fibre biocatalytic supramolecular transformation of an aromatic peptide amphiphile*. Chemical Communications, 2011. **47**(2): p. 728-730.
30. Shahi, P., et al., *Formation of amyloid fibrils via longitudinal growth of oligomers*. Biochemistry, 2007. **46**(25): p. 7365-7373.
31. Yang, Z.M., et al., *Enzymatic formation of supramolecular hydrogels*. Advanced Materials, 2004. **16**(16): p. 1440-+.
32. Shapiro, Y.E., *Structure and dynamics of hydrogels and organogels: An NMR spectroscopy approach*. Progress in Polymer Science, 2011. **36**(9): p. 1184-1253.
33. Hughes, M., et al., *Differential supramolecular organisation of Fmoc-dipeptides with hydrophilic terminal amino acid residues by biocatalytic self-assembly*. Soft Matter, 2012. **8**(45): p. 11565-11574.
34. Braun, H.-G. and A.Z. Cardoso, *Self-assembly of Fmoc-diphenylalanine inside liquid marbles*. Colloids and Surfaces B: Biointerfaces, 2012. **97**(0): p. 43-50.
35. Urry, D.W., et al., *Nanometric Design Of Extraordinary Hydrophobic-Induced Pka Shifts For Aspartic-Acid - Relevance To Protein MechanissS*. Biopolymers, 1994. **34**(7): p. 889-896.
36. Urry, D.W., et al., *Comparison Of Electrostatic-Induced And Hydrophobic-Induced Pka Shifts In Polypentapeptides - The Lysine Residue*. Chemical Physics Letters, 1994. **225**(1-3): p. 97-103.
37. Marek, P.J., et al., *Ionic Strength Effects on Amyloid Formation by Amylin Are a Complicated Interplay among Debye Screening, Ion Selectivity, and Hofmeister Effects*. Biochemistry, 2012. **51**(43): p. 8478-8490.
38. Hong, Y., et al., *Effect of NaCl and peptide concentration on the self-assembly of an ionic-complementary peptide EAK16-II*. Colloids and Surfaces B-Biointerfaces, 2005. **46**(3): p. 152-161.
39. Xu, X.D., et al., *Coassembly of Oppositely Charged Short Peptides into Well-Defined Supramolecular Hydrogels*. Journal of Physical Chemistry B, 2010. **114**(7): p. 2365-2372.
40. Junnila, S., et al., *Effect of Double-Tailed Surfactant Architecture on the Conformation, Self-Assembly, and Processing in Polypeptide-Surfactant Complexes*. Biomacromolecules, 2009. **10**(10): p. 2787-2794.
41. Saiani, A., et al., *Self-assembly and gelation properties of alpha-helix versus beta-sheet forming peptides*. Soft Matter, 2009. **5**(1): p. 193-202.
42. Xu, X.D., et al., *Self-assembly behavior of peptide amphiphiles (PAs) with different length of hydrophobic alkyl tails*. Colloids and Surfaces B-Biointerfaces, 2010. **81**(1): p. 329-335.
43. Gallardo, I.F. and L.J. Webb, *Tethering Hydrophobic Peptides to Functionalized Self-Assembled Mono layers on Gold through Two Chemical Linkers Using the Huisgen Cycloaddition*. Langmuir, 2010. **26**(24): p. 18959-18966.
44. Gallardo, I.F. and L.J. Webb, *Demonstration of alpha-Helical Structure of Peptides Tethered to Gold Surfaces Using Surface Infrared and Circular Dichroic Spectroscopies*. Langmuir, 2012. **28**(7): p. 3510-3515.



## **Chapter 4. Developing Depsipeptides as Novel Biomaterials with Predictable Self-Assembling Characteristics with Hydrophobicity, Secondary Prediction, and Biocompatibility**

### **4.1 CHAPTER SUMMARY**

The synthesis of a depsipeptide family described has been summarized in Chapter 2. Standard Fmoc-methods were used to synthesize the depsipeptide with despi-building block, which were synthesized on the gram scale. Chapter 3 describes various environmental effects that promote self-assembly into spherical nanoparticles, fibers, or hydrogels. Of those tested conditions, the fastest rate of gelation was observed with 20 mg/ml of depsipeptide (4) after 18 hours in a solution with PBS and 10 mM NaCl. This condition is not ideal for scaffolding vivo applications, due to the relatively long aggregation time. A change in the chemical backbone may influence gelation, as seen with the introduction of hydrophobic residues within self-assembling peptide families. As we investigate the potential for these materials to be implanted into the body, biocompatibility studies must be conducted. This chapter will describe some of the methods to increase the rate of gelation by increasing the overall hydrophobicity of depsipeptide (4) and also describe the *in vitro* and *in vivo* biocompatibility studies from other self-assembling peptide and modified-peptide systems.

## 4.2 EXPERIMENTAL RESULTS

### 4.2.1 Increasing overall hydrophobicity

Increasing the overall hydrophobicity of a molecule has been shown to influence gelation, gelation strength, and secondary structure. The first, and perhaps most facile method to achieve this within our depsipeptide library would be with preloaded resins. Chapter 3 describes the use of a commercial Fmoc-Ala-Wang resin during solid phase synthesis, and it is not unlikely that self-assembly processes will be affected by the synthesis of Fmoc-Leu-Wang or Fmoc-Phe-Wang resins by adding the respective residue to the C-terminal. The Phe residue may potentially stack with the fluorenyl group, as seen with other Fmoc-families [1-3] to drive self-assembling processes.

Another strategy is to increase the hydrophobicity of the ester residues. The synthesis methods described in Chapter 2 used L-lactic acid because of its commercial availability. Other commonly used  $\alpha$ -hydroxy acids were not appropriate, as glycolic acid has no side chain functionality and mandelic acid would not be the equivalent of phenylalanine. The diazotization of amino acids has been reported to yield  $\alpha$ -hydroxy-acid equivalents [4]. The amino acid of interest will be dissolved in 2.5N sulfuric acid and added dropwise to a solution of sodium nitrate in water for 1 hour at 0°C. The reaction will stir for 2 hours at 0°C, then 9 hours at room temperature. The reaction mixture will be extracted with ether, and washed with brine, dried over magnesium sulfate, filtered, and concentrated. The crude product will be purified by recrystallization from chloroform/hexane or ether/petroleum ether. These methods could potentially be applied to commercial Fmoc-amino acids and protected with benzyl chloride as reported

in Chapter 2. Diazotization will convert the L-amino acid to the D-hydroxy acid equivalent. Because the synthesis methods in Chapter 2 used L-lactic acid, Fmoc-L-Ala-OH will be used to observe any enantiomeric changes. As the overall hydrophobicity of the depsipeptide increases, the role of the fluorenyl group in the self-organization process may change. Self-assembly requires a balance between hydrophobic and hydrophilic conditions, thus this modified synthesis may lead to removal of the Fmoc-group for these depsipeptide families.

#### **4.2.3 Secondary analysis and self-assembly of depsipeptides: Peptide control**

IR and CD analysis of depsipeptides can be used to monitor changes in the backbone due to differences in sequence, solvent, and concentration. However, it may not be accurate to dictate the secondary structure of a peptide backbone with regular ester substitutions. One possible way to monitor the folding process is to observe changes of the native peptide structure. Collecting CD upon substituting with the depsi-moiety may help determine how the presence of the ester affects secondary structure. It is likely that the fluorenyl group may dominate the CD signal, thus IR will also be performed.

The slow rate of gelation has allowed us to sufficiently monitor the self-assembling processes over a period of days. The rate of gelation may be affected by the conformational flexibility of the depsipeptides, as the torsion angle of the ester bond is more flexible than the peptide bond. It would be interesting to observe how a pure peptide backbone influences the self-assembly of depsipeptide (4) under similar ionic and concentration effects. Ester substitutions have commonly been used to monitor structural changes within proteins and peptide residues. We have shown that the presence of ester

residues does not hinder the self-assembly of spherical nanostructures, fibers, or gels. Do the esters simply slow down the process? The steric hindrance of the fluorenyl group may also be a factor for the self-assembly of depsipeptide (4) and has been reported to influence the rate of gelation for a family of short Fmoc-peptides [5]. Fmoc-VRGDV and Fmoc-GRGDG formed gels at 5 mg/ml at pH 3.8. When mixed with Fmoc-KRGDK, gels formed after 12 hours at pH 7 with a total peptide concentration range of 11-20 mg/ml. The authors suggest that the steric hindrance of the fluorenyl group may contribute to the relatively slow coassembly of the oppositely charged peptides.

### **4.2.3 Biocompatibility of self-assembling peptides and modified peptides**

#### ***4.2.3.1 Fmoc-FF/RGD gels as 3D scaffolds***

Applying self-assembled systems for tissue engineering applications requires that the material supports, and in some instances, drives cellular function. Fmoc-FF/RGD (Figure 4.1) was examined for its utility as a biomimetic, 3D-scaffold for anchorage dependent cells [3]. Fmoc-FF/RGE gels were prepared as a control. Human adult dermal fibroblasts (HDFa) were embedded into the hydrogels. The cell-gel constructs formed quickly, ensuring that cells were evenly distributed throughout the hydrogels. The self-assembly process did not affect cell viability after 24 hours, as confirmed with a Live-Dead assay. Living cells with well-defined round morphology were observed, and the presence of dead cells were not detected. Cell spreading occurred within the first 24 hours of culture in the Fmoc-FF/RGD gels, and after 48 hours the spread cells formed 3D-networks. The cells in the Fmoc-FF/RGE gels were rounded after 48 hours.

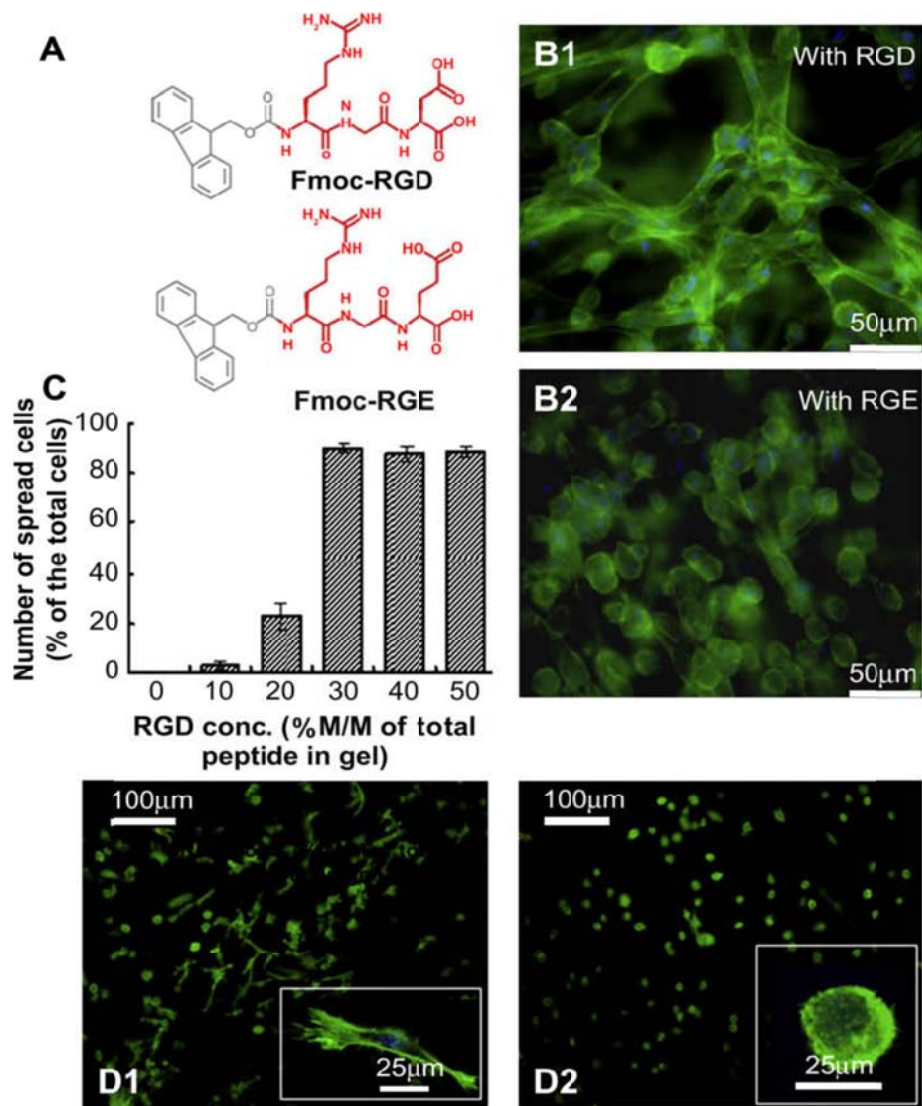


Figure 4.1 The Fmoc-FF/RGD hydrogel promotes cell adhesion with subsequent cell spreading and proliferation. The chemical structures Fmoc-RGD and Fmoc-RGE are provided (A). Cell adhesion and morphology in the Fmoc-FF/RGD and Fmoc-FF/RGE hydrogels (B). HDFa are well-spread in the Fmoc-FF/RGD hydrogels, and form a 3D cell network (B1), compared to the round morphology observed in the Fmoc-FF/RGE hydrogels (B2). The Fmoc-RGD concentration also influenced cell spreading, as hydrogels with 30–50% Fmoc-RGD shows over 90% cell spreading (C). Integrin blocking experiments (D) show that cells with unblocked  $\alpha 5\beta 1$  integrins spread and attach to RGD (D1), while cells with blocked  $\alpha 5\beta 1$  maintain rounded morphology (D2). Used with permission [3]

The extent of cell spreading in the coassembled Fmoc-FF/RGD gel was influenced by the Fmoc-RGD concentration, as 30-50% incorporation yielded over 90% cell spreading. RGD–integrin binding was investigated by incubating cells with a blocking antibody to  $\alpha 5\beta 1$  integrin before 3D-culture. Results show that cells with unblocked integrins exhibited similar cell spreading as observed earlier while cells with blocked  $\alpha 5\beta 1$  integrins failed to attach and spread. This work shows that self-assembled hydrogels from short Fmoc-peptide structures are a viable scaffold for dermal fibroblasts.

#### ***4.2.3.2 PuraMatrix™: Commercial synthetic peptide that exhibits self-assembling behavior***

The self-assembling peptide RAD16 is commercially available as PuraMatrix™ and is derived from a family of self-assembling peptides. Initial investigations of PuraMatrix™ before it was commercialized focused on understanding the influence of peptide sequence on nanofiber formation and stability. PuraMatrix™ is a unique example showing that a firm understanding of how the properties of amino acids affect peptide secondary folding is imperative in the development of self-assembled, gelled materials [6].

PuraMatrix™ is synthetic, sterile, and is currently manufactured in large scale quantities. It can be used for closed, sterile system culture *in vitro* or as injectable applications *in vivo*. PuraMatrix™ has been successfully used to culture variety of cell types, including mouse fibroblasts, bovine calf and adult chondrocytes, chicken embryo fibroblast, bovine endothelial cells, and human neural cells to name a few. [6] In a preliminary study, PuraMatrix™ was used as a scaffold for brain lesion repair in Syrian

hamsters. The animals were treated to injection of PuraMatrix™ upon injury and sacrificed at 1, 3, 6, 30 and 60 days, and the histological results suggest the formation of new tissue. These findings were not observed in untreated animals or those treated with saline as a control.

#### **4.3 CONCLUSIONS**

The synthesis and self-assembly of a depsipeptide family shows that incorporation of regular esters into a native peptide backbone does not disrupt the formation of higher order structures. This initial study has demonstrated that the potential to synthesis a wide range of depsipeptides with variable side chains and hydrophobic character. While the ultimate goal for this work is in vivo implantation, understanding how the interplay between hydrophobic and hydrophilic residues drive self-assembly and hydrogel formation is still needed.

## References

1. Jayawarna, V., et al., *Nanostructured hydrogels for three-dimensional cell culture through self-assembly of fluorenylmethoxycarbonyl-dipeptides*. *Advanced Materials*, 2006. **18**(5): p. 611-+.
2. Mahler, A., et al., *Rigid, self-assembled hydrogel composed of a modified aromatic dipeptide*. *Advanced Materials*, 2006. **18**(11): p. 1365-+.
3. Zhou, M., et al., *Self-assembled peptide-based hydrogels as scaffolds for anchorage-dependent cells*. *Biomaterials*, 2009. **30**(13): p. 2523-2530.
4. Shin, I., et al., *Synthesis of optically active phthaloyl D-aminoxy acids from L-amino acids or L-hydroxy acids as building blocks for the preparation of aminoxy peptides*. *Journal of Organic Chemistry*, 2000. **65**(22): p. 7667-7675.
5. Xu, X.-D., et al., *Coassembly of Oppositely Charged Short Peptides into Well-Defined Supramolecular Hydrogels*. *Journal of Physical Chemistry B*, 2010. **114**(7): p. 2365-2372.
6. Xiaojun, Z., Z. Shuguang, and S. Lisa, *PuraMatrix*, in *Scaffolding In Tissue Engineering*. 2005, CRC Press. p. 217-238.



## Bibliography

- Abdelmelek, M., M. Nguyen, et al. (2010). Synthesis of Morpholine-2,5-dione Monomers for the Preparation of Polydepsipeptides. Biomaterials. A. S. Kulshrestha, A. Mahapatro and L. A. Henderson. Washington, Amer Chemical Soc. **1054**: 185-196.
- Adams, D. J., L. M. Mullen, et al. (2010). "Relationship between molecular structure, gelation behaviour and gel properties of Fmoc-dipeptides." Soft Matter **6**(9): 1971-1980.
- Amblard, M., J. A. Fehrentz, et al. (2006). "Methods and Protocols of modern solid phase peptide synthesis." Molecular Biotechnology **33**(3): 239-254.
- Avan, I., S. R. Tala, et al. (2011). "Benzotriazole-Mediated Syntheses of Depsipeptides and Oligoesters." Journal of Organic Chemistry **76**(12): 4884-4893.
- Barrera, D. A., E. Zylstra, et al. (1995). "Copolymerization and Degradation of Poly(Lactic Acid Co-Lysine)." Macromolecules **28**(2): 425-432.
- Betre, H., S. R. Ong, et al. (2006). "Chondrocytic differentiation of human adipose-derived adult stem cells in elastin-like polypeptide." Biomaterials **27**(1): 91-99.
- Betre, H., L. A. Setton, et al. (2002). "Characterization of a Genetically Engineered Elastin-like Polypeptide for Cartilaginous Tissue Repair." Biomacromolecules **3**(5): 910-916.
- Bezemer, J. M., P. O. Weme, et al. (2000). "Amphiphilic poly(ether ester amide) multiblock copolymers as biodegradable matrices for the controlled release of proteins." Journal of Biomedical Materials Research **52**(1): 8-17.
- Bouget, K., S. Aubin, et al. (2003). "Hydrazino-aza and N-azapeptoids with therapeutic potential as anticancer agents." Bioorganic & Medicinal Chemistry **11**(23): 4881-4889.
- Bowerman, C. J., W. Liyanage, et al. (2011). "Tuning beta-Sheet Peptide Self-Assembly and Hydrogelation Behavior by Modification of Sequence Hydrophobicity and Aromaticity." Biomacromolecules **12**(7): 2735-2745.
- Braun, H.-G. and A. Z. Cardoso (2012). "Self-assembly of Fmoc-diphenylalanine inside liquid marbles." Colloids and Surfaces B: Biointerfaces **97**(0): 43-50.
- Brown, N. J., J. Johansson, et al. (2008). "Biomimicry of Surfactant Protein C." Accounts of Chemical Research **41**(10): 1409-1417.
- Burch, R. M., M. Weitzberg, et al. (1991). "N-(FLUORENYL-9-METHOXYCARBONYL) AMINO-ACIDS, A CLASS OF ANTIINFLAMMATORY AGENTS WITH A DIFFERENT MECHANISM OF ACTION." Proceedings of the National Academy of Sciences of the United States of America **88**(2): 355-359.
- Caplan, M. R., E. M. Schwartzfarb, et al. (2002). "Control of self-assembling oligopeptide matrix formation through systematic variation of amino acid sequence." Biomaterials **23**(1): 219-227.
- Caves, J. M., W. X. Cui, et al. (2011). "Elastin-like protein matrix reinforced with collagen microfibers for soft tissue repair." Biomaterials **32**(23): 5371-5379.

- Chongsiriwatana, N. P., J. A. Patch, et al. (2008). "Peptoids that mimic the structure, function, and mechanism of helical antimicrobial peptides." Proceedings of the National Academy of Sciences **105**(8): 2794-2799.
- Chow, D., M. L. Nunalee, et al. (2008). "Peptide-based biopolymers in biomedicine and biotechnology." Materials Science & Engineering R-Reports **62**(4): 125-155.
- Coin, I., M. Beyermann, et al. (2007). "Solid-phase peptide synthesis: from standard procedures to the synthesis of difficult sequences." Nature Protocols **2**(12): 3247-3256.
- Cudic, P. and M. Stawikowski (2007). "Pseudopeptide synthesis via Fmoc solid-phase synthetic methodology." Mini-Reviews in Organic Chemistry **4**(4): 268-280.
- Davis, M. E., J. P. M. Motion, et al. (2005). "Injectable self-assembling peptide nanofibers create intramyocardial microenvironments for endothelial cells." Circulation **111**(4): 442-450.
- Deng, C., X. S. Chen, et al. (2007). "RGD peptide grafted biodegradable amphiphilic triblock copolymer poly(glutamic acid)-b-poly(L-lactide)-b-poly(glutamic acid): Synthesis and self-assembly." Journal of Polymer Science Part a-Polymer Chemistry **45**(15): 3218-3230.
- Deshmukh, R. and H. J. Purohit (2012). "Peptide Scaffolds: Flexible Molecular Structures With Diverse Therapeutic Potentials." International Journal of Peptide Research and Therapeutics **18**(2): 125-143.
- Dijkstra PJ, F. J. (2000). "Synthetic Pathways to Polydepsipeptides." Macromol Symp **153**: 67-76.
- Elgersma, R. C., T. Meijneke, et al. (2006). "Self-assembly of amylin(20-29) amide-bond derivatives into helical ribbons and peptide nanotubes rather than fibrils." Chemistry-a European Journal **12**(14): 3714-3725.
- Fan, W., X. Li, et al. (2009). "Enhanced Brain Targeting of Tegafur Using Novel Lactyl Cholesterol Liposome as a Carrier." Letters in Drug Design & Discovery **6**(7): 542-547.
- Feng, Y., D. Klee, et al. (2002). "Synthesis of poly[(lactic acid)-alt- or co-((S)-aspartic acid)] from (3S,6R,S)-3-[(benzyloxycarbonyl)methyl]6-methylmorpholine-2,5-dione." Macromolecular Chemistry and Physics **203**(5-6): 819-824.
- Gallardo, I. F. and L. J. Webb (2010). "Tethering Hydrophobic Peptides to Functionalized Self-Assembled Mono layers on Gold through Two Chemical Linkers Using the Huisgen Cycloaddition." Langmuir **26**(24): 18959-18966.
- Gallardo, I. F. and L. J. Webb (2012). "Demonstration of alpha-Helical Structure of Peptides Tethered to Gold Surfaces Using Surface Infrared and Circular Dichroic Spectroscopies." Langmuir **28**(7): 3510-3515.
- Geisler, I. M. and J. P. Schneider (2012). "Evolution-Based Design of an Injectable Hydrogel." Advanced Functional Materials **22**(3): 529-537.
- Gelain, F., A. Horii, et al. (2007). "Designer self-assembling peptide scaffolds for 3-D tissue cell cultures and regenerative medicine." Macromolecular Bioscience **7**(5): 544-551.

- Godballe, T., L. L. Nilsson, et al. (2011). "Antimicrobial  $\beta$ -Peptides and  $\alpha$ -Peptoids." Chemical Biology & Drug Design **77**(2): 107-116.
- Gomes, S., I. B. Leonor, et al. (2012). "Natural and genetically engineered proteins for tissue engineering." Progress in Polymer Science **37**(1): 1-17.
- Goodman, M. and K. C. Stueben (1959). "Peptide Syntheses Via Amino Acid Active Esters." J. Am. Chem. Soc. **81**(15): 3980-3983.
- Hamuro, Y., J. P. Schneider, et al. (1999). "De Novo Design of Antibacterial  $\beta^2$ -Peptides." Journal of the American Chemical Society **121**(51): 12200-12201.
- Hauser, C. A. E., R. S. Deng, et al. (2011). "Natural tri- to hexapeptides self-assemble in water to amyloid beta-type fiber aggregates by unexpected alpha-helical intermediate structures." Proceedings of the National Academy of Sciences of the United States of America **108**(4): 1361-1366.
- Heilshorn, S. C., J. C. Liu, et al. (2005). "Cell-binding domain context affects cell behavior on engineered proteins." Biomacromolecules **6**(1): 318-323.
- Helder, J., F. E. Kohn, et al. (1985). "Synthesis of Poly[Oxyethylidenecarbonylimino-(2-Oxoethylene)] [Poly(Glycine-D,L-Lactic Acid)] by Ring-Opening Polymerization." Makromolekulare Chemie-Rapid Communications **6**(1): 9-14.
- Hong, Y., M. D. Pritzker, et al. (2005). "Effect of NaCl and peptide concentration on the self-assembly of an ionic-complementary peptide EAK16-II." Colloids and Surfaces B-Biointerfaces **46**(3): 152-161.
- Horii, A., X. Wang, et al. (2007). "Biological Designer Self-Assembling Peptide Nanofiber Scaffolds Significantly Enhance Osteoblast Proliferation, Differentiation and 3-D Migration." PLoS ONE **2**(2): e190.
- Hughes, M., L. S. Birchall, et al. (2012). "Differential supramolecular organisation of Fmoc-dipeptides with hydrophilic terminal amino acid residues by biocatalytic self-assembly." Soft Matter **8**(45): 11565-11574.
- Ingwall, R. T., C. Gilon, et al. (1978). Polydepsipeptides. 7. Conformational Analysis of Poly(L-alanyl-L-alanyl-L-lactic acid). **11**: 540-545.
- Jayawarna, V., M. Ali, et al. (2006). "Nanostructured hydrogels for three-dimensional cell culture through self-assembly of fluorenylmethoxycarbonyl-dipeptides." Advanced Materials **18**(5): 611-614.
- Jayawarna, V., S. M. Richardson, et al. (2009). "Introducing chemical functionality in Fmoc-peptide gels for cell culture." Acta Biomaterialia **5**(3): 934-943.
- Jun, H.-W. and J. L. West (2005). "Modification of polyurethaneurea with PEG and YIGSR peptide to enhance endothelialization without platelet adhesion." Journal of Biomedical Materials Research Part B: Applied Biomaterials **72B**(1): 131-139.
- Junnila, S., S. Hanski, et al. (2009). "Effect of Double-Tailed Surfactant Architecture on the Conformation, Self-Assembly, and Processing in Polypeptide-Surfactant Complexes." Biomacromolecules **10**(10): 2787-2794.
- Katritzky, A. R., M. Yoshioka, et al. (2008). "N-Fmoc-protected(alpha-dipeptidoyl)benzotriazoles for efficient solid-phase peptide synthesis by segment condensation." Chemical Biology & Drug Design **72**(3): 182-188.

- Kisfaludy, L. and I. Schon (1983). "PREPARATION AND APPLICATIONS OF PENTAFLUOROPHENYL ESTERS OF 9-FLUORENYLMETHYLOXYCARBONYL AMINO-ACIDS FOR PEPTIDE-SYNTHESIS." Synthesis-Stuttgart(4): 325-327.
- Kudirka, R., H. Tran, et al. (2011). "Folding of a single-chain, information-rich polypeptoid sequence into a highly ordered nanosheet." Peptide Science **96**(5): 586-595.
- Kuisle, O., E. Quinoa, et al. (1999). "A general methodology for automated solid-phase synthesis of depsides and depsipeptides. Preparation of a valinomycin analogue." Journal of Organic Chemistry **64**(22): 8063-8075.
- Kuisle, O., E. Quinoa, et al. (1999). "Solid phase synthesis of depsides and depsipeptides." Tetrahedron Letters **40**(6): 1203-1206.
- Lammel, A. S., X. Hu, et al. (2010). "Controlling silk fibroin particle features for drug delivery." Biomaterials **31**(16): 4583-4591.
- Lawrence, B. D., J. K. Marchant, et al. (2009). "Silk film biomaterials for cornea tissue engineering." Biomaterials **30**(7): 1299-1308.
- Loo, Y., S. G. Zhang, et al. (2012). "From short peptides to nanofibers to macromolecular assemblies in biomedicine." Biotechnology Advances **30**(3): 593-603.
- Mahler, A., M. Reches, et al. (2006). "Rigid, self-assembled hydrogel composed of a modified aromatic dipeptide." Advanced Materials **18**(11): 1365-1370.
- Marek, P. J., V. Patsalo, et al. (2012). "Ionic Strength Effects on Amyloid Formation by Amylin Are a Complicated Interplay among Debye Screening, Ion Selectivity, and Hofmeister Effects." Biochemistry **51**(43): 8478-8490.
- Martino, M., A. Coviello, et al. (2000). "Synthesis and structural characterization of poly(LGGVG), an elastin-like polypeptide." International Journal of Biological Macromolecules **27**(1): 59-64.
- Martino, M. and A. M. Tamburro (2001). "Chemical synthesis of cross-linked poly(KGGVG), an elastin-like biopolymer." Biopolymers **59**(1): 29-37.
- Mathias, L. J., W. D. Fuller, et al. (1978). "Polydepsipeptides .6. Synthesis of Sequential Polymers Containing Varying Ratios of L-Alanine and L-Lactic Acid." Macromolecules **11**(3): 534-539.
- Matsuda, A., H. Kobayashi, et al. (2005). "Immobilization of laminin peptide in molecularly aligned chitosan by covalent bonding." Biomaterials **26**(15): 2273-2279.
- Merrifield, R. B. (1963). "SOLID PHASE PEPTIDE SYNTHESIS .1. SYNTHESIS OF A TETRAPEPTIDE." Journal of the American Chemical Society **85**(14): 2149-&
- Miller, S. M., R. J. Simon, et al. (1994). "Proteolytic studies of homologous peptide and N-substituted glycine peptoid oligomers." Bioorganic & Medicinal Chemistry Letters **4**(22): 2657-2662.
- Mu, X., K. M. Eckes, et al. (2012). "Experimental and Computational Studies Reveal an Alternative Supramolecular Structure for Fmoc-Dipeptide Self-Assembly." Biomacromolecules **13**(11): 3562-3571.

- Murnen, H. K., A. M. Rosales, et al. (2010). "Hierarchical Self-Assembly of a Biomimetic Diblock Copolypeptoid into Homochiral Superhelices." Journal of the American Chemical Society **132**(45): 16112-16119.
- Nettles, D. L., A. Chilkoti, et al. (2010). "Applications of elastin-like polypeptides in tissue engineering." Advanced Drug Delivery Reviews **62**(15): 1479-1485.
- Nguyen, M. M., N. Ong, et al. (2013). "A general solid phase method for the synthesis of depsipeptides." Organic & Biomolecular Chemistry **11**(7): 1167-1170.
- Ohyama, T., H. Oku, et al. (2001). "Crystal structure of a depsipeptide, Boc-(Leu-Leu-Lac)(3)-Leu-Leu-OEt." Biopolymers **58**(7): 636-642.
- Oku, H., T. Ohyama, et al. (2004). "Addition of a peptide fragment on an  $\alpha$ -helical depsipeptide induces  $\alpha/3(10)$ -conjugated helix: Synthesis, crystal structure, and CD spectra of Boc-Leu-Leu-Ala-(Leu-Leu-Lac)(3)-Leu-Leu-OEt." Biopolymers **75**(3): 242-254.
- Oku, H., K. Yamada, et al. (2008). "Conformational change from antiparallel beta-sheet to alpha-helix in a series of depsipeptide, -(Leu-Leu-Lac)(n)-: Syntheses, spectroscopic studies, and crystal structures of Boc-Leu-Lac-OEt and Boc-(Leu-Leu-Lac)(n)-OEt (n=1, 2)." Biopolymers **89**(4): 270-283.
- Ouchi, T., A. Hamada, et al. (1999). "Biodegradable microspheres having reactive groups prepared from L-lactic acid-depsipeptide copolymers." Macromolecular Chemistry and Physics **200**(2): 436-441.
- Ouchi, T., H. Miyazaki, et al. (2002). "Synthesis of biodegradable amphiphilic AB-type diblock copolymers of lactide and depsipeptide with pendant reactive groups." Journal of Polymer Science Part a-Polymer Chemistry **40**(9): 1218-1225.
- Ouchi, T., T. Nozaki, et al. (1997). "Synthesis and enzymatic hydrolysis of lactic acid depsipeptide copolymers with functionalized pendant groups." Journal of Polymer Science Part a-Polymer Chemistry **35**(2): 377-383.
- Ouchi, T., T. Nozaki, et al. (1996). "Synthesis and enzymatic hydrolysis of polydepsipeptides with functionalized pendant groups." Macromolecular Chemistry and Physics **197**(6): 1823-1833.
- Ouchi, T. and Y. Ohya (2004). "Design of lactide copolymers as biomaterials." Journal of Polymer Science Part a-Polymer Chemistry **42**(3): 453-462.
- Ouchi, T., M. Sasakawa, et al. (2004). "Preparation of poly[DL-lactide-co-glycolide]-based microspheres containing protein by use of amphiphilic diblock copolymers of depsipeptide and lactide having ionic pendant groups as biodegradable surfactants by W/O/W emulsion method." Polymer **45**(5): 1583-1589.
- Ouchi, T., H. Seike, et al. (2000). "Synthesis of a block copolymer of L-lactide and depsipeptide with pendant thiol groups." Designed Monomers and Polymers **3**(3): 279-287.
- Ouchi, T., M. Shiratani, et al. (1993). "Synthesis of poly[(glycolic acid)-alt-(l-aspartic acid)] and its biodegradation behavior in-vitro." Makromolekulare Chemie-Rapid Communications **14**(12): 825-831.
- Rathore, O. and D. Y. Sogah (2001). "Nanostructure Formation through Beta-Sheet Self-Assembly in Silk-Based Materials." Macromolecules **34**(5): 1477-1486.

- Rathore, O. and D. Y. Sogah (2001). "Self-Assembly of Beta-Sheets into Nanostructures by Poly(alanine) Segments Incorporated in Multiblock Copolymers Inspired by Spider Silk." Journal of the American Chemical Society **123**(22): 5231-5239.
- Ratner, B. D. and S. J. Bryant (2004). "Biomaterials: Where we have been and where we are going." Annual Review of Biomedical Engineering **6**: 41-75.
- Rotem, S. and A. Mor (2009). "Antimicrobial peptide mimics for improved therapeutic properties." Biochimica Et Biophysica Acta-Biomembranes **1788**(8): 1582-1592.
- Ryan, D. M., T. M. Doran, et al. (2011). "Complementary pi-pi Interactions Induce Multicomponent Coassembly into Functional Fibrils." Langmuir **27**(17): 11145-11156.
- Sadownik, J. W., J. Leckie, et al. (2011). "Micelle to fibre biocatalytic supramolecular transformation of an aromatic peptide amphiphile." Chemical Communications **47**(2): 728-730.
- Saiani, A., A. Mohammed, et al. (2009). "Self-assembly and gelation properties of alpha-helix versus beta-sheet forming peptides." Soft Matter **5**(1): 193-202.
- Sanii, B., R. Kudirka, et al. (2011). "Shaken, Not Stirred: Collapsing a Peptoid Monolayer To Produce Free-Floating, Stable Nanosheets." Journal of the American Chemical Society **133**(51): 20808-20815.
- Schakenraad, J. M., P. Nieuwenhuis, et al. (1989). "Invivo and Invitro Degradation of Glycine Dl-Lactic Acid Copolymers." Journal of Biomedical Materials Research **23**(11): 1271-1288.
- Seebach, D., M. Overhand, et al. (1996). " $\beta$ -Peptides: Synthesis by Arndt-Eistert homologation with concomitant peptide coupling. Structure determination by NMR and CD spectroscopy and by X-ray crystallography. Helical secondary structure of a  $\beta$ -hexapeptide in solution and its stability towards pepsin." Helvetica Chimica Acta **79**(4): 913-941.
- Shahi, P., R. Sharma, et al. (2007). "Formation of amyloid fibrils via longitudinal growth of oligomers." Biochemistry **46**(25): 7365-7373.
- Shalaby, W. and D. F. Koelmel (1984). Copolymers of p-dioxanone and 2,5-morpholinediones and surgical devices form therefrom having accelerated absorption characteristics, Ethicon, Inc.
- Shapiro, Y. E. (2011). "Structure and dynamics of hydrogels and organogels: An NMR spectroscopy approach." Progress in Polymer Science **36**(9): 1184-1253.
- Shin, I., M. R. Lee, et al. (2000). "Synthesis of optically active phthaloyl D-aminoxy acids from L-amino acids or L-hydroxy acids as building blocks for the preparation of aminoxy peptides." Journal of Organic Chemistry **65**(22): 7667-7675.
- Smith, A. M., R. J. Williams, et al. (2008). "Fmoc-Diphenylalanine self assembles to a hydrogel via a novel architecture based on pi-pi interlocked beta-sheets." Advanced Materials **20**(1): 37-+.
- Soffer, L., X. Wang, et al. (2008). "Silk-based electrospun tubular scaffolds for tissue-engineered vascular grafts." Journal of Biomaterials Science, Polymer Edition **19**(5): 653-664.

- Spengler, J., B. Kokschi, et al. (2007). "Simple machine-assisted protocol for solid-phase synthesis of depsipeptides." Biopolymers **88**(6): 823-828.
- Stewart, F. H. C. (1965). "The synthesis and polymerization of peptide p-nitrophenyl esters." Australian Journal of Chemistry **18**(6): 887-901.
- Stewart, F. H. C. (1966). "The preparation of some sequential polypeptides by the p-Nitrophenyl ester method." Australian Journal of Chemistry **19**(8): 1503-1509.
- Stewart, F. H. C. (1967). "Formation of depsipeptide ester bonds by accelerated active ester coupling." Chemistry and Industry **46**: 1960-1961.
- Stewart, F. H. C. (1968). "Pentamethylbenzyl esters of  $\alpha$ -hydroxy acids and their use in depsipeptide synthesis." Australian Journal of Chemistry **21**(5): 1327-1335.
- Stewart, F. H. C. (1969). "Synthesis of polydepsipeptides with regularly repeating unit sequences." Australian Journal of Chemistry **22**(6): 1291-1298.
- Tang, C., R. V. Ulijn, et al. (2011). "Effect of Glycine Substitution on Fmoc-Diphenylalanine Self-Assembly and Gelation Properties." Langmuir **27**(23): 14438-14449.
- Urry, D. W. (1997). "Physical Chemistry of Biological Free Energy Transduction As Demonstrated by Elastic Protein-Based Polymers." The Journal of Physical Chemistry B **101**(51): 11007-11028.
- Urry, D. W., D. C. Gowda, et al. (1994). "NANOMETRIC DESIGN OF EXTRAORDINARY HYDROPHOBIC-INDUCED PKA SHIFTS FOR ASPARTIC-ACID - RELEVANCE TO PROTEIN MECHANISMS." Biopolymers **34**(7): 889-896.
- Urry, D. W., S. Q. Peng, et al. (1994). "COMPARISON OF ELECTROSTATIC-INDUCED AND HYDROPHOBIC-INDUCED PKA SHIFTS IN POLYPENTAPEPTIDES - THE LYSINE RESIDUE." Chemical Physics Letters **225**(1-3): 97-103.
- Vandermeulen, G. W. M. and H. A. Klok (2004). "Peptide/protein hybrid materials: Enhanced control of structure and improved performance through conjugation of biological and synthetic polymers." Macromolecular Bioscience **4**(4): 383-398.
- Veld, P., P. J. Dijkstra, et al. (1992). "Synthesis of Biodegradable Polyesteramides with Pendant Functional-Groups." Makromolekulare Chemie-Macromolecular Chemistry and Physics **193**(11): 2713-2730.
- Wang, D. and X. D. Feng (1997). "Synthesis of poly(glycolic acid-alt-L-aspartic acid) from a morpholine-2,5-dione derivative." Macromolecules **30**(19): 5688-5692.
- Wong, J. Y., Z. Weng, et al. (2002). "Identification and validation of a novel cell-recognition site (KNEED) on the 8th type III domain of fibronectin." Biomaterials **23**(18): 3865-3870.
- Wu, C. W., K. Kirshenbaum, et al. (2003). "Structural and Spectroscopic Studies of Peptoid Oligomers with  $\hat{\pm}$ -Chiral Aliphatic Side Chains." Journal of the American Chemical Society **125**(44): 13525-13530.
- Wu, C. W., T. J. Sanborn, et al. (2001). "Peptoid Oligomers with  $\alpha$ -Chiral, Aromatic Side Chains: Sequence Requirements for the Formation of Stable Peptoid Helices." Journal of the American Chemical Society **123**(28): 6778-6784.

- XiaoJun, Z., Z. Shuguang, et al. (2005). PuraMatrix. Scaffolding In Tissue Engineering, CRC Press: 217-238.
- Xu, X.-D., C.-S. Chen, et al. (2010). "Coassembly of Oppositely Charged Short Peptides into Well-Defined Supramolecular Hydrogels." Journal of Physical Chemistry B **114**(7): 2365-2372.
- Xu, X. D., Y. Jin, et al. (2010). "Self-assembly behavior of peptide amphiphiles (PAs) with different length of hydrophobic alkyl tails." Colloids and Surfaces B-Biointerfaces **81**(1): 329-335.
- Yang, X. Y., M. Wang, et al. (2004). "Analysis of protein folding and function using backbone modified proteins." Bioorganic Chemistry **32**(5): 438-449.
- Yang, Y., U. Khoe, et al. (2009). "Designer self-assembling peptide nanomaterials." Nano Today **4**(2): 193-210.
- Ye, Z. Y., H. Y. Zhang, et al. (2008). "Temperature and pH effects on biophysical and morphological properties of self-assembling peptide RADA16-1." Journal of Peptide Science **14**(2): 152-162.
- Yokoi, H., T. Kinoshita, et al. (2005). "Dynamic reassembly of peptide RADA16 nanofiber scaffold." Proceedings of the National Academy of Sciences of the United States of America **102**(24): 8414-8419.
- Zhang, D. H., S. H. Lahasky, et al. (2012). "Polypeptoid Materials: Current Status and Future Perspectives." Macromolecules **45**(15): 5833-5841.
- Zhang, J. J., M. King, et al. (2007). "Molecular modeling of conformational properties of oligodepsipeptides." Biomacromolecules **8**(10): 3015-3024.
- Zhang, S. G., T. Holmes, et al. (1993). "Spontaneous Assembly of a Self-Complementary Oligopeptide to Form a Stable Macroscopic Membrane." Proceedings of the National Academy of Sciences of the United States of America **90**(8): 3334-3338.
- Zhou, J., C. Cao, et al. (2010). "Electrospinning of silk fibroin and collagen for vascular tissue engineering." International Journal of Biological Macromolecules **47**(4): 514-519.
- Zhou, M., A. M. Smith, et al. (2009). "Self-assembled peptide-based hydrogels as scaffolds for anchorage-dependent cells." Biomaterials **30**(13): 2523-2530.



## **Vita**

Mary Minh Chau (MC) Nguyen was born August 28, 1982 in St. Paul, MN to Tong Nguyen and Thuha Truong. She graduated from Como Park Senior High School and obtained a degree Biomedical Engineering and minor in Chemistry from the University of Minnesota. She taught English as a second language in Vietnam upon entering the Graduate Program in Biomedical Engineering at the University of Texas at Austin. In 2008, she was awarded a CESRI fellowship and worked under the Hecht group at Humboldt University in Berlin, Germany. She has completed a certification in the Societal Impacts of Science and Technology from UT and presented her portfolio work at the Gordon Research Seminar in Science Policy in the Summer of 2012. She was also a Senior Associate in the Biosciences division at the Austin Technology Incubator.

Permanent address: 1314 Travis Heights Blvd, Unit A. Austin, TX 78704

This dissertation was typed by the author.